



# Acoustic and Laser Doppler Anemometer Results for Confluent, 22-Lobed, and Unique-Lobed Mixer Exhaust Systems for Subsonic Jet Noise Reduction

M. Salikuddin, S. Martens, H. Shin, and R.K. Majjigi  
General Electric Aircraft Engines Company, Cincinnati, Ohio

## The NASA STI Program Office . . . in Profile

Since its founding, NASA has been dedicated to the advancement of aeronautics and space science. The NASA Scientific and Technical Information (STI) Program Office plays a key part in helping NASA maintain this important role.

The NASA STI Program Office is operated by Langley Research Center, the Lead Center for NASA's scientific and technical information. The NASA STI Program Office provides access to the NASA STI Database, the largest collection of aeronautical and space science STI in the world. The Program Office is also NASA's institutional mechanism for disseminating the results of its research and development activities. These results are published by NASA in the NASA STI Report Series, which includes the following report types:

- **TECHNICAL PUBLICATION.** Reports of completed research or a major significant phase of research that present the results of NASA programs and include extensive data or theoretical analysis. Includes compilations of significant scientific and technical data and information deemed to be of continuing reference value. NASA's counterpart of peer-reviewed formal professional papers but has less stringent limitations on manuscript length and extent of graphic presentations.
- **TECHNICAL MEMORANDUM.** Scientific and technical findings that are preliminary or of specialized interest, e.g., quick release reports, working papers, and bibliographies that contain minimal annotation. Does not contain extensive analysis.
- **CONTRACTOR REPORT.** Scientific and technical findings by NASA-sponsored contractors and grantees.

- **CONFERENCE PUBLICATION.** Collected papers from scientific and technical conferences, symposia, seminars, or other meetings sponsored or cosponsored by NASA.
- **SPECIAL PUBLICATION.** Scientific, technical, or historical information from NASA programs, projects, and missions, often concerned with subjects having substantial public interest.
- **TECHNICAL TRANSLATION.** English-language translations of foreign scientific and technical material pertinent to NASA's mission.

Specialized services that complement the STI Program Office's diverse offerings include creating custom thesauri, building customized databases, organizing and publishing research results . . . even providing videos.

For more information about the NASA STI Program Office, see the following:

- Access the NASA STI Program Home Page at <http://www.sti.nasa.gov>
- E-mail your question via the Internet to [help@sti.nasa.gov](mailto:help@sti.nasa.gov)
- Fax your question to the NASA Access Help Desk at 301-621-0134
- Telephone the NASA Access Help Desk at 301-621-0390
- Write to:  
NASA Access Help Desk  
NASA Center for AeroSpace Information  
7121 Standard Drive  
Hanover, MD 21076

NASA/CR—2002-211598



# Acoustic and Laser Doppler Anemometer Results for Confluent, 22-Lobed, and Unique-Lobed Mixer Exhaust Systems for Subsonic Jet Noise Reduction

M. Salikuddin, S. Martens, H. Shin, and R.K. Majjigi  
General Electric Aircraft Engines Company, Cincinnati, Ohio

Prepared under Contract NAS3-26617

National Aeronautics and  
Space Administration

Glenn Research Center

## Acknowledgments

This report is prepared by GE Aircraft Engines, Cincinnati, Ohio for NASA Glenn Research Center, Cleveland, Ohio under LET Contract NAS3-26617, Task Order 31. Mr. Gene Krejsa was the Project Manager for NASA Glenn Research Center and Dr. R.K. Majjigi was the Project Manager for GEAE. The authors are thankful to Mr. J. Brausch and Mr. R.R. Babbitt for their contributions in designing and acquiring the model hardware and helping the installation of the hardware in GEAE's Cell 41 for testing. The authors are also thankful to Mr. J. Hencheck and Ms. S. Thomson for running the test facility, and to Dr. K. Kinzie for helping in data analysis. The authors are particularly thankful to Dr. B.A. Janardan for his useful suggestions and discussions during the course of this work.

Trade names or manufacturers' names are used in this report for identification only. This usage does not constitute an official endorsement, either expressed or implied, by the National Aeronautics and Space Administration.

Available from

NASA Center for Aerospace Information  
7121 Standard Drive  
Hanover, MD 21076

National Technical Information Service  
5285 Port Royal Road  
Springfield, VA 22100

Available electronically at <http://gltrs.grc.nasa.gov>

## SUMMARY

The objective of this task was to develop a design methodology and noise reduction concepts for high bypass exhaust systems which could be applied to both existing production and new advanced engine designs. Special emphasis was given to engine cycles with bypass ratios in the range of 4:1 to 7:1, where jet mixing noise was a primary noise source at full power takeoff conditions. The goal of this effort was to develop the design methodology for mixed-flow exhaust systems and other novel noise reduction concepts that would yield 3 EPNdB noise reduction relative to 1992 baseline technology.

Two multi-lobed mixers, a 22-lobed axisymmetric and a 21-lobed with a unique lobe, were designed. These mixers along with a confluent mixer were tested with several fan nozzles of different lengths with and without acoustic treatment in GEAE's Cell 41 under the current subtask (Subtask C). In addition to the acoustic and LDA tests for the model mixer exhaust systems, a semi-empirical noise prediction method for mixer exhaust system is developed. Effort was also made to implement flowfield data for noise prediction by utilizing MGB code. In general, this study established an aero and acoustic diagnostic database to calibrate and refine current aero and acoustic prediction tools. Following conclusions are made on the basis of the measured acoustic and LDA data:

- Significant noise reduction can be achieved by using a lower core velocity engine cycle for multi-lobed and confluent mixer exhaust systems.
- While the low frequency noise is significantly reduced by 22- and unique-21-Lobed mixers compared to the confluent mixer, high frequency noise increase is large.
- The Task objective of 3 EPNdB reduction relative to 1992 technology level was demonstrated in Task - A Tests: 12-lobed mixer configuration (F9B) resulted in a 3.5 EPNdB reduction compared to the confluent mixer at  $V_{mix}=1000$  ft/sec.
- 22- and unique-21-lobed mixer tests in Task - C along a reduced core velocity cycle (High Bypass Mixed Flow Cycle) resulted in an EPNdB lower than the F9B at  $V_{mix}=1000$  ft/sec due to a combination of cycle and mixer design, even though a 2 EPNdB reduction relative to confluent mixer is achieved.
- Increased fan nozzle length reduces noise level at all frequencies at lower velocity conditions due to improved mixing. The trend is reversed at higher velocity conditions possibly due to increased turbulence level.
- Internal pylon for unique-lobed mixer has very little effect on noise level compared to the 22-lobed axisymmetric mixer configuration.
- Acoustic treatment on fan nozzle is more effective in reducing noise at higher velocity conditions.

- Also, the treatment effectiveness is more for E<sup>3</sup> mixed flow cycle conditions, possibly due to higher internal noise caused by higher core velocity.
- Treated configuration introduces excess noise at lower velocity conditions at higher frequencies (2 to 4 kHz) possibly due to increased small scale turbulence by liner perforations. However, these levels are small compared to noise reduction due to treatment at other frequencies at higher velocity conditions.

## CONTENTS

	Page
SUMMARY	iii
1.0 INTRODUCTION	1
2.0 ANECHOIC FREE-JET NOISE FACILITY	3
3.0 COMPONENTS, ASSEMBLIES OF EXHAUST SYSTEM, AND EXHAUST SYSTEM CONFIGURATIONS	5
4.0 TEST PROCEDURE AND DATA ACQUISITION	23
4.1 Acoustic Tests	23
4.2 LDA Tests	26
5.0 VARIOUS MIXED & SEPARATE FLOW ENGINE CYCLE CONDITIONS	31
6.0 EXPERIMENTAL RESULTS	42
6.1 Acoustic Data for 20.5 in <sup>2</sup> Conic Nozzle	42
6.2 Acoustic and LDA Data for Confluent and 22-Lobed Mixers with Standard Fan Nozzle Showing the Effect of Engine Cycle on Farfield Noise Level and Plume Flowfield	54
Confluent Mixer	54
22-Lobed Mixer	62
6.3 Effect of Mixer Geometry on farfield Noise Level and Plume Flowfield	73
6.4 Effect of Fan Nozzle Length on Farfield Noise Level and Plume Flowfield	89
22-Lobed Mixer	89
Confluent Mixer	102
6.5 Effect of Internal Pylon on farfield Noise Level	102

	Page
6.4 Effect of Fan Nozzle Treatment on Farfield Noise Level and Plume Flowfield	102
Treatment Design	102
Acoustic and Flowfield Results for 22-Lobed Mixer	116
Acoustic Results for Unique-Lobed Mixer	116
6.7 Farfield Noise for Multi-Lobed Configurations Compared to Confluent Mixer & Conic Nozzle	127
6.8 Conclusions	146
<b>APPENDIX A TABULATED RESULTS FOR VARIOUS EXHAUST SYSTEM CONFIGURATIONS</b>	<b>147</b>
<b>APPENDIX B DEVELOPMENT OF NOISE PREDICTION CODE FOR INTERNAL MIXER NOZZLE SYSTEMS</b>	<b>167</b>
<b>APPENDIX C IMPLEMENTATION AND IMPROVEMENT OF MGB CODE TO PREDICT FARFIELD NOISE USING CFD PREDICTED/MEASURED FLOWFIELD DATA</b>	<b>177</b>

## 1.0 INTRODUCTION

Jet mixing noise limits the engine noise reduction that can be achieved at higher power settings for current high bypass engines, and for advanced engines with bypass ratios less than about 10:1. Methods for reducing jet mixing noise are therefore needed for engines with bypass ratios less than 10:1 that do not introduce significant performance and weight penalties. Current production engines have bypass ratios in the range of 3:1 to 6:1, and the potential of increased future noise certification rule stringency requires development of jet noise reduction concepts that are applicable to, and practical for, this class of engines, so that they can remain competitive in the marketplace and compliant with prevailing regulations well into the 21st century. Because of the long lead time required to introduce new engines into the marketplace with sufficient fleet penetration to have a significant impact on community noise exposure, only by reducing the noise of existing production engine models can it be hoped to reduce community noise impact in the next 15 to 20 years.

The objective of this task is to develop a design methodology and noise reduction concepts for high bypass exhaust systems, which can be applied to both existing production and new advanced engine designs. Special emphasis is given to engine cycles with bypass ratios in the range of 4:1 to 7:1, where jet-mixing noise is a primary noise source at full power takeoff conditions. The goal of this effort is to develop the design methodology for mixed-flow exhaust systems and other novel noise reduction concepts that will yield 3 EPNdB noise reduction relative to 1992 baseline technology.

Development of the design methodology is based upon a previously developed jet noise model and code for exhaust nozzles (MGB), which will be coupled with a CFD flow field analysis. The modeling is envisioned to be in two steps. The first step is to adapt an existing CFD code to predict the velocity, temperature, and turbulence intensity profiles at the exit plane of the mixer, and these profiles are then the starting conditions for the MGB aeroacoustic computations. By coupling the CFD flow fields with the MGB code, the noise generated by the internal mixing will be assessed. The second step is to adapt the existing CFD code to also predict the external jet plume aerodynamics as well, rather than using the MGB aerodynamic mixing algorithms (based on Reichardt's momentum and enthalpy transport theory). The first step provides the capability for studying mixer exit profile shape effects on the noise generation, and can provide some guidance on possible new mixer designs that may provide lower noise. The second step provides a more accurate simulation of the jet plume mixing characteristics. This two-step approach, the CFD-MGB integrated model, will provide a useful design tool for developing low noise exhaust nozzle designs.

In concert with the development of advanced aeroacoustic design tools, the CFD-MBG model, a carefully selected set of baseline and example mixer test and diagnostic measurements with simulated forward flight in the GEAE Cell 41 Anechoic Free-Jet Wind Tunnel Facility were performed to validate and calibrate the model. For this purpose, the several existing mixers developed during the Energy Efficient Engine (E<sup>3</sup>)

program in the 1970's were tested under Subtask A. The scale models tested under Subtask A in Cell 41 were selected Energy Efficient Engine, E<sup>3</sup> Long Duct Mixed Flow (LDMF) exhaust system configurations with 12-lobed mixers. Subtask A establishes an aero and acoustic diagnostic database from which to calibrate and refine current aero and acoustic prediction tools. The acoustic and LDA results for this subtask are presented in a report, "Acoustic & Laser Doppler Anemometer Results for Confluent and 12-Lobed E<sup>3</sup> Mixer Exhaust Systems for Subsonic Jet Noise Reduction."

The next step consists of designing, fabricating, and testing candidate low-noise mixer designs, using the validated CFD-MGB tool and experimental results from E<sup>3</sup> mixer tests. This activity is a demonstration that the modeling and understanding gained from the experiments will provide the capability to design an exhaust system capable of meeting the objective goal of reducing jet mixing noise of a high bypass exhaust system by 3 EPNdB.

Two multi-lobed mixers, a 22-lobed axisymmetric and a 21-lobed with a unique lobe, were designed. These mixers along with a confluent mixer were tested with several fan nozzles of different lengths with and without acoustic treatment in GEAE's Cell 41 under the current subtask, Subtask C. In addition to the acoustic and LDA tests for the model mixer exhaust systems, a semi-empirical noise prediction method for mixer exhaust system is developed. Effort is also made to implement flowfield data for noise prediction by utilizing MGB code. In general, this study establishes an aero and acoustic diagnostic database to calibrate and refine current aero and acoustic prediction tools.

## 2.0 ANECHOIC FREE-JET JET NOISE FACILITY

The GEAE anechoic free-jet jet noise facility, shown in Figure 1, is a cylindrical chamber 43' (13.1 meters) in diameter and 72' (21.95 meters) tall. The inner surfaces of the chamber are lined with anechoic wedges made of fiberglass wool to render the facility anechoic above 220 Hz. The facility can accommodate model configurations up to 5.3" (13.5 cm) and 5.5" (14.0 cm) equivalent flow diameter in the inner and outer flow streams, respectively. The corresponding throat areas for these streams are 22 and 24 square inches. The streams of heated air for the dual flow arrangement, produced by two separate natural gas burners, flow through silencers and plenum chambers before entering the test nozzle. Each stream can be heated to a maximum of  $1960^{\circ}\text{R}$  with nozzle pressure ratios as high as 5.5, resulting in a maximum jet velocity of 3000 feet/second.

The tertiary air stream system, which is used to simulate external flow, consists of a 250,000 scfm (at 50" of water column static pressure) fan and a 3,500 horsepower electric motor. The transition duct work and silencer route the air from the fan discharge through the 48" (1.2 meter) diameter free-jet exhaust. The silencer reduces the fan noise by 30 dB to 50 dB. Tertiary flow at its maximum permits simulation up to a Mach number of about 0.4. Mach number variation is achieved by adjusting the fan inlet vanes. The combined model and free-jet airflow is exhausted through a "T" stack silencer directly over the models in the ceiling of the chamber. The "T" stack is acoustically treated to prevent high levels of noise to the surrounding community.

The facility is equipped with two systems of microphone arrays to measure the acoustic characteristics of the test models in the farfield, a fixed array of microphones and an array on a traversing tower. The fixed array has 17 microphones mounted from the false floor, the wall, and the ceiling of the test cell, which provides measurements at a minimum distance of 26.75' (8.15 meter) from the nozzle reference location covering the polar angle ( $\theta$ ) range from  $50^{\circ}$  to  $155^{\circ}$ . The traversing tower contains 13 microphones, mounted at polar angles  $\theta$  ranging from  $45^{\circ}$  to  $155^{\circ}$ , and provides measurements at a distance of 22' (6.7 meter) from the nozzle reference location. The traversing tower can be positioned at any azimuthal angle  $\phi$  between  $+55^{\circ}$  to  $-55^{\circ}$  with respect to the fixed microphone array (or  $\phi = -10^{\circ}$  to  $100^{\circ}$ ).

The facility is also equipped with a laser Doppler anemometer (LDA) system for jet flowfield measurement.

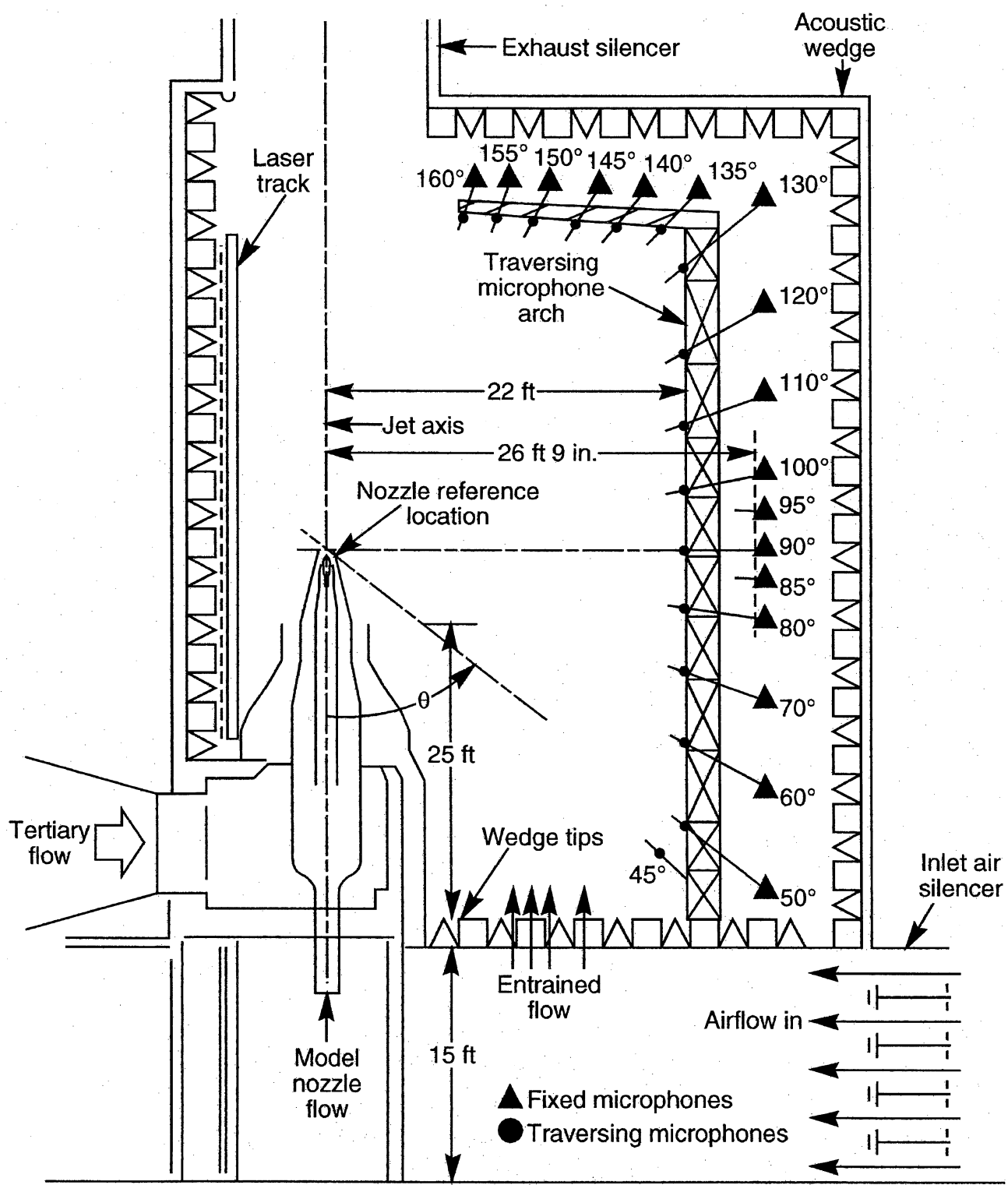


Figure 1. GEAE Test Cell 41 anechoic free-jet noise facility

### **3.0 COMPONENTS, ASSEMBLIES OF EXHAUST SYSTEM AND EXHAUST SYSTEM CONFIGURATIONS**

Two multi-lobe mixers, a baseline 22-lobed axisymmetric mixer and a baseline 21-lobed mixer with one unique lobe and a confluent mixer, shown in Figure 2, are designed and fabricated. These mixers are tested with three fan nozzles with different lengths (see Figure 3), namely, the baseline fan nozzle, the short fan nozzle representing a 1/3rd reduction in the nozzle mixing/tailpipe length, and the long fan nozzle representing a 1/3rd increase in the nozzle mixing/tailpipe length. The assembly of mixers and the fan nozzles is schematically shown in Figure 4. The baseline 22-lobe mixer is defined by reflecting the half lobe surface about the lobe center-plane that passes through the engine centerline. The full lobe pattern is then revolved around the engine centerline to create the 22 common lobe pattern (see Figure 5). The baseline mixer with unique lobe has the same common lobe shape as the baseline 22 lobe mixer. However, two of the common lobes are replaced with one unique lobe as shown in Figure 6. The confluent mixer (see Figure 4), which is a fan and core flow side surface of revolution, with approximately the same core area of the baseline mixers and with axial length consistent with the baseline mixers is also tested for comparison purpose. The fan nozzles consist of both internal and external surfaces of revolution. Figure 7 shows the general model hardware setup with lobed mixer nozzles on the upper half and the confluent mixer on the lower half with the standard or baseline fan nozzle. Figure 8 shows the long and short fan nozzles mounted to the lobed mixer nozzles on the upper half and the confluent mixer on the lower half on each case. Figure 9 shows views of the unique lobe mixer and the confluent mixer integrated with the internal pylon systems. The integration of internal pylon with the unique lobe mixer without and with the baseline fan are shown in Figures 10 and 11, respectively.

In addition to the above described configurations, a treated long fan nozzle (see Figure 12) is also designed and tested with various mixers to evaluate noise suppression due to treatment. A 0.4"-deep bulk material treatment is used for this purpose. The inner surface of the nozzle remains the same as the long untreated fan nozzle of Figure 8 (a). However, the outer surface is modified to accommodate 0.4"-deep treatment. Two different bulk materials, Feltmetal, made out of a high temperature steel and astroquartz, with a perforated facesheet were used as the treatments. An insert with six components is fabricated to hold the treatment on fan nozzle surface. The feltmetal treatment is shaped into six pieces to fit the insert compartment. To obtain a proper assessment of noise suppression due to treatment a similar insert with hardwall surface is also fabricated and tested. These components are shown in Figure 13. A nozzle shell is fabricated to hold the treatment insert or the hardwall insert as required. The nozzle shell and the nozzle shell with the treatment insert are shown in Figure 14.

All the different mixer configurations and fan nozzle lengths employed the same plug nozzle. A 5.09" diameter conic nozzle is also tested at the mass averaged mixed flow conditions corresponding to the various engine cycles for the mixer configurations.

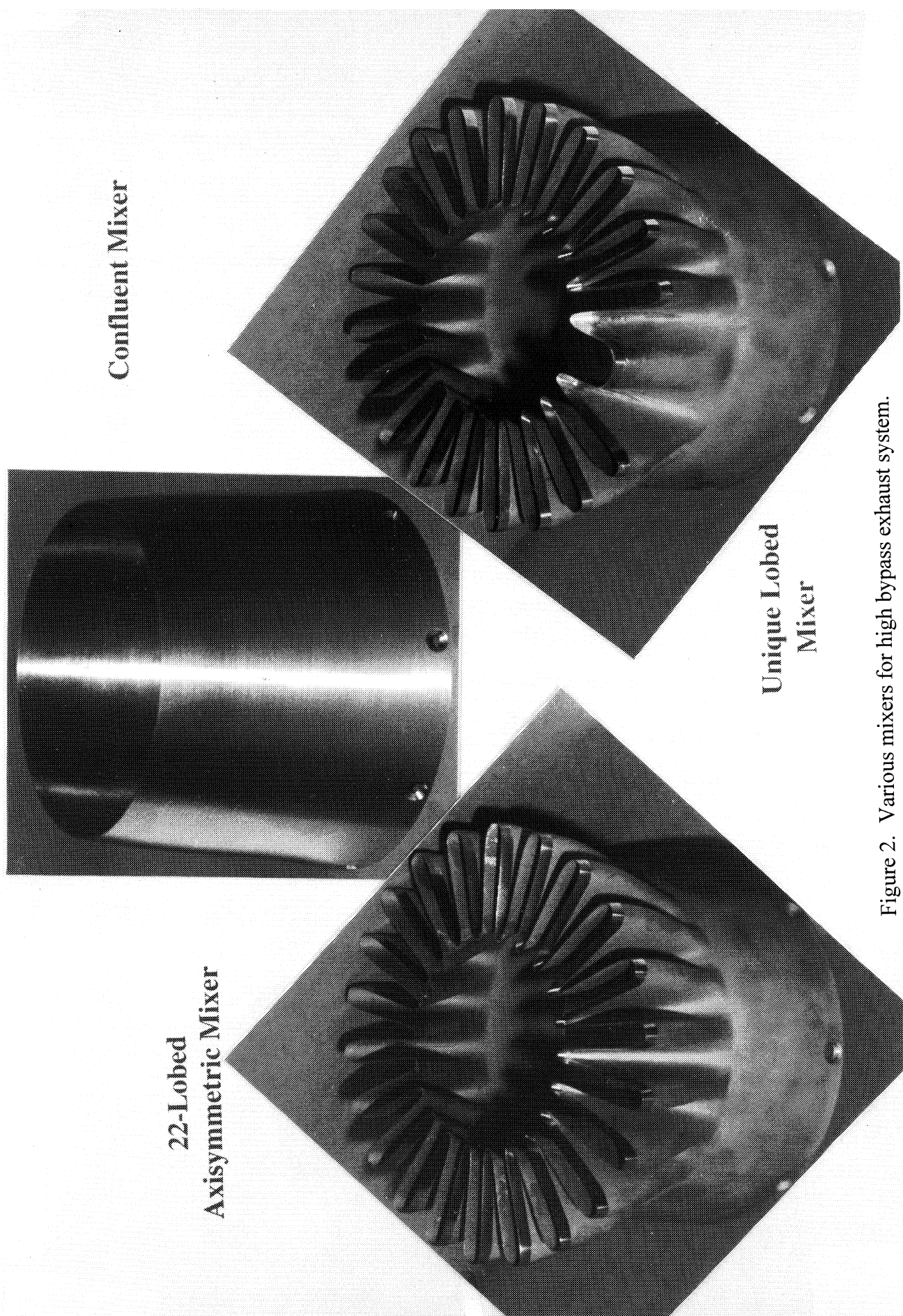


Figure 2. Various mixers for high bypass exhaust system.

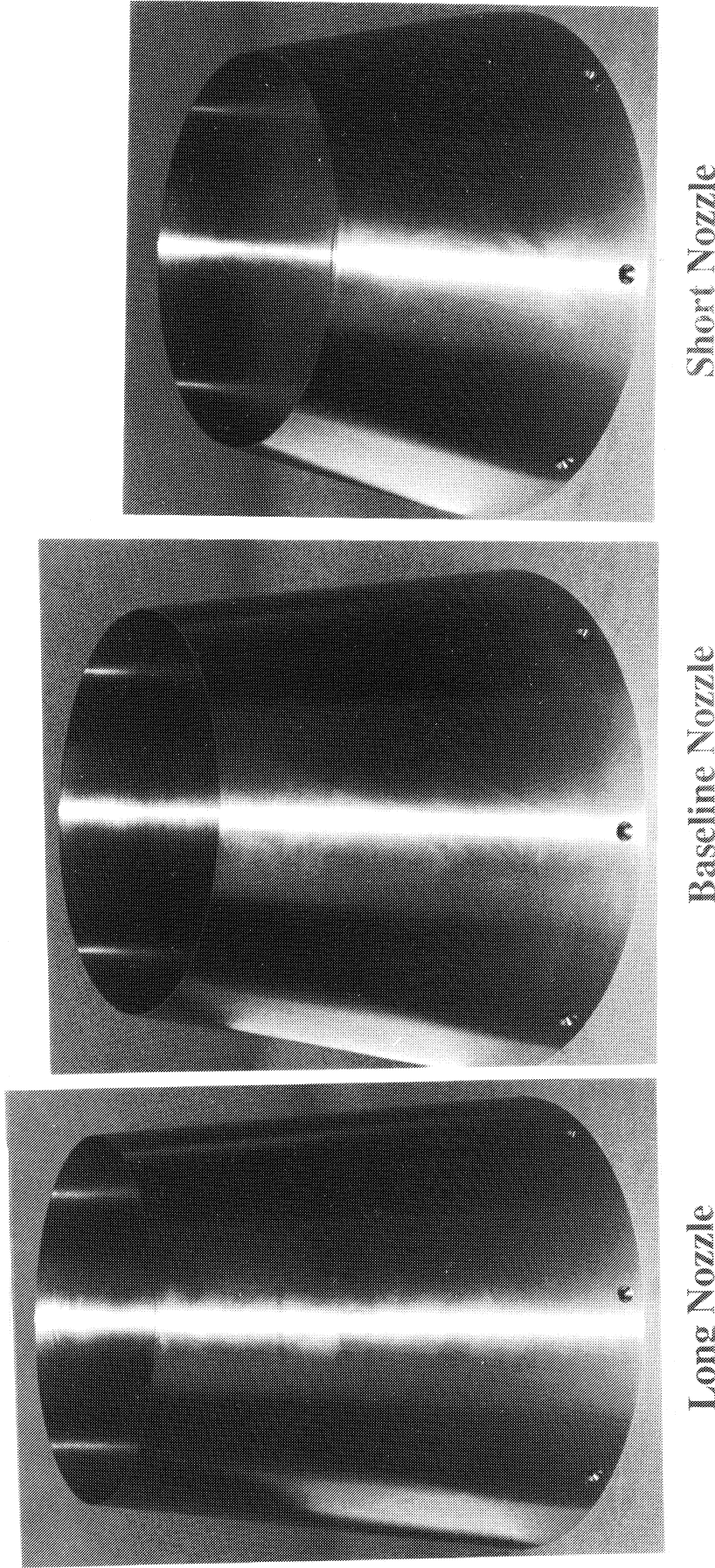


Figure 3. Fan stream nozzles of different lengths for high bypass exhaust system.

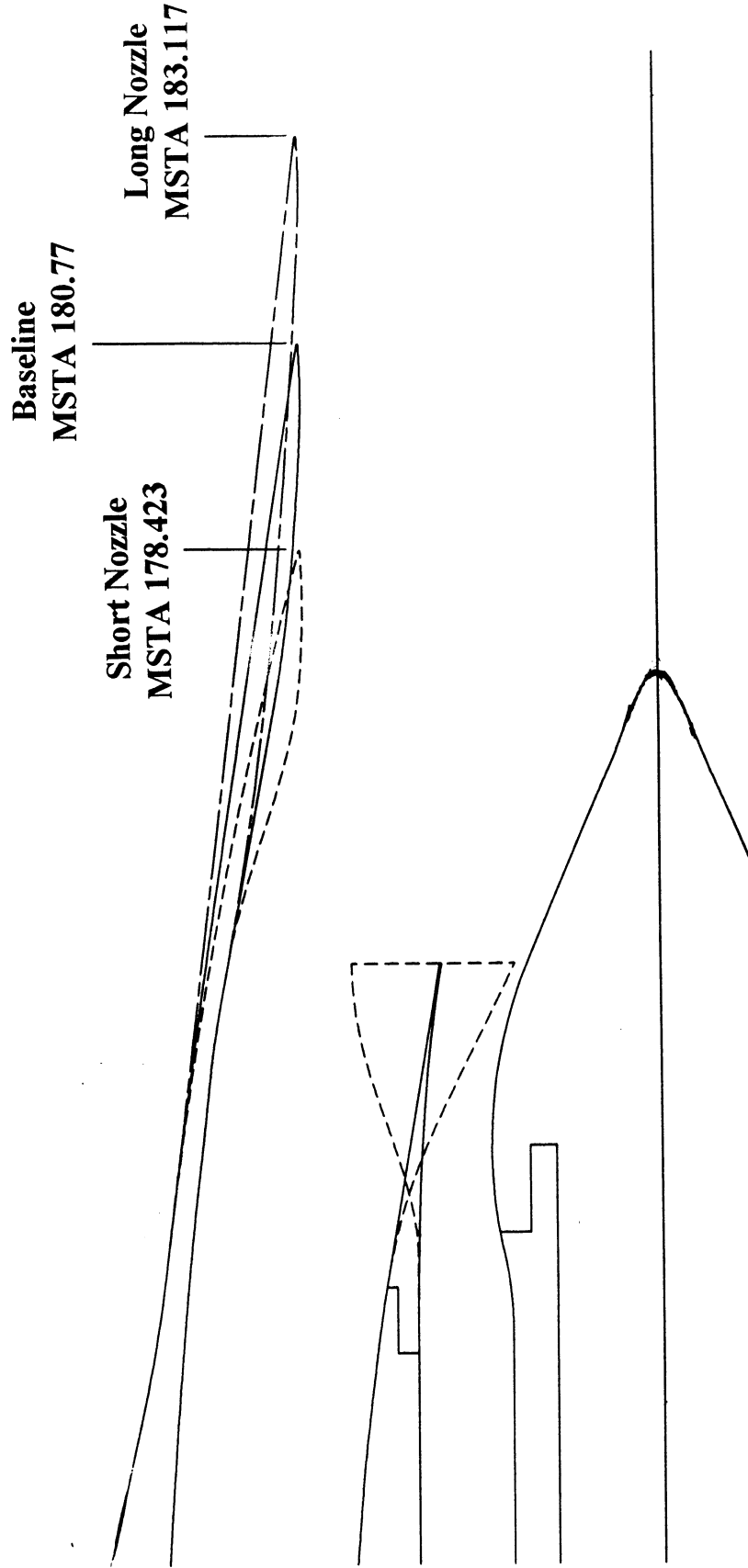


Figure 4. Fan stream nozzles of different lengths mounted with the core stream mixer.

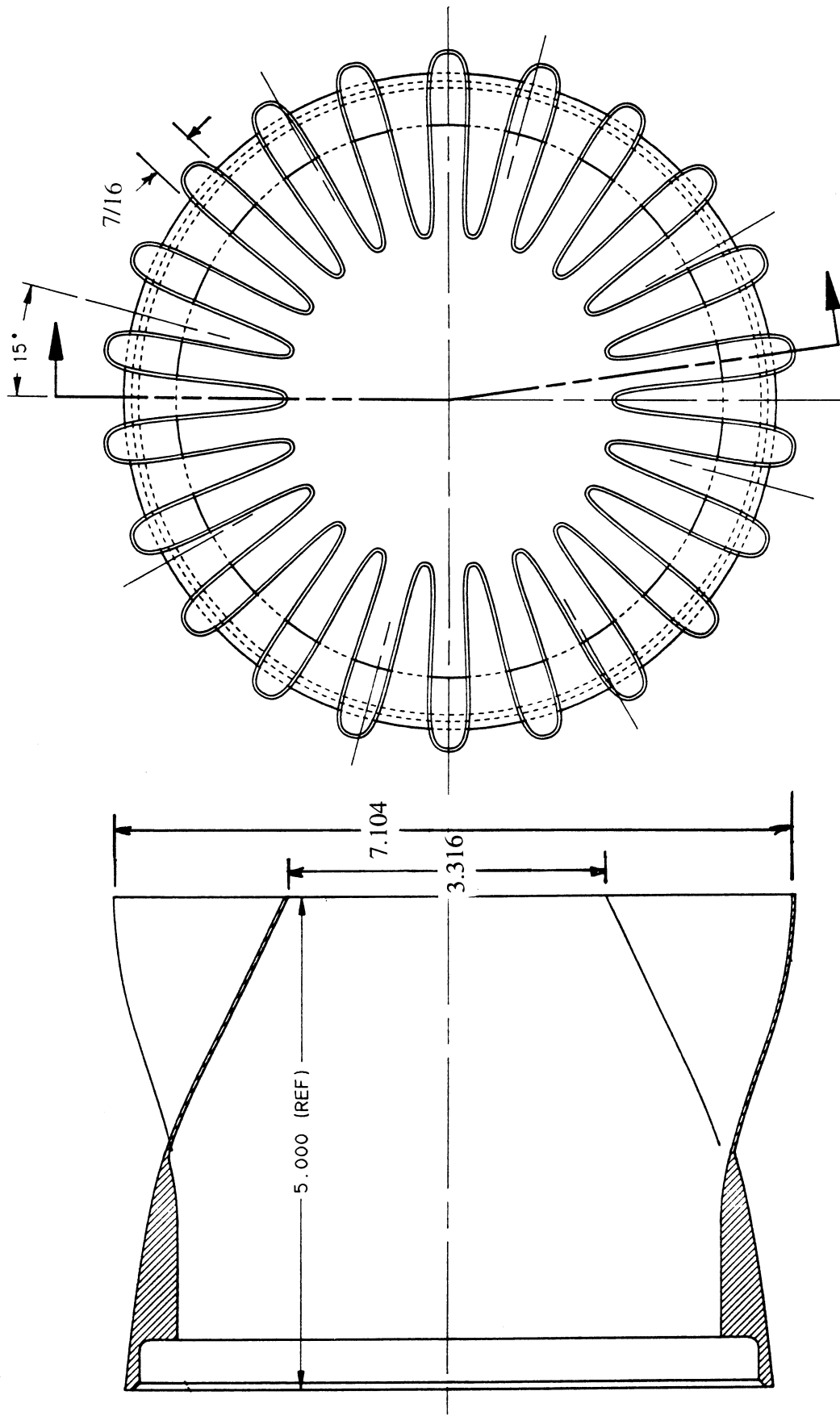


Figure 5. Side and front views of the 22 lobed axisymmetric mixer (all dimensions are in inches).

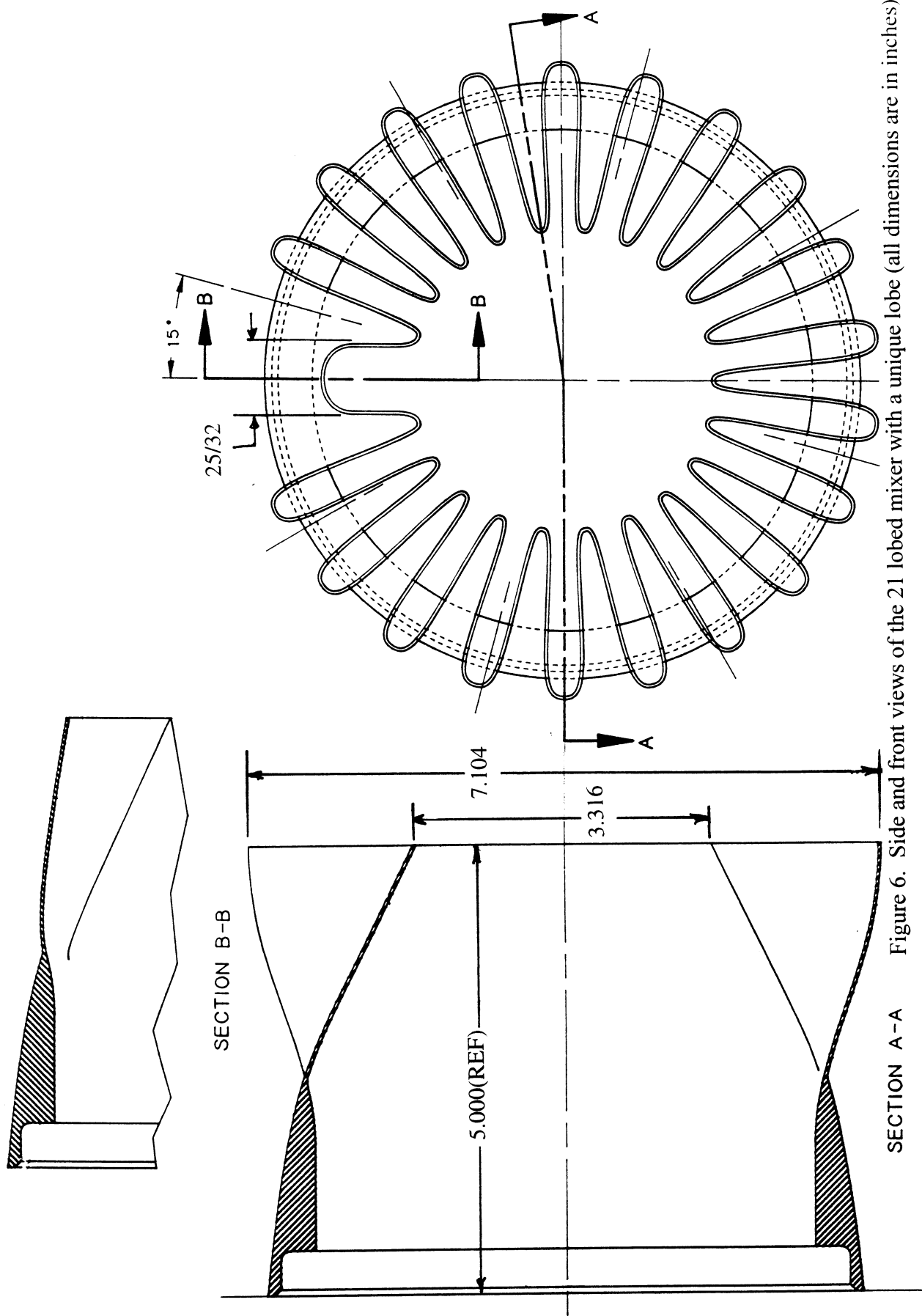


Figure 6. Side and front views of the 21 lobed mixer with a unique lobe (all dimensions are in inches).

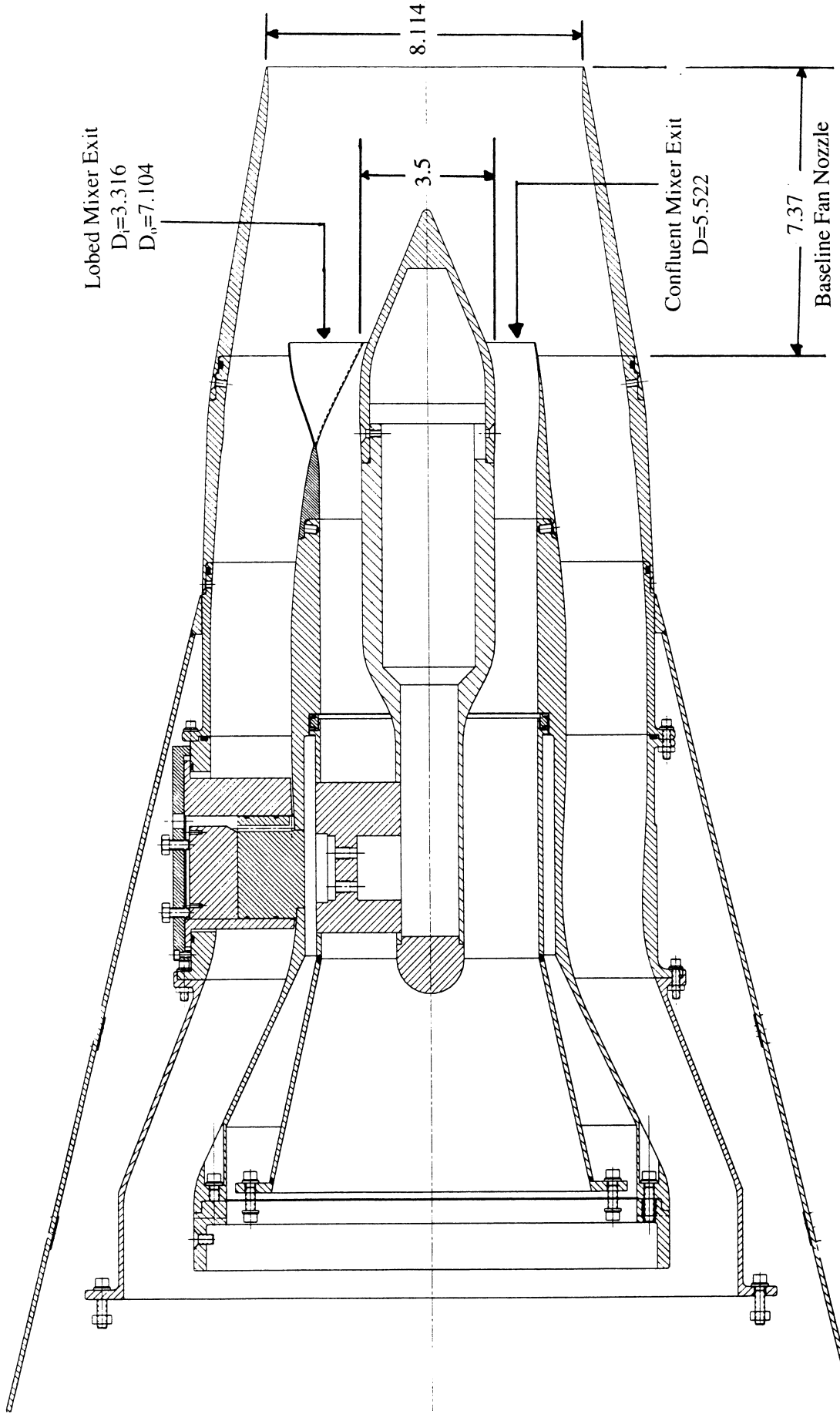
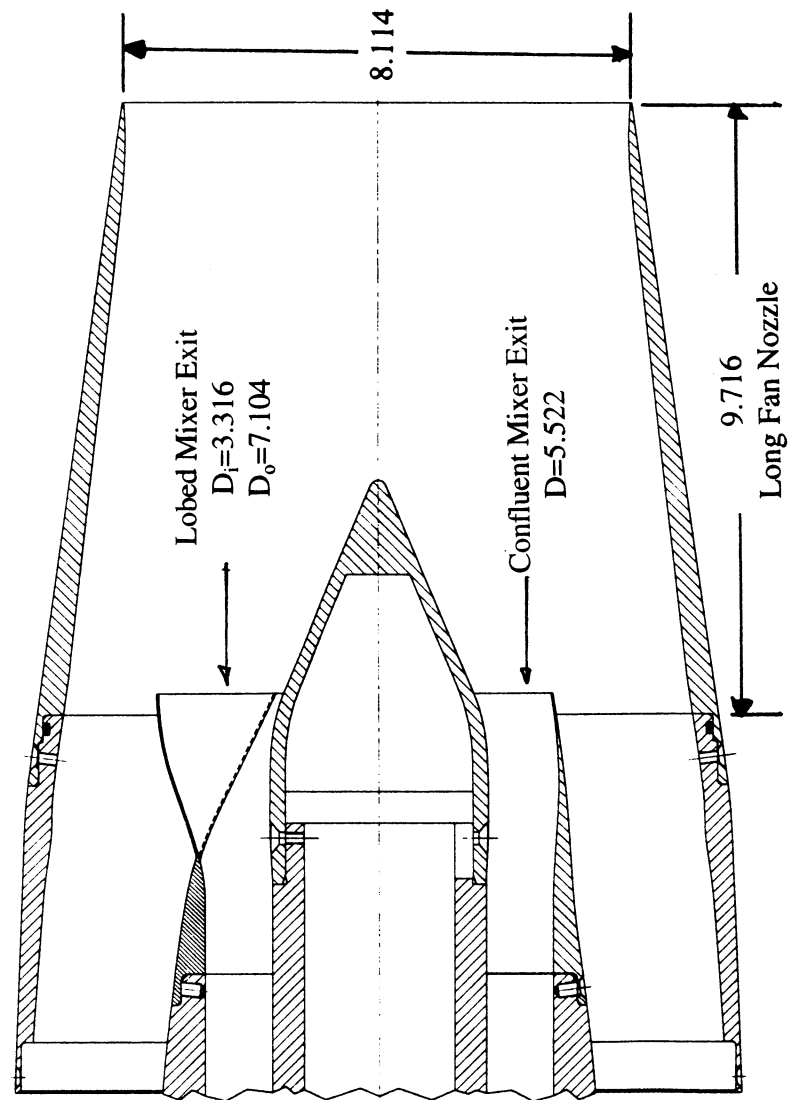


Figure 7. General mixer nozzle hardware assembly (all dimensions are in inches).

(a) Long Fan Nozzle Assembly



(b) Short Fan Nozzle Assembly

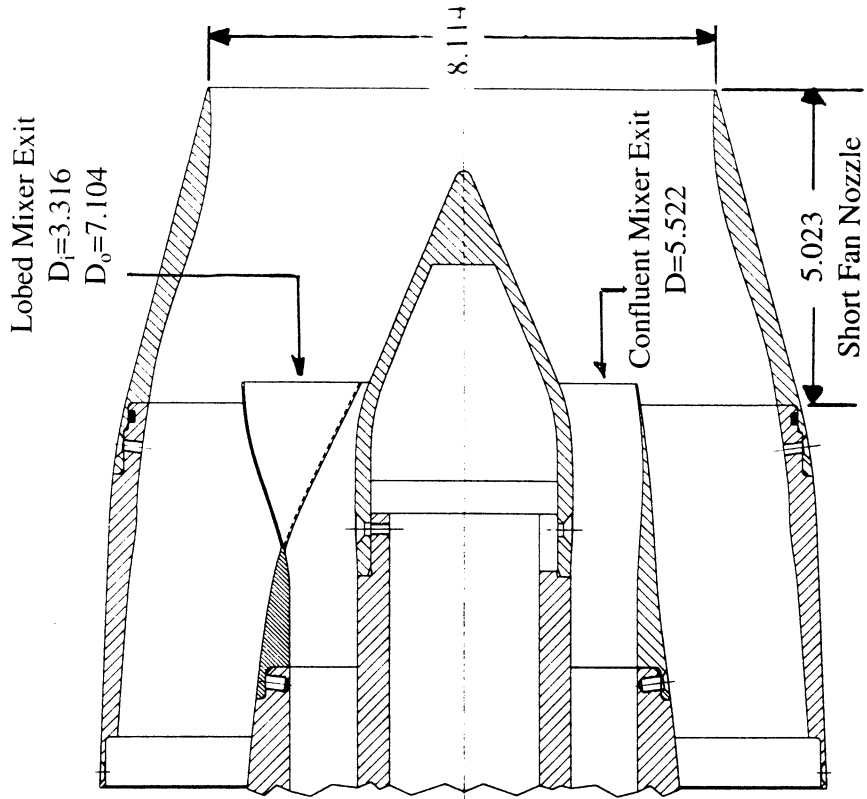


Figure 8. Side view of the long and the short fan nozzle assemblies (all dimensions are in inches).

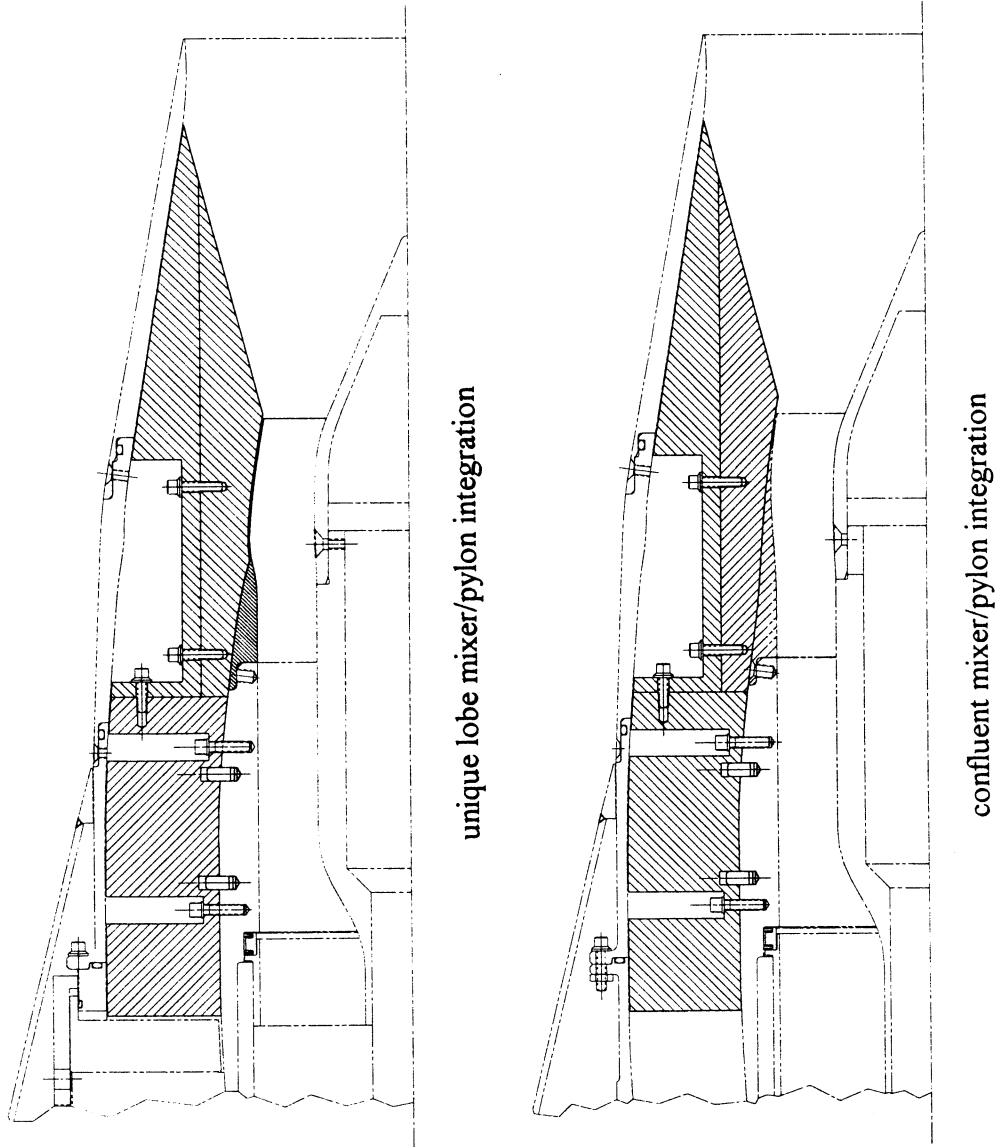


Figure 9. Side views of unique lobed mixer and the confluent mixer with pylon integration for baseline fan.

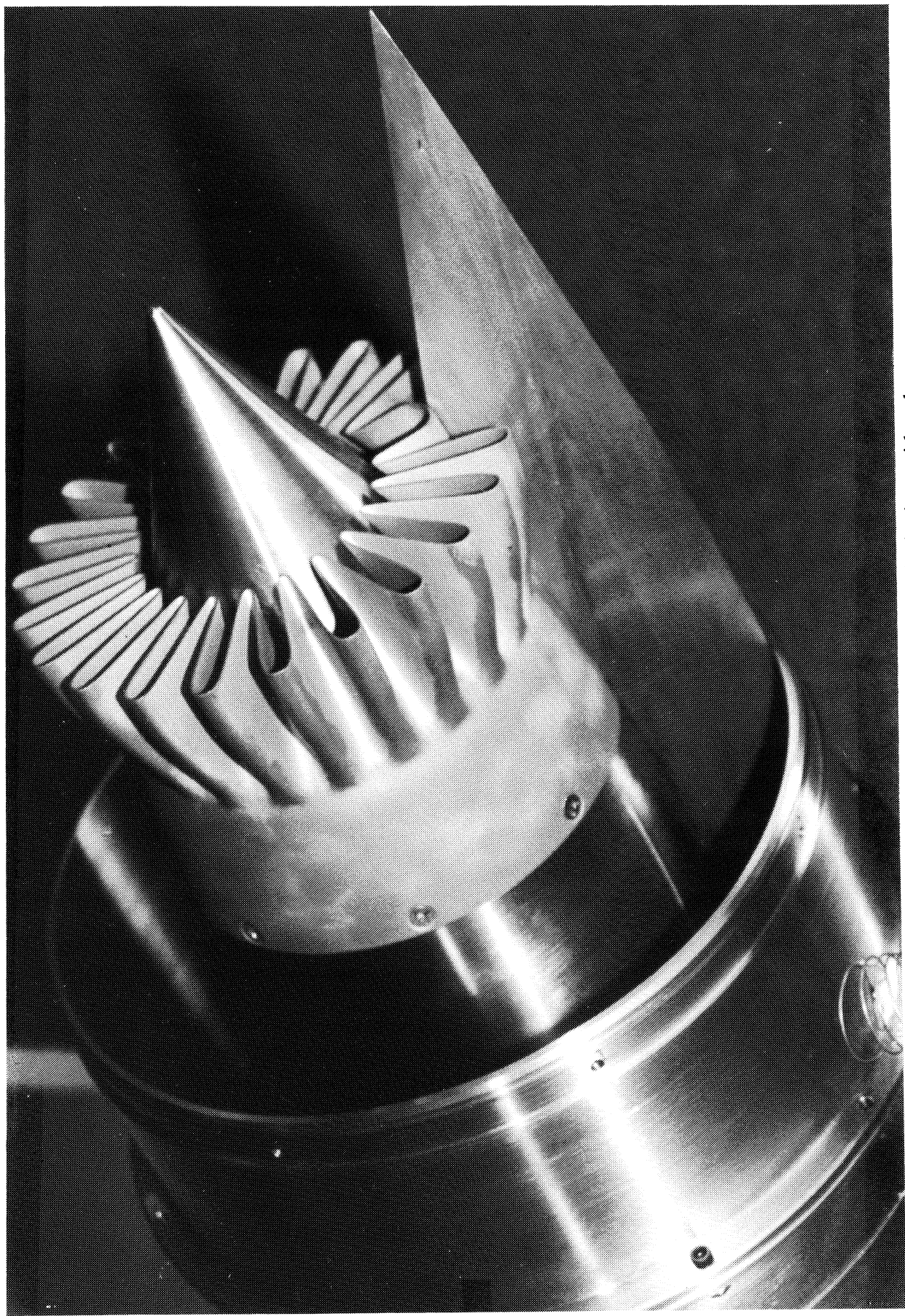


Figure 10. View of unique lobed mixer with pylon.

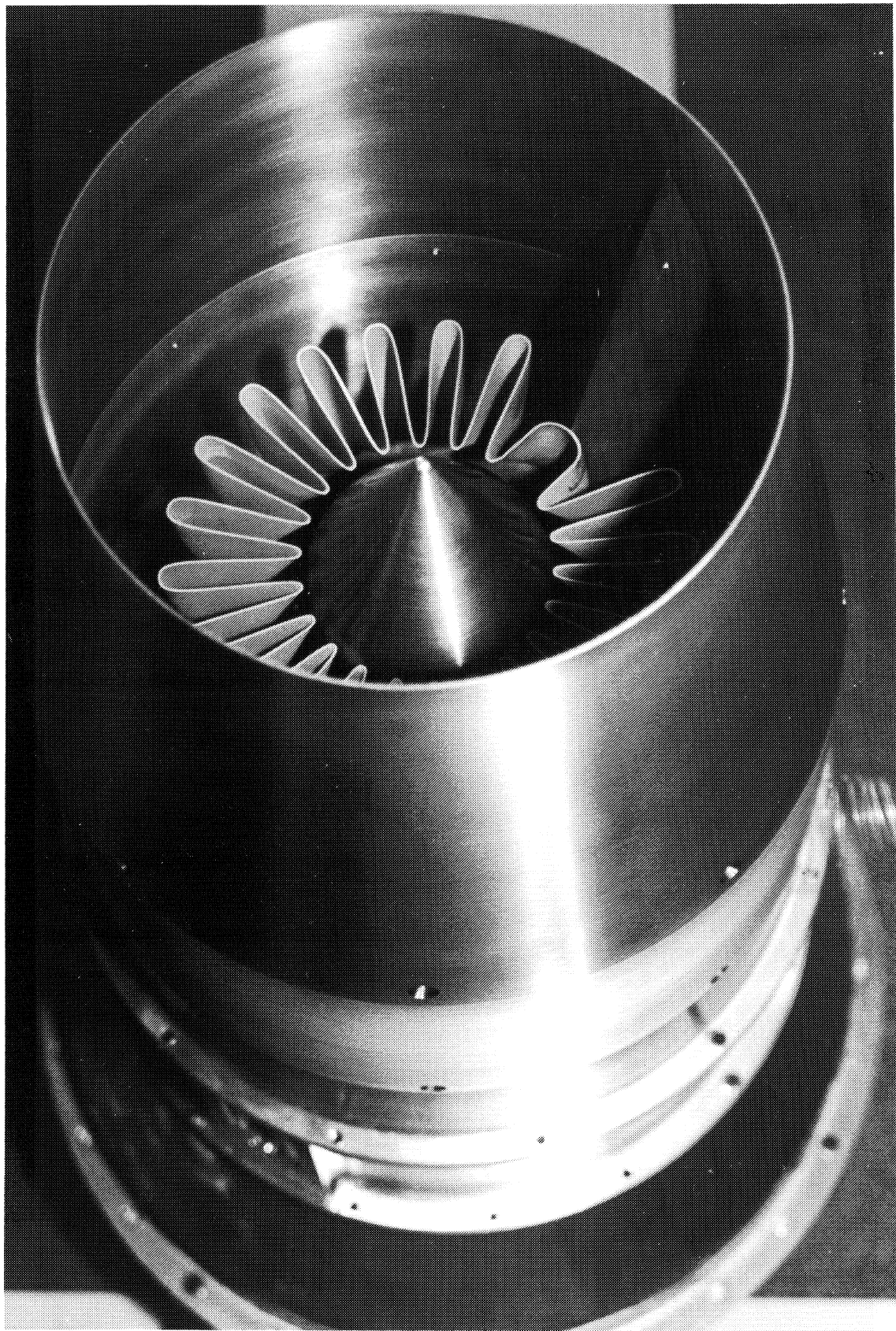


Figure 11. View of unique lobed mixer with pylon integration for baseline fan.

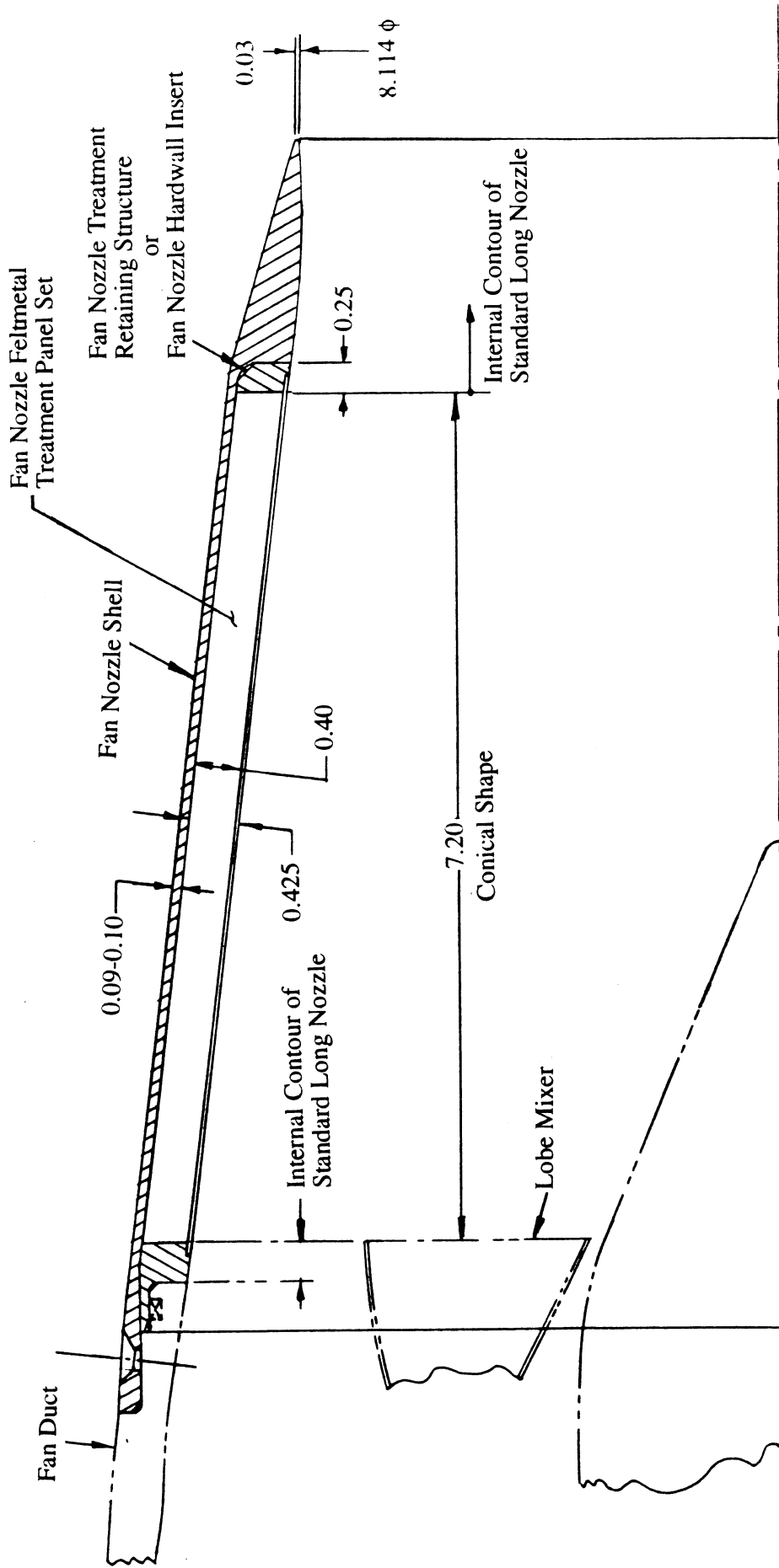
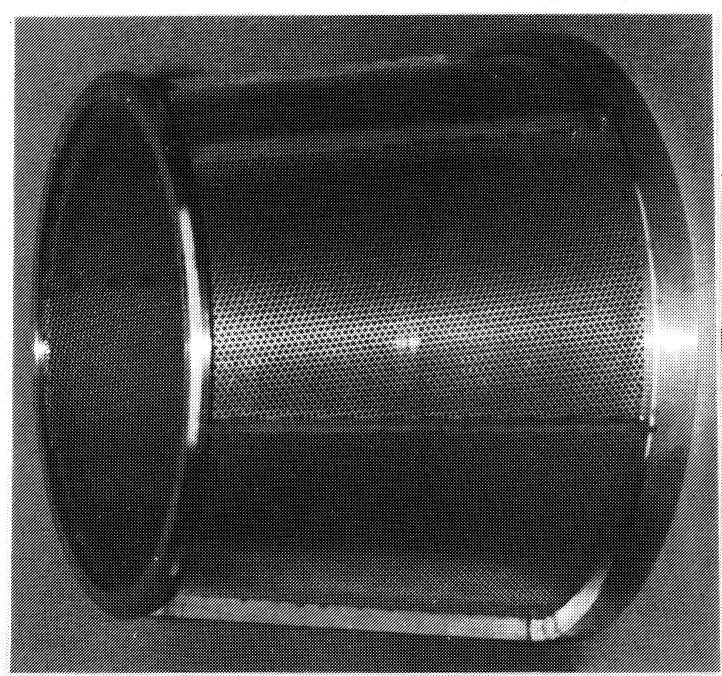
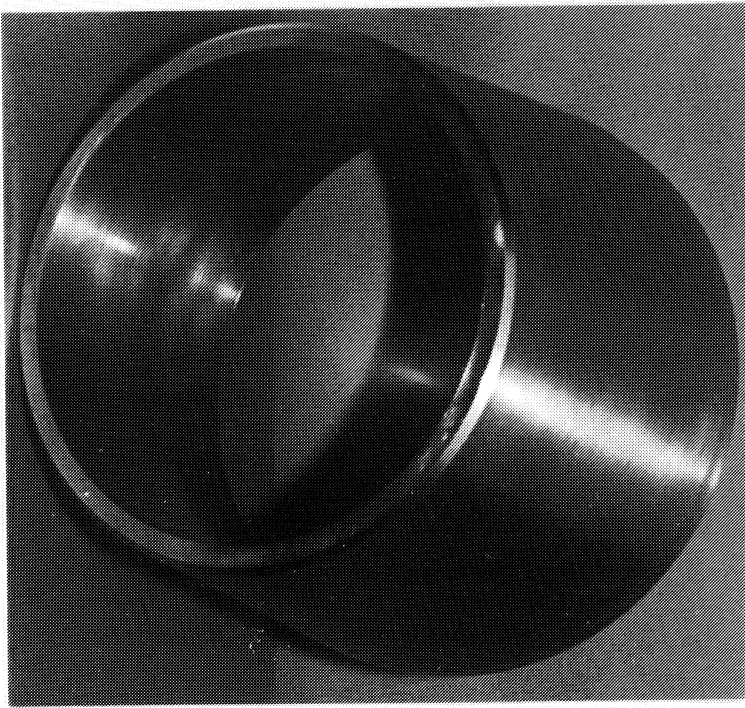


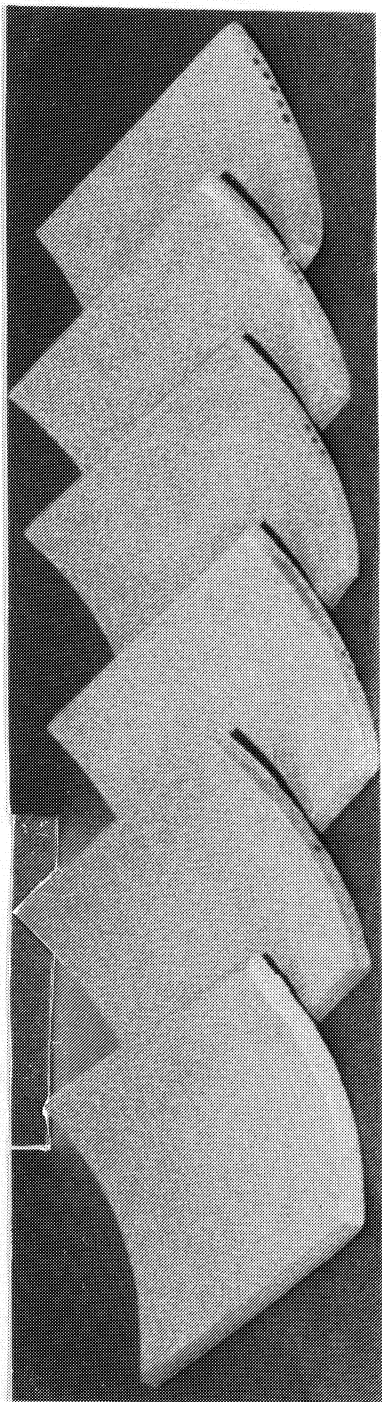
Figure 12. Treated and hardwalled fan nozzle components (all dimensions are in inches).



Acoustic Treatment  
Structure



Hardwall Insert



Feltmetal Insert  
(Bulk Absorber)

Figure 13. Components for fan nozzle treatment.

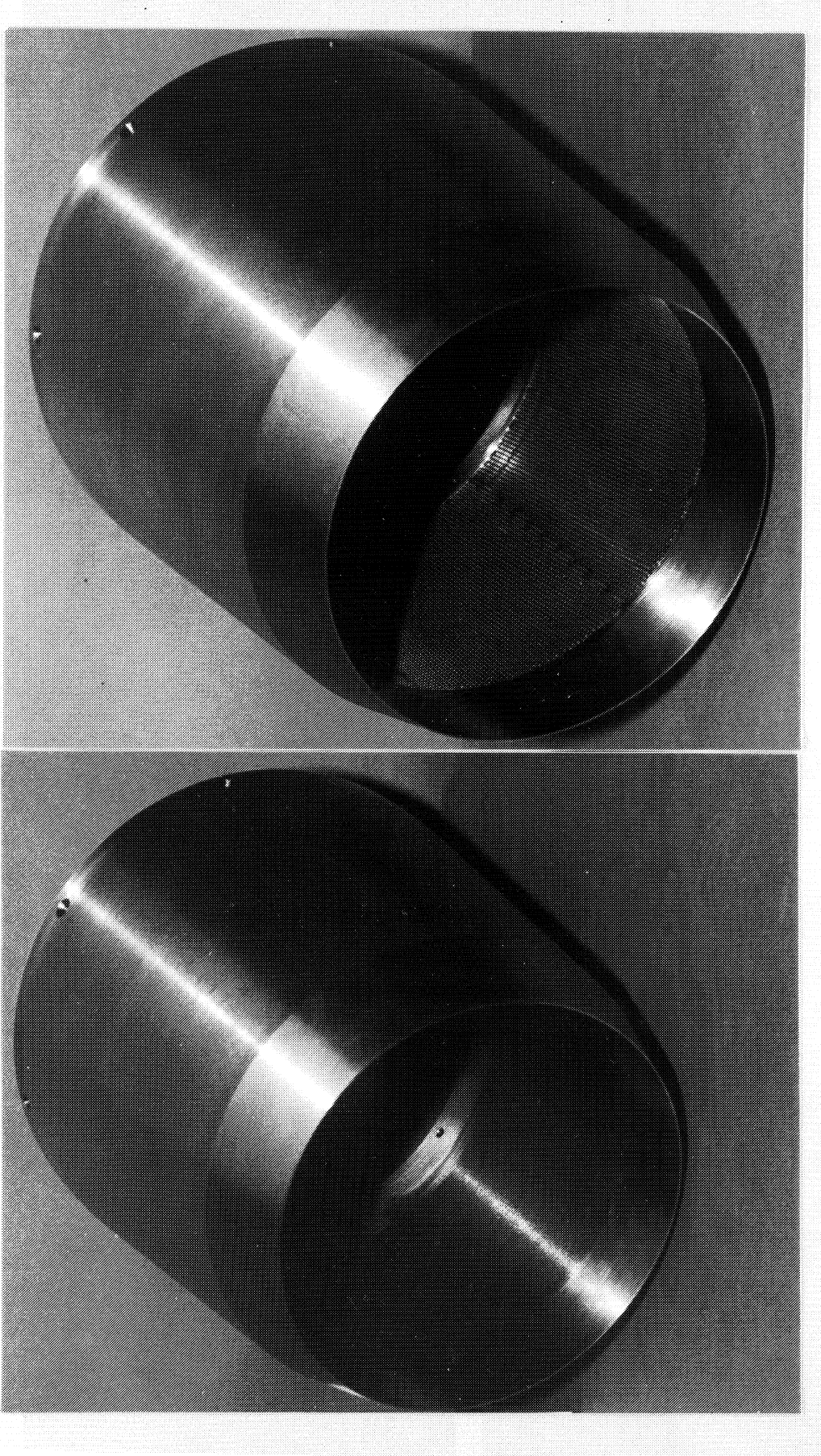


Figure 14. Long fan nozzle with acoustic treatment

Several 12-lobed mixers and a confluent mixer were tested earlier under Task A of this program (see Figure 15). The 12-lobed scalloped and staggered with quarter periodic mixer (F9B) and the confluent mixer (V1) were also tested under the current task to evaluate the noise impact due to mixer geometry.

Based on the various mixers and fan nozzles, described above, a number of configurations for high bypass exhaust system (see Table 1) are assembled and tested in the anechoic freejet facility. While the acoustic tests were conducted for all these configurations, LDA tests were conducted for a few selected configurations at a limited number of aerothermodynamic conditions.



Table 1. Model Scale High Bypass Exhaust System Configurations for Cell 41 Test, Full Scale Area = 3078 in<sup>2</sup>.

Configuration Code	Core Nozzle/Mixer	Fan Nozzle	Internal Pylon	Treatment	Core Area at Mixer Exit, in <sup>2</sup>	Fan Area at Mixer Exit, in <sup>2</sup>	Model Scale Exit Area, in <sup>2</sup>
1000	Conic	-	-	-	20.5	-	20.5
2100	Confluent	Standard	No	-	16.688	53.619	51.7
2110	Confluent	Standard	Yes	-	16.688	50.542	51.7
2200	Confluent	Short	No	-	16.688	53.619	51.7
3100	22 Lobed	Standard	No	-	14.719	53.176	51.7
3200	22 Lobed	Short	No	-	14.719	53.176	51.7
3300	22 Lobed	Long	No	-	14.719	53.176	51.7
3401	22 Lobed	Long	No	Hardwall	14.719	53.176	51.7
3402	22 Lobed	Long	No	Feltmetal	14.719	53.176	51.7
3403	22 Lobed	Long	No	Astroquartz	14.719	53.176	51.7
4110	Unique Lobed	Standard	Yes	-	14.188	50.794	51.7
4411	Unique Lobed	Long	Yes	Hardwall	14.188	50.794	51.7
4412	Unique Lobed	Long	Yes	Feltmetal	14.188	50.794	51.7
V1	Confluent (Task A)	Standard	No	-	10.9	49.6	45.7
F9B	12 Lobed (Task A)	Standard	No	-	10.9	49.6	45.7

Note : Configuration Code consists of 4 numbers (ABCD). Each number is defined as follows, except for V1, the :confluent mixer, and F9B (the 12-lobed scalloped and staggered with quarter periodic mixer), tested under Task A:

First number A stands for the type of core nozzle/mixer :

- A=1- Conic,
- A=2 - Confluent,
- A=3 - 22 Lobed,
- A=4 - Unique Lobed

Third number C stands for with or without internal pylon:

- C=0 - No Pylon,
- C=1 - With Pylon

Second number B stands for the type of fan nozzle:

- B=0 - No Fan Nozzle,
- B=1 - Baseline Fan,
- B=2 - Short Fan,
- B=3 - Long Fan,
- B=4 - Treated Long Fan

Fourth number D stands for type of fan treatment:

- D=0 - No Treatment,
- D=1 - Hardwall,
- D=2 - Feltmetal,
- D=3 - Astroquartz



## 4.0 TEST PROCEDURE AND DATA ACQUISITION

All of the acoustic and LDA tests for the model scale nozzles are conducted in the General Electric Anechoic Free-Jet Facility (Cell 41). A photograph of a model scale exhaust nozzle, mounted in the anechoic chamber is shown in Figure 16. The traversing microphone tower and the fiber flow probe of the LDA system mounted on a three dimensional actuator table system are shown in this figure. During the acoustic measurement the LDA system is removed from the anechoic chamber and the actuator system is lowered down to avoid any possible acoustic interference

**4.1 Acoustic Tests :** Cell 41 is supported by well-calibrated acoustic and aerodynamic data acquisition systems. Acoustic data measured by both the microphone arrays is analyzed by an on-line system, which computes 1/3-octave band data for model scale at a 40' arc corrected to standard day conditions (i.e., 59°F and 70 % humidity) and narrowband data as measured. In addition, this data can be recorded if required on magnetic tapes for post processing. All static and total pressures including model surface pressures are measured using an aerodynamic data acquisition system consisting of multiport scanivalve contained pressure transducers, signal conditioner, and analog/digital converters. The online acoustic system is operated by a work-station computer. The data is transferred to other computer systems for further analysis. Concurrently, a front-end computer with touch-screen application is used for signal and facility control and for real time data monitoring. Temperature data (thermocouple signals) are fed directly to the front-end computer.

Both the flow streams, core and fan, were utilized for the current dual flow model exhaust system in the anechoic freejet facility (Cell 41). The 13-microphone tower array was used for farfield acoustic measurement and only online data was acquired for all the configurations. For axisymmetric configurations the farfield data is measured at one tower location of  $\phi = 34^\circ$ . For a few conditions the measurement is taken at several tower locations to examine the symmetry of the noise field. For non-axisymmetric configuration the data is acquired at two tower locations, namely  $\phi = 34^\circ$  for sideline and  $\phi = 90^\circ$  for community. Again, for limited conditions the data is measured at several tower locations. Online 1/3-octave data is further analyzed as per the flow chart of Figure 17 for scaling, flight transformation, and extrapolation to any sideline or arc location. The scale model data is scaled to an engine size of 3078 in<sup>2</sup> and extrapolated to a range of sideline distances from one to two thousand feet. Acoustic data extrapolated to a sideline distance of 1500 feet is presented in this report. The acoustic data is corrected to standard day conditions of ARP 77°F and 70 % humidity.

Mass flow rate through the individual streams  $m$  are calculated by using the following expression;

$$m = m_b \cdot P_t \cdot A / ((T_t)^{1/2})$$

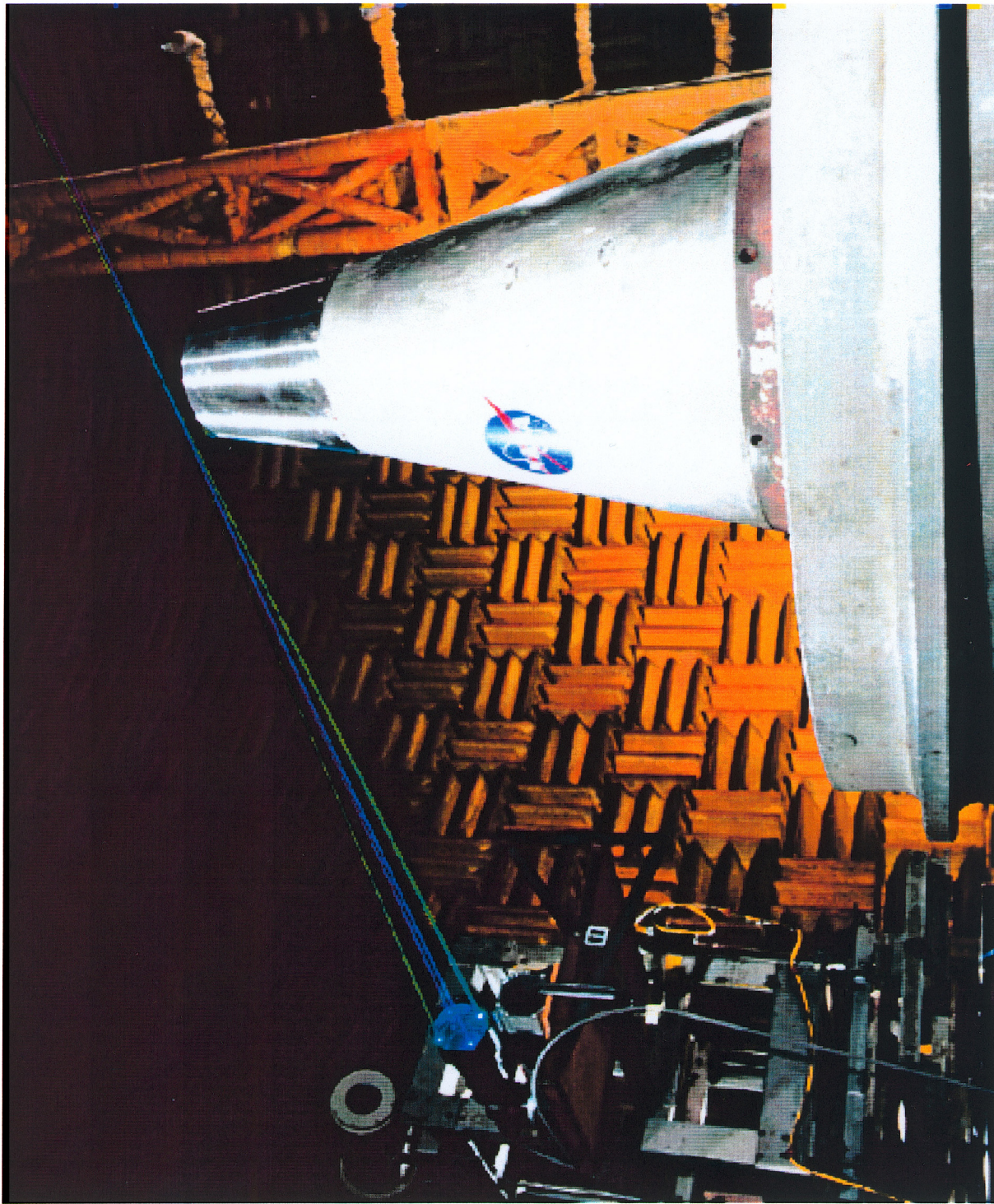


Figure 16. Laser Doppler Anemometer setup for scale model nozzle test in Cell 41.

## On-Line Data Acquisition System

## Data Processing System

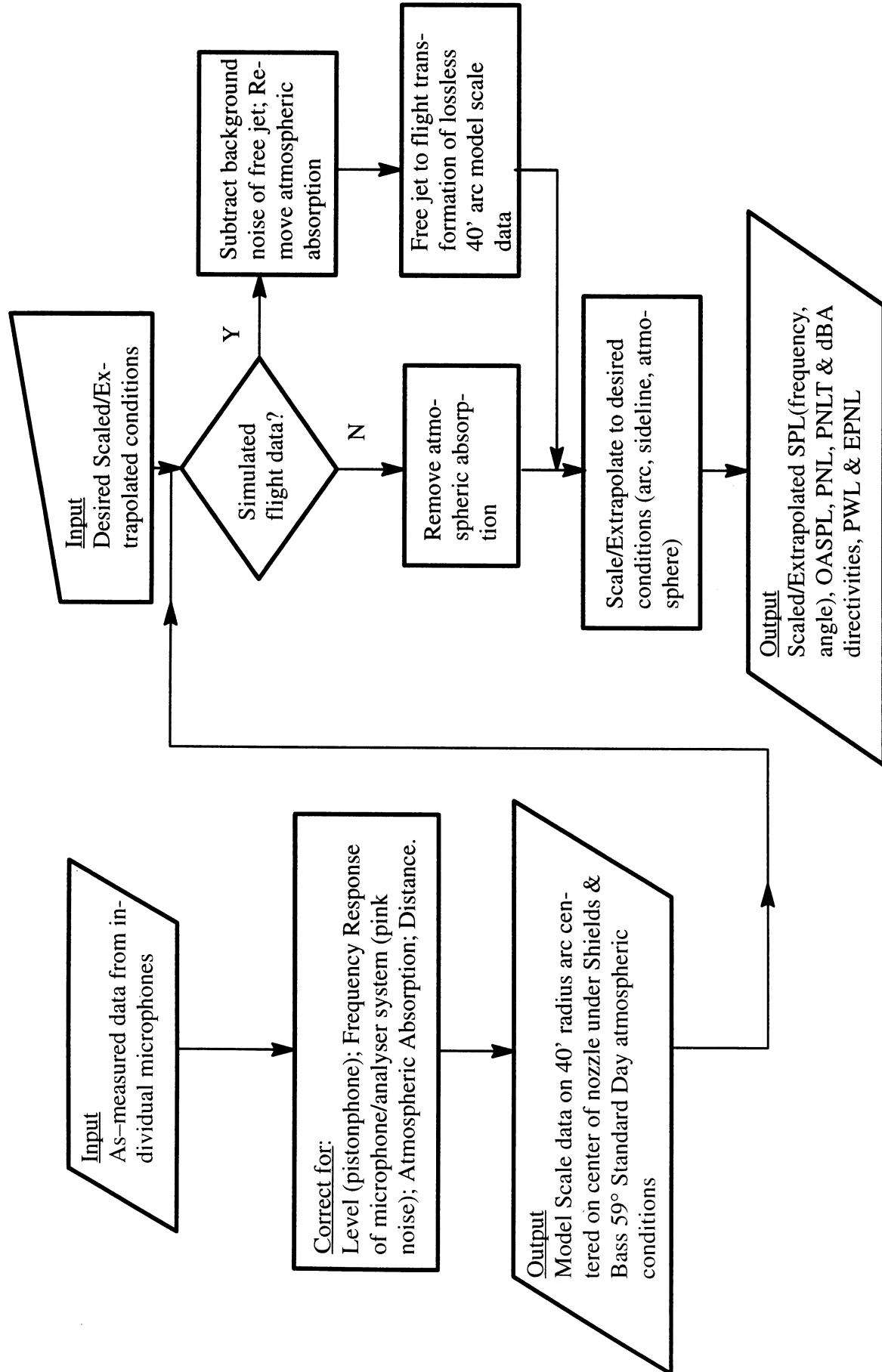


Figure 17. Cell 41 acoustic data acquisition and processing flow chart.

where;

$$m_b = [(2g\gamma/((\gamma-1)R)(1-(1/nprp)^{(\gamma-1)/\gamma})^{1/2}(1/nprp)^{1/\gamma}]$$

$P_t$  = Total pressure of the stream

$T_t$  = Total temperature of the stream

A = Cross sectional area of the stream at the pressure and temperature measurement location

g = Acceleration due to gravity

$\gamma$  = Specific heat ratio

R = Gas constant

nprp = Pressure ratio of the stream at the pressure measurement location

For the current test configurations the mass flow rates are calculated in the following three different ways;

1. Mass flow through charging station using scanivalve data:

$$nprp = [(Average \ total \ pressure)/(Average \ static \ pressure)]_{(in \ charging \ station)}$$

Area of core charging station=57 in<sup>2</sup>

Area of fan charging station=154.45 in<sup>2</sup>

2. Mass flow through charging station using differential pressure transducer in charging station:

$$nprp = [(Average \ total \ pressure)/$$

$$( Average \ total \ pressure-Average \ static \ pressure)]_{(in \ charging \ station)}$$

Area of core charging station=57 in<sup>2</sup>

Area of fan charging station=154.45 in<sup>2</sup>

3. Mass flow through charging station using model static pressure data:

$$nprp = [(Average \ total \ pressure)_{(in \ charging \ station)}] / (Average \ model \ static \ pressure)$$

Area of core at the static pressure location=15.268 in<sup>2</sup>

Area of fan at the static pressure location=60.242 in<sup>2</sup>(51.477 in<sup>2</sup> for F9B configuration)

The mass flow rates calculated by model static pressure data (Method 3) are utilized in the current data analysis. The acoustic data is normalized with respect to a constant reference thrust of 60,000 lbs.

**4.2 LDA Tests :** Laser Doppler Anemometer (LDA) system was employed for velocity measurements. The LDA system was a DANTEC four-beam, two-color Laser Fiber Optics system which measured two mutually perpendicular velocity components simultaneously. The optical head was rotated by 45 degree so that the measurement capability of maximum velocity increased by a factor of 1.4. The optical system had a 3.22 deg. beam angle, 112.67mm beam distance, 2000mm focal length, 36 fringes, and 9.136 micron fringe spacing for the green beam (514.5nm) and a 3.23 deg. beam angle, 112.92mm beam distance, and 8.646 micron fringe spacing for the blue beam (488.0nm).

The optics consisted of a 60 mm diameter fiber optic probe and 1.9 and 1.5 beam expanders.

The LDA system was operated in two modes. The first mode was a conventional method in which the LDA collected data from each measurement point providing histogram data. For the second mode, the LDA system was modified to obtain online data using two counter processors, an x-y plotter, three Fluke digital voltmeters and a Compaq computer. Employing these methods allowed the acquisition of large amounts of Laser data in a short time period thus keeping test time at a minimum.

Velocity information was obtained from the analog output of the two counter processor through D/A converters which provided voltages related to the Doppler frequency plus Bragg Cell frequency (40MHz). Laser position was read from a Laser positioning actuator simultaneously using a Compaq computer. Instantaneous axial velocities were plotted on an xy plotter against Laser position as data were acquired for the data quality check.

The data acquisition process for the LDA system is shown in Figure 18. All the velocity and position data were transferred to a workstation for further analysis. The seeding was provided from downstream of the burner using three 100psi vacuum pumps. The Laser seeding material was one micron aluminum powder.

Online data was taken at six axial locations, 0.5", 0.5D, 1.0D, 1.5D, 3.0D, and 5.0D, measured from the nozzle exit plane, D being the nozzle exit diameter. At each axial locations the LDA system was traversed along Y (N-S) and Z (E-W), as shown in Figure 19. Histogram data was acquired at five axial locations, 0.5", 0.5D, 1.0D, 1.5D, and 3.0D. At each location the LDA was traversed along Y (N-S) direction and positioned at 11 equispaced points, measured from the nozzle center, at 9 equispaced Z (E-W) locations. Thus, LDA data at 99 points on a grid were acquired at fixed axial locations, as shown in Figure 20. The grid spacing along Y and Z were 0.45" and 0.3", respectively, at axial locations of 0.5", 0.5D, and 1.0D. At axial locations of 1.5D and 3.0D these spacings are increased to 0.5" & 0.375" and 0.6" & 0.45", respectively.

Two dimensional four-beam, two-color, LDA measurements of axial mean velocity ( $u$ ), horizontal mean velocity ( $v$ ) which is perpendicular to axial velocity and parallel to horizontal centerline, and the axial and horizontal component of turbulence velocities ( $u'$ ,  $v'$ ) were made on different engine exhaust configurations.

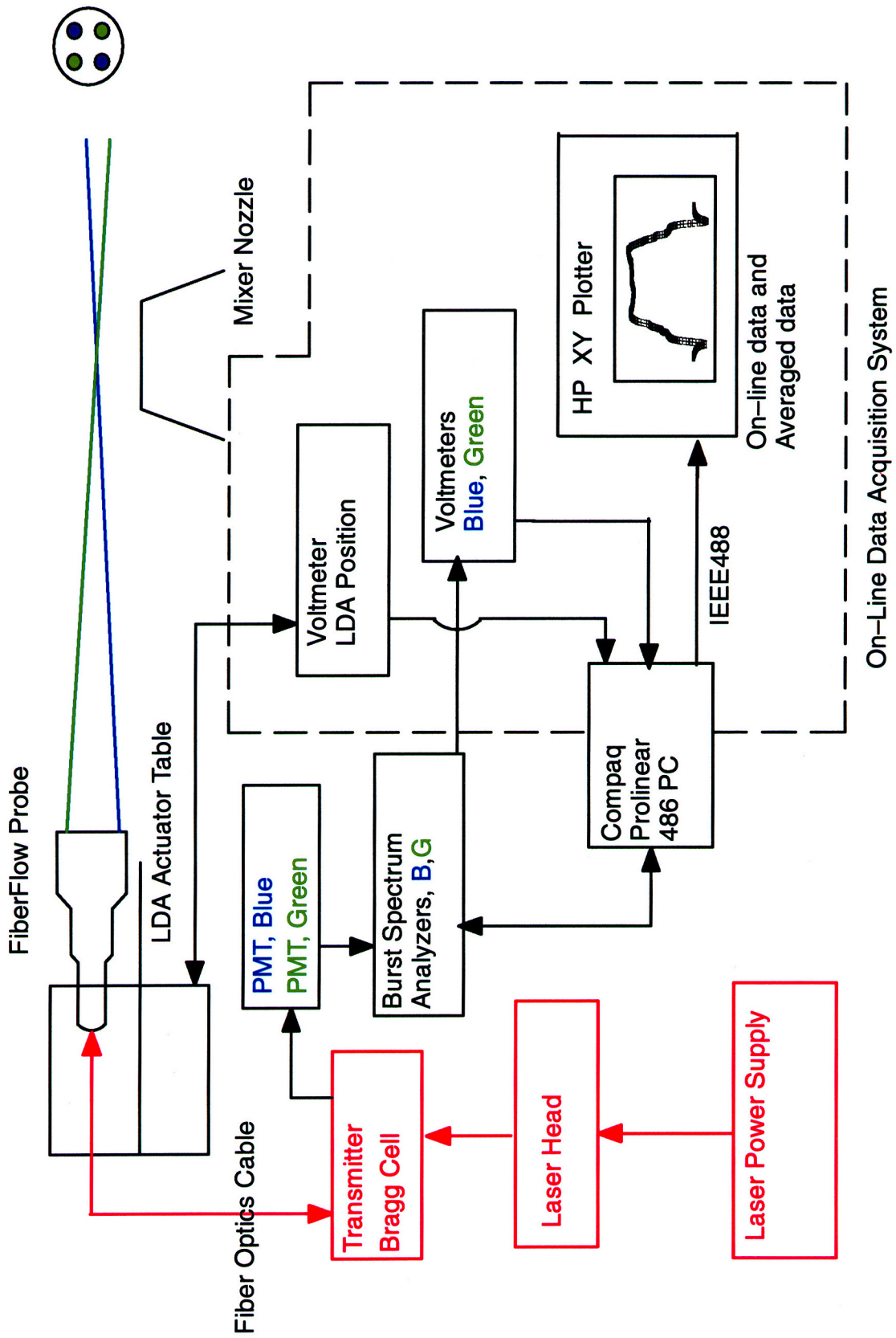


Figure 18. Data Acquisition System for the LDA

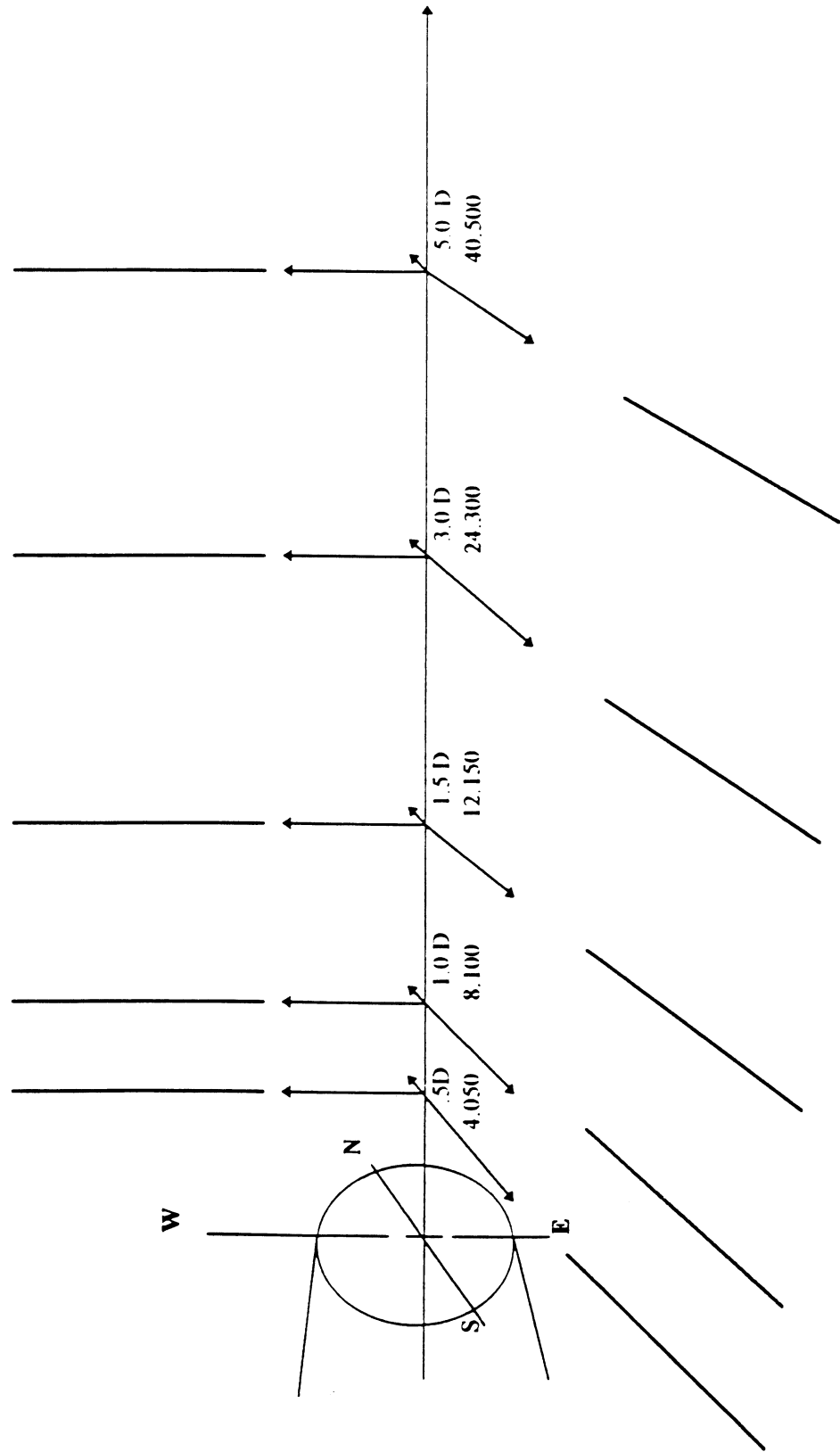


Figure 19. LDV traverse summary for plume survey.

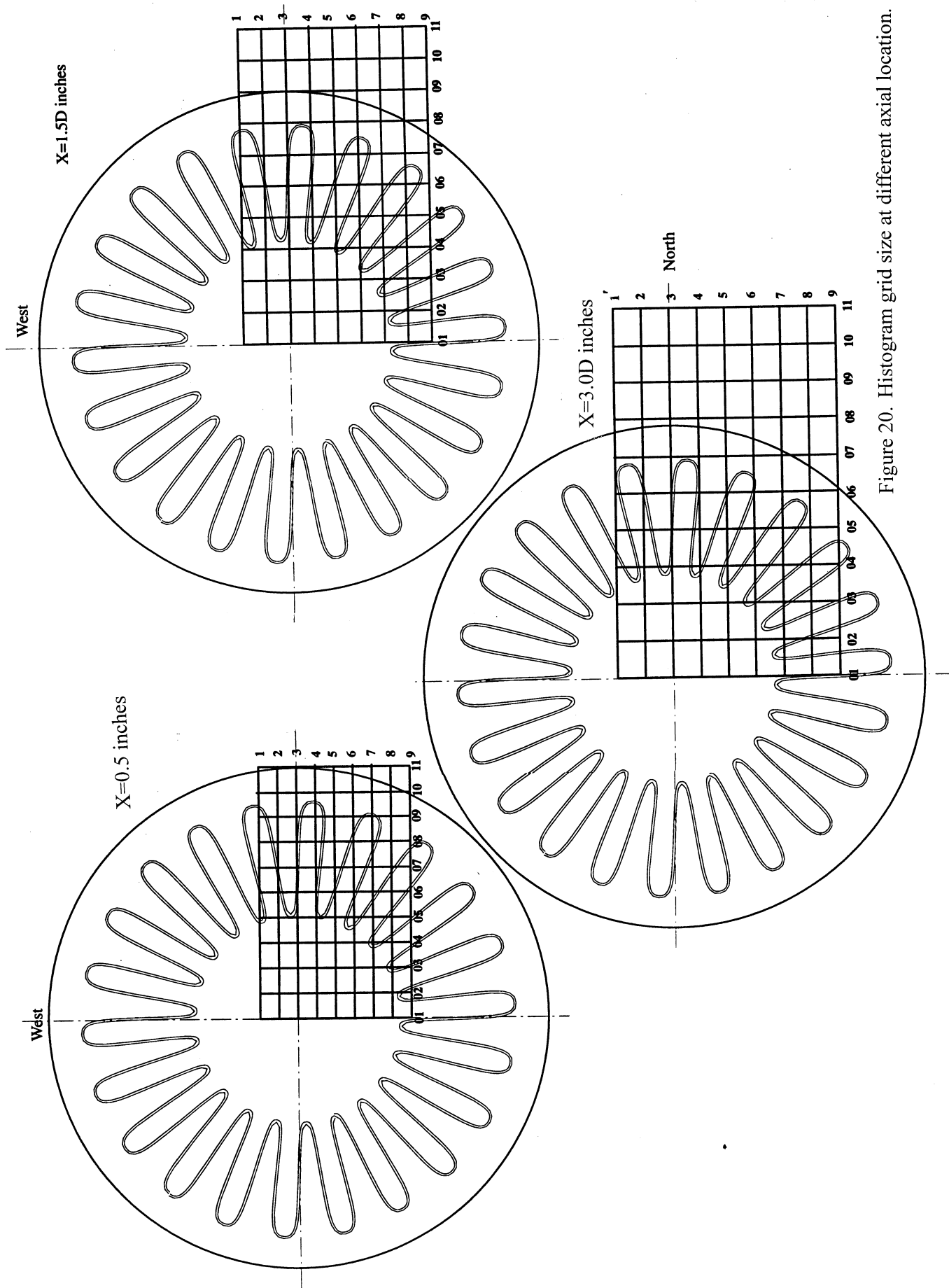


Figure 20. Histogram grid size at different axial location.

## 5.0 VARIOUS MIXED & SEPARATE FLOW ENGINE CYCLE CONDITIONS

Acoustic tests for the model scale exhaust configurations were conducted by following two typical high bypass ratio separate flow and mixed flow cycle lines applicable to the current design. In addition, some configurations are also tested at the two cycle lines used for E<sup>3</sup> configurations, tested under LET TO #31A. The aerothermodynamic conditions for these four cycle lines are listed in Tables 2 and 3. Two additional points with higher pressure ratios are included in the existing E<sup>3</sup> mixed flow cycle. The aerothermodynamic conditions for conic nozzle tests are designed to result in exit conditions matching the mixed flow exit conditions of the mixed and separate flow cycle lines of Tables 2 and 3 for high bypass exhaust system. The conditions for separate flow cycle are very close to those of mixed flow cycle. Thus, only one set of these parameters are selected for conic nozzle tests and are listed in Table 4. Table 4 also contains a few aerothermodynamic conditions at which the same conic nozzle was tested under LET TO #31A for E<sup>3</sup> configurations. The nomenclature for various parameters included in tables 2 through 4 are defined as follows:

- P<sub>r,p</sub> = Primary or core stream nozzle pressure ratio  
T<sub>t,p</sub> = Primary or core stream nozzle total temperature in degree R  
W<sub>p</sub> = Mass Flow Rate for primary or core stream in lbs/sec  
V<sub>j,p</sub> = Ideal Nozzle Exhaust Velocity for primary (core) stream in ft/sec  
P<sub>r,s</sub> = Secondary or fan stream nozzle pressure ratio  
T<sub>t,s</sub> = Secondary or fan stream nozzle total temperature in degree R  
W<sub>s</sub> = Mass Flow Rate for secondary stream in lbs/sec  
V<sub>j,s</sub> = Ideal Nozzle Exhaust Velocity for secondary (fan) stream in ft/sec  
V<sub>mix</sub> = (V<sub>j,p</sub> · W<sub>p</sub> + V<sub>j,s</sub> · W<sub>s</sub>) / (W<sub>p</sub> + W<sub>s</sub>) = Mass averaged mixed velocity in ft/sec  
V<sub>r</sub> = V<sub>j,s</sub> / V<sub>j,p</sub> = Velocity ratio  
W<sub>r</sub> = W<sub>s</sub> / W<sub>p</sub> = Mass flow ratio  
T<sub>sr</sub> = Static temperature ratio  
P<sub>amb</sub> = Ambient pressure in psi  
T<sub>amb</sub> = Ambient temperature in degree R  
P<sub>r</sub> = Nozzle pressure ratio for single stream nozzle  
T<sub>t</sub> = Total temperature for single stream nozzle in degree R  
W = Mass Flow Rate for single stream nozzle in lbs/sec  
V<sub>j</sub> = Ideal Exhaust Velocity or jet velocity for single stream nozzle in ft/sec

For the dual flow exhaust system the core and fan stream jet velocities are computed assuming ideal expansion of each stream to the atmosphere. The individual mass flow rates are computed using the core and fan areas of 16.7 in<sup>2</sup> and 50.5 in<sup>2</sup>, respectively, at the mixer exit plane. Thus, the mixed jet velocity, mass flow ratio, and velocity ratio are based on these assumptions. The actual mass flow rates are determined utilizing experimental pressure measurements in the flow system as described in section 4.

Table 2. Separate flow cycle conditions for High bypass model scale exhaust system, Core and Fan areas at mixer exit being  $16.7 \text{ in}^2$  and  $50.5 \text{ in}^2$ , respectively.

TEST POINT	$P_{r,p}$	$T_{t,p}$ $^{\circ}\text{R}$	$W_p$ lb/sec	$V_{j,p}$ ft/sec	$P_{r,s}$	$T_{t,s}$ $^{\circ}\text{R}$	$W_s$ lb/sec	$V_{j,s}$ ft/sec	$V_{\text{mix}}$ ft/sec	$V_r$	$W_r$	$T_{sr}$	$P_{\text{amb}}$ psi	$T_{\text{amb}}$ $^{\circ}\text{R}$
Cycle 1 - High Bypass Separate Flow Cycle														
11	1.077	1126.	2.17	533.	1.203	535.	15.46	575.	570.	1.08	7.11	0.46	14.4	520.0
12	1.116	1169.	2.61	659.	1.278	535.	18.04	660.	660.	1.00	6.90	0.44	14.4	520.0
13	1.154	1204.	2.96	762.	1.342	535.	19.96	720.	725.	0.94	6.74	0.42	14.4	520.0
14	1.219	1248.	3.46	909.	1.442	640.	20.68	874.	879.	0.96	5.98	0.49	14.4	520.0
15	1.272	1281.	3.80	1012.	1.513	640.	22.22	926.	939.	0.92	5.85	0.47	14.4	520.0
16	1.337	1318.	4.15	1124.	1.589	640.	23.75	976.	998.	0.87	5.72	0.46	14.4	520.0
17	1.416	1356.	4.53	1243.	1.666	640.	25.19	1022.	1055.	0.82	5.56	0.45	14.4	520.0
18	1.506	1395.	4.91	1363.	1.727	640.	26.27	1054.	1103.	0.77	5.35	0.44	14.4	520.0
19	1.579	1431.	5.17	1454.	1.773	640.	27.04	1077.	1138.	0.74	5.23	0.43	14.4	520.0
20	1.679	1468.	5.50	1562.	1.832	640.	28.00	1105.	1180.	0.71	5.09	0.42	14.4	520.0
21	1.792	1508.	5.83	1673.	1.892	640.	28.94	1132.	1222.	0.68	4.96	0.41	14.4	520.0
22	1.920	1550.	6.17	1785.	1.952	640.	29.86	1157.	1264.	0.65	4.84	0.41	14.4	520.0
Cycle 8 - E <sup>3</sup> Separate Flow Cycle														
82	1.293	1260.	3.97	1036.	1.483	535.	23.61	827.	857.	0.80	5.95	0.41	14.4	520.0
84	1.389	1291.	4.50	1181.	1.589	535.	25.98	893.	935.	0.76	5.77	0.40	14.4	520.0
86	1.505	1327.	5.03	1328.	1.698	535.	28.18	950.	1007.	0.72	5.60	0.39	14.4	520.0

Table 3. Mixed Flow cycle conditions for High bypass model scale exhaust system, Core and Fan areas at mixer exit being  $16.7 \text{ in}^2$  and  $50.5 \text{ in}^2$ , respectively.

TEST POINT	$P_{r,p}$	$T_{r,p}$	$W_p$	$V_{j,p}$	$P_{r,s}$	$T_{r,s}$	$W_s$	$V_{j,s}$	$V_{mix}$	$V_r$	$W_r$	$T_{sr}$	$P_{amb}$	$T_{amb}$
		$^{\circ}\text{R}$	lb/sec	ft/sec		$^{\circ}\text{R}$	lb/sec	ft/sec	ft/sec			psi	psi	$^{\circ}\text{R}$
Cycle 3 - High Bypass Mixed Flow Cycle														
31	1.115	1126.	2.65	644.	1.195	535.	15.15	565.	577.	0.88	5.71	0.47	14.4	520.0
32	1.170	1169.	3.16	785.	1.268	535.	17.72	649.	670.	0.83	5.61	0.45	14.4	520.0
33	1.222	1204.	3.55	898.	1.330	535.	19.62	709.	738.	0.79	5.53	0.43	14.4	520.0
34	1.318	1248.	4.15	1068.	1.422	640.	20.22	858.	894.	0.80	4.87	0.50	14.4	520.0
35	1.380	1281.	4.47	1165.	1.485	640.	21.63	906.	951.	0.78	4.84	0.49	14.4	520.0
36	1.462	1318.	4.84	1278.	1.560	640.	23.18	958.	1013.	0.75	4.79	0.47	14.4	520.0
37	1.560	1356.	5.23	1397.	1.635	640.	24.62	1004.	1073.	0.72	4.71	0.46	14.4	520.0
38	1.650	1395.	5.53	1498.	1.690	640.	25.62	1035.	1117.	0.69	4.63	0.45	14.4	520.0
39	1.735	1431.	5.79	1586.	1.730	640.	26.32	1056.	1151.	0.67	4.55	0.44	14.4	520.0
40	1.832	1468.	6.05	1678.	1.785	640.	27.24	1083.	1191.	0.65	4.50	0.43	14.4	520.0
41	1.950	1508.	6.36	1780.	1.845	640.	28.21	1111.	1234.	0.62	4.44	0.43	14.4	520.0
Cycle 7 - E <sup>3</sup> Mixed Flow Cycle														
71	1.365	1357.	4.25	1179.	1.400	535.	21.55	768.	835.	0.65	5.07	0.39	14.4	520.0
72	1.428	1382.	4.55	1270.	1.450	535.	22.82	805.	882.	0.63	5.01	0.38	14.4	520.0
73	1.493	1405.	4.83	1354.	1.500	535.	24.01	839.	925.	0.62	4.97	0.38	14.4	520.0
74	1.560	1430.	5.09	1435.	1.550	535.	25.14	870.	965.	0.61	4.94	0.37	14.4	520.0
75	1.631	1454.	5.34	1513.	1.600	535.	26.21	899.	1003.	0.59	4.91	0.37	14.4	520.0
76	1.703	1479.	5.57	1588.	1.650	535.	27.24	926.	1038.	0.58	4.89	0.36	14.4	520.0
77	1.776	1502.	5.79	1657.	1.700	535.	28.22	951.	1071.	0.57	4.87	0.36	14.4	520.0
78	1.857	1525.	6.02	1729.	1.750	535.	29.16	975.	1104.	0.56	4.85	0.35	14.4	520.0
79	1.966	1550.	6.32	1815.	1.800	535.	30.07	997.	1139.	0.55	4.76	0.35	14.4	520.0

Table 4. Cycle conditions for 20.5 in<sup>2</sup> conic nozzle, determine on the basis of matched mixed flow conditions for various high bypass exhaust system cycles.

TEST POINT	P <sub>r</sub>	T <sub>t</sub> °R	W lb/sec	V <sub>j</sub> ft/sec	P <sub>amb</sub> psi	T <sub>amb</sub> °F
Mixed Conditions of High Bypass Separate & Mixed Flow Cycles						
11	1.173	604.	5.451	569.	14.4	520.0
12	1.237	615.	6.311	660.	14.4	520.0
13	1.293	619.	6.979	726.	14.4	520.0
14	1.385	723.	7.375	879.	14.4	520.0
15	1.448	732.	7.894	939.	14.4	520.0
16	1.519	737.	8.442	999.	14.4	520.0
17	1.592	746.	8.941	1056.	14.4	520.0
18	1.656	756.	9.327	1105.	14.4	520.0
19	1.706	765.	9.608	1140.	14.4	520.0
20	1.771	772.	9.969	1183.	14.4	520.0
21	1.841	781.	10.328	1226.	14.4	520.0
22	1.912	793.	10.652	1269.	14.4	520.0
Mixed Conditions of E <sup>3</sup> Mixed Flow Cycle						
72	1.439	643.	8.339	874.	14.4	520.0
75	1.595	655.	9.568	991.	14.4	520.0
77	1.701	662.	10.294	1058.	14.4	520.0
Mixed Conditions of E <sup>3</sup> Separate Flow Cycle						
86	1.650	627.	10.203	1002.	14.4	520.0

Variation of cycle parameters, listed in Tables 2 through 4, are graphically illustrated in Figures 21 through 26. Figures 21 and 22 show the variation of core and fan stream pressure ratios and total temperatures with respect to mixed jet velocity, respectively. The pressure ratios for both the streams are relatively lower for the current cycles compared to E<sup>3</sup> cycles at fixed mixed jet velocities. The fan stream temperatures at higher mixed jet velocities for the current cycles are higher compared to E<sup>3</sup> cycles. Thus, for the same mixed jet velocity, the E<sup>3</sup> cycle generates much higher core velocity compared to current cycles. These cycle differences are further illustrated in Figure 23 by plotting core stream pressure ratios with respect to fan stream pressure ratio. The dashed and dotted lines connecting points between mixed flow and separate flow cycles, current and E<sup>3</sup>, respectively, are the fixed ideal thrust lines. Variation of velocity ratio and mass flow ratio with respect to mixed jet velocity for different cycles are shown in Figure 24. The corresponding variations of mass flow ratio with respect to velocity ratio are shown in Figure 25. The sudden mass flow jump for the current cycles (see Figure 25) is due to the abrupt fan stream total temperature variation from atmospheric condition to a heated condition. The implication of these cycle characteristics are expected to influence the noise characteristics of the exhaust systems.

The variation of nozzle pressure ratio and total temperature with respect to the ideal jet velocity for the conic nozzle are illustrated in Figure 26. Again, the mixed pressure ratios for E<sup>3</sup> cycles are relatively higher compared to the current cycles.

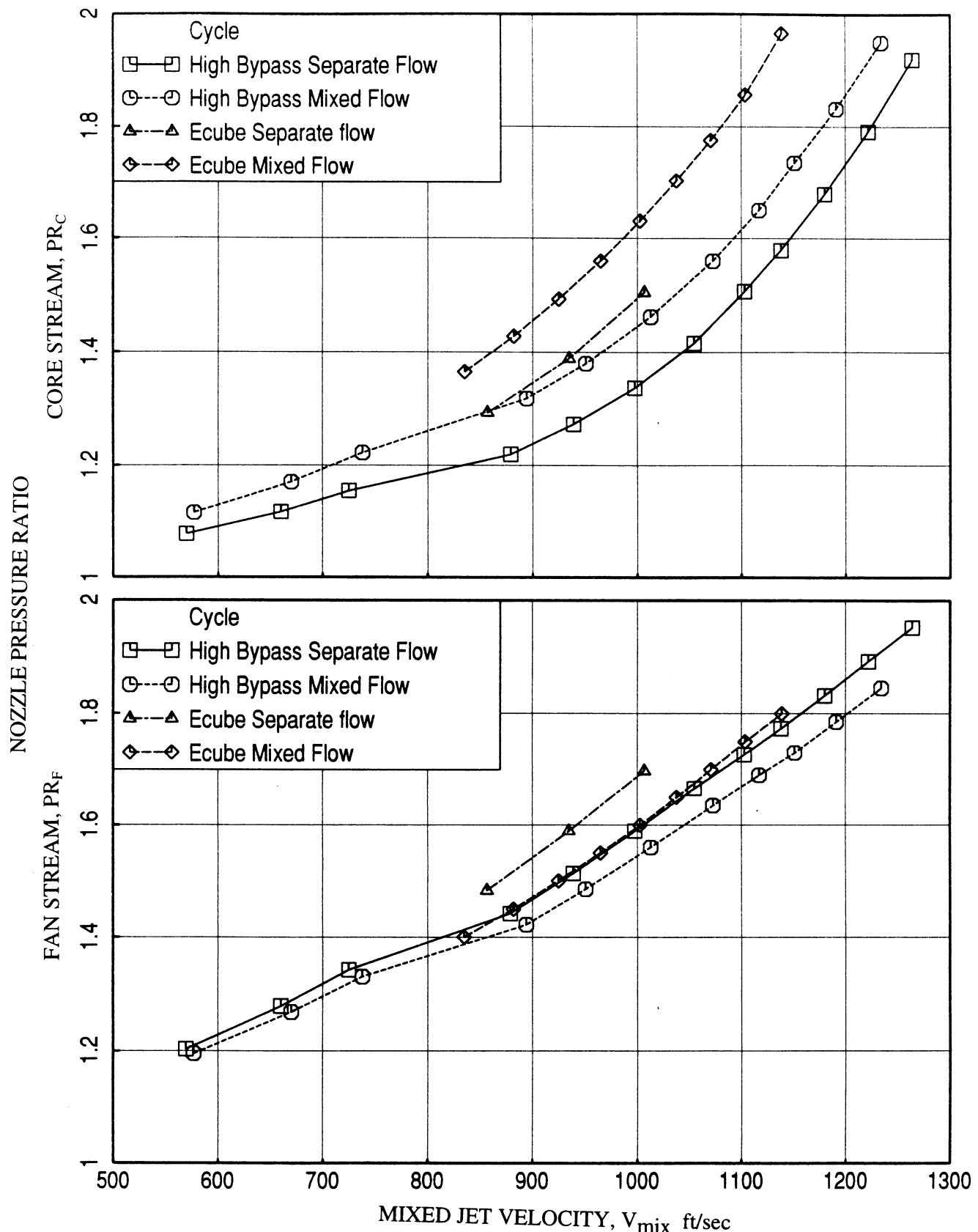


Figure 21. Core and fan stream pressure ratio variation with respect to mixed jet velocity for different cycles.

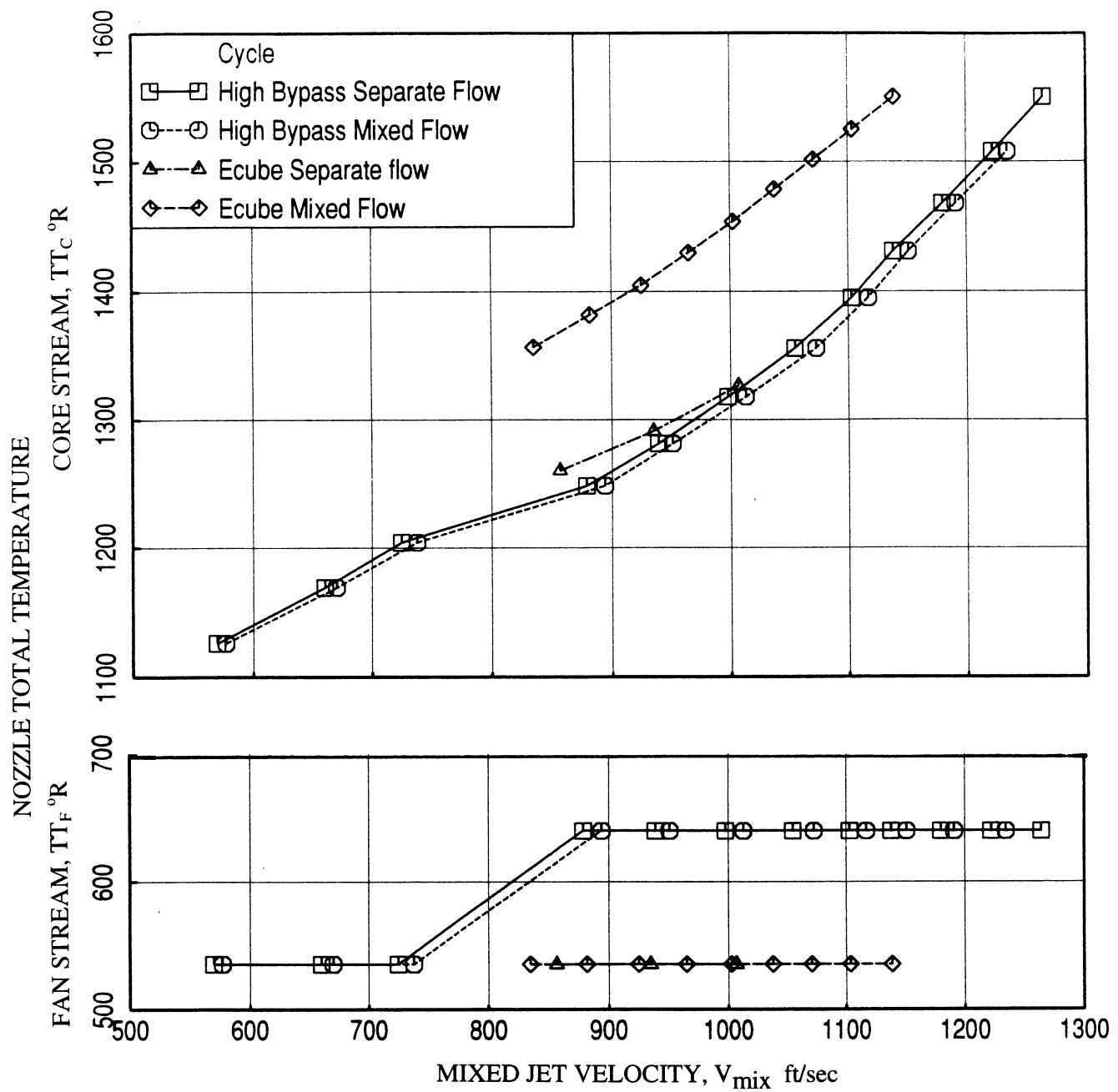


Figure 22. Core and fan stream total temperature variation with respect to mixed jet velocity for different cycles.

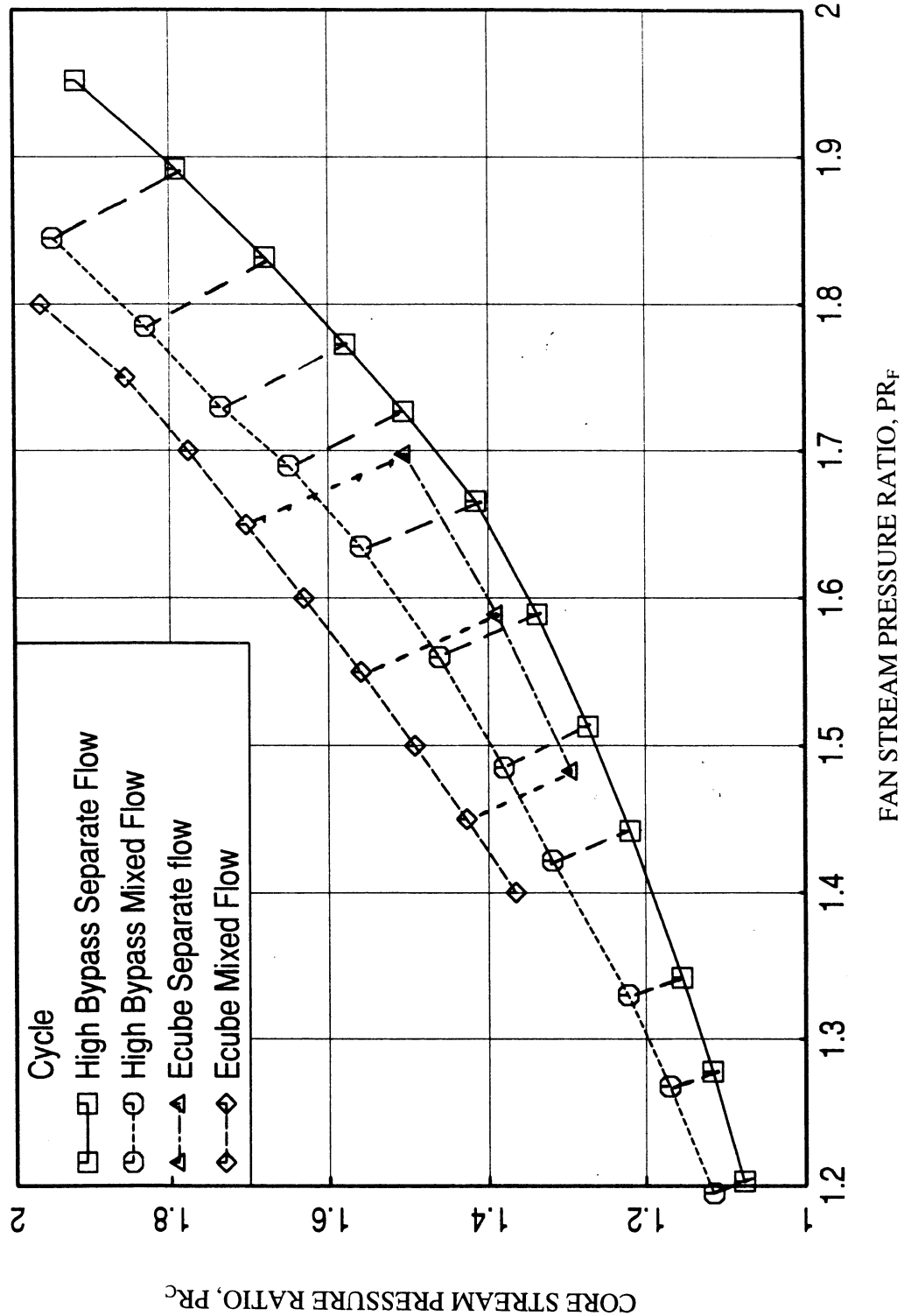


Figure 23. Variation of core stream pressure ratio with respect to fan stream pressure ratio for different cycles.

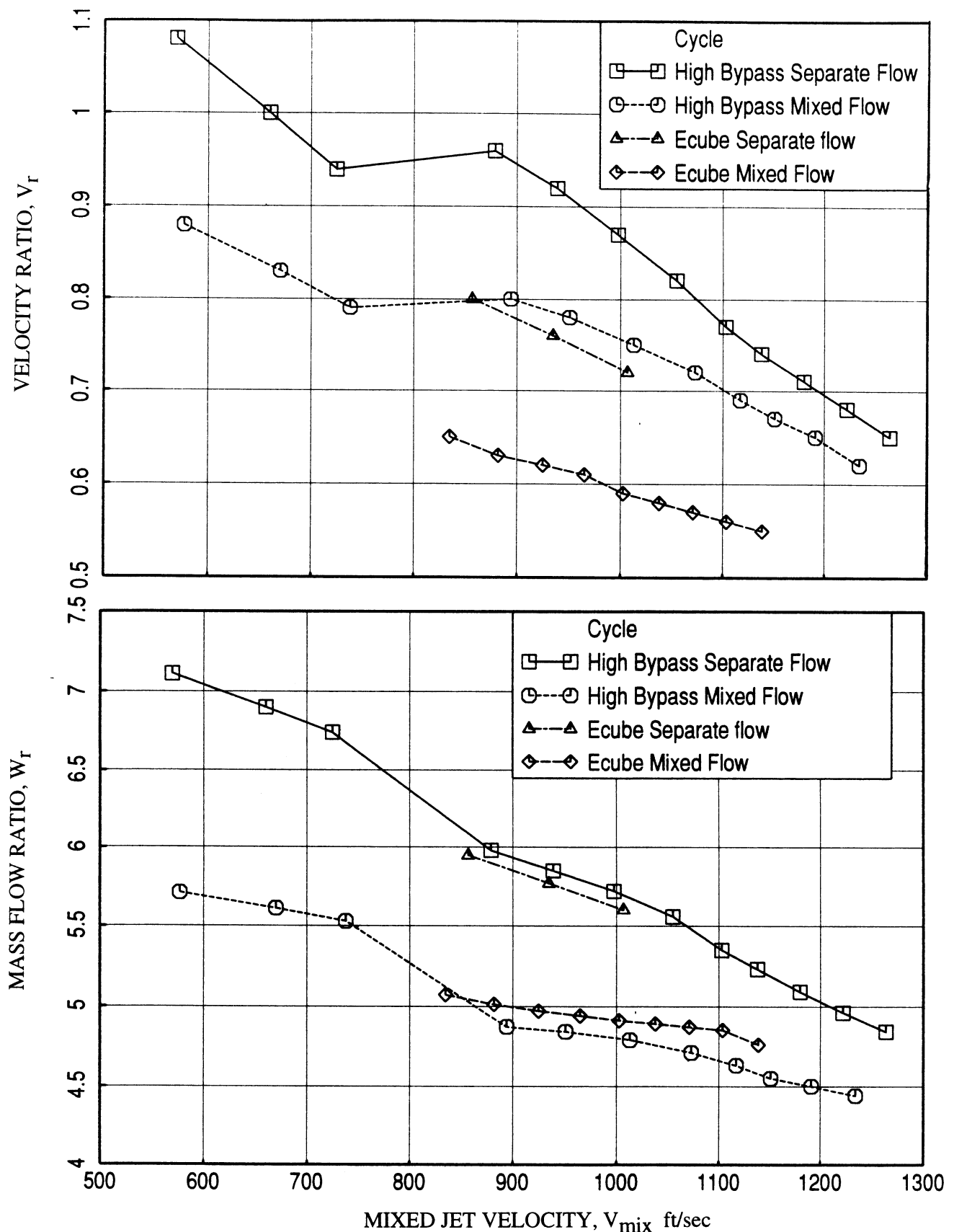


Figure 24. Velocity and mass flow ratio variation with respect to mixed jet velocity for different cycles.

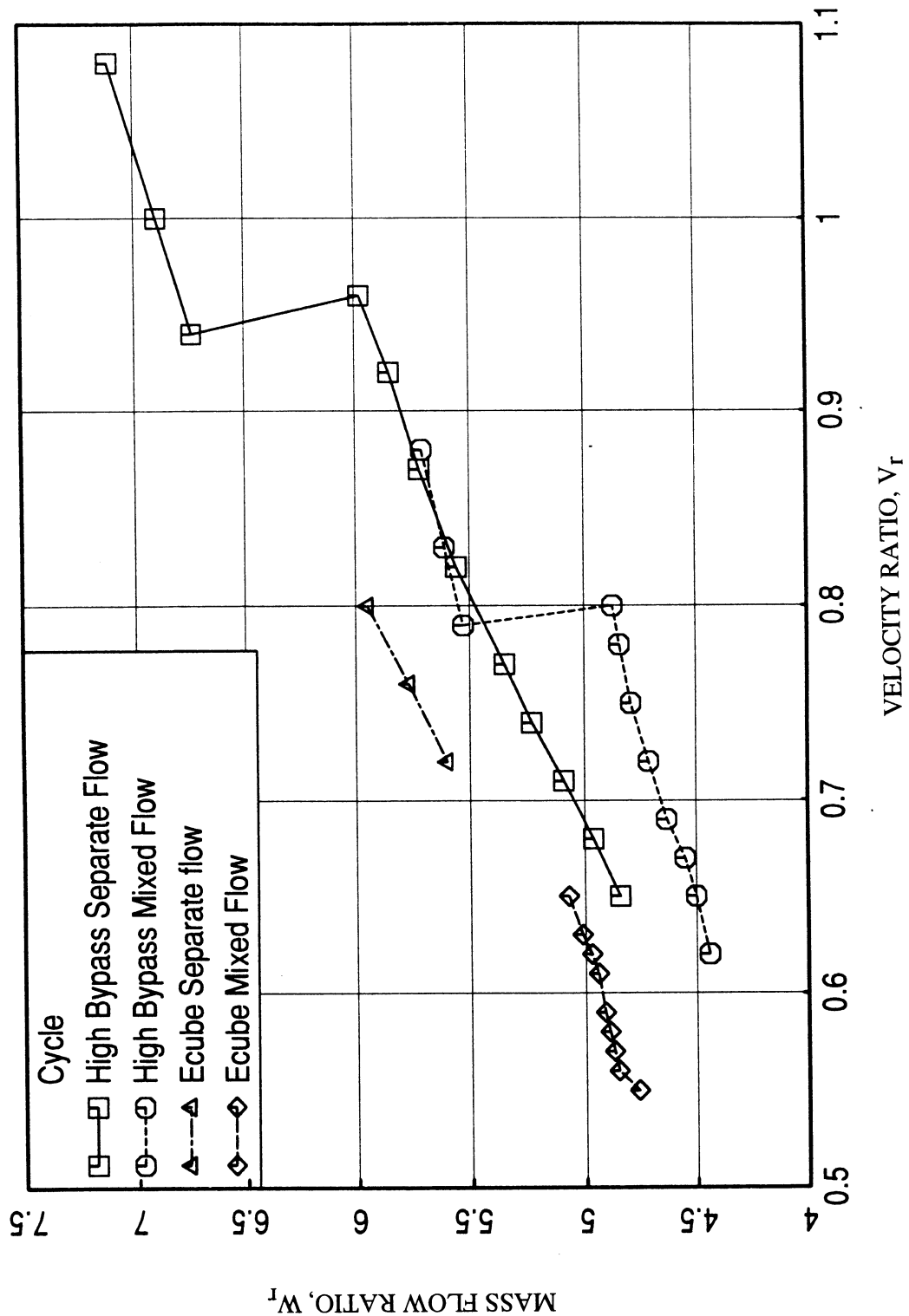


Figure 25. Variation of mass flow ratio with respect to velocity ratio for different cycles.

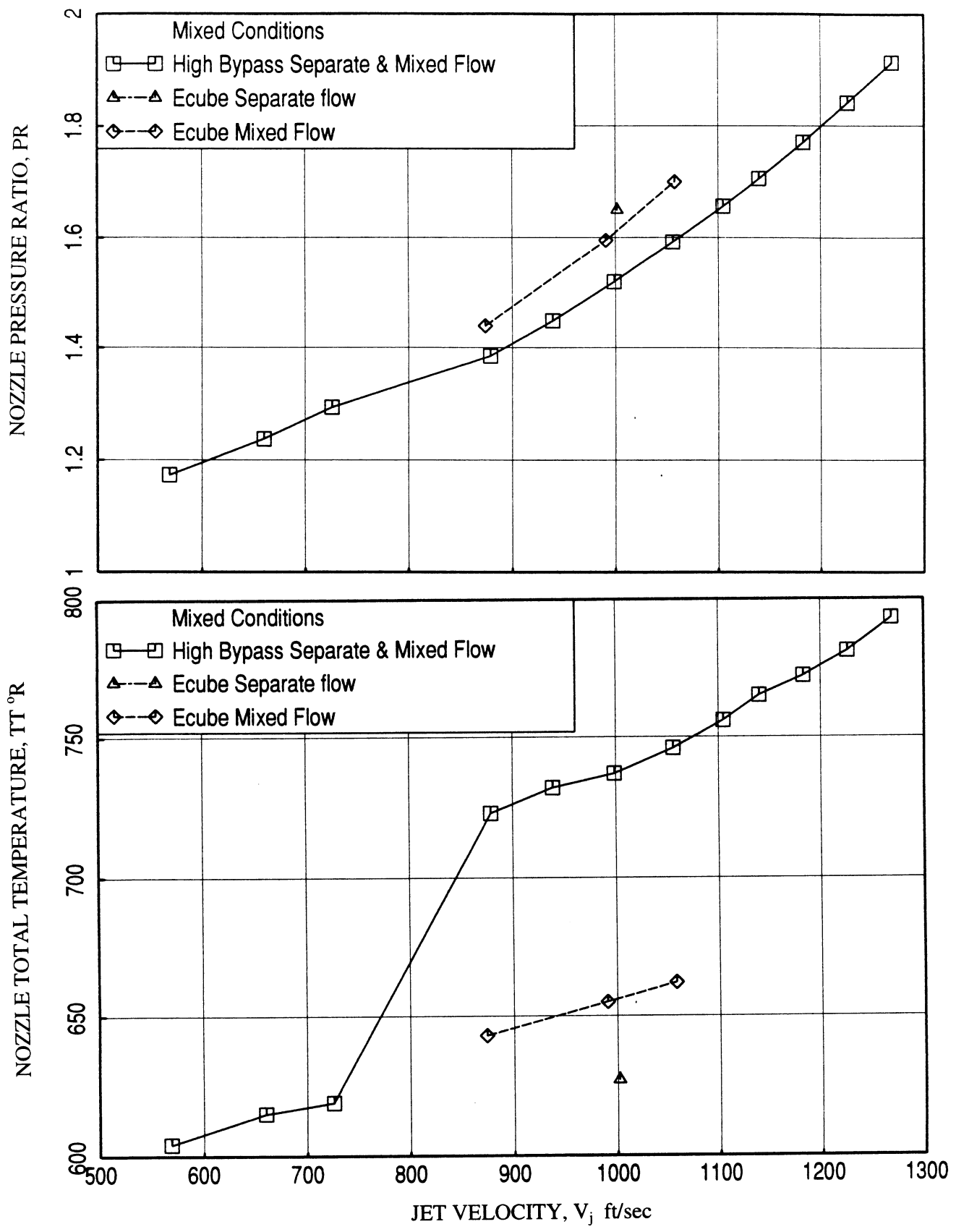


Figure 26. Nozzle pressure ratio and total temperature variations with respect to ideal jet velocity for different cycles.

## 6.0 EXPERIMENTAL RESULTS

Acoustic and LDV tests were conducted for a number of configurations, listed in Table 1, with and without flight simulation. Freejet Mach numbers of 0.24 and 0.28 were used as flight simulation. Limited numbers of tests with relatively lower aerothermodynamic conditions were conducted with simulated flight Mach number of 0.24.

**6.1 Acoustic Data for 20.5 in<sup>2</sup> Conic Nozzle:** Acoustic data for the conic nozzle is analyzed and examined to assess the quality and the repeatability of the results. In addition, the current tests (Task C) include the mixed aerothermodynamic conditions for high bypass exhaust system cycle conditions for higher ideal jet velocity. These high jet velocity results will be used to assess relative noise characteristics of the high bypass exhaust systems compared to conic nozzle.

OASPL and PNLT directivities at a number of aerothermodynamic conditions along the conic nozzle cycle line are plotted in Figure 27 for static condition. The impact of increasing ideal jet velocity  $V_j$  due to increasing NPR ( $P_r$ ) and  $T_t$  on noise level is clearly observed in this figure, that the noise level increases with increasing ideal jet velocity. The corresponding SPL spectra at a number of polar angles  $\theta$  are plotted in Figure 28, which also indicates increasing noise level with ideal jet velocity. Similar results with simulated flight of  $M_F=0.28$  are shown in Figures 29 and 30, respectively. The sound power level (PWL) spectra for both static and flight cases at different aerothermodynamic conditions are shown in Figure 31.

The same 20.5 in<sup>2</sup> conic nozzle was tested earlier under Task A of the current program, mostly at lower ideal jet velocity conditions, up to about 1000 ft/sec. Results from Task A are compared with those of the current task (i.e., Task C). In these comparisons all the noise levels are normalized to an ideal gross thrust of 60,000 lbs. Figure 32 shows the comparison of EPNL and PNLT at several polar angle  $\theta$  with respect to  $V_j$  between the two tasks. EPNL agreement between the results is excellent for flight-simulated conditions. In addition, the agreement seems to be better at higher jet velocity conditions. Similar comparisons of OASPL and PNLT directivities at three different  $V_j$  are shown in Figures 33 and 34, respectively. Again the agreement is much better with flight simulation and at higher velocity conditions. The spectral comparison of sound pressure level (SPL) for the same three jet velocities is shown in Figures 35 through 37.

The observation leads to conclude that the agreement between the two sets of data is excellent at higher velocity conditions. At lower velocity conditions the agreement is still good with flight simulation. The observed differences between the two sets of data are possibly due to the differences in the internal noise, anechoic chamber background noise, and the atmospheric conditions during the tests for the two tasks. At higher velocity conditions the impact of these parameters is negligible, since the jet noise component is relatively high. At lower velocity conditions these differences, especially the internal noise component, could influence the noise levels significantly. At higher jet velocities, above 1000 ft/sec, conic nozzle data repeatability is expected to be excellent.

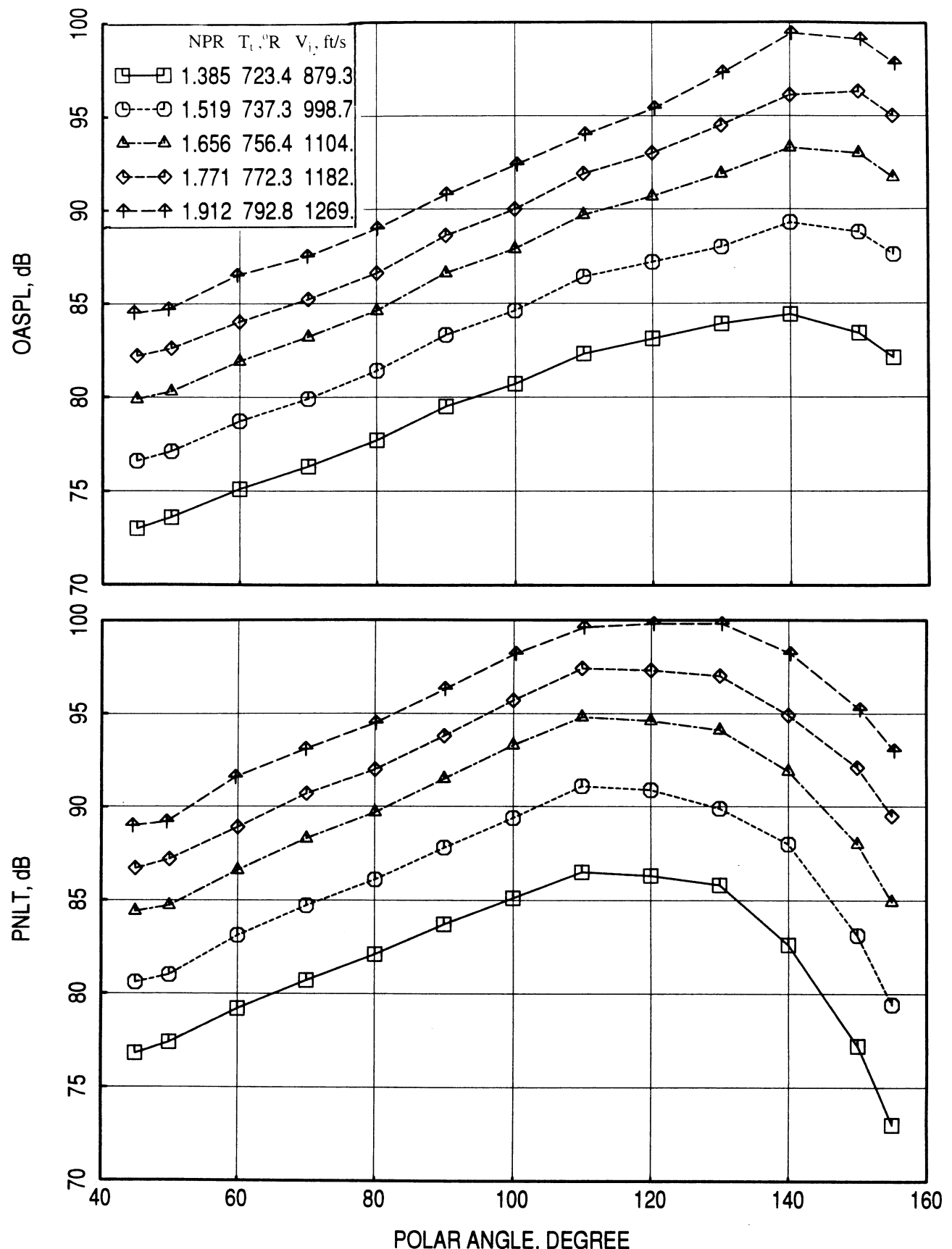


Figure 27. OASPL and PNLT directivities at different aerothermodynamic conditions along the conic nozzle cycle for a 20.5 in<sup>2</sup> conic nozzle at SAE 77° standard day conditions, M<sub>F</sub>=0, A<sub>8</sub>=3078 in<sup>2</sup>, Sideline Distance=1500 ft.

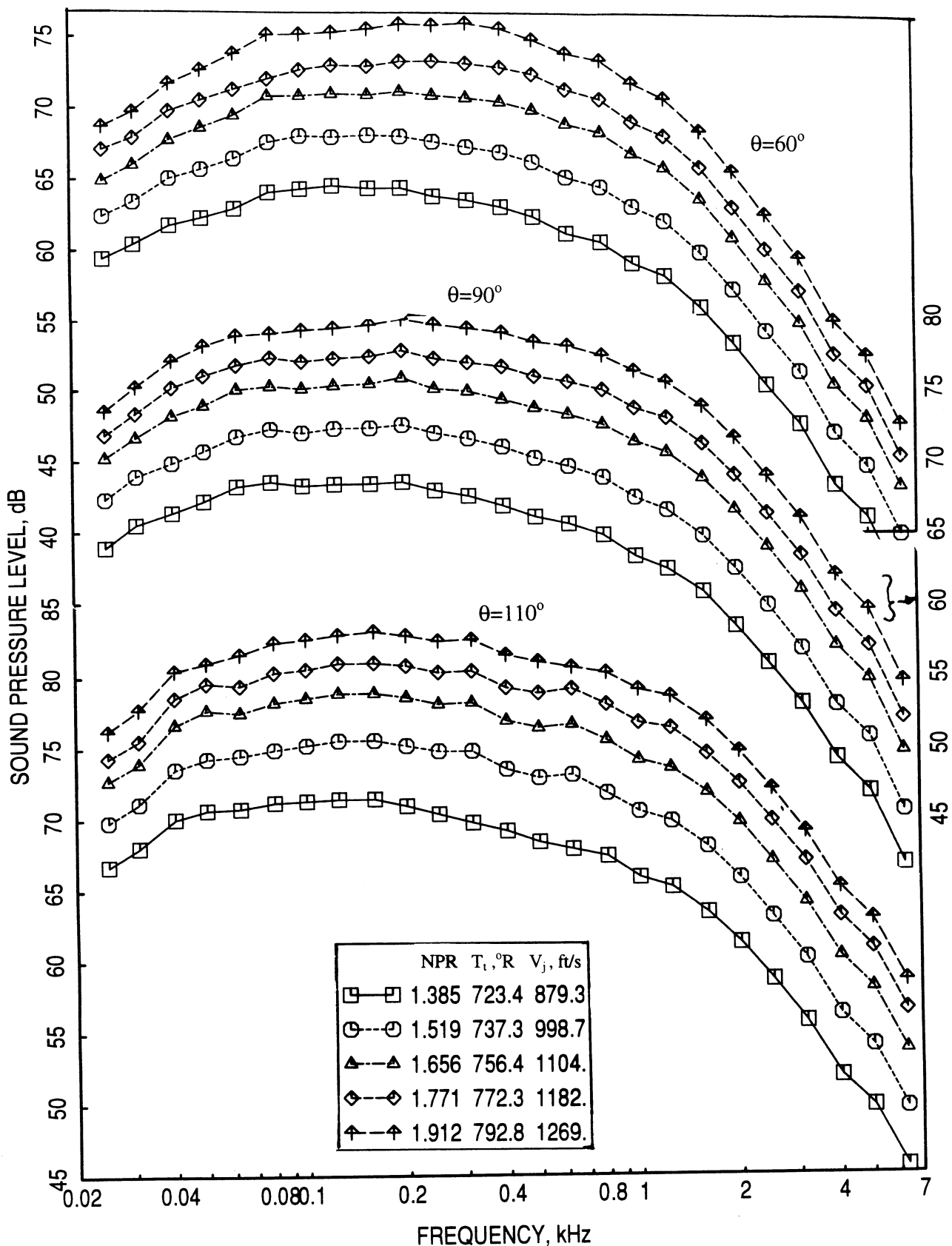


Figure 28. SPL spectra at a number of polar angles  $\theta$  for different aerothermodynamic conditions along the conic nozzle cycle for a  $20.5 \text{ in}^2$  conic nozzle at SAE  $77^\circ$  standard day conditions,  $M_F=0$ ,  $A_8=3078 \text{ in}^2$ , Sideline Distance=1500 ft.

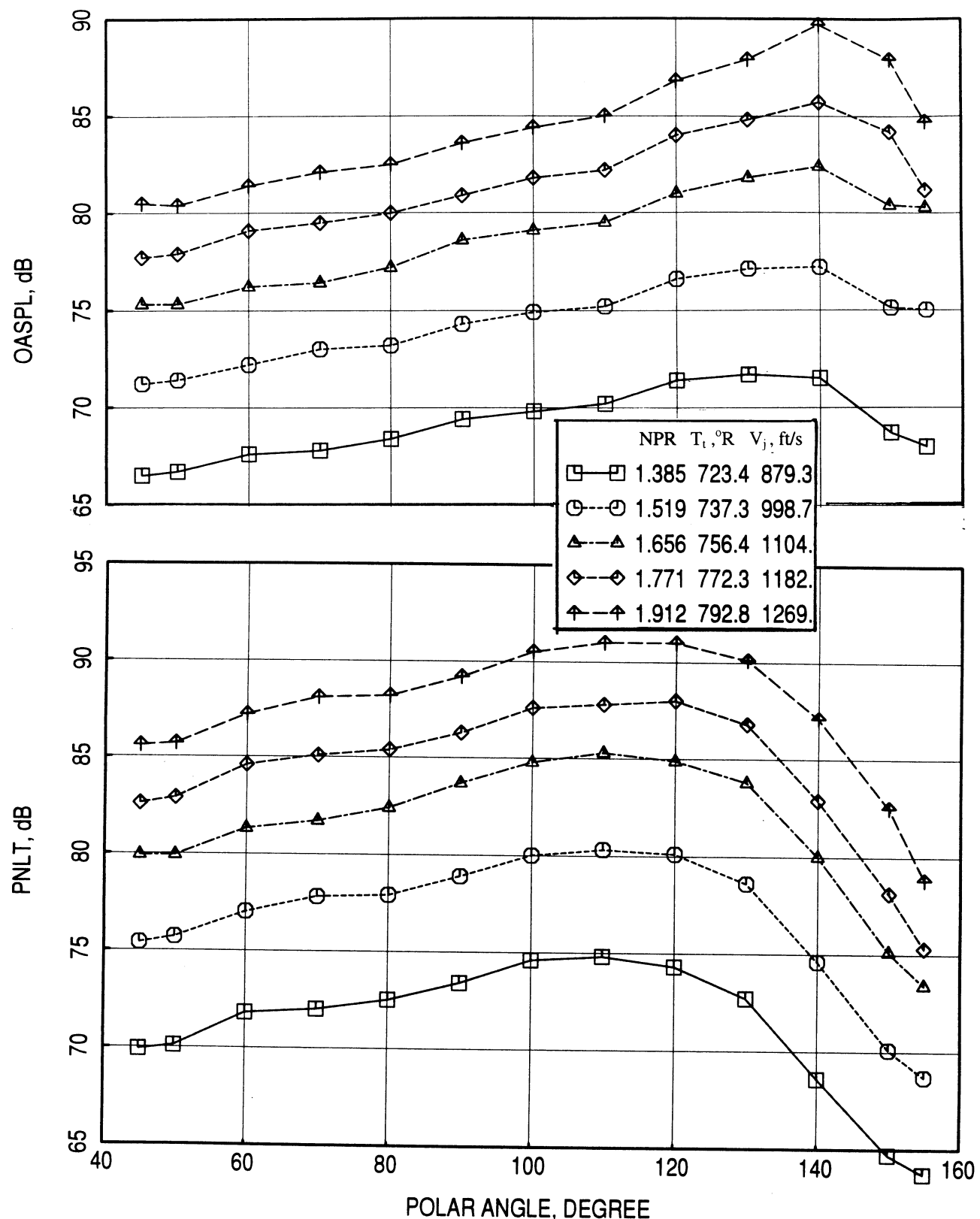


Figure 29. OASPL and PNLT directivities at different aerothermodynamic conditions along the conic nozzle cycle for a 20.5 in<sup>2</sup> conic nozzle at SAE 77° standard day conditions,  $M_F=0.28$ ,  $A_8=3078$  in<sup>2</sup>, Sideline Distance=1500 ft.

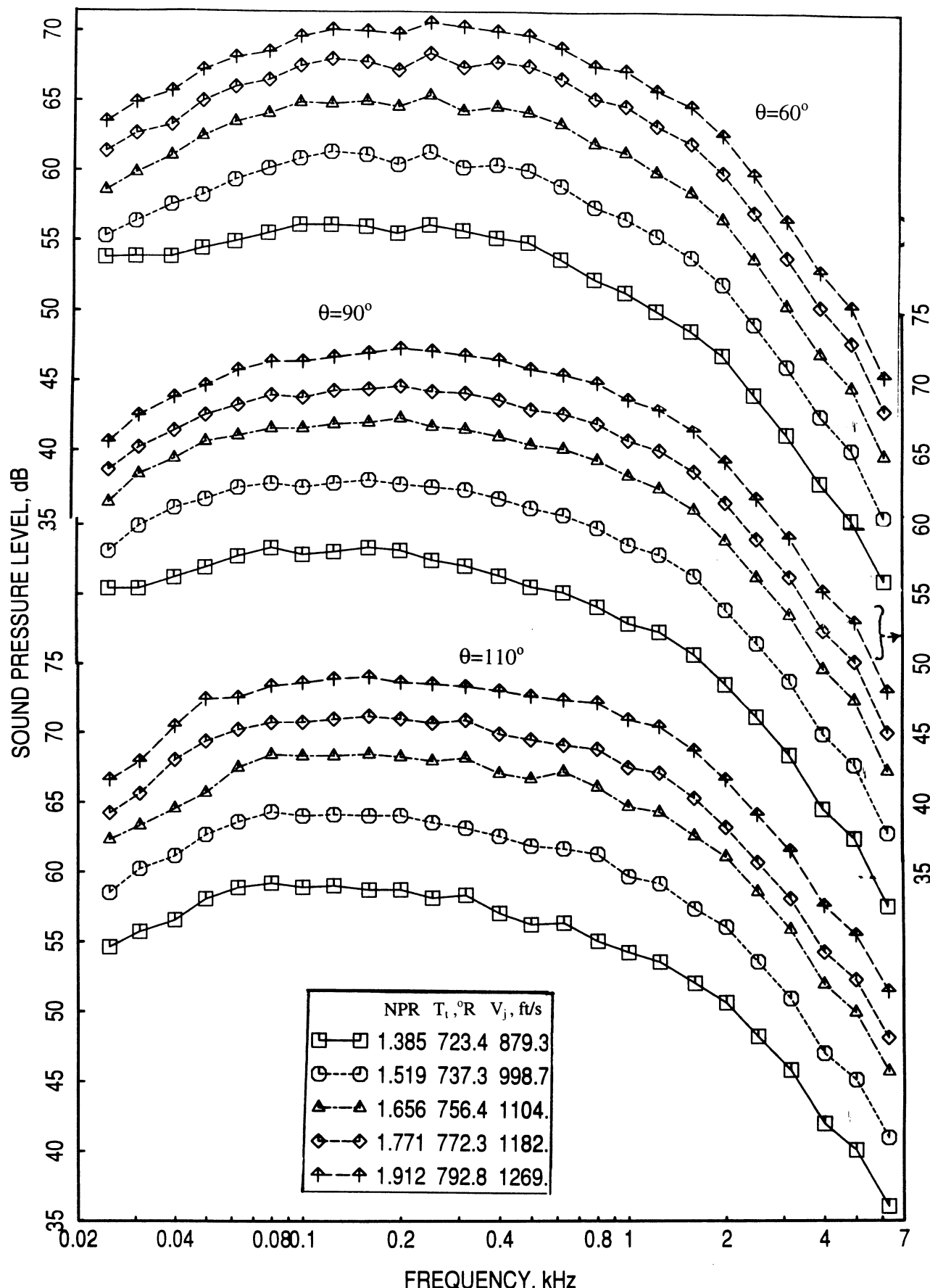


Figure 30. SPL spectra at a number of polar angles  $\theta$  for different aerothermodynamic conditions along the conic nozzle cycle for a 20.5 in<sup>2</sup> conic nozzle at SAE 77° standard day conditions,  $M_F=0.28$ ,  $A_8=3078$  in<sup>2</sup>, Sideline Distance=1500 ft.

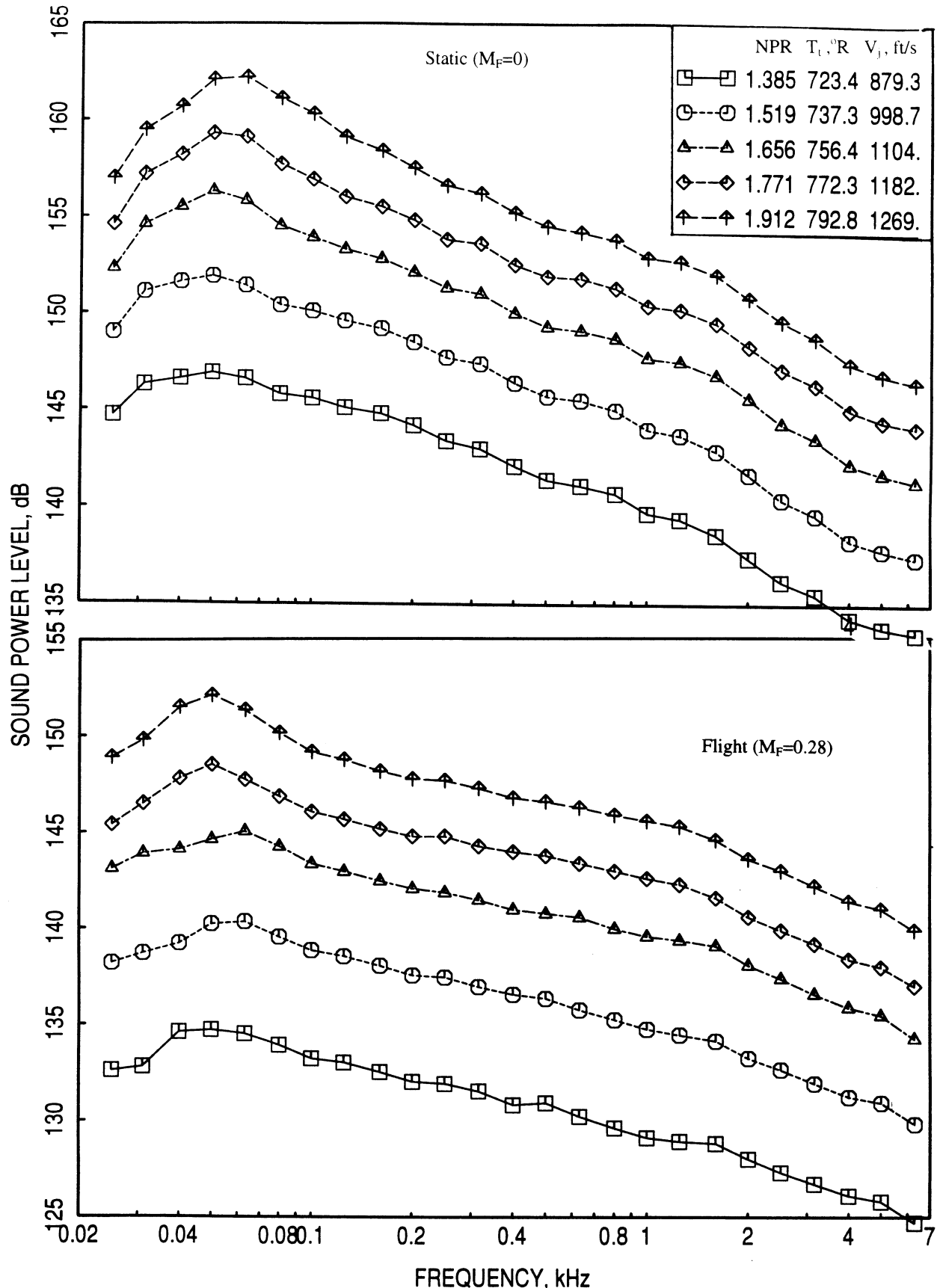


Figure 31. Sound Power Level spectra at different aerothermodynamic conditions along the conic nozzle cycle for a 20.5 in<sup>2</sup> conic nozzle at SAE 77° standard day conditions, A8=3078 in<sup>2</sup>, Sideline Distance=1500 ft.

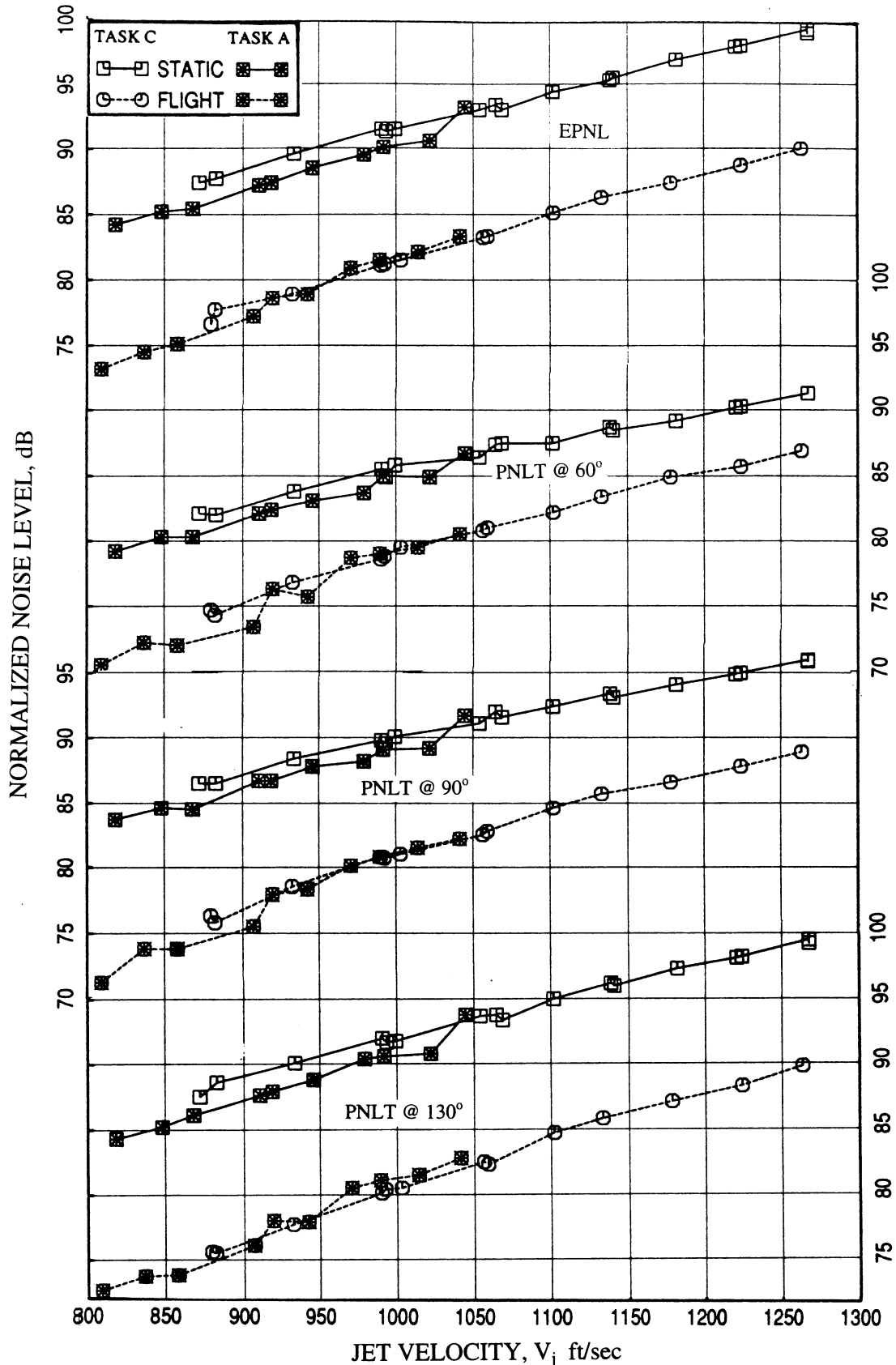


Figure 32. Comparison of Normalized EPNL and PNLT at a number of polar angles  $\theta$  along the conic nozzle cycle for a 20.5 in<sup>2</sup> conic nozzle between the current tests (Task C) and the previously conducted tests (Task A) for Static ( $M_F=0$ ) and Flight ( $M_F=0.28$ ) at SAE 77° standard day conditions,  $A_8=3078$  in<sup>2</sup>, Sideline Distance=1500 ft.

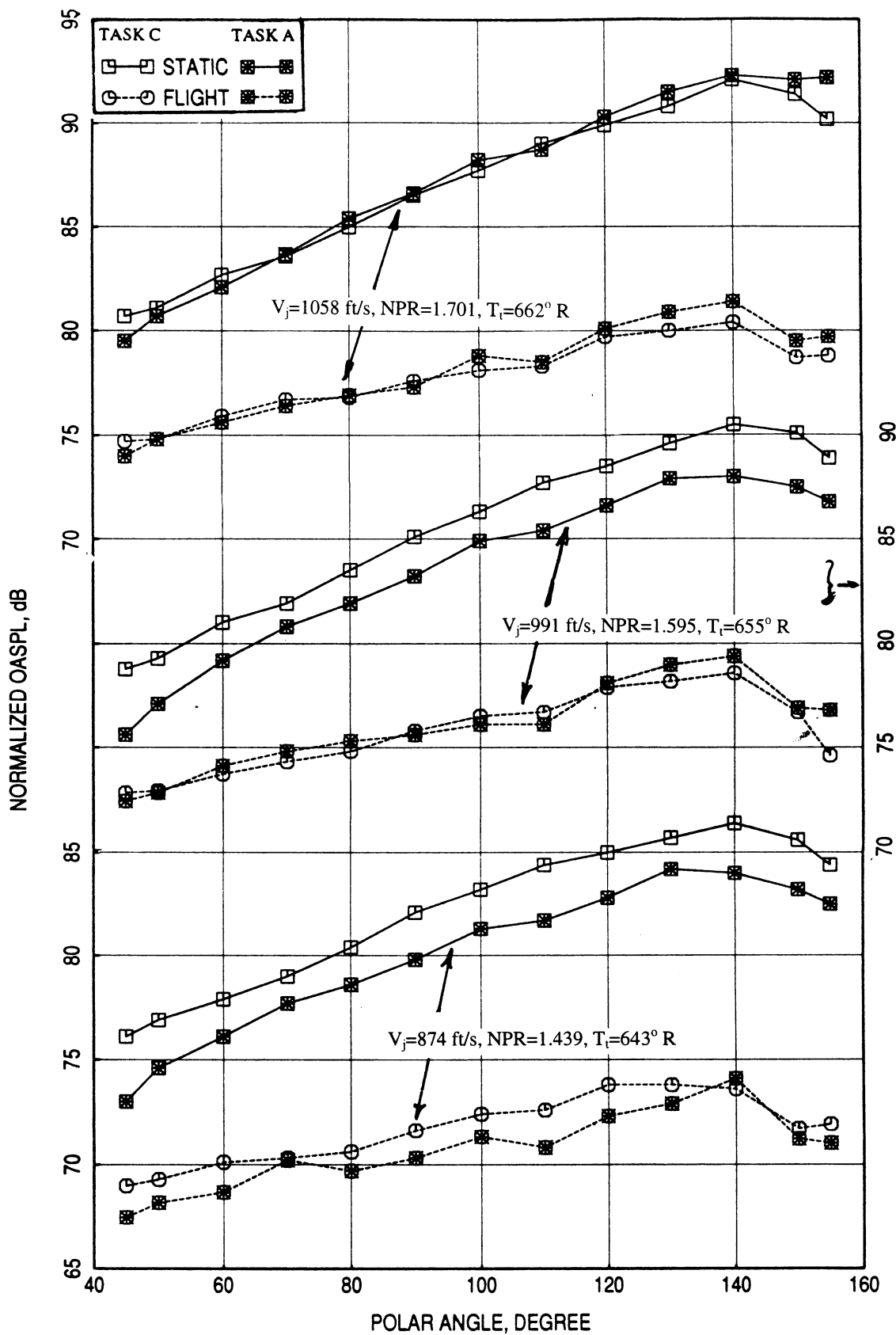


Figure 33. Comparison of Normalized OASPL directivities at a number aerothermodynamic conditions along the conic nozzle cycle for a  $20.5 \text{ in}^2$  conic nozzle between the current tests (Task C) and the previously conducted tests (Task A) for Static ( $M_F=0$ ) and Flight ( $M_F=0.28$ ) at SAE  $77^\circ$  standard day conditions,  $A_8=3078 \text{ in}^2$ , Sideline Distance=1500 ft.

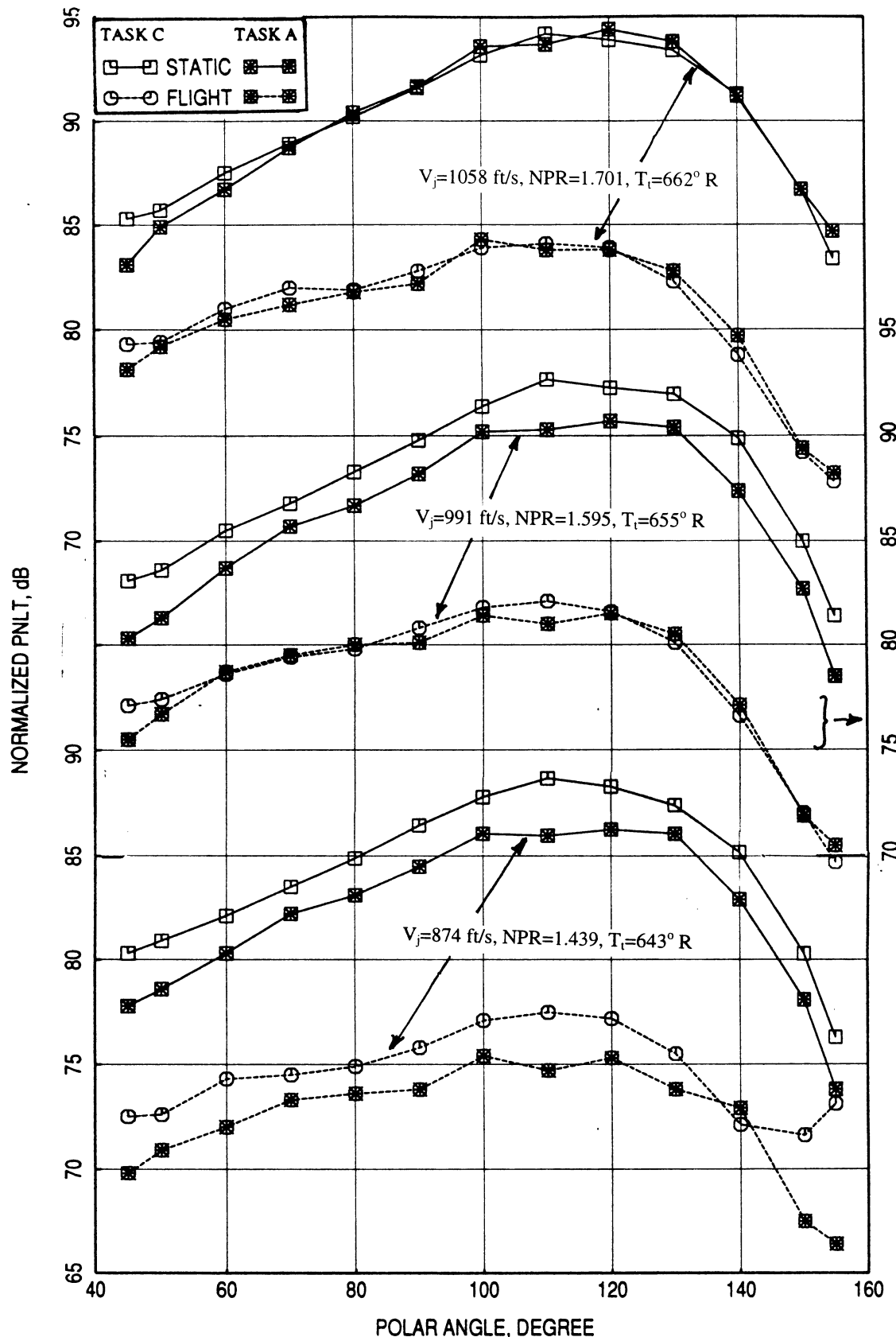


Figure 34. Comparison of Normalized PNLT directivities at a number aerothermodynamic conditions along the conic nozzle cycle for a 20.5 in<sup>2</sup> conic nozzle between the current tests (Task C) and the previously conducted tests (Task A) for Static ( $M_F=0$ ) and Flight ( $M_F=0.28$ ) at SAE 77° standard day conditions,  $A_8=3078 \text{ in}^2$ , Sideline Distance=1500 ft.

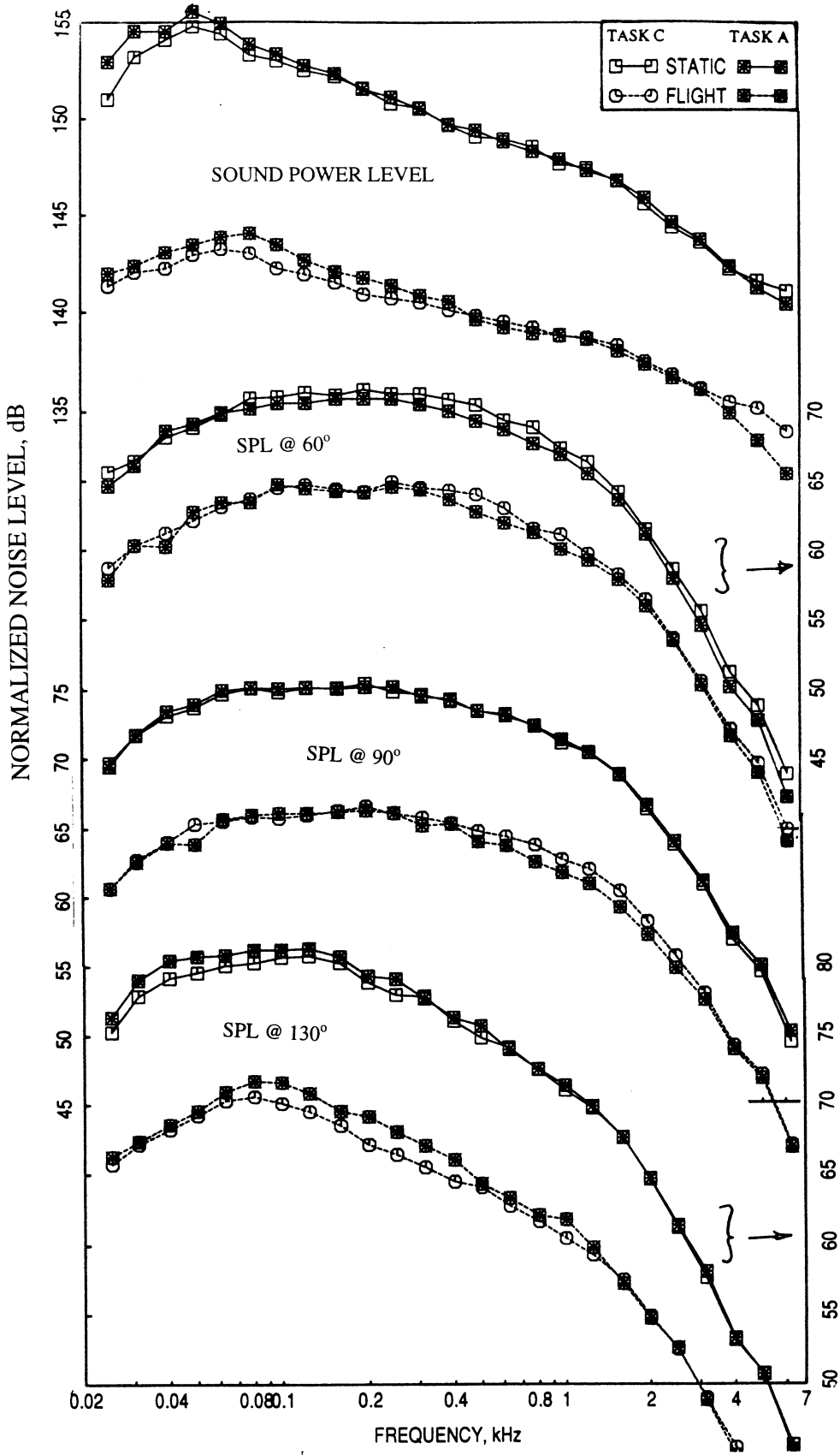


Figure 35. Comparison of Normalized PWL spectra and SPL spectra at a number of polar angles  $\theta$  for a 20.5 in<sup>2</sup> conic nozzle between the current tests (Task C) and the previously conducted tests (Task A) for Static ( $M_F=0$ ) and Flight ( $M_F=0.28$ ) at SAE 77° standard day conditions,  $V_j=1058$  ft/s,  $NPR=1.701$ ,  $T_t=662^\circ R$ ,  $A_8=3078$  in<sup>2</sup>, Sideline Distance=1500 ft.

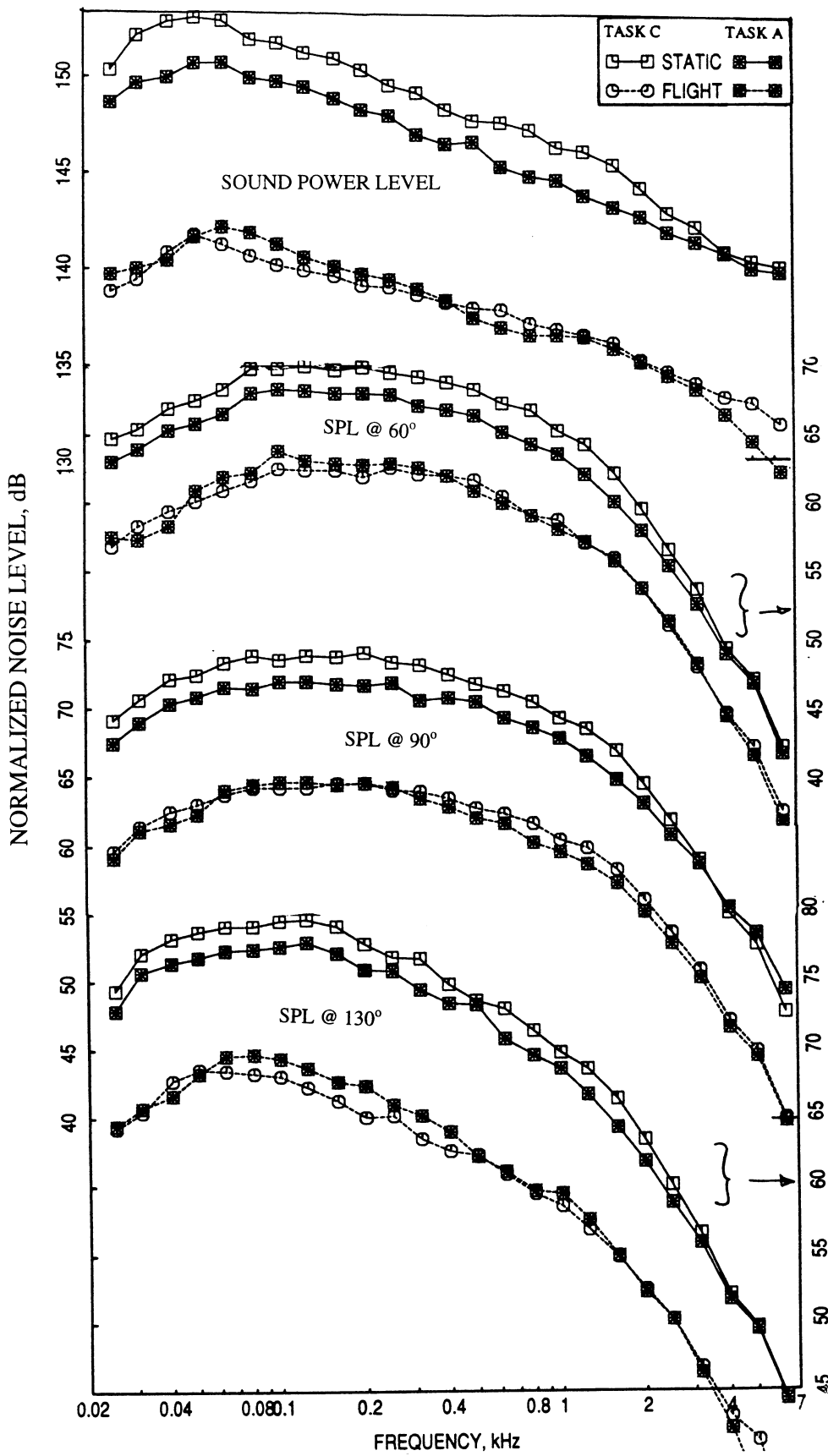


Figure 36. Comparison of Normalized PWL spectra and SPL spectra at a number of polar angles  $\theta$  for a 20.5 in<sup>2</sup> conic nozzle between the current tests (Task C) and the previously conducted tests (Task A) for Static ( $M_F=0$ ) and Flight ( $M_F=0.28$ ) at SAE 77° standard day conditions,  $V_j=991$  ft/s,  $NPR=1.595$ ,  $T_t=655^\circ$  R,  $A_8=3078$  in<sup>2</sup>, Sideline Distance=1500 ft.

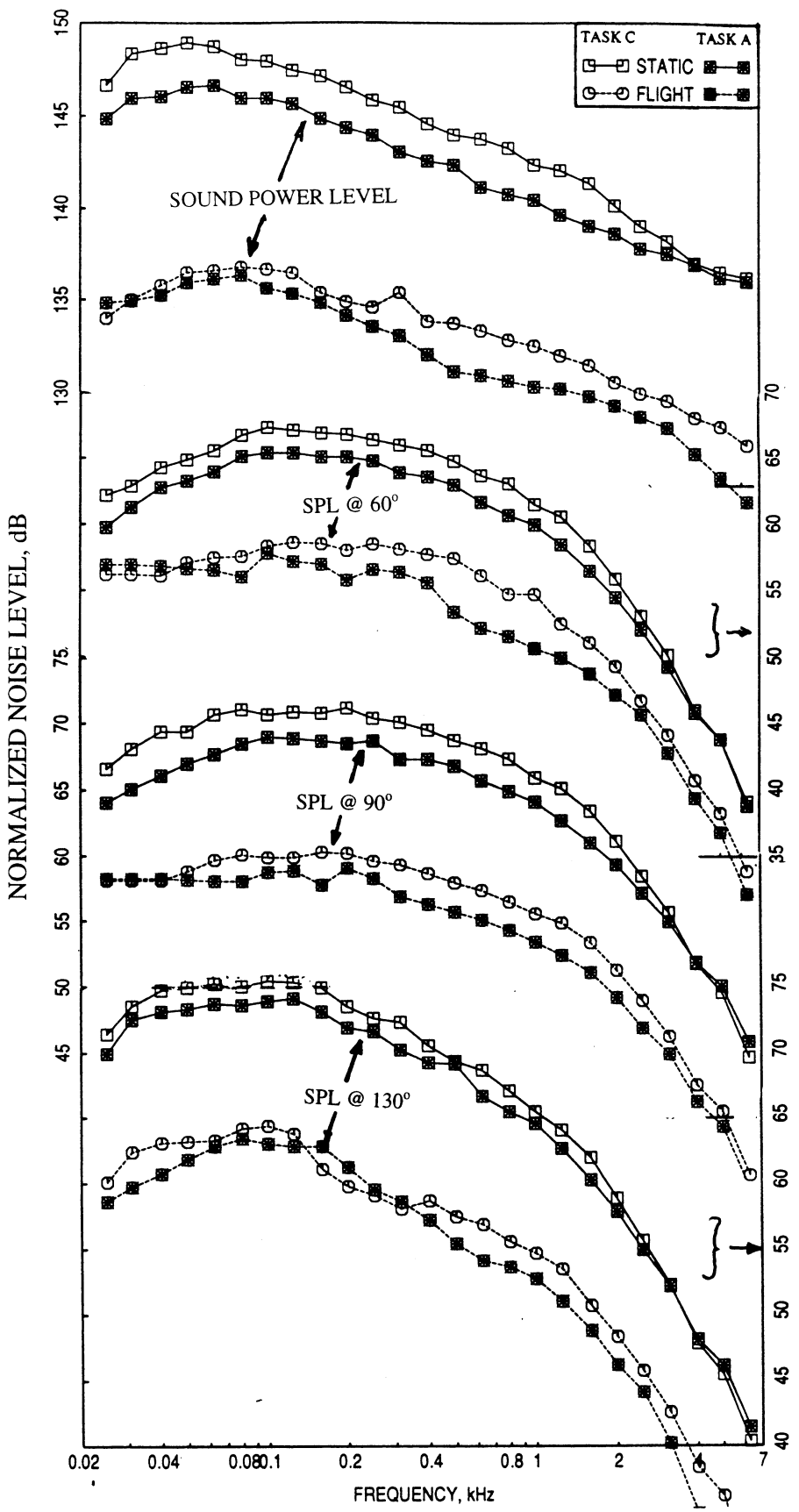


Figure 37. Comparison of Normalized PWL spectra and SPL spectra at a number of polar angles  $\theta$  for a 20.5 in<sup>2</sup> conic nozzle between the current tests (Task C) and the previously conducted tests (Task A) for Static ( $M_F=0$ ) and Flight ( $M_F=0.28$ ) at SAE 77° standard day conditions,  $V_j=874$  ft/s,  $NPR=1.439$ ,  $T_t=643^\circ R$ ,  $A_8=3078$  in<sup>2</sup>, Sideline Distance=1500 ft.

## **6.2 Acoustic and LDA Data for Confluent and 22-Lobed Mixers with Standard Fan Nozzle Showing the Effect of Engine Cycle on Farfield Noise Level and Plume Flowfield:**

Tests for confluent and 22-lobed mixers with standard fan were conducted at various engine cycle conditions, namely, High Bypass Separate Flow (HBSF), High Bypass Mixed Flow (HBMF) and E<sup>3</sup> Mixed Flow (E<sup>3</sup>MF) cycles.

Figure 38 shows the EPNL variation with respect to  $V_{mix}$  for confluent and 22-lobed mixers with standard fan. The effect of engine cycle seems to be more prominent for the confluent mixer compared to 22-lobed mixer. In addition, the EPNL variation with respect to different cycles is dominant with flight simulation compared to static, especially for 22-lobed mixer. Axial velocity profiles in 3-dimensional form at 0.5" downstream of the nozzle exit plane shown in Figures 39 and 40 for the confluent and 22-lobed mixers with standard fan for different engine cycles at nominal  $V_{mix}$  of 1000 ft/sec. For the confluent mixer (see Figure 39) the core velocity distinctly steps up over the fan velocity for HBMF and E<sup>3</sup>MF cycles compared to HBSF cycle and the increase is higher for E<sup>3</sup>MF cycle. Each profile has a dip at the center due to the center plug of the exhaust system. The step between the core and fan velocity is highest for E<sup>3</sup>MF cycle and least for HBSF cycle. For the 22-lobed mixer (see Figure 40) the core velocity steps up over the fan velocity with rising conical shape profiles along the core flow lobes. For HBSF cycle the heights of the cones are small and thus the entire profile looks more uniform. For the other two cycles the velocity at the center steps up in the form of a cone along with the cones through the core flow lobes. The heights of these velocity cones are significant.

**Confluent Mixer:** Noise levels due to aerothermodynamic variation along the HBMF cycle for the confluent nozzle with standard fan is shown in Figure 41. Sound pressure levels at all polar angles increase with increasing aerothermodynamic conditions for the entire frequency range. Similar effect is also observed for OASP and PNLT directivities at all polar angles. The effect of aerothermodynamic condition on the flowfield is shown in Figure 42 in the form of 3-dimensional velocity profiles measured at 0.5" downstream of the nozzle exit at different test points along the HBMF cycle. The core velocity distinctly steps up over the fan velocity with a dip at the center due to the center plug of the exhaust system and the relative difference between core and fan velocities increases with increasing  $V_{mix}$  conditions. This effect on the axial velocity contour and axial velocity (i.e., mean and unsteady) distributions at 0.5" downstream of the nozzle exit plane is shown in Figure 43. Axial velocity levels are higher for TP38 compared to TP36, especially the difference of velocities between these test points is much higher for the core region, resulting into a higher uneven velocity profile at the higher aerothermodynamic conditions.

The evolution of mean and random unsteady axial velocity distributions along the nozzle axis, downstream of the nozzle exit plane, for a nominal  $V_{mix}$  of 1000 ft/sec (TP36) for HBMF cycle is shown in Figure 44. Due to the center plug in the exhaust system a significant velocity drop is observed at the center. This velocity drop decreases along the axis, downstream of the nozzle exit, as shown in Figure 44. The fan and core streams are very distinct at the nozzle exit plane. The mixing process continues outside the nozzle

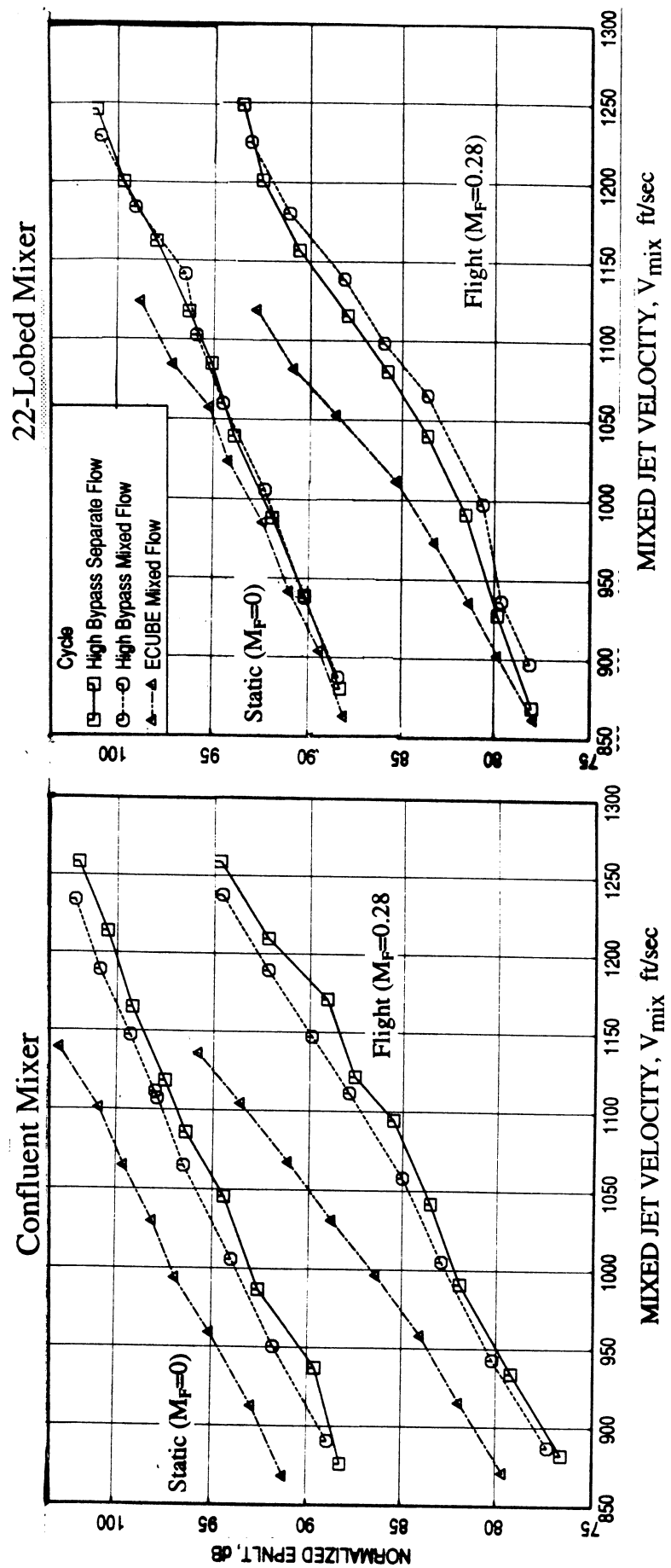


Figure 38. Effect of engine cycle on normalized EPNL for confluent and 22-lobed mixers with standard fan of exit area 51.7 in<sup>2</sup> at SAE 77° standard day conditions,  $A_8=3078$  in<sup>2</sup>, Sideline Distance=1500 ft.

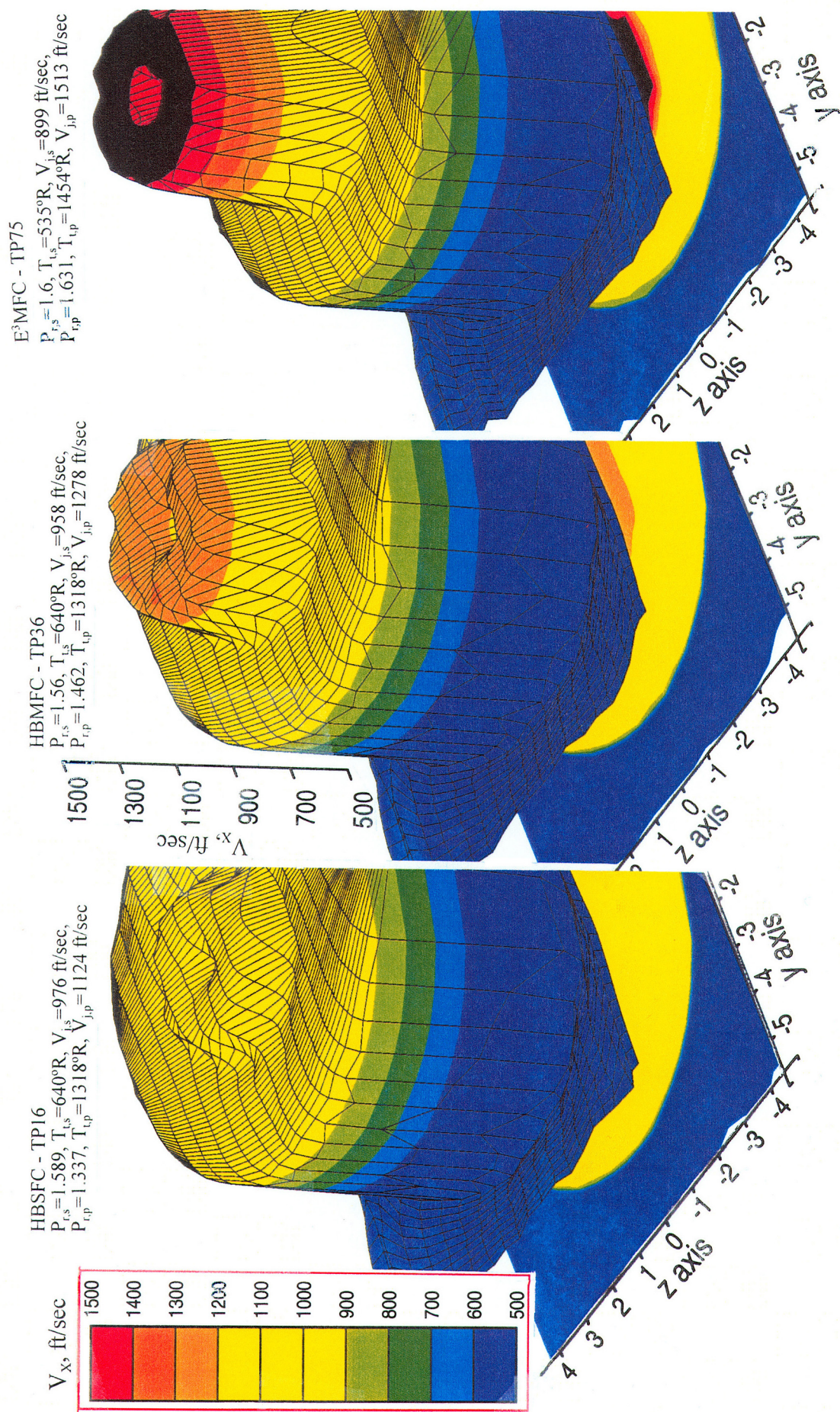


Figure 39. Effect of engine cycle on axial velocity profiles in 3-dimensional form at 0.5" downstream of the nozzle exit plane for a nominal  $V_{\text{mix}} = 1000 \text{ ft/sec}$  for model scale confluent mixer with standard fan of exit area 51.7 in<sup>2</sup>,  $M_f = 0.28$ .

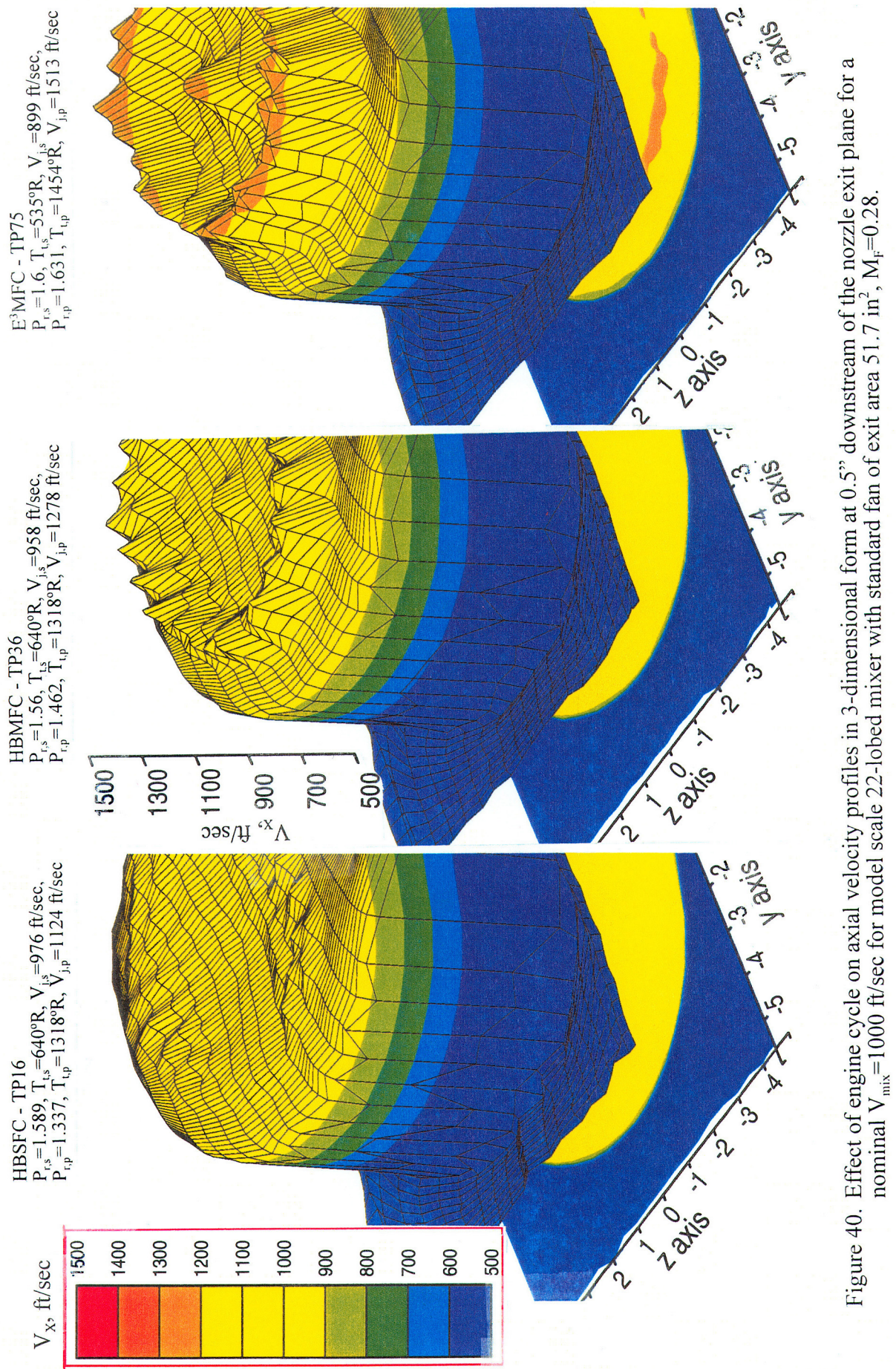


Figure 40. Effect of engine cycle on axial velocity profiles in 3-dimensional form at 0.5" downstream of the nozzle exit plane for a nominal  $V_{\text{mix}} = 1000 \text{ ft/sec}$  for model scale 22-lobed mixer with standard fan of exit area 51.7 in<sup>2</sup>,  $M_f = 0.28$ .

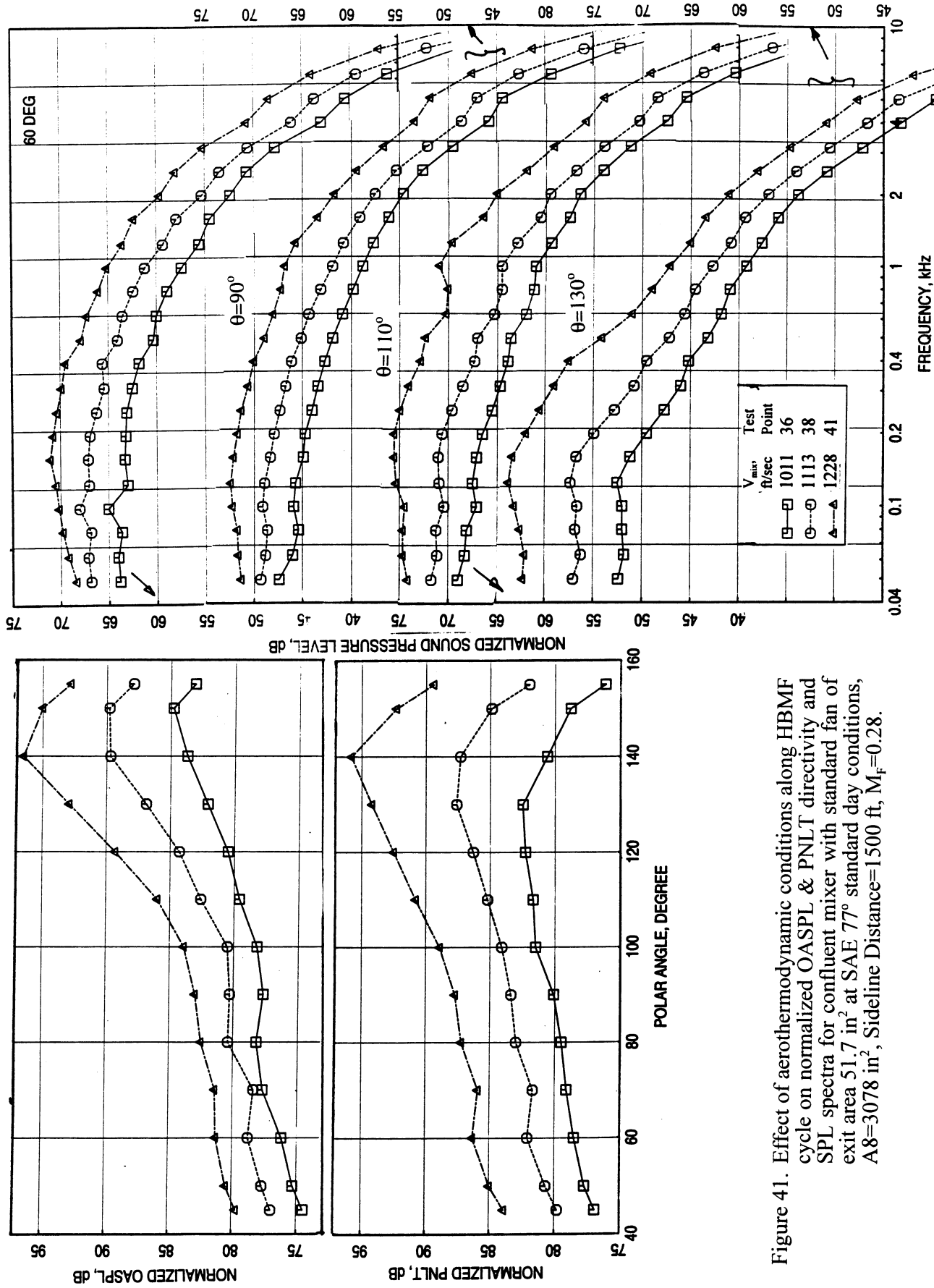


Figure 41. Effect of aerothermodynamic conditions along HBMF cycle on normalized OA SPL & PNLT directivity and SPL spectra for confluent mixer with standard fan of exit area  $51.7 \text{ in}^2$  at SAE  $77^\circ$  standard day conditions,  $A8=3078 \text{ in}^2$ , Sideline Distance=1500 ft,  $M_F=0.28$ .

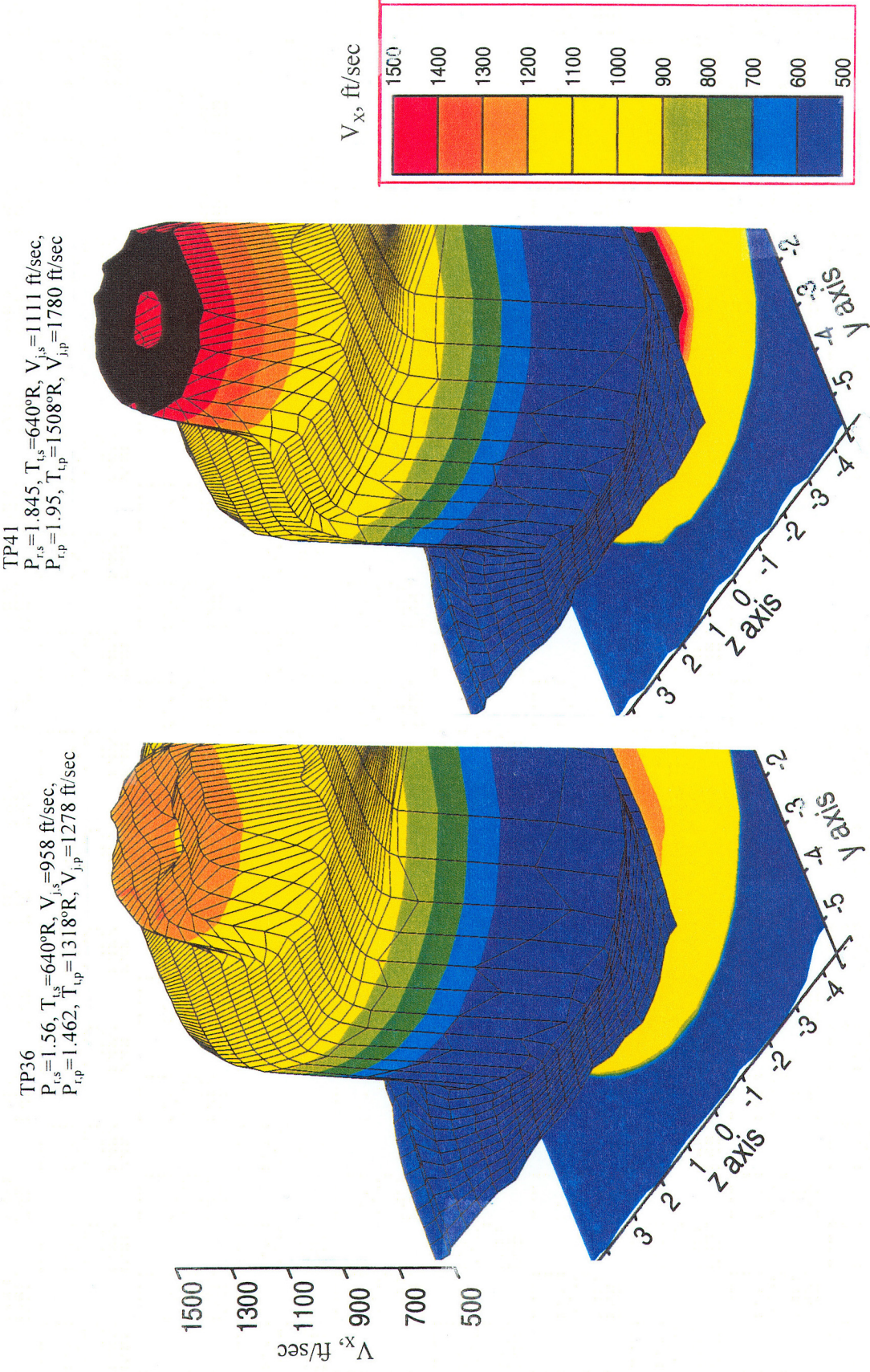


Figure 42. Effect of HBMF cycle aerothermodynamic conditions on axial velocity profiles in 3-dimensional form at 0.5" downstream of the nozzle exit plane for model scale confluent mixer with standard fan of exit area 51.7 in<sup>2</sup>,  $M_f = 0.28$ .

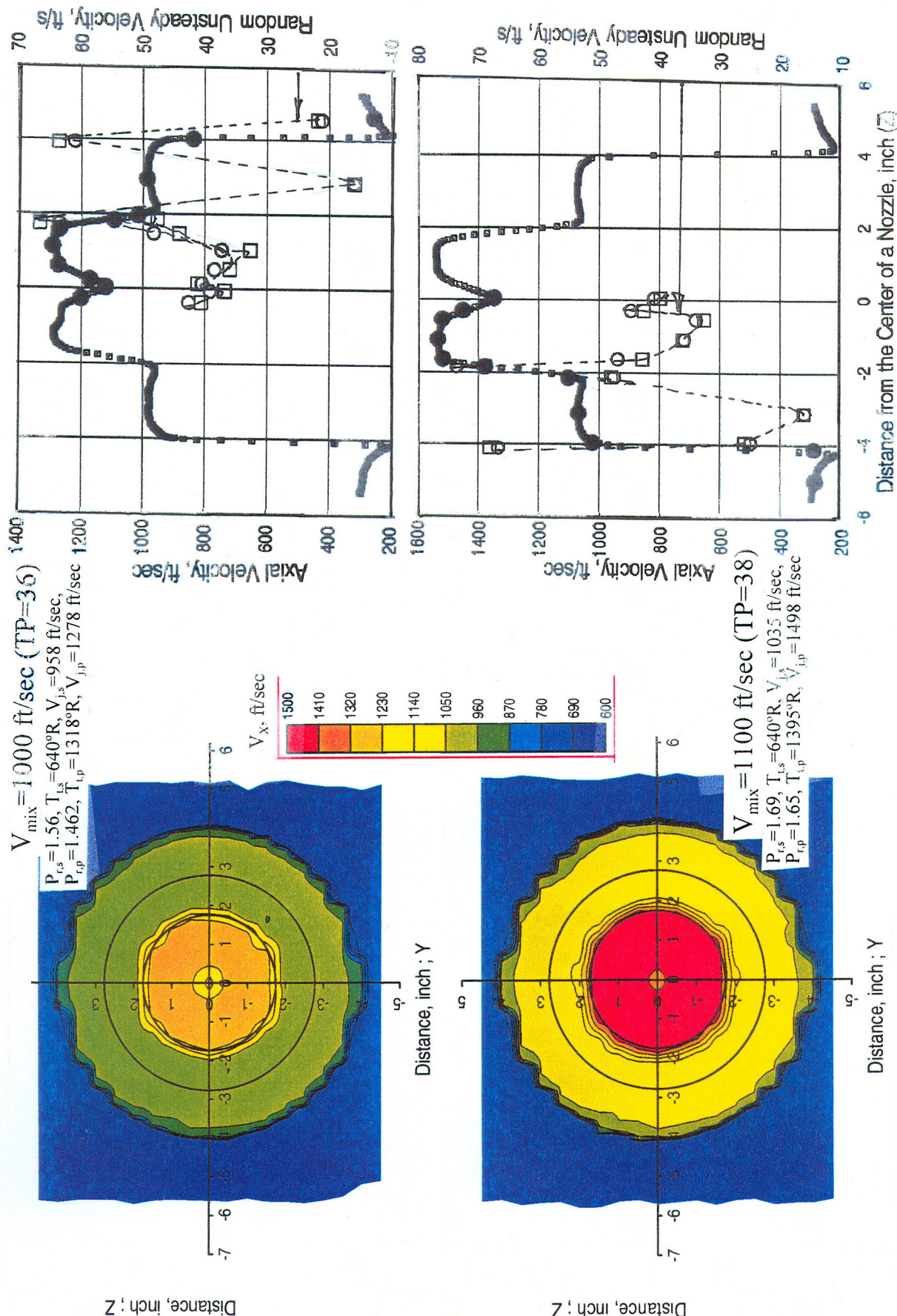


Figure 43. Effect of HBMF cycle aerothermodynamic conditions on axial velocity contours and axial velocity distributions for model scale confluent mixer with standard fan of exit area 51.7 in<sup>2</sup>, at the nozzle exit plane (X=0.5", Y=0), M<sub>f</sub>=0.28.

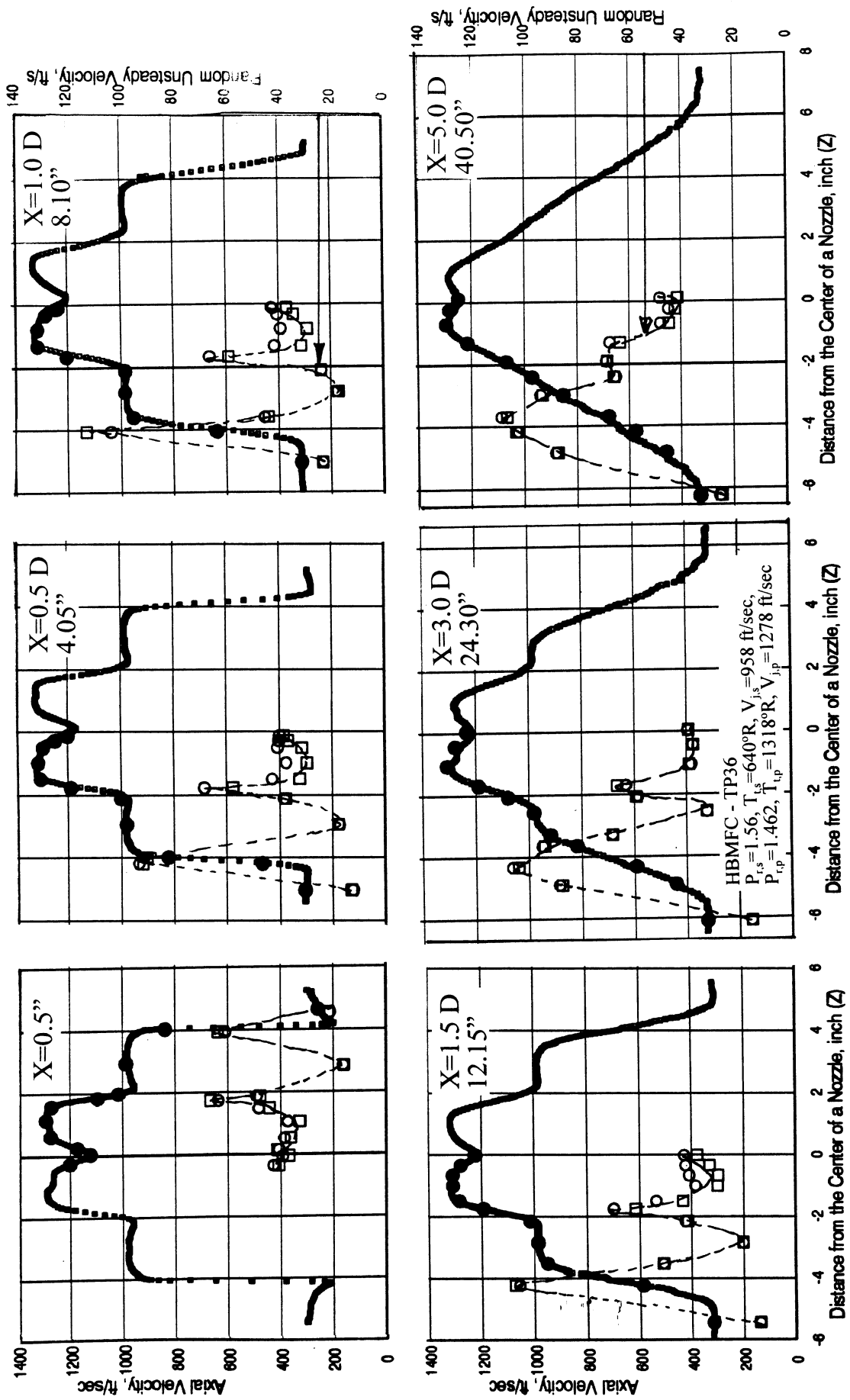


Figure 44. Axial mean and random unsteady velocity distributions at various axial locations ( $X$ ) along the centerline ( $Y=0$ ) from the nozzle exit plane for model scale confluent mixer with standard fan of exit area  $51.7 \text{ in}^2$  for high bypass mixed flow cycle (TP=36), Nominal  $V_{\text{mix}} = 1000 \text{ ft/sec}$ ,  $M_F = 0.28$ .

exit plane, at least, up to about 5 nozzle diameters downstream of the nozzle exit for this aerothermodynamic conditions (see Figure 44). Similar effects are also observed with the random unsteady velocity distributions.

Figures 45 and 46 show the effect of engine cycles on PNLT directivity and SPL spectra for confluent mixer with standard fan at nominal  $V_{mix}$  of 1000 ft/sec and 1125 ft/sec, respectively. The cycle effects on noise field are more dominant with flight simulation. The effect of simulated flight on axial velocity contours at the nozzle exit plane and axial velocity distributions at various downstream locations from the nozzle exit plane for a nominal  $V_{mix}$  of 1000 ft/sec (TP36) for HBMF cycle are shown in Figures 47 and 48, respectively. The velocity contours and profiles within the plume shear layer are not effected much by flight simulation. However, the relative velocity change due to flight simulation is the cause for noise reduction.

Noise levels are the highest for  $E^3MF$  cycle conditions and lowest for HBSF cycle conditions. The effect is more prominent at lower frequencies and at higher polar angles. The axial velocity contours and axial velocity distributions at nominal  $V_{mix}$  of 1000 ft/sec at the nozzle exit plane for different cycles are shown in Figure 49. The velocity profile is most uniform for HBSF cycle and extremely unmixed for  $E^3MF$  cycle, which is the reason for noise field variations among the cycles shown in Figure 45. The effect of engine cycle on axial velocity distributions at various axial downstream locations from the nozzle exit plane at nominal  $V_{mix}$  of 1000 ft/sec are shown in Figure 50. The nonuniformity of velocity profile continues further downstream for HBMF cycle compared to HBSF cycle.

**22-Lobed Mixer:** a Noise level due to aerothermodynamic variation along the HBMF cycle for the 22-lobed mixer nozzle with standard fan is shown in Figure 51. Sound pressure levels at all polar angles increase with increasing aerothermodynamic conditions for the entire frequency range. Similar effect is also observed for OASPL and PNLT directivities at all polar angles. Substantial sound pressure level increase is observed at higher frequency range for very high aerothermodynamic conditions (namely, at  $V_{mix}=1220$  ft/sec). The effect of aerothermodynamic condition on the flowfield is shown in Figure 52 in the form of 3-dimensional velocity profiles measured at 0.5" downstream of the nozzle exit at different test points along the HBMF cycle. The cone heights along the mixer core flow lobes and the cone height at the center increases relative to the secondary flow velocity with increasing  $V_{mix}$  condition. This effect on axial velocity contours and axial velocity distributions at 0.5" downstream of the nozzle exit plane is shown in Figure 53. Axial velocity levels increase with increasing aerothermodynamic conditions. The core stream velocity increase due to aerothermodynamic condition is higher compared to fan stream velocity, resulting into a higher uneven velocity profile at the higher aerothermodynamic conditions.

The evolution of mean axial velocity distributions along the nozzle axis, downstream of the nozzle exit plane, for different aerothermodynamic conditions for HBMF cycle is shown in Figure 54. Distinct velocity peaks due to mixer lobes are observed in the

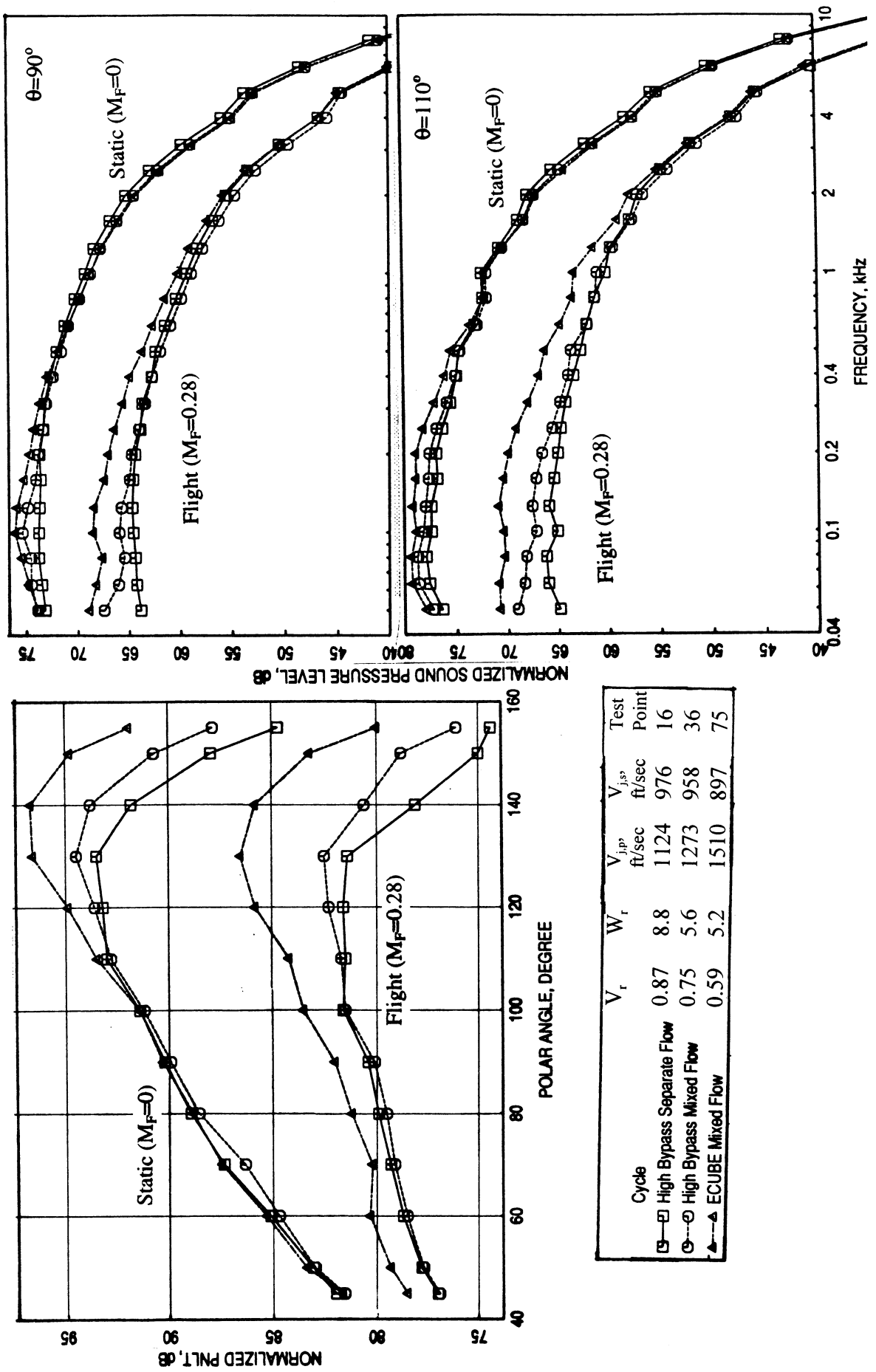


Figure 45. Effect of engine cycle on normalized PNLT directivity and SPL spectra at a nominal  $V_{\text{mix}} = 1000$  ft/sec for confluent mixer with standard fan of exit area  $51.7 \text{ in}^2$  at SAE 77° standard day conditions,  $A_8 = 3078 \text{ in}^2$ , Sideline Distance = 1500 ft.

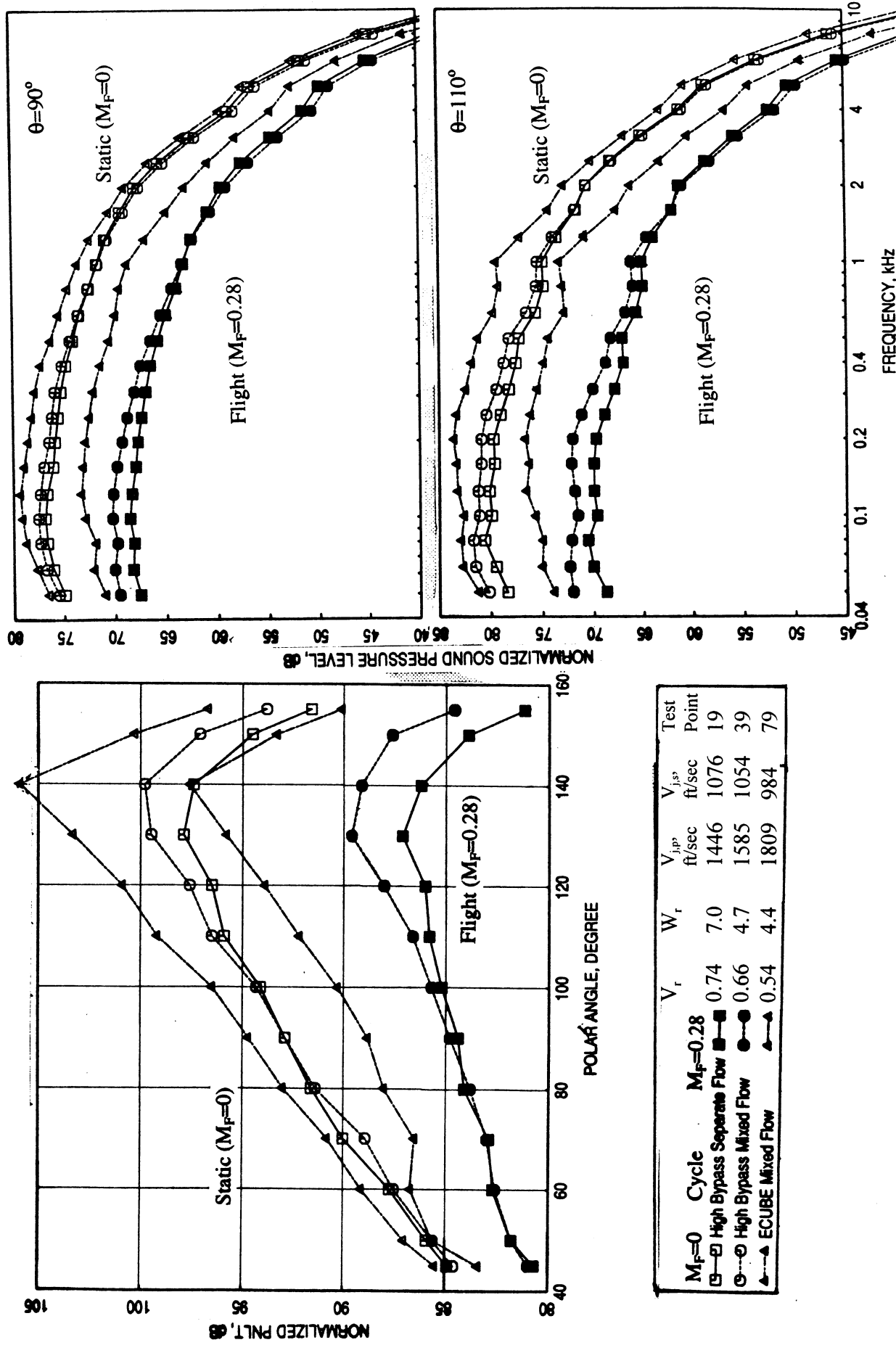


Figure 46. Effect of engine cycle on normalized PNLT directivity and SPL spectra at a nominal  $V_{\text{mix}} = 1125$  ft/sec for confluent mixer with standard fan of exit area  $51.7 \text{ in}^2$  at SAE  $77^\circ$  standard day conditions,  $A_8 = 3078 \text{ in}^2$ , Sideline Distance = 1500 ft.

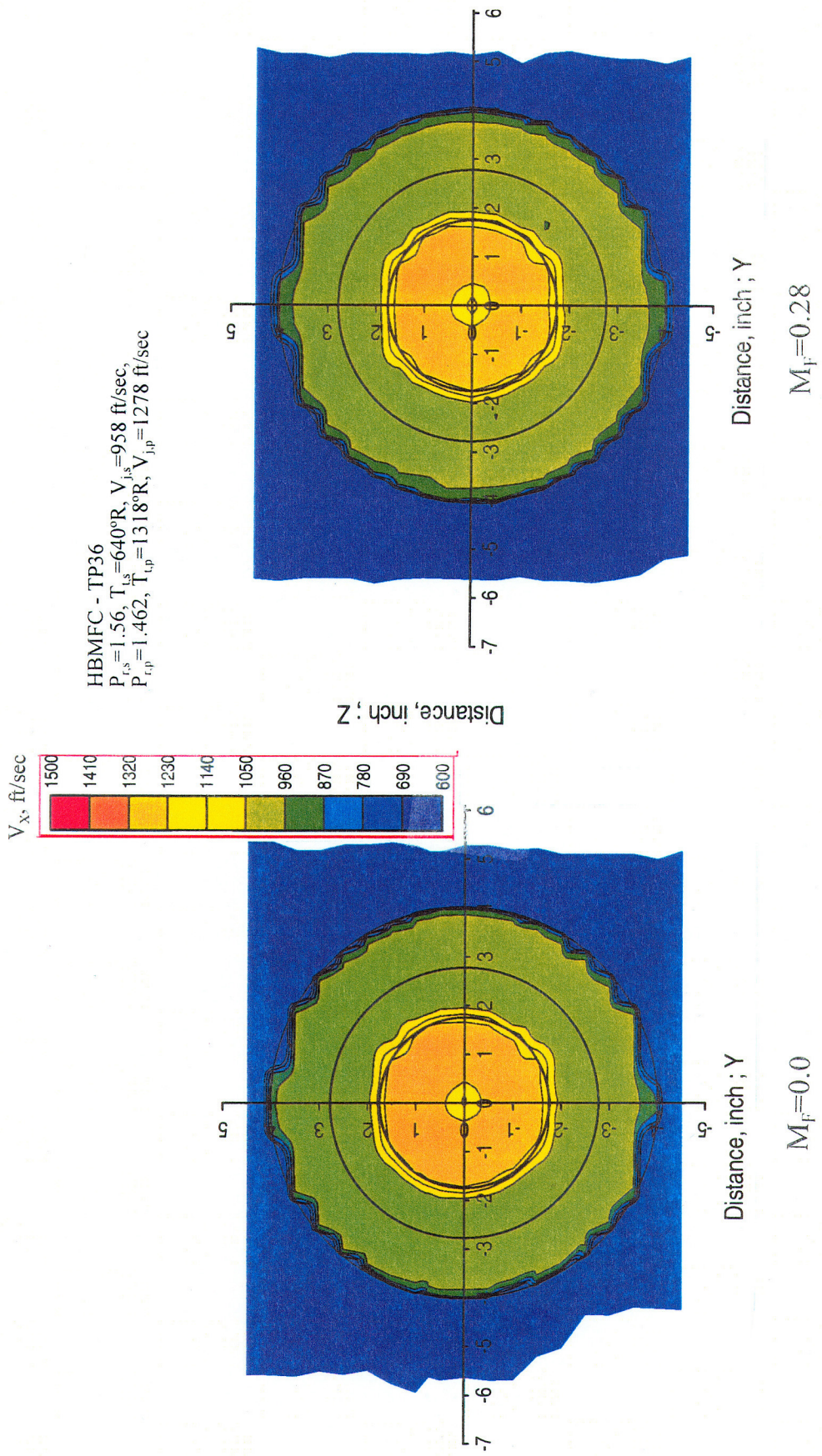
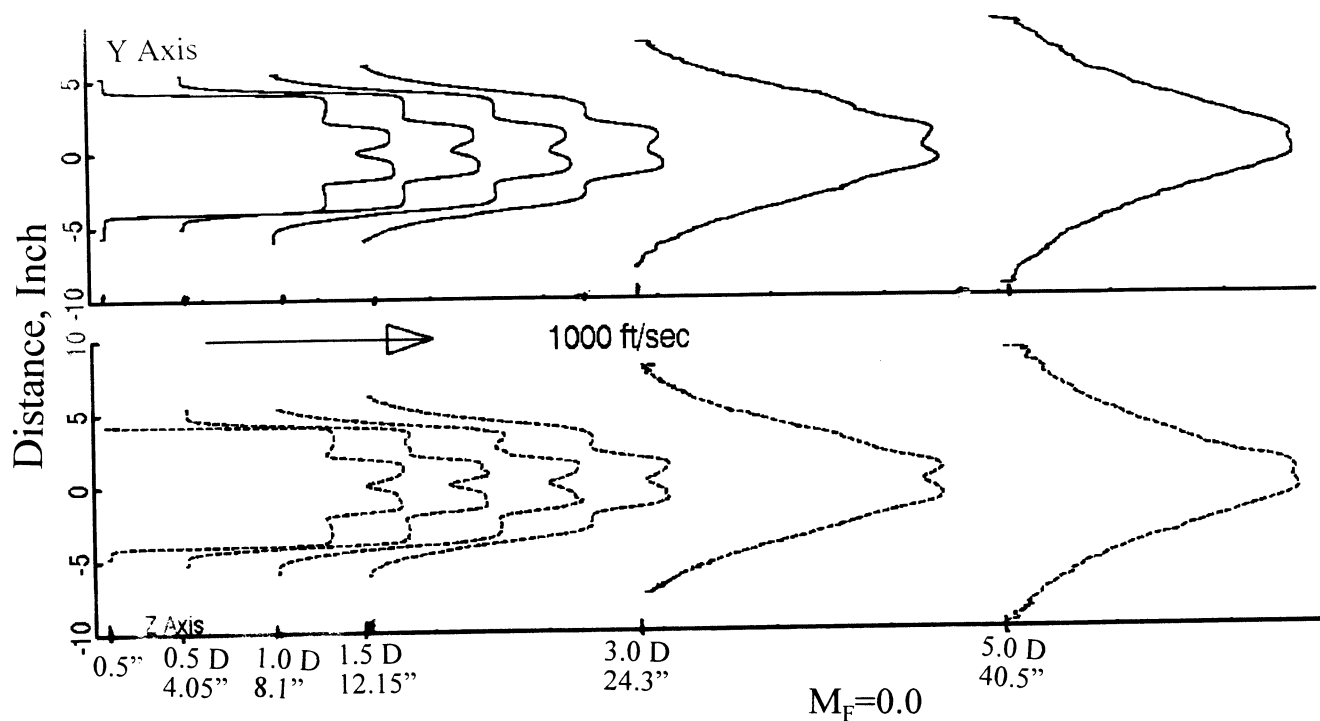


Figure 47. Effect of simulated flight on axial velocity contours for model scale confluent mixer with standard fan of exit area  $51.7 \text{ in}^2$ , at the nozzle exit plane ( $X=0.5''$ ,  $Y=0$ ) for high bypass mixed flow cycle (TP=36), Nominal  $V_{mix} = 1000 \text{ ft/sec}$ .



$$P_{r,s} = 1.56, T_{t,s} = 640^\circ R, V_{j,s} = 958 \text{ ft/sec}, \\ P_{r,p} = 1.462, T_{t,p} = 1318^\circ R, V_{j,p} = 1278 \text{ ft/sec}$$

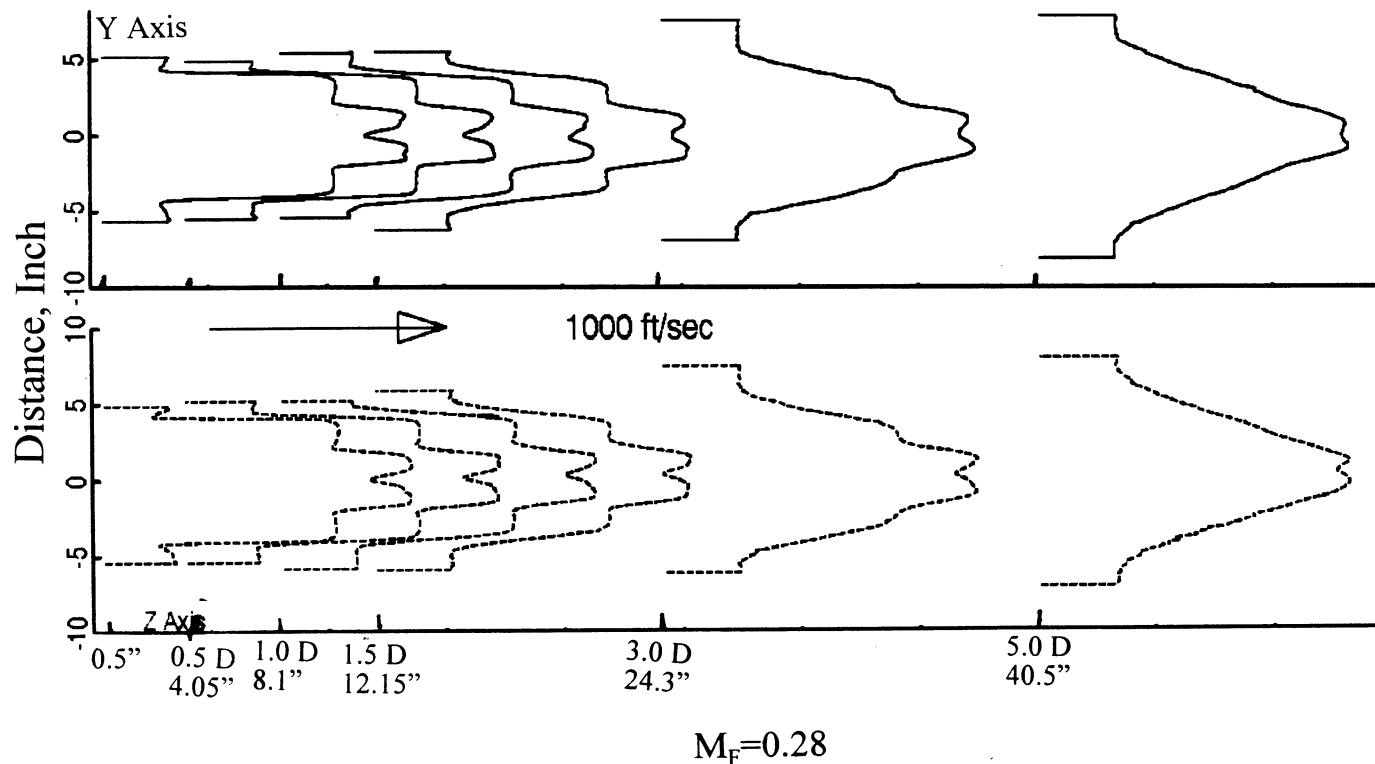
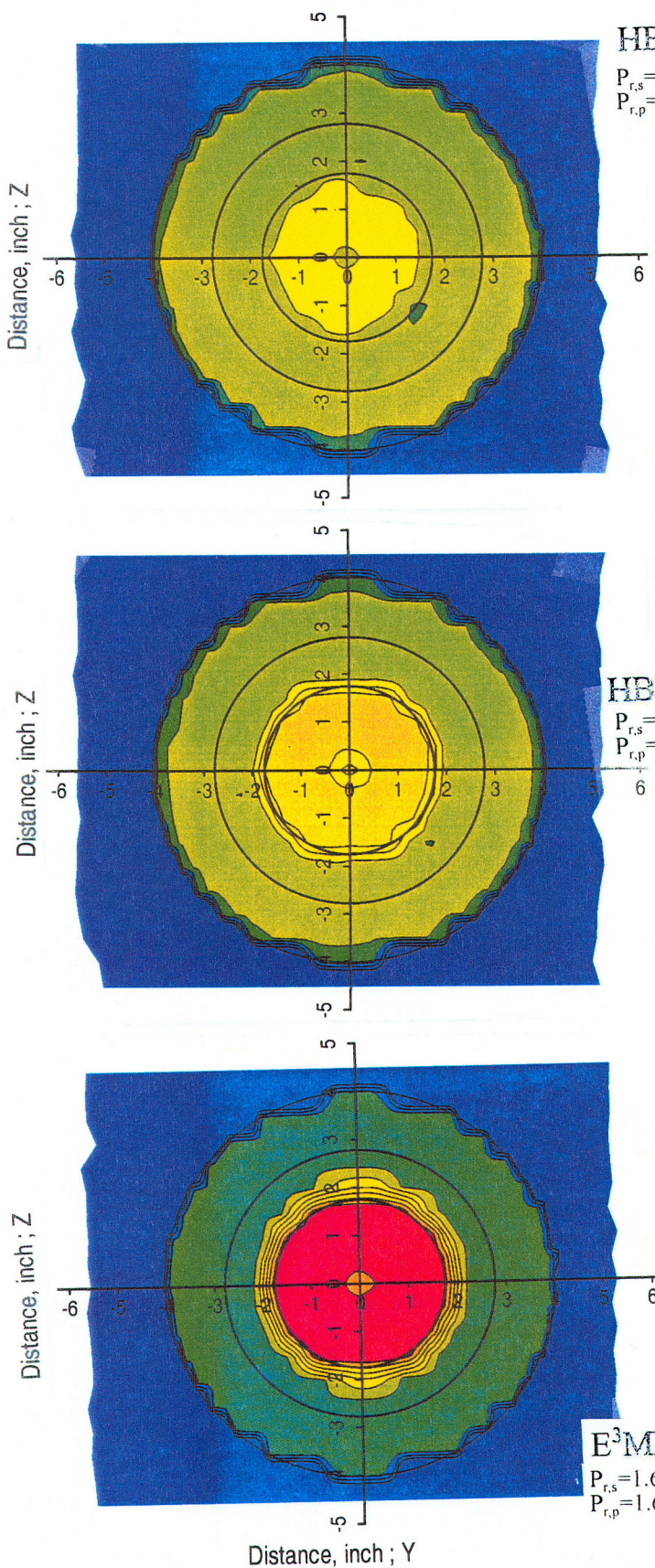


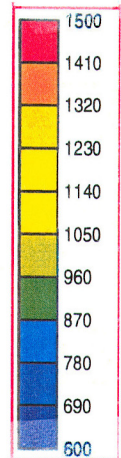
Figure 48. Effect of simulated flight on axial velocity distribution at various axial downstream locations from the nozzle exit plane for model scale confluent mixer with standard fan of exit area  $51.7 \text{ in}^2$  for high bypass mixed flow cycle ( $TP=36$ ), Nominal  $V_{\text{mix}} = 1000 \text{ ft/sec}$ .



HBSFC (TP16)

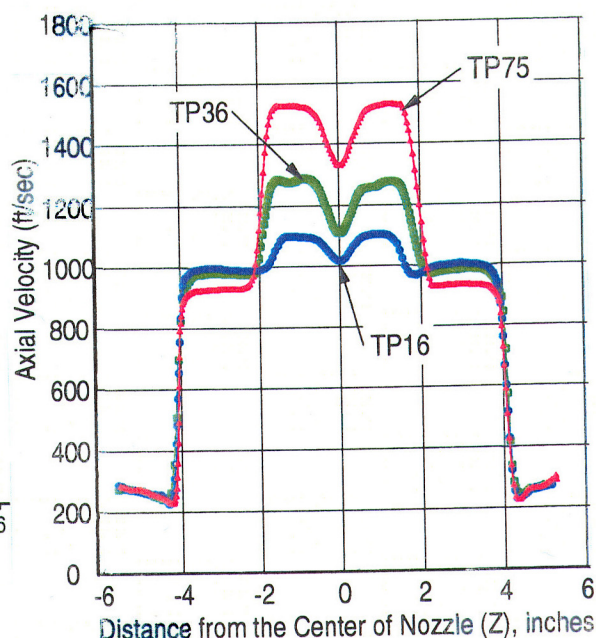
$P_{r,s} = 1.589, T_{t,s} = 640^\circ R, V_{j,s} = 976 \text{ ft/sec}$ ,  
 $P_{r,p} = 1.337, T_{t,p} = 1318^\circ R, V_{j,p} = 1124 \text{ ft/sec}$

$V_x, \text{ ft/sec}$



HBMFC (TP36)

$P_{r,s} = 1.56, T_{t,s} = 640^\circ R, V_{j,s} = 958 \text{ ft/sec}$ ,  
 $P_{r,p} = 1.462, T_{t,p} = 1318^\circ R, V_{j,p} = 1278 \text{ ft/sec}$



E<sup>3</sup>MFC (TP75)

$P_{r,s} = 1.6, T_{t,s} = 535^\circ R, V_{j,s} = 899 \text{ ft/sec}$ ,  
 $P_{r,p} = 1.631, T_{t,p} = 1454^\circ R, V_{j,p} = 1513 \text{ ft/sec}$

Figure 49. Effect of engine cycle on axial velocity contours and axial velocity distributions for model scale confluent mixer with standard fan of exit area  $51.7 \text{ in}^2$  at the nozzle exit plane ( $X=0.5''$ ,  $Y=0$  ), Nominal  $V_{\text{mix}}=1000 \text{ ft/sec}$ ,  $M_F=0.28$ .

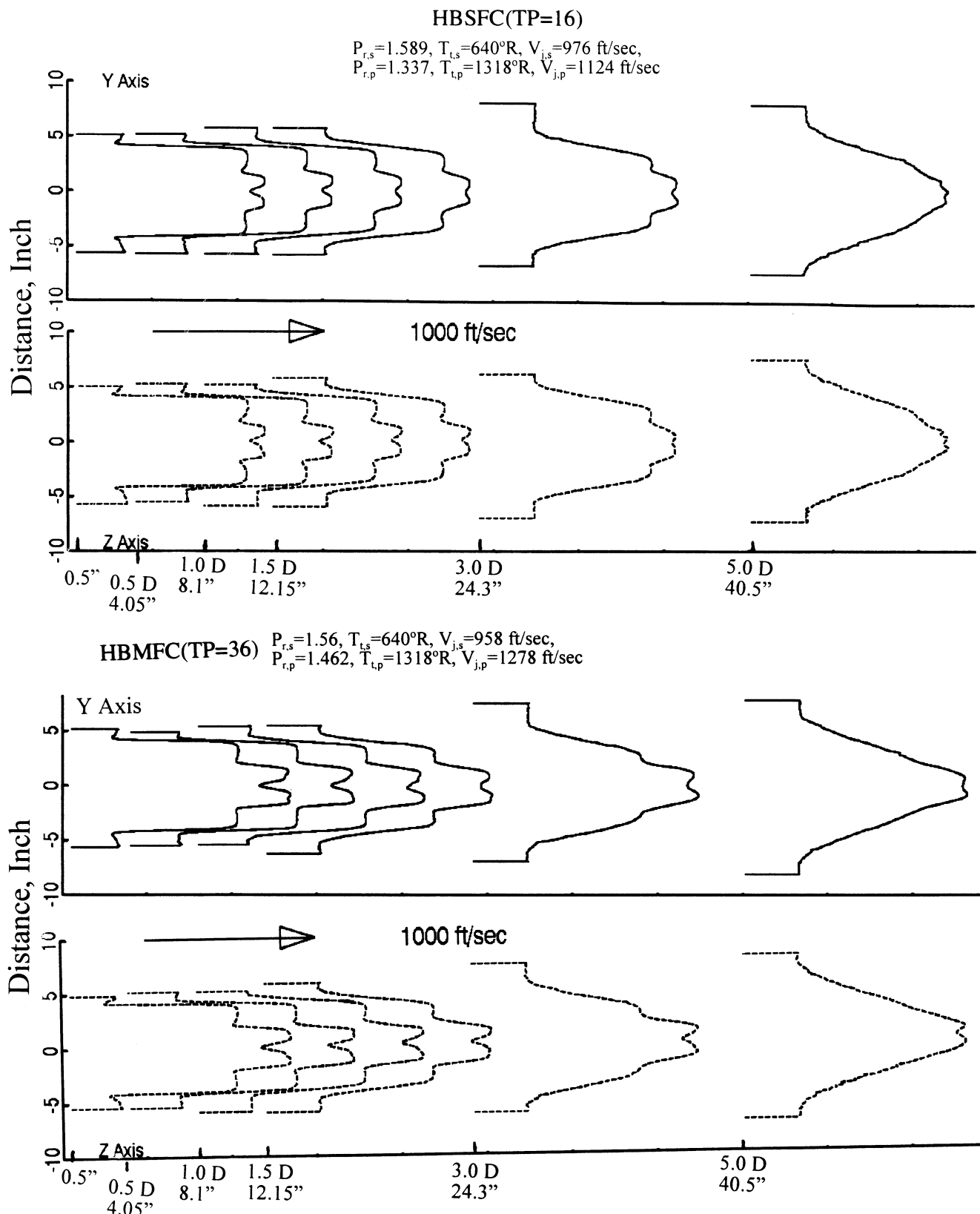


Figure 50. Effect of engine cycle on axial velocity distributions at various axial downstream locations (X) from the nozzle exit plane for model scale confluent mixer with standard fan of exit area  $51.7 \text{ in}^2$ , Nominal  $V_{\text{mix}}=1000 \text{ ft/sec}$ ,  $M_F=0.28$ .

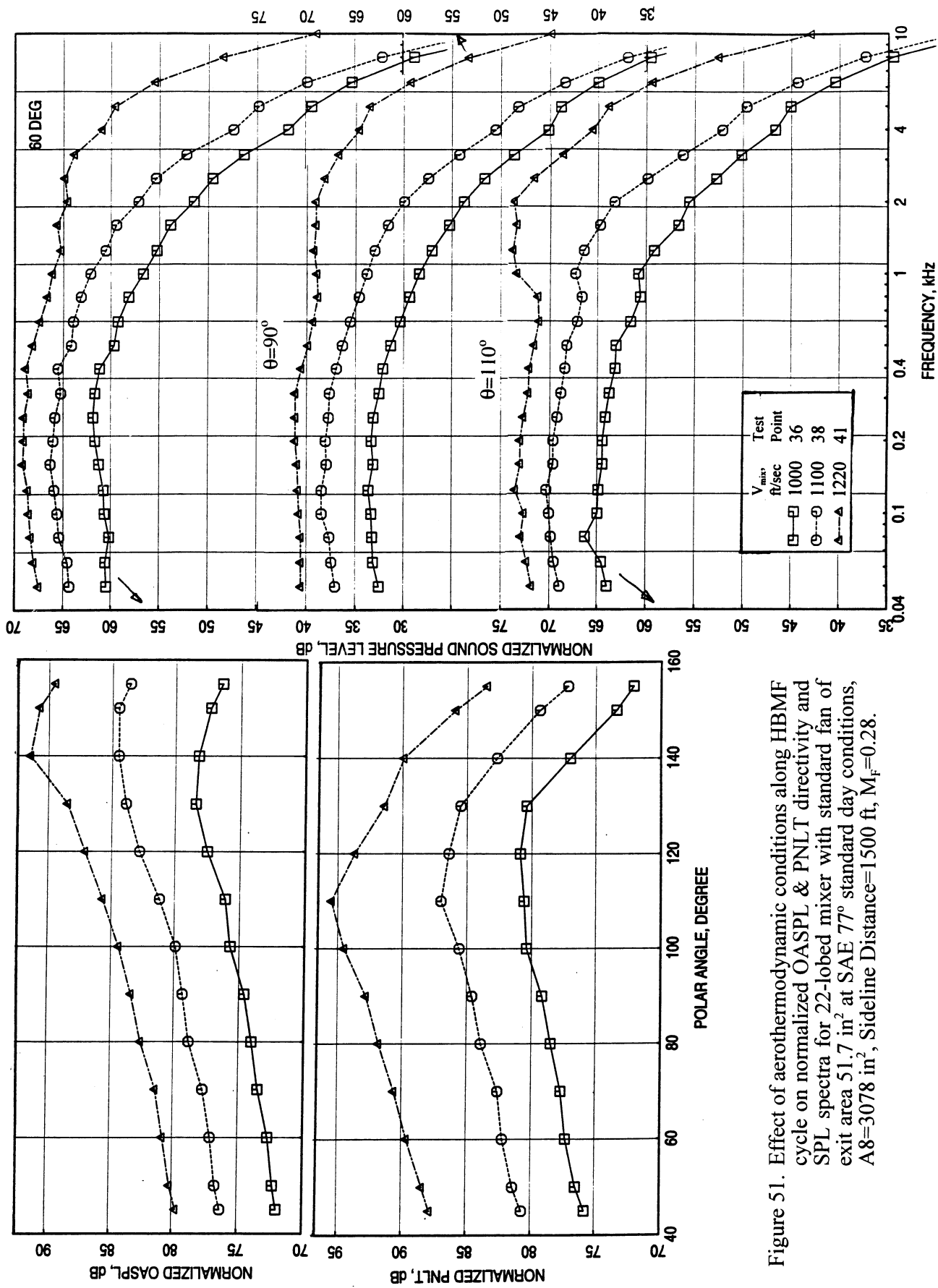
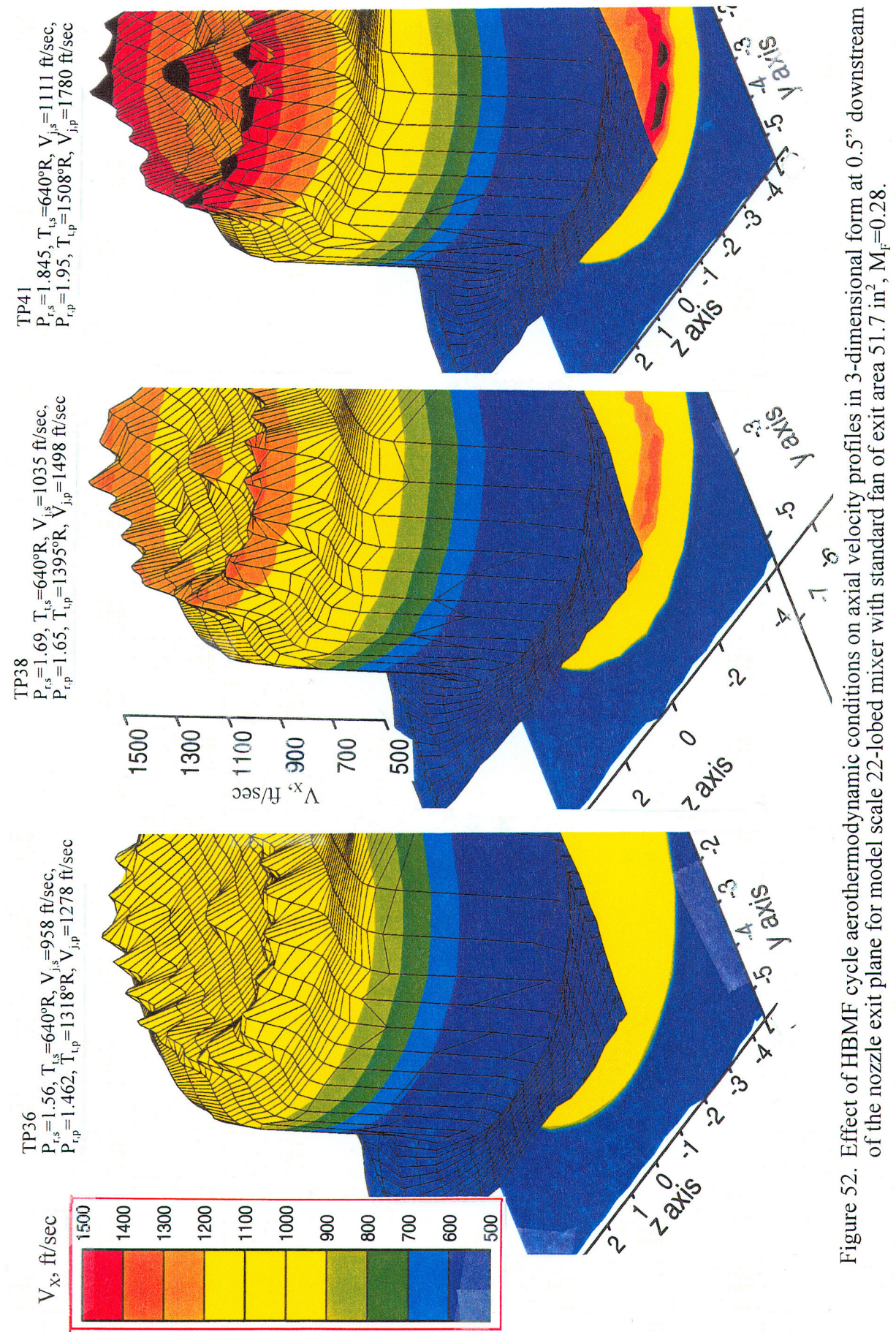


Figure 51. Effect of aerothermodynamic conditions along HBMF cycle on normalized OASPL & PNLT directivity and SPL spectra for 22-lobed mixer with standard fan of exit area  $51.7 \text{ in}^2$  at SAE  $77^\circ$  standard day conditions,  $A_8=3078 \text{ in}^2$ , Sideline Distance=1500 ft,  $M_F=0.28$ .



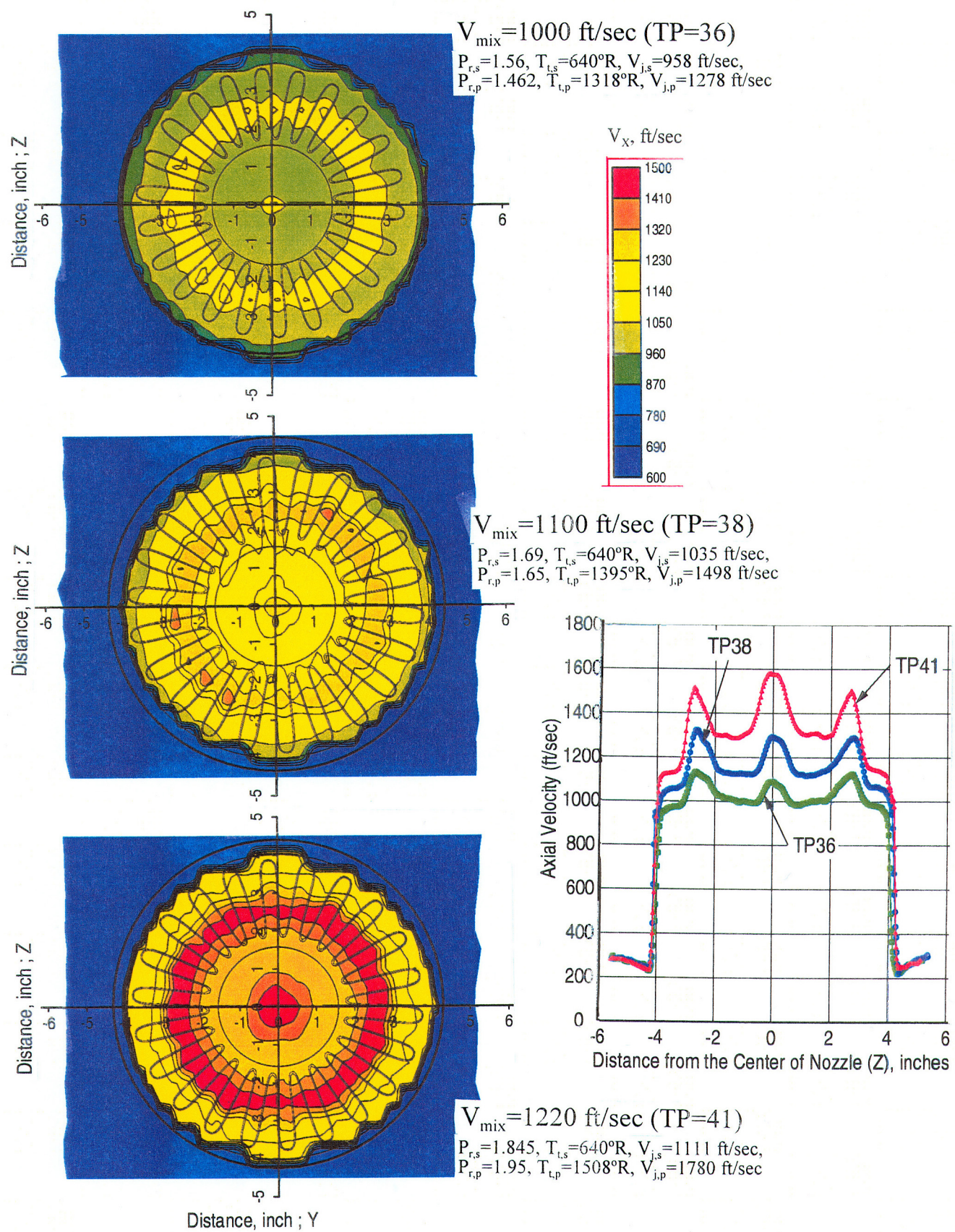


Figure 53. Effect of aerothermodynamic conditions on axial velocity contours and axial velocity distributions for the model scale 22-lobed mixer with standard fan of exit area  $51.7 \text{ in}^2$  at the nozzle exit plane ( $X=0.5"$ ,  $Y=0$ ) for high bypass mixed flow cycle,  $M_F=0.28$ .

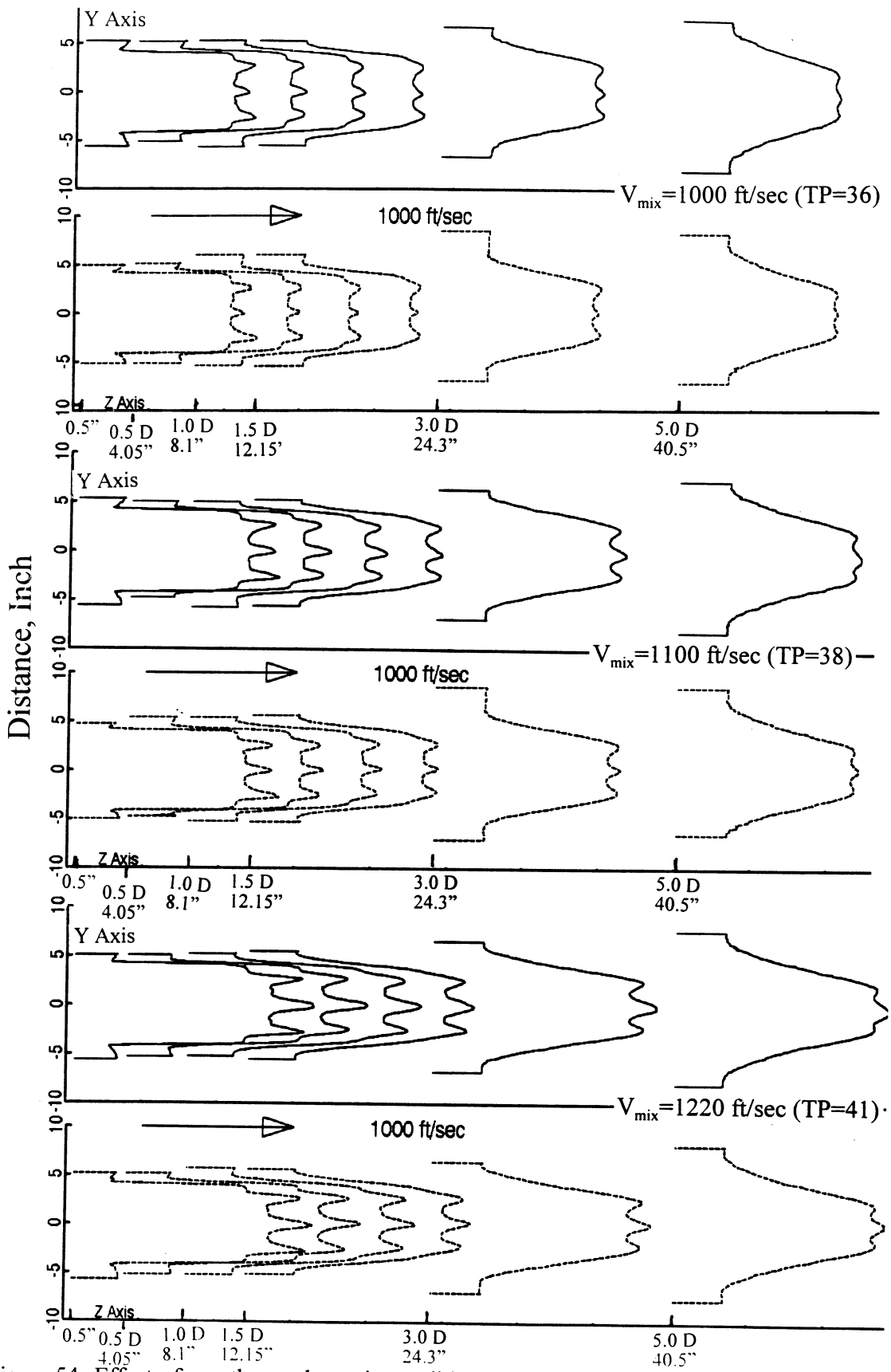


Figure 54. Effect of aerothermodynamic conditions on axial velocity distributions at various axial downstream locations (X) from the nozzle exit plane for the model scale 22-lobed mixer with standard fan of exit area  $51.7 \text{ in}^2$  for high bypass mixed flow cycle,  $M_F=0.28$ .

velocity profiles closer to the nozzle exit. The mixing process continues outside the nozzle exit plane downstream of the nozzle exit. For higher aerothermodynamic conditions the velocity peaks and valleys continue to exist even at 5 nozzle diameters, downstream of the nozzle exit.

Figures 55 and 56 show the effect of engine cycles on PNLT directivity and SPL spectra for 22-lobed mixer with standard fan at nominal  $V_{mix}$  of 1000 ft/sec and 1125 ft/sec, respectively. The cycle effects on noise field are more dominant with flight simulation. The effect of simulated flight on axial velocity contours and velocity distributions at the nozzle exit plane and axial velocity distributions at various downstream locations from the nozzle exit plane for a nominal  $V_{mix}$  of 1000 ft/sec (TP36) for HBMF cycle are shown in Figures 57 and 58, respectively. The velocity contours and profiles within the plume shear layer are not effected much by flight simulation. However, the relative velocity change due to flight simulation is the cause for noise reduction.

Noise levels are the highest for  $E^3$ MF cycle conditions, similar to confluent mixer. However, the lowest noise levels are achieved for HBMF cycle points, especially at lower  $V_{mix}$  conditions, indicating the effectiveness of the lobed mixer in mixing process. The axial velocity contours and axial velocity distributions at nominal  $V_{mix}$  of 1000 ft/sec at the nozzle exit plane for different cycles are shown in Figure 59. The velocity profile is most uniform for HBSF cycle and extremely unmixed for  $E^3$ MF cycle, which is the reason for noise field variations among the cycles shown in Figure 55. The effect of engine cycle on axial velocity distributions at various axial downstream locations from the nozzle exit plane at nominal  $V_{mix}$  of 1000 ft/sec are shown in Figure 60. The nonuniformity of velocity profile continues further downstream, especially for  $E^3$ MF cycle compared to HBSF cycle.

The pressure ratios for both the streams are relatively lower for the current high bypass cycles compared to  $E^3$  mixed flow cycle at fixed mixed jet velocities. The fan stream temperatures at higher mixed jet velocities for the current high bypass cycles are higher compared to  $E^3$  mixed flow cycle. Thus, for the same mixed jet velocity, the  $E^3$  mixed flow cycle generates much higher core velocity compared to the current high bypass cycles. Thus the noise level for  $E^3$  mixed flow cycle is higher relative to the high bypass mixed flow cycle due to higher core velocity. Noise reduction due to simulated flight is lower for  $E^3$  mixed flow cycle conditions compared to the high bypass mixed flow cycle due to reduced velocity ratio effect (shear effect based on flight to jet velocity ratio) due to higher core velocity at lower frequencies and higher level of "Unmixedness" possibly due to lower secondary to primary stream velocity ratio at higher frequencies.

Substantial noise reduction is achievable by lowering core velocity with appropriate engine cycles.

**6.3 Effect of Mixer Geometry on Farfield Noise Level and Plume Flowfield:** Figure 61 shows the EPNL variation with respect to  $V_{mix}$  for confluent and multi-lobed mixers with standard fan at different cycle conditions. The multi-lobed mixers include a 12-lobed

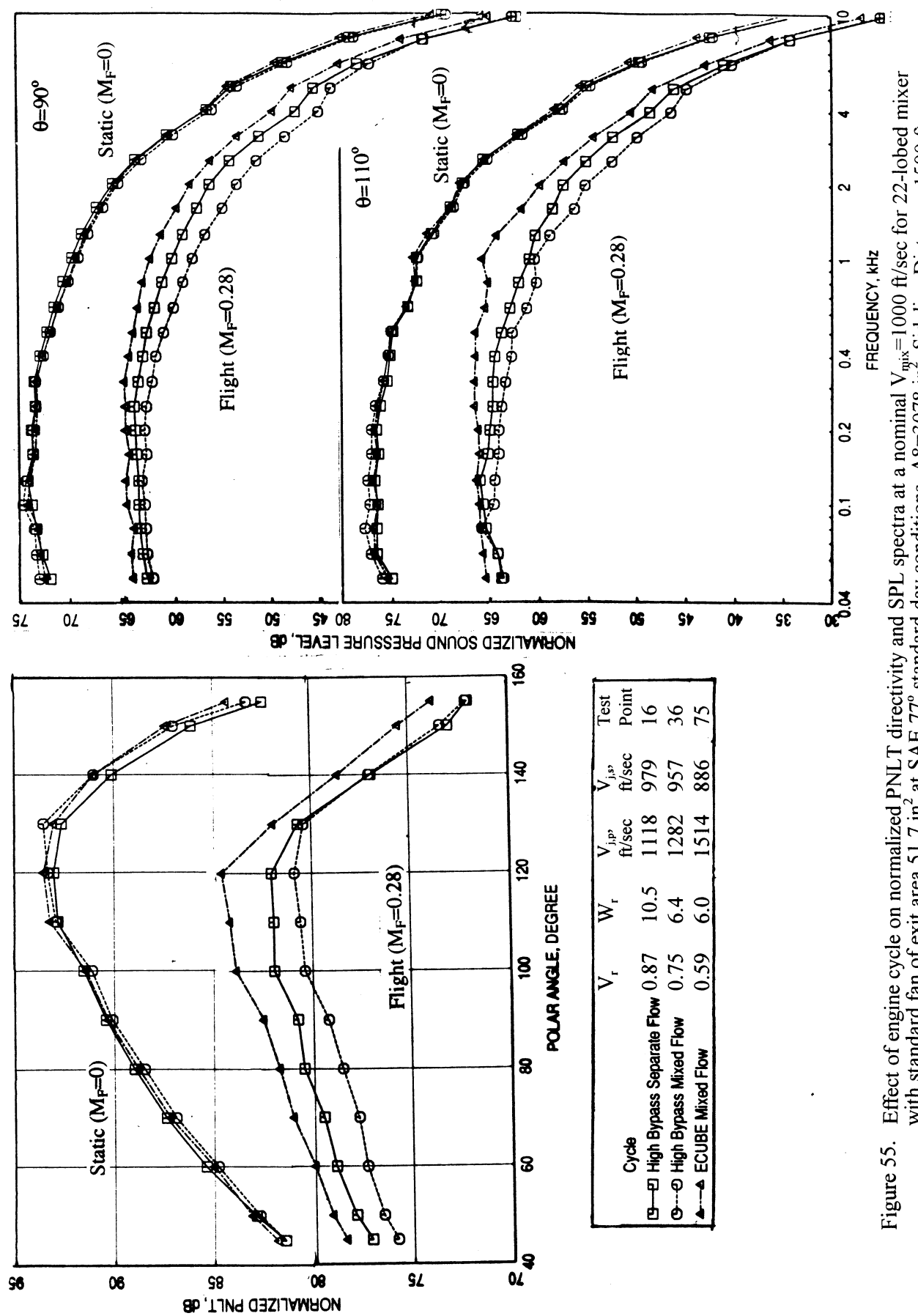


Figure 55. Effect of engine cycle on normalized PNLT directivity and SPL spectra at a nominal  $V_{\text{mix}} = 1000$  ft/sec for 22-lobed mixer with standard fan of exit area  $51.7 \text{ in}^2$  at SAE 77° standard day conditions,  $A_8 = 3078 \text{ in}^2$ , Sideline Distance = 1500 ft.

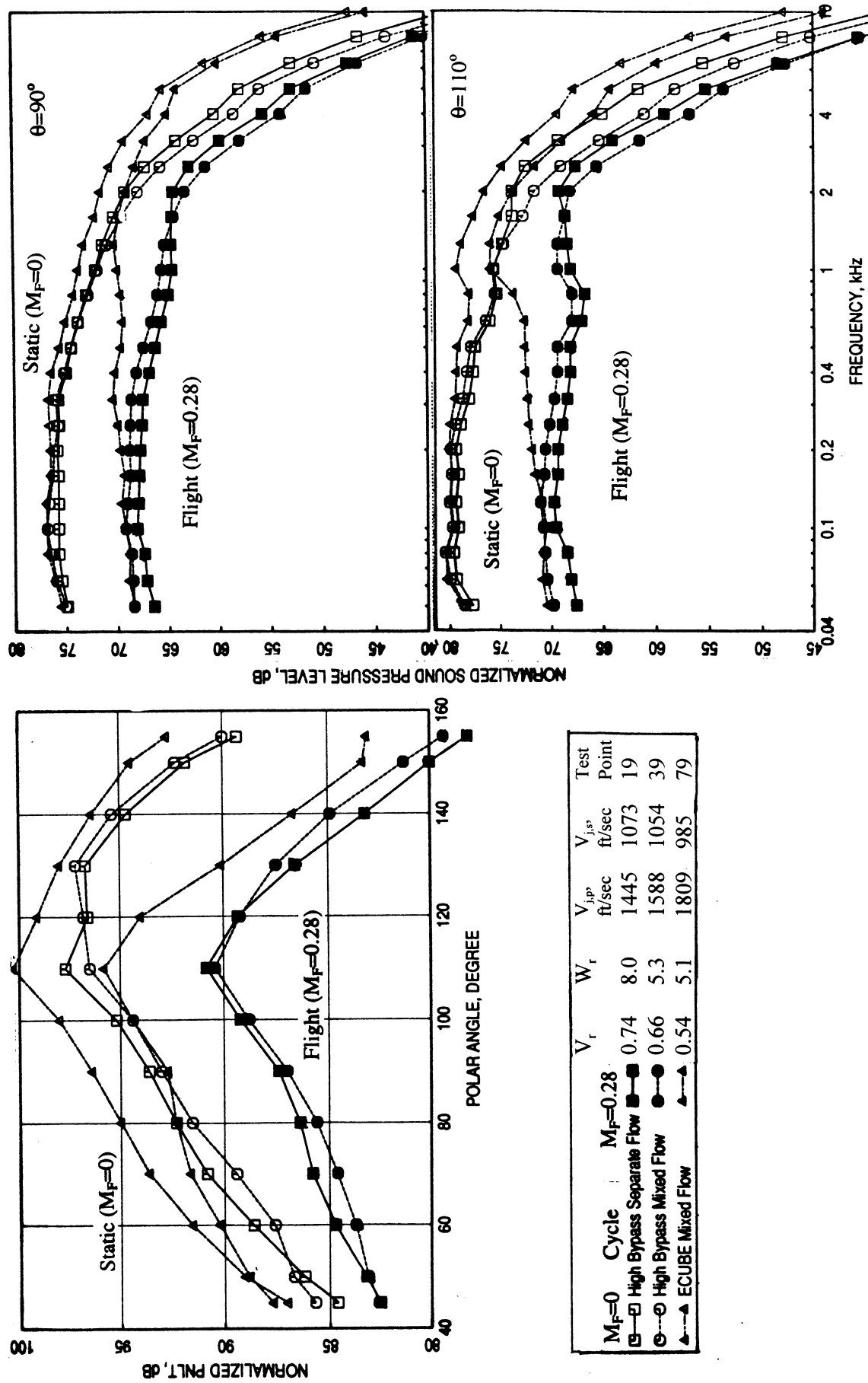


Figure 56. Effect of engine cycle on normalized PNLT directivity and SPL spectra at a nominal  $V_{mix}^2 = 1125$  ft/sec for 22-lobed mixer with standard fan of exit area  $51.7 \text{ in}^2$  at SAE 77° standard day conditions,  $A_8 = 3078 \text{ in}^2$ , Sideline Distance = 1500 ft.

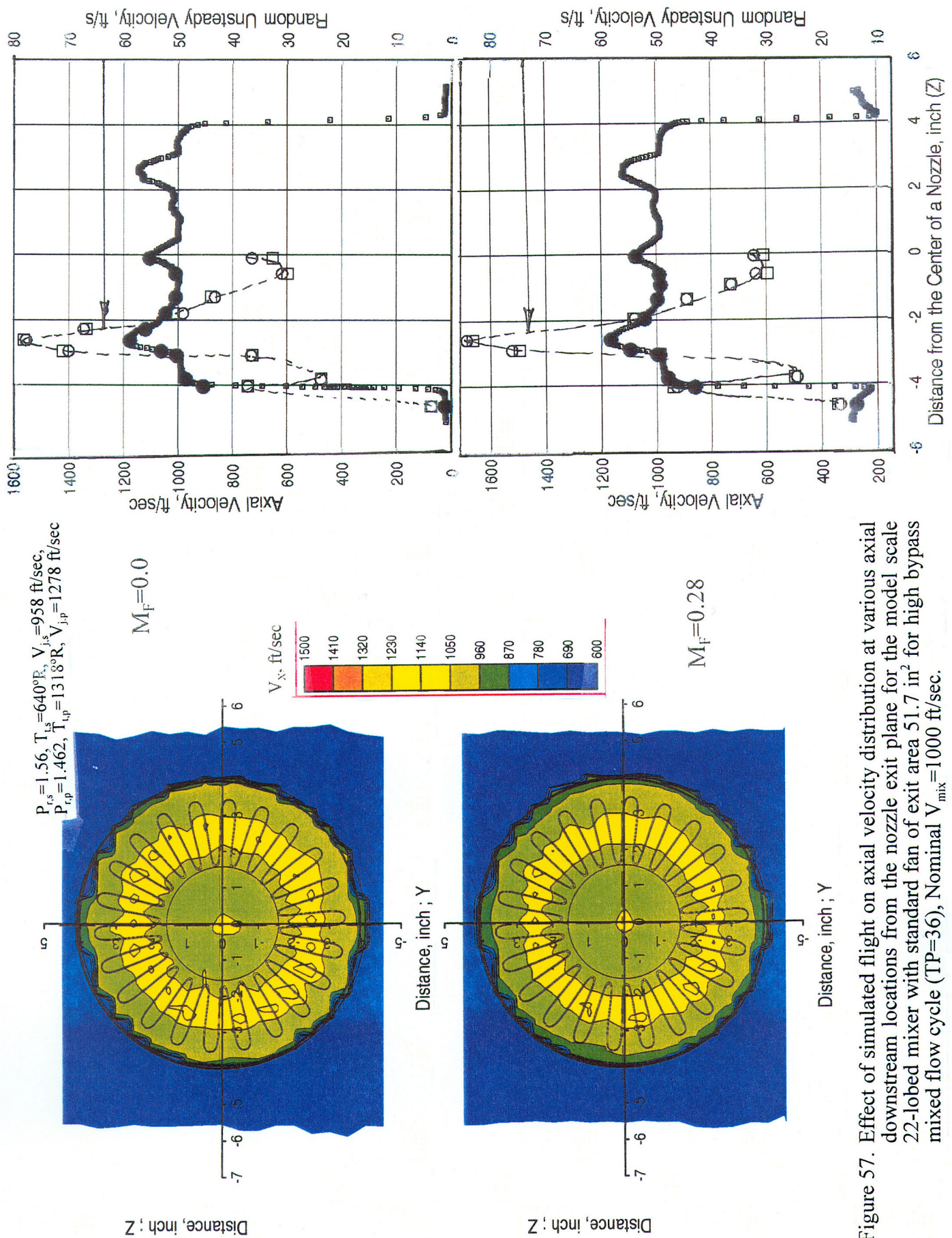
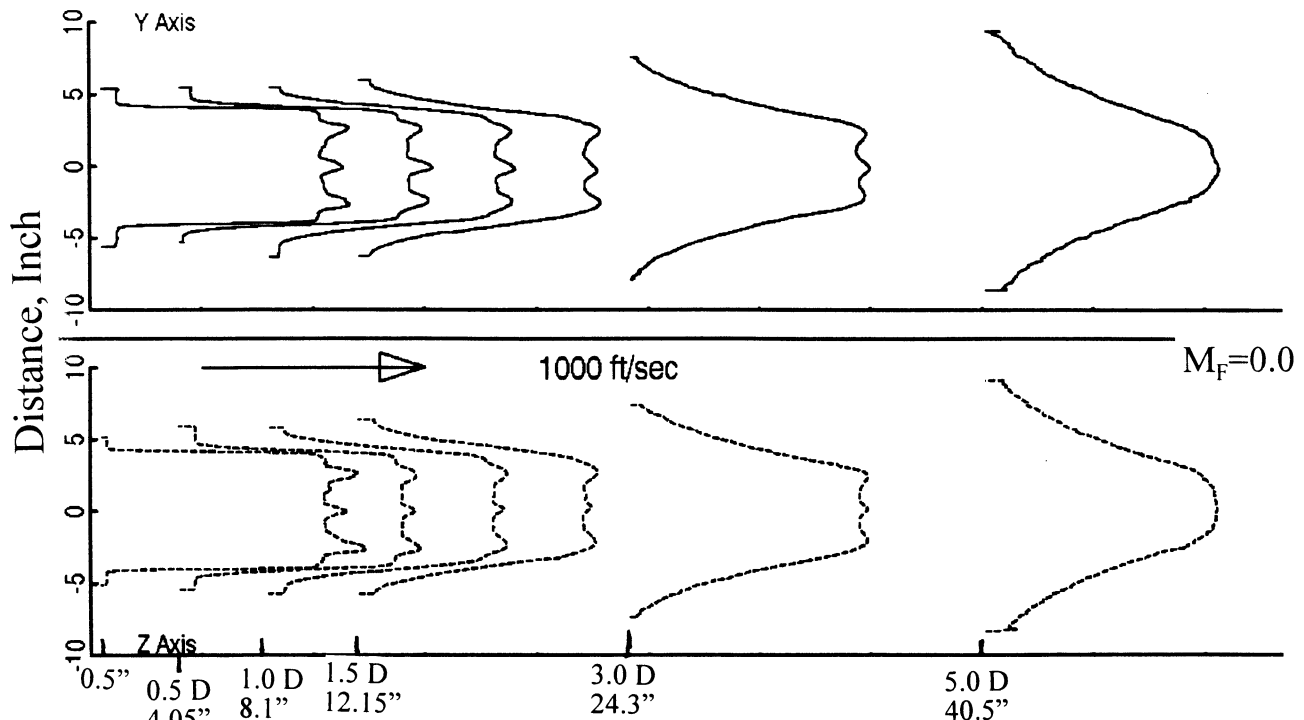


Figure 57. Effect of simulated flight on axial velocity distribution at various axial downstream locations from the nozzle exit plane for the model scale 22-lobe mixer with standard fan of exit area 51.7 in<sup>2</sup> for high bypass mixed flow cycle (TP=36), Nominal  $V_{mix} = 1000$  ft/sec.



$P_{r,s} = 1.56, T_{t,s} = 640^{\circ}\text{R}, V_{j,s} = 958 \text{ ft/sec}$ ,  
 $P_{r,p} = 1.462, T_{t,p} = 1318^{\circ}\text{R}, V_{j,p} = 1278 \text{ ft/sec}$

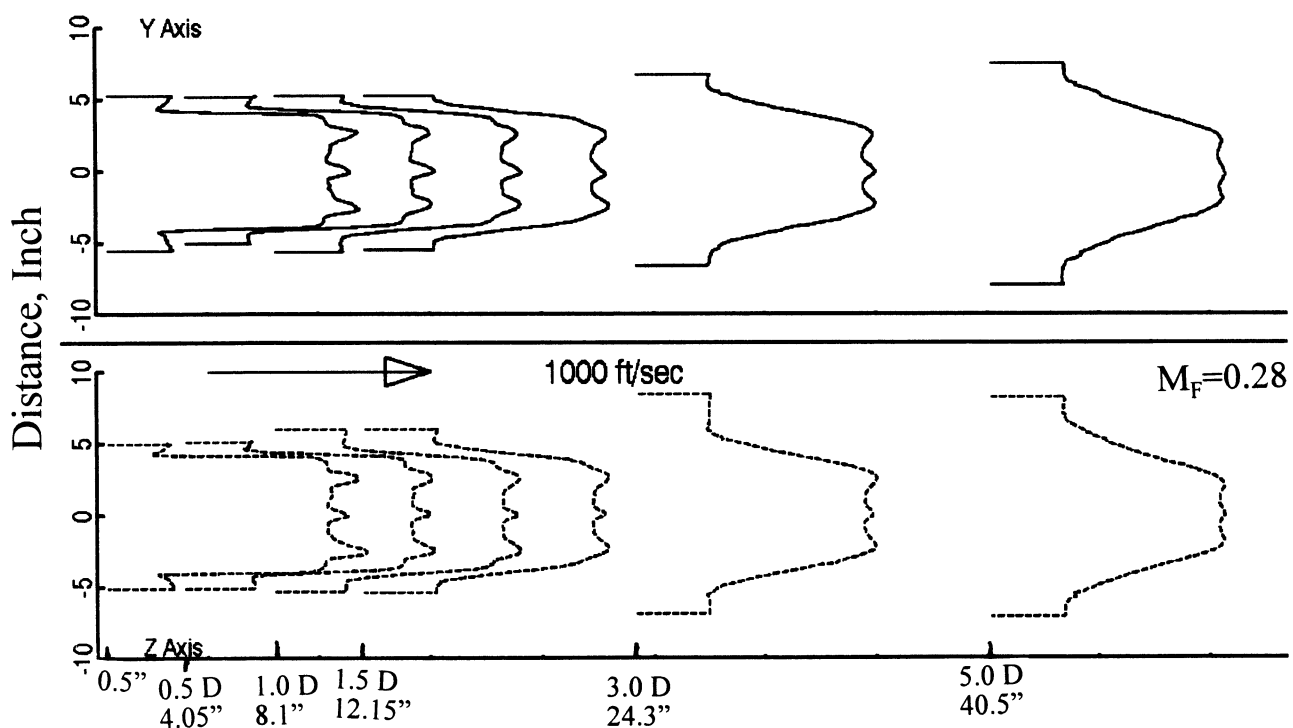


Figure 58. Effect of simulated flight on axial velocity distribution at various axial downstream locations from the nozzle exit plane for the model scale 22-lobed mixer with standard fan of exit area  $51.7 \text{ in}^2$  for high bypass mixed flow cycle (TP=36), Nominal  $V_{\text{mix}} = 1000 \text{ ft/sec}$ .

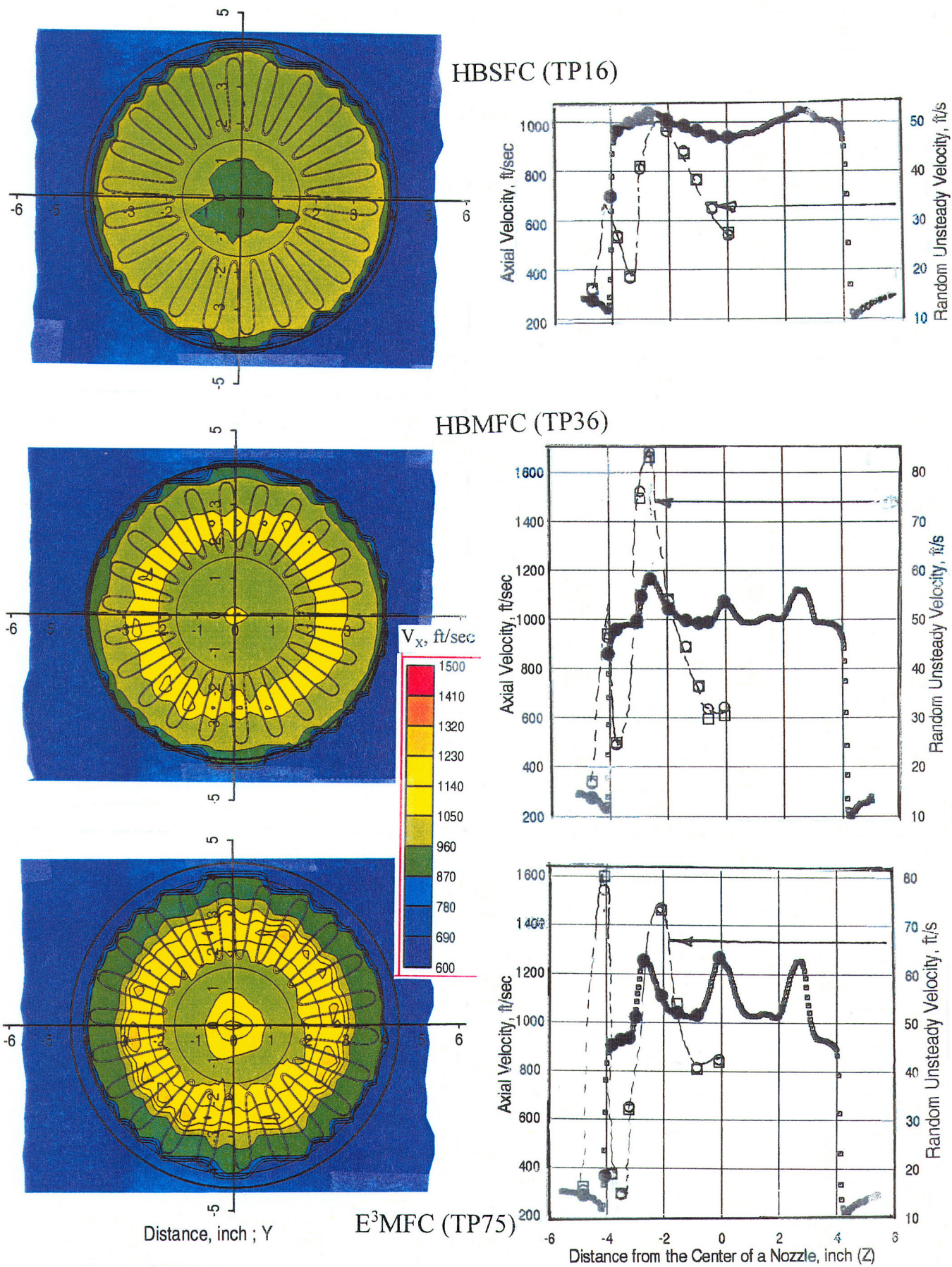


Figure 59. Effect of engine cycle on axial velocity contours and axial velocity distributions for the model scale 22-lobed mixer with standard fan of exit area  $51.7 \text{ in}^2$  at the nozzle exit plane ( $X=0.5"$ ,  $Y=0"$ ), Nominal  $V_{\text{mix}}=1000 \text{ ft/sec}$ ,  $M_F=0.28$ .

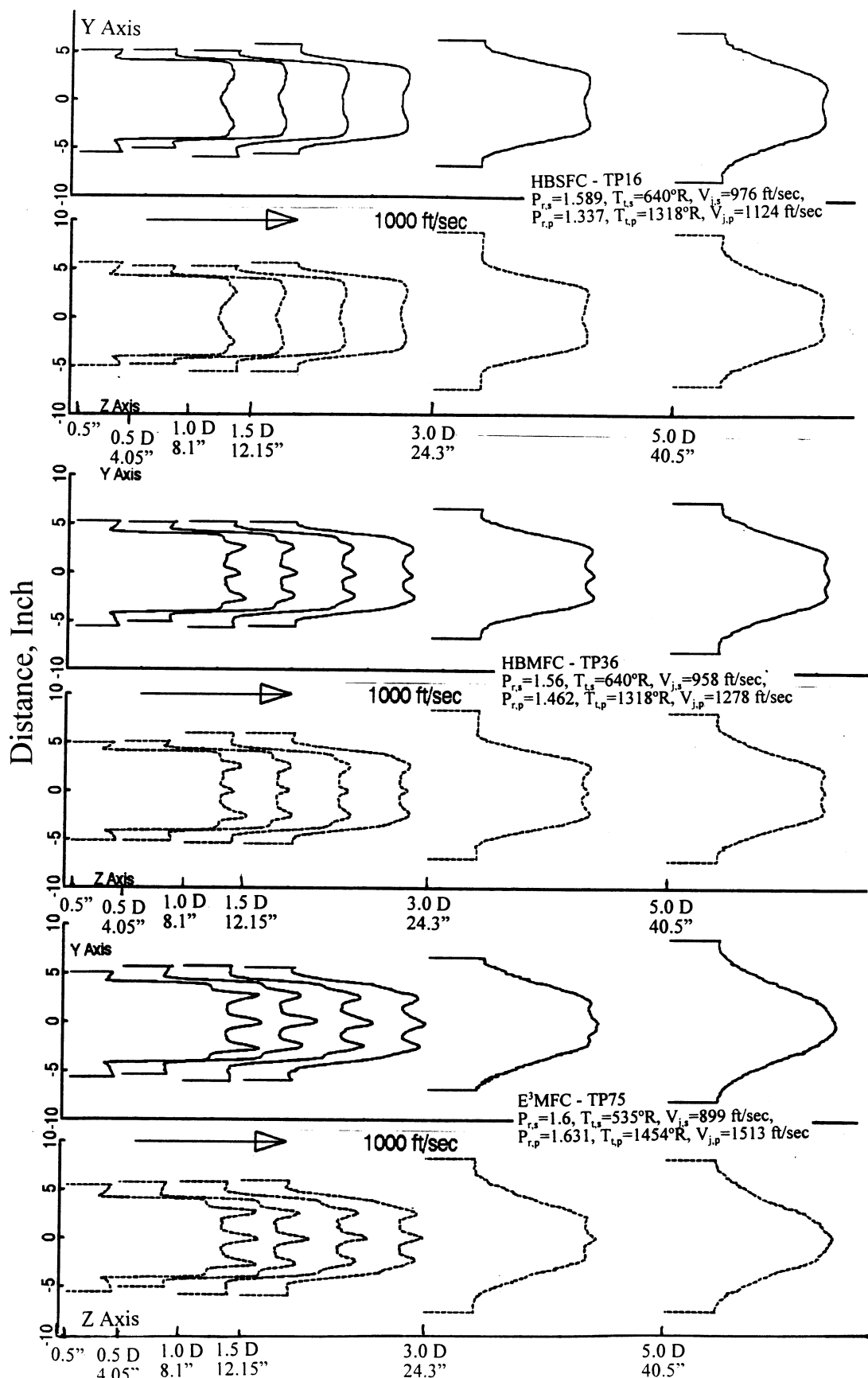


Figure 60. Effect of engine cycle on axial velocity distributions at various axial downstream locations (X) from the nozzle exit plane for the model scale 22-lobed mixer with standard fan of exit area  $51.7 \text{ in}^2$ , Nominal  $V_{\text{mix}} = 1000 \text{ ft/sec.}$ ,  $M_F = 0.28$ .

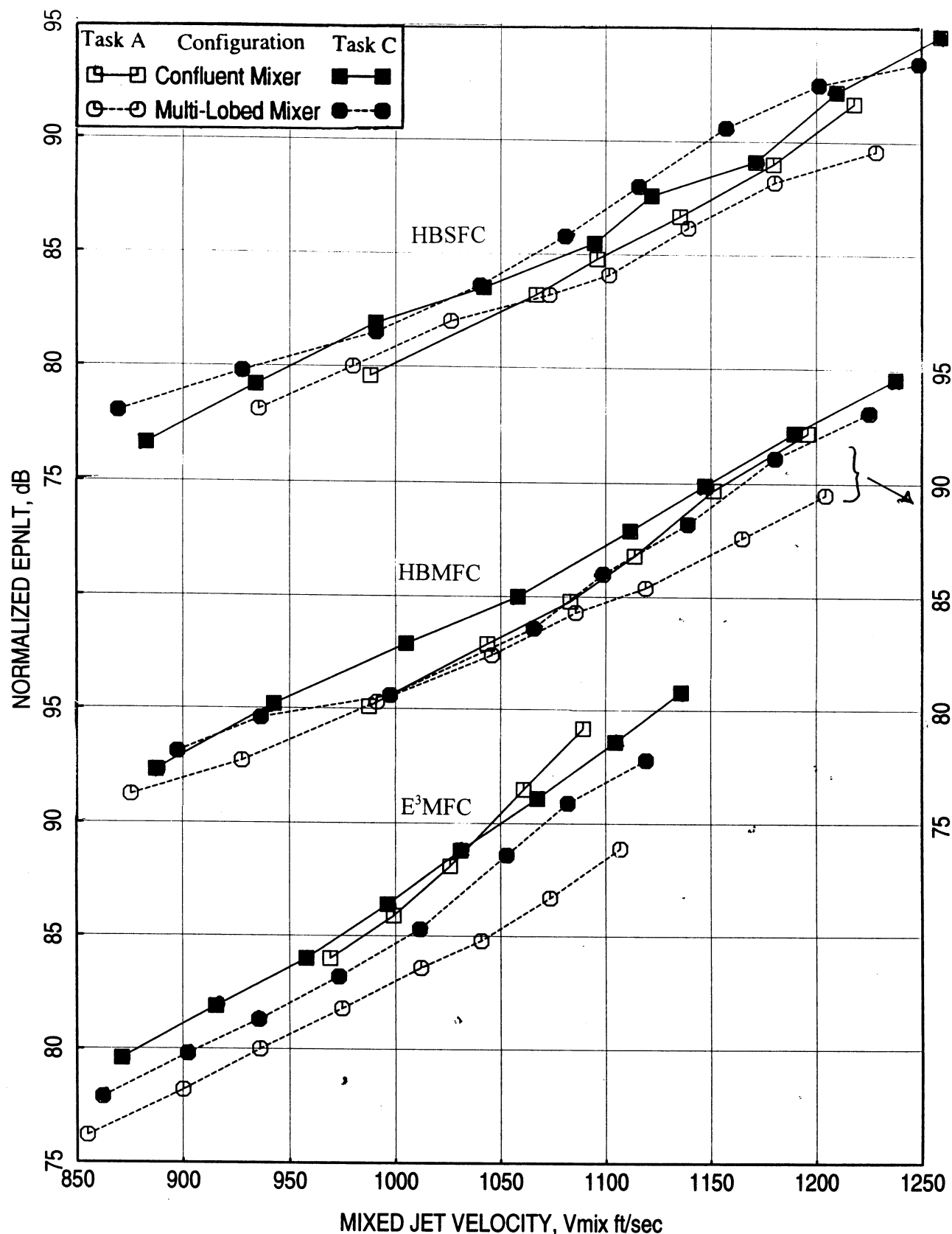


Figure 61. Effect of mixer geometry on normalized EPNL for confluent and multi-lobed mixers with standard fan for different engine cycles at SAE 77° standard day conditions,  $A_8=3078 \text{ in}^2$ , Sideline Distance=1500 ft.

scalloped and staggered with quarter periodic mixer (F9B) and a 22-lobed axisymmetric mixer. Data for two confluent mixers compatible to each of the lobed mixers are included in Figure 61. The 12-lobed mixer and the corresponding confluent mixer (V1) were tested earlier under Task A of this program. These configurations are again tested under Task C for all the cycle conditions for appropriate comparison. The dimensions including the fan nozzle length for mixers tested under Task A are significantly different compared to the mixers of the current task. However, the acoustic results are scaled to the same full scale size. Normalized EPNL levels are distinctly higher for the Task C mixers compared to those of Task A for HBSF cycle at all mixed velocities. For HBMF cycle EPNL for 22-lobed mixer is comparable to 12-lobed mixer at mid mixed velocity range. For E<sup>3</sup>MFC while the confluent mixer noise levels are comparable the 12-lobed mixer seems to be quieter compared to 22-lobed mixer for entire velocity range.

Figure 62 shows the effect of mixer geometry on PNLT & OASL directivities and SPL spectra at a nominal  $V_{mix}$  of 1000 ft/sec (TP75) for E<sup>3</sup>MF cycle. For 22-lobed mixer the SPL levels are slightly higher at higher frequency range at a few polar angle locations between 110° to 130° compared to the 12-lobed mixer. In the forward arc the 22-lobed mixer is quieter than the 12-lobed mixer. The axial velocity contours and axial velocity distributions at the same aerothermodynamic conditions (i.e., at TP75) at the nozzle exit plane for different mixers are shown in Figure 63. Distinctly, the unmixedness is most prominent for the confluent mixer. Between the lobed mixers the mixing seems to be slightly better for the 12-lobed mixer compared to 22-lobed one. Velocity profiles for the lobed mixers are further compared in Figure 64 for the nominal  $V_{mix}$  of 1000 ft/sec (TP75). In this figure the distance from the nozzle center is normalized with respect to the exit radius for proper comparison. The data for 12-lobed mixer is compared with 22-lobed mixer with two different fan nozzles of different lengths. The fan nozzle length for the 12-lobed mixer lies between the short and standard fan lengths of 22-lobed nozzle. However, for both the cases the axial velocity levels for 12-lobed mixer are lower compared to the 22-lobed data.

Figures 65 and 66 show the effect of mixer geometry on SPL & Noy spectra and PNLT & OASL directivities, respectively, at a nominal  $V_{mix}$  of 1060 ft/sec (TP77) for E<sup>3</sup>MF cycle. Sound pressure levels for 22-lobed nozzle are lower at lower frequencies compared to the 12-lobed nozzle. However, the trend is reversed at higher frequencies. Thus, the Annoyance levels at higher frequencies are much higher for 22-lobed mixer influencing the PNLT to increase significantly (see Figure 66), even though the OASLs are lower for 22-lobed mixer.

The noise level differences between the two multi-lobed mixers are further examined by plotting the mixed velocity with respect to ideal gross thrust at different cycles in Figure 67. For a fixed mixed velocity the ideal gross thrust is higher for the 22-lobed nozzle compared to 12-lobed nozzle, especially for E<sup>3</sup>MF cycle. The EPNL for the multi-lobed nozzles are again compared in Figure 68 at three different cycle conditions with respect to mixed velocity. Clearly, the EPNL for 12-lobed mixer is lower compared to 22-lobed mixer, even though the levels are normalized with respect to ideal gross thrust. However,

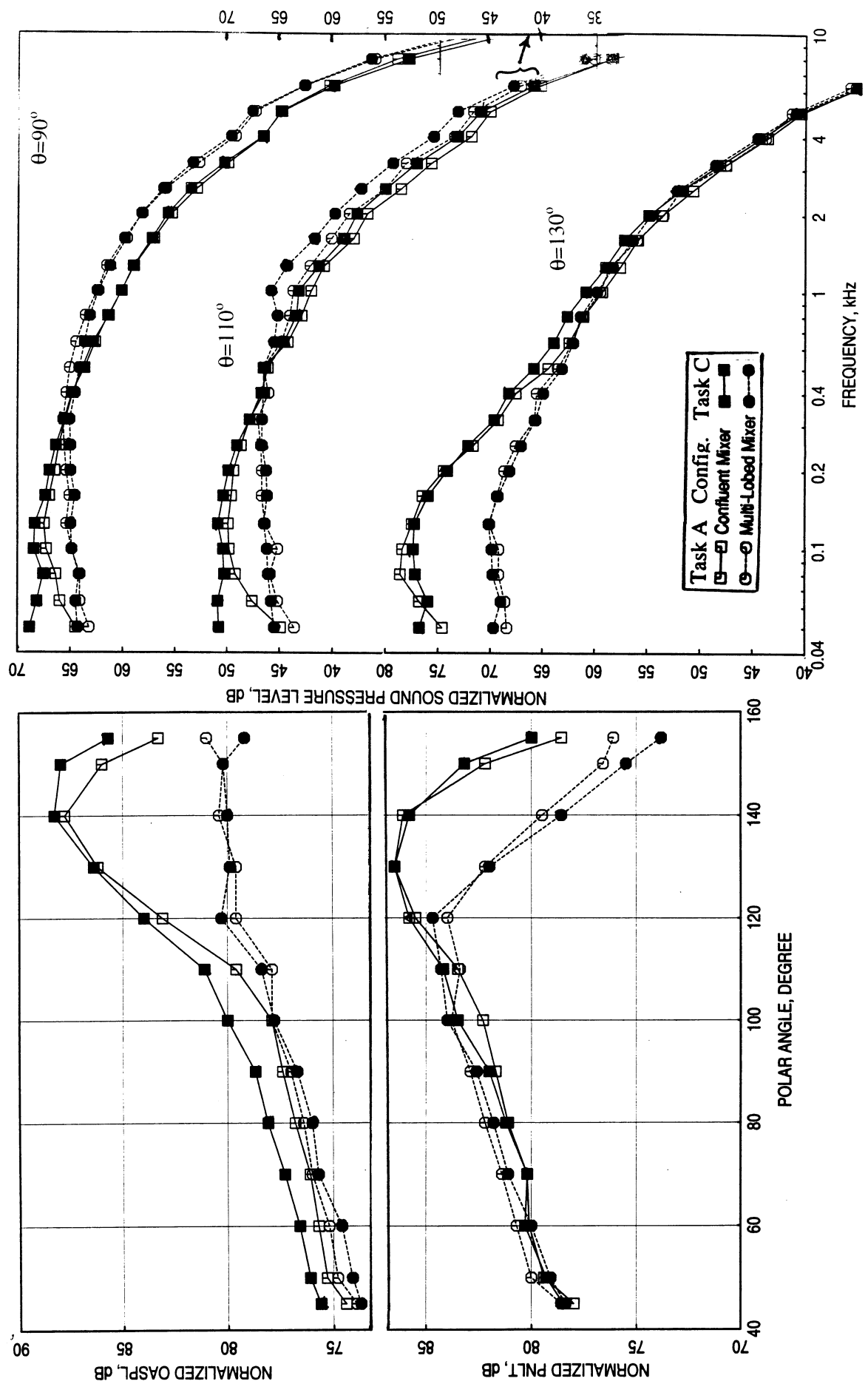


Figure 62. Effect of mixer geometry on normalized OASPL & PNLT directivities and SPL spectra at a nominal  $V_{\text{mix}} = 1000 \text{ ft/sec}$  (TP75 of E<sub>3</sub>MFC) for confluent and multi-lobed mixers with standard fan at SAE 77° standard day conditions,  $A_8 = 3078 \text{ in}^2$ , Sideline Distance = 1500 ft.

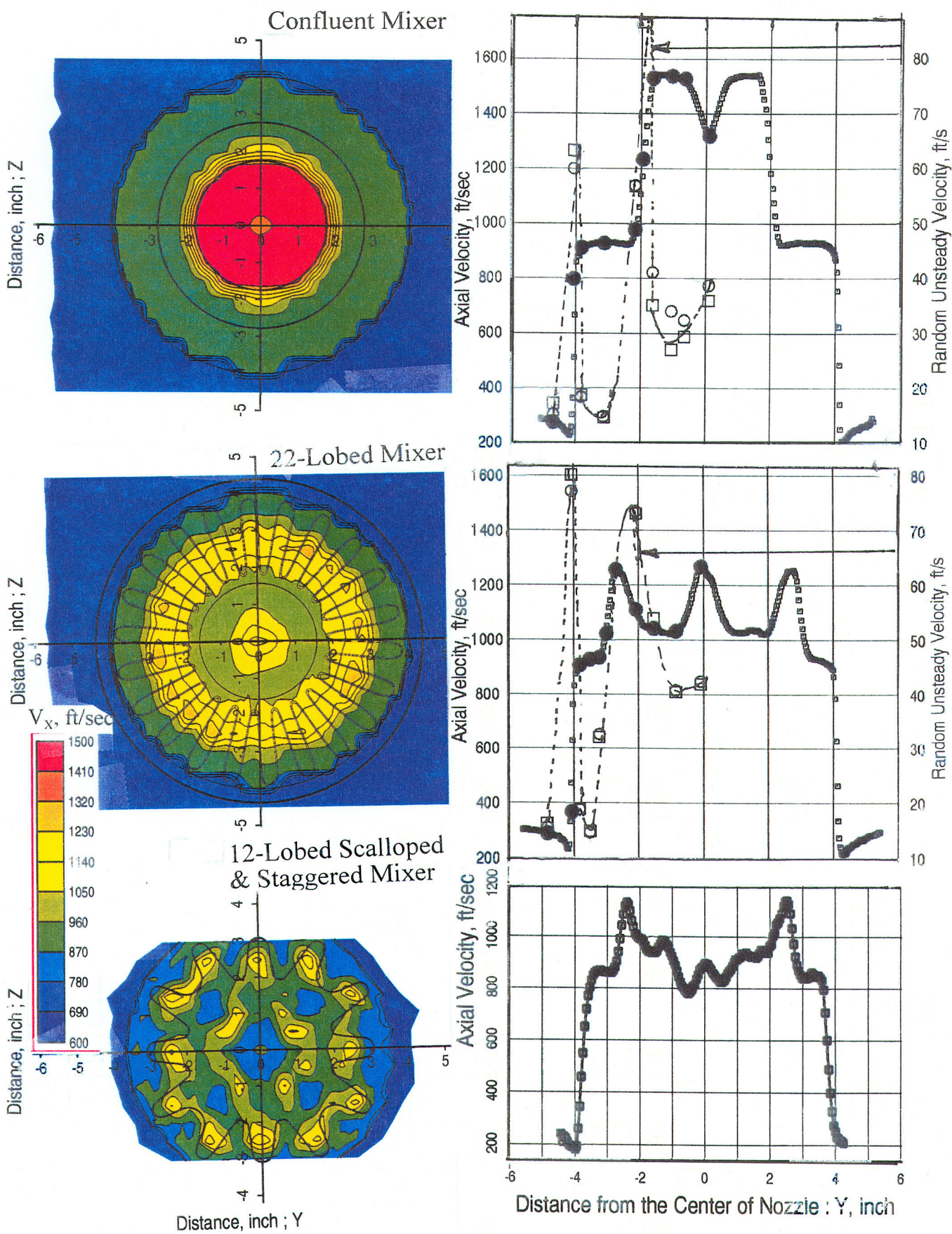


Figure 63. Effect of mixer geometry on axial velocity contours and axial velocity distributions for model scale mixers with standard fans at the nozzle exit plane ( $X=0.5"$ ,  $Y=0"$ ) for  $E^3$  Mixed Flow Cycle, Nominal  $V_{mix}=1000$  ft/sec (TP75),  $M_F=0.28$ .

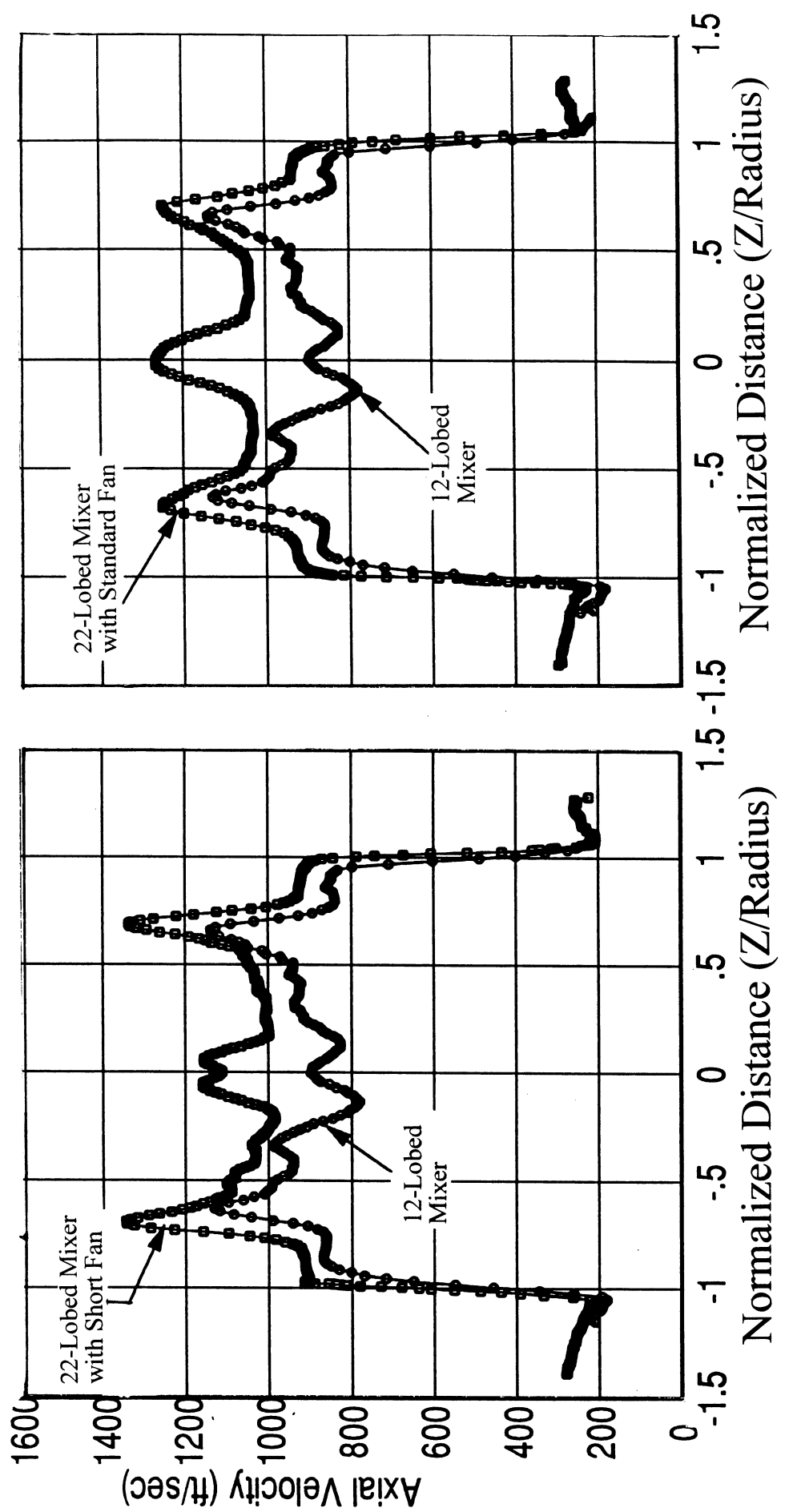


Figure 64. Effect of mixer geometry on axial velocity distributions for model scale confluent and multi-lobed mixers at a nominal  $V_{mix} = 1000$  ft/sec (TP75 of E<sup>3</sup>MFC) at the nozzle exit plane ( $X=0.5"$ ,  $Y=0$ ).

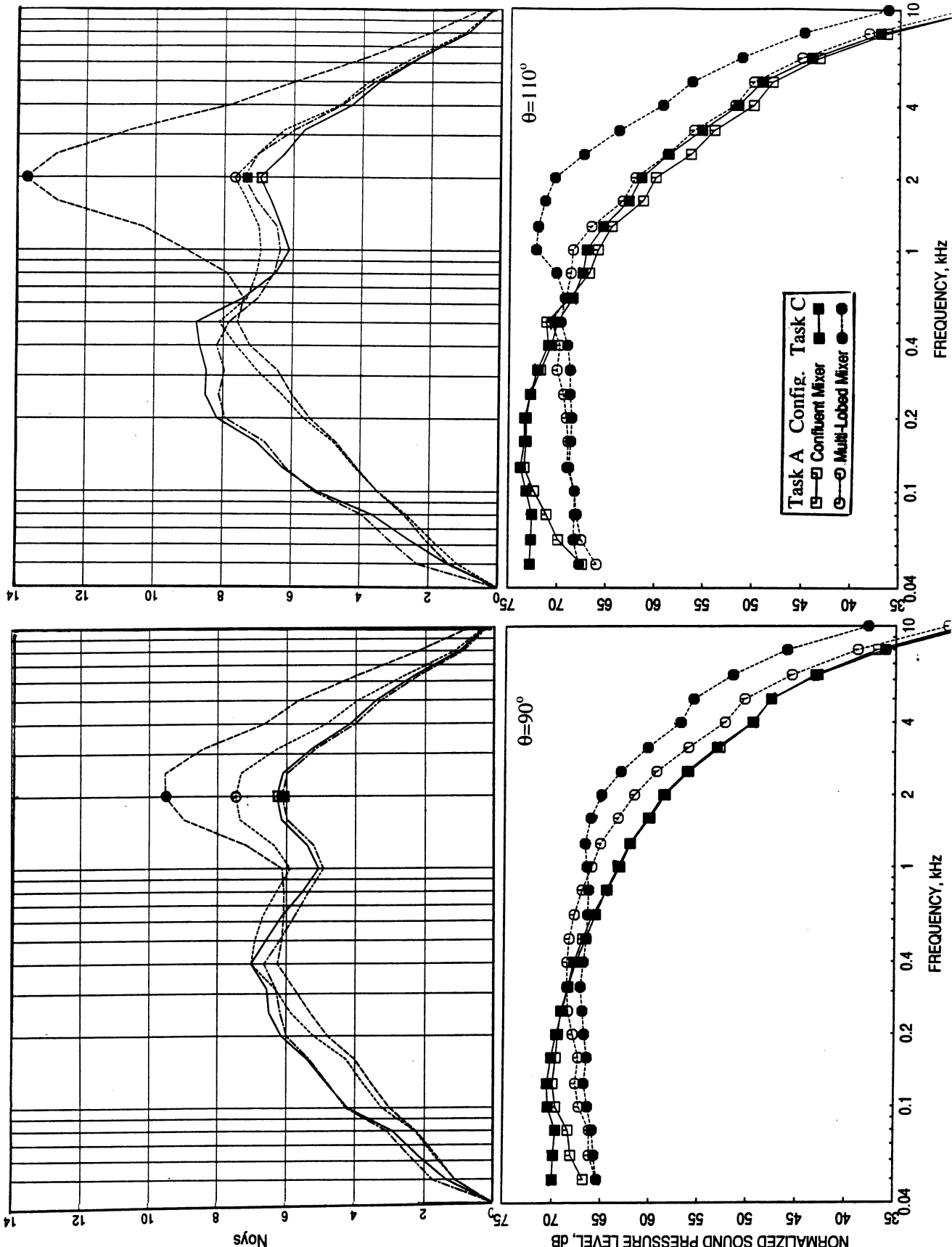


Figure 65. Effect of mixer geometry on normalized SPL & NOy spectra at a nominal  $V_{mix} = 1060$  ft/sec (TP77 of E<sup>3</sup>MFC) for confluent and multi-lobed mixers with standard day conditions,  $A_8 = 3078 \text{ in}^2$ , Sideline Distance = 1500 ft.

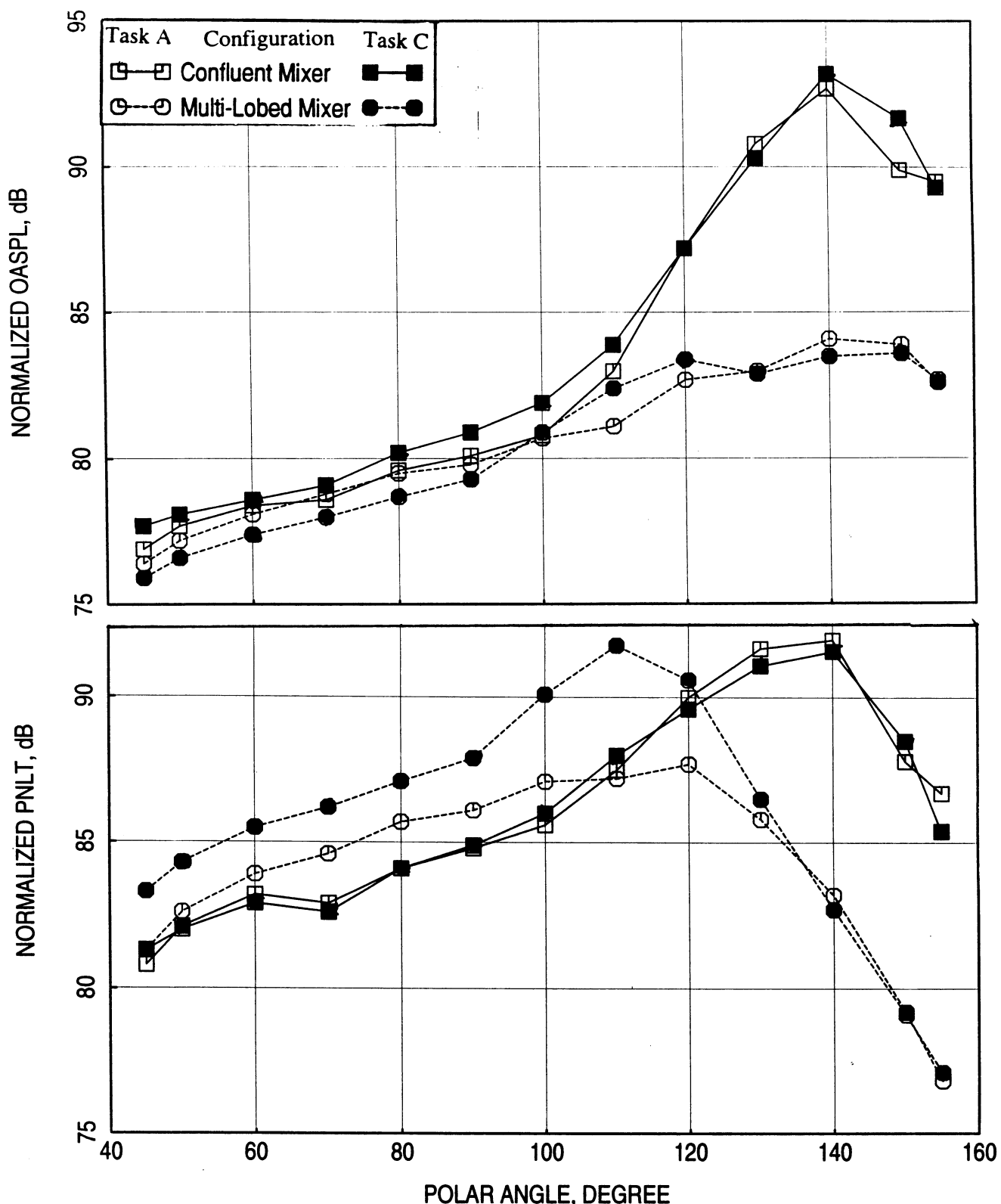


Figure 66. Effect of mixer geometry on normalized OSPL & PNLT directivities at a nominal  $V_{\text{mix}} = 1060$  ft/sec (TP77 of E<sup>3</sup>MFC) for confluent and multi-lobed mixers with standard fan at SAE 77° standard day conditions,  $A_8 = 3078$  in<sup>2</sup>, Sideline Distance = 1500 ft.

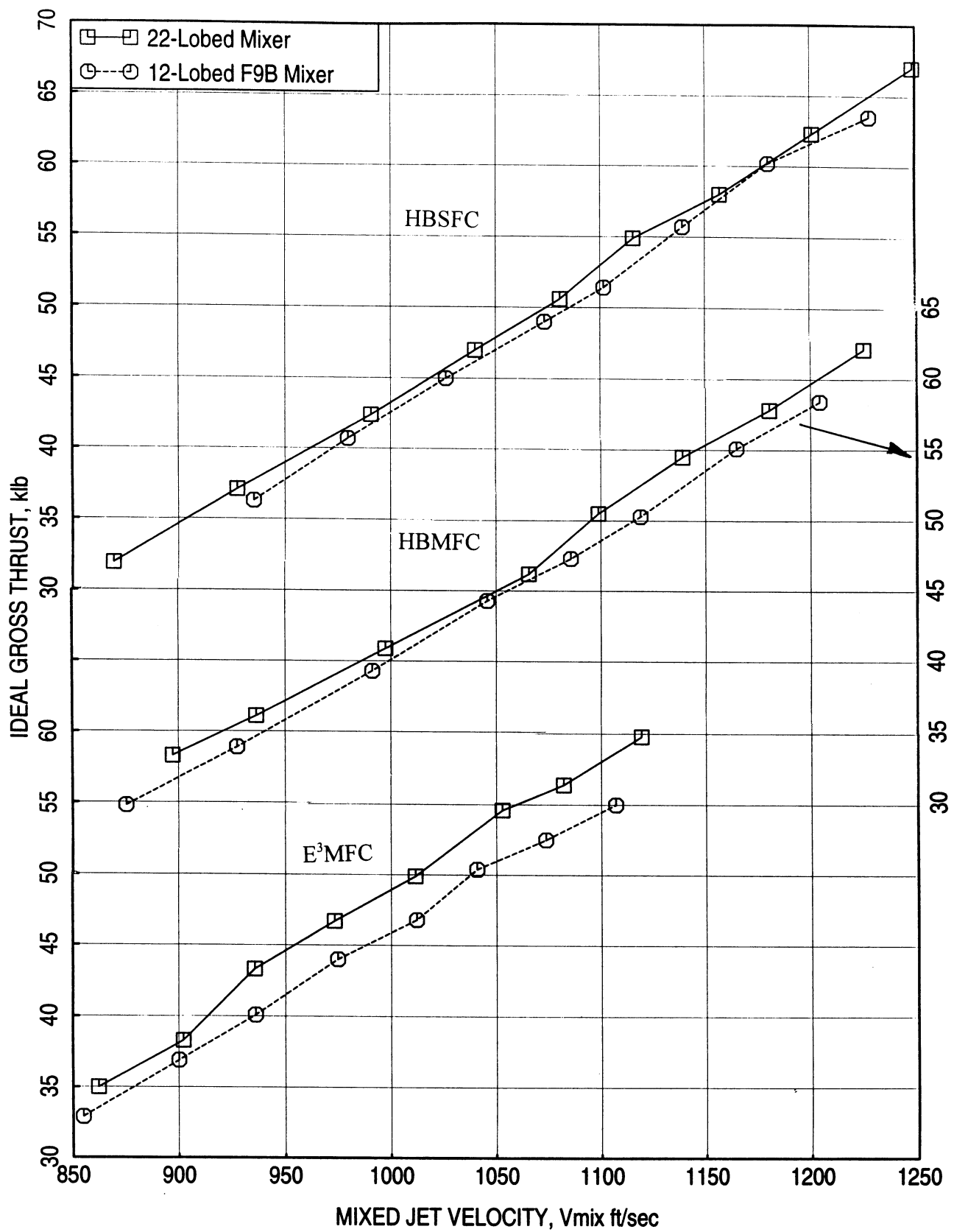


Figure 67. Effect of mixer geometry on ideal gross thrust with respect to mixed velocity for multi-lobed mixers with standard fan for different engine cycles at SAE 77° standard day conditions,  $A_8=3078 \text{ in}^2$ , Sideline Distance=1500 ft.

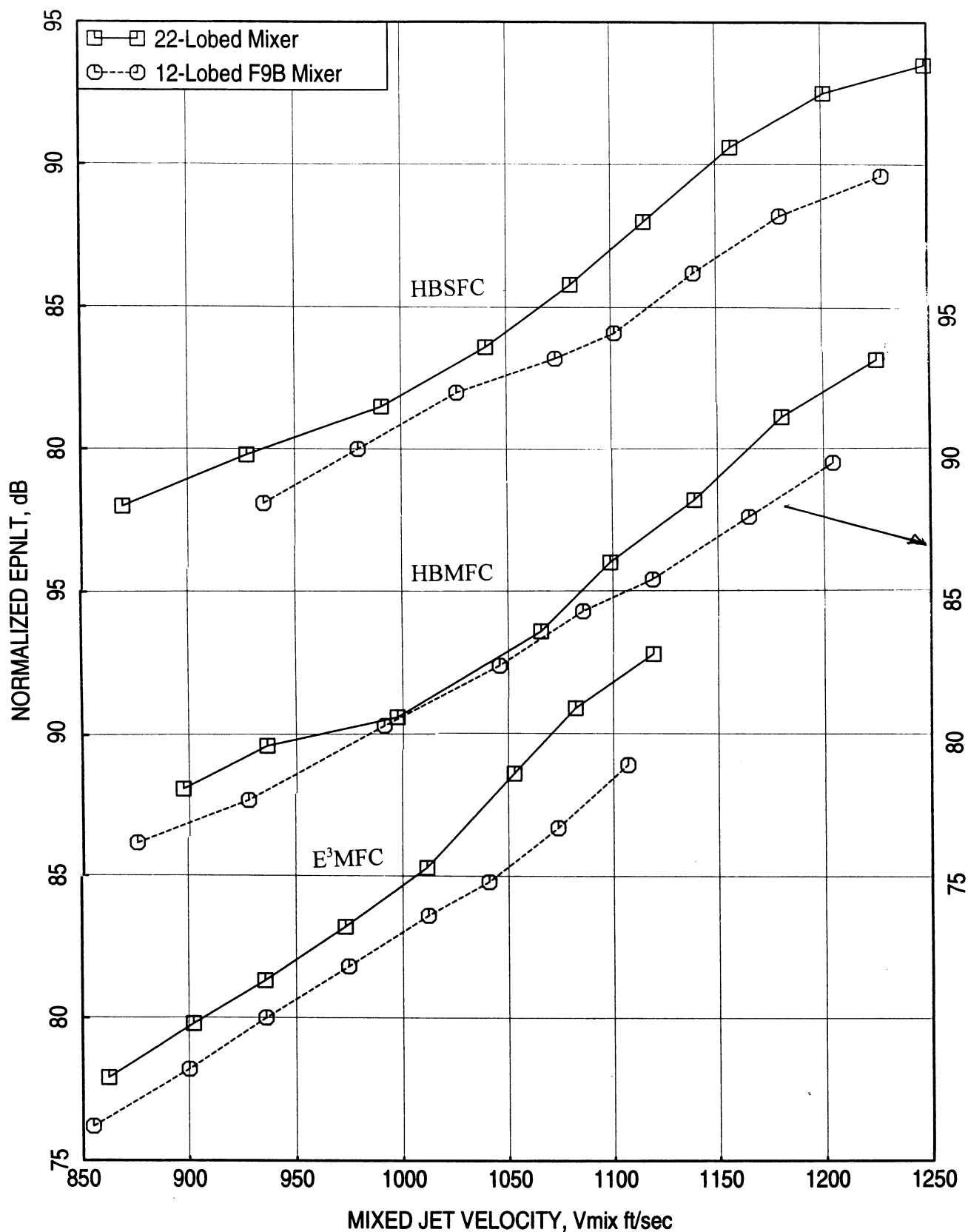


Figure 68. Effect of mixer geometry on normalized EPNL with respect to mixed velocity for multi-lobe mixers with standard fan for different engine cycles at SAE 77° standard day conditions, A8=3078 in<sup>2</sup>, Sideline Distance=1500 ft.

the EPNL with respect to ideal gross thrust, shown in Figure 69, shows good agreement between the mixers for both the mixed flow cycles. Thus, both the mixers are similar in their performance with respect to the ideal gross thrust for mixed flow cycles.

#### 6.4 Effect of Fan Nozzle Length on Farfield Noise Level and Plume Flowfield:

**22-Lobed Mixer:** Figure 70 shows the EPNL variation with respect to  $V_{mix}$  for the 22-lobed mixer with fan nozzles of different lengths at two different cycle conditions. For E<sup>3</sup>MF Cycle the EPNL increases and then decreases with increasing fan nozzle length. However, for HBMF cycle the noise levels in terms of EPNL seem to be lowest with shortest fan.

To illustrate the effect of fan nozzle on the velocity profiles generated by the multi-lobed mixer, LDV measurements are taken at the mixer exit plane without any fan nozzle. Figures 71 and 72 show these results for a flow condition with relatively lower pressure conditions. The velocity profiles from individual lobes are distinctly isolated above the secondary velocity profile. However, similar results with fan nozzles, measured at the nozzle exit plane and shown in Figure 73 (at a different flow condition compared to the data of Figures 71 and 72) indicate substantial mixing between primary and secondary flow. In fact, the velocity profile is more uniform with longer fan nozzle compared to the shorter fan nozzle configuration.

Figure 74 shows the effect of fan nozzle length for 22-lobed mixer on PNLT & OASL directivities and PWL & SPL spectra at a nominal  $V_{mix}$  of 1000 ft/sec (TP75) for E<sup>3</sup>MF cycle. At higher frequencies, above 400 Hz, the SPL and PWL decrease with increasing fan nozzle length, indicating improved mixing due to longer fan nozzle. However, at lower frequencies the standard fan configuration seems to be noisiest. The axial velocity contours and axial velocity distributions at the same aerothermodynamic conditions (i.e., at TP75) at the nozzle exit plane for different fan nozzle lengths are shown in Figure 75. Again the mixing seems to be better for the standard fan nozzle compared to the short fan configuration. Figure 76 shows the effect of fan nozzle length on PNLT & OASL directivities and PWL & SPL spectra at a higher nominal  $V_{mix}$  of 1100 ft/sec (TP79) for E<sup>3</sup>MF cycle. The impact of fan nozzle length on the noisefield seems to be insignificant.

Fan nozzle effect for 22-lobed mixer on PNLT & OASL directivities and PWL & SPL spectra for HBMF cycle at three nominal  $V_{mix}$  of 1000 ft/sec (TP36), 1140 ft/sec (TP36), and 1230 ft/sec (TP41) are shown in Figures 77 through 79, respectively. In general, noise levels at higher frequencies seem to decrease with increasing fan length. However, the impact is small compared to E<sup>3</sup>MF cycle and limited to very high frequencies. In terms of OASPL and PNLT directivities the longest fan nozzle seems to be noisiest compared to short and standard fan lengths.

The effect of fan nozzle length on the flowfield for HBMF cycle at a nominal  $V_{mix}$  of 1230 ft/sec (TP41) is shown in Figure 80 in the form of 3-dimensional velocity profiles measured at 0.5" downstream of the nozzle exit. The peaks and valleys of the velocity

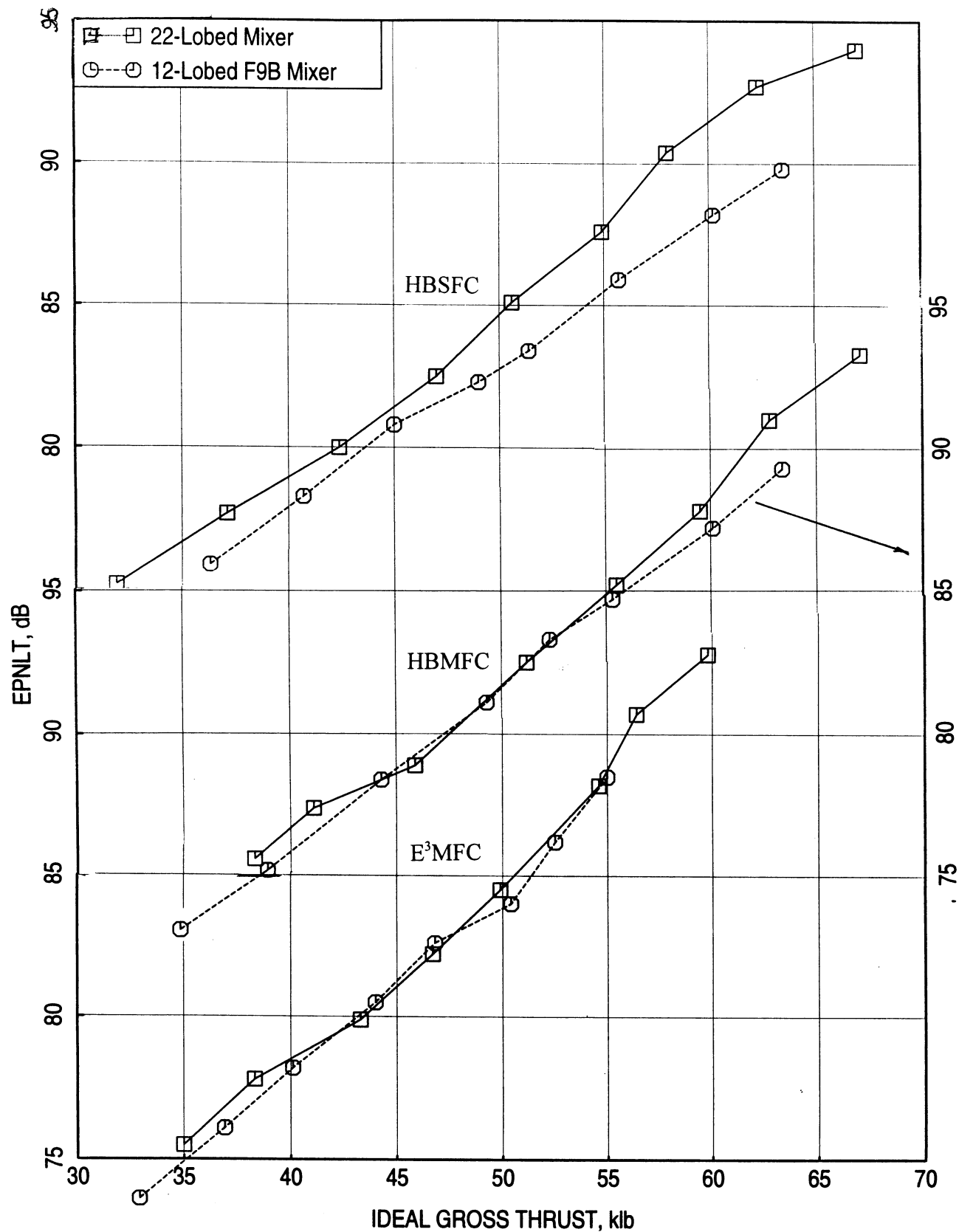


Figure 69. Effect of mixer geometry on EPNL with respect to ideal gross thrust for multi-lobed mixers with standard fan for different engine cycles at SAE 77° standard day conditions,  $A_8=3078 \text{ in}^2$ , Sideline Distance=1500 ft,  $M_F=0.28$ .

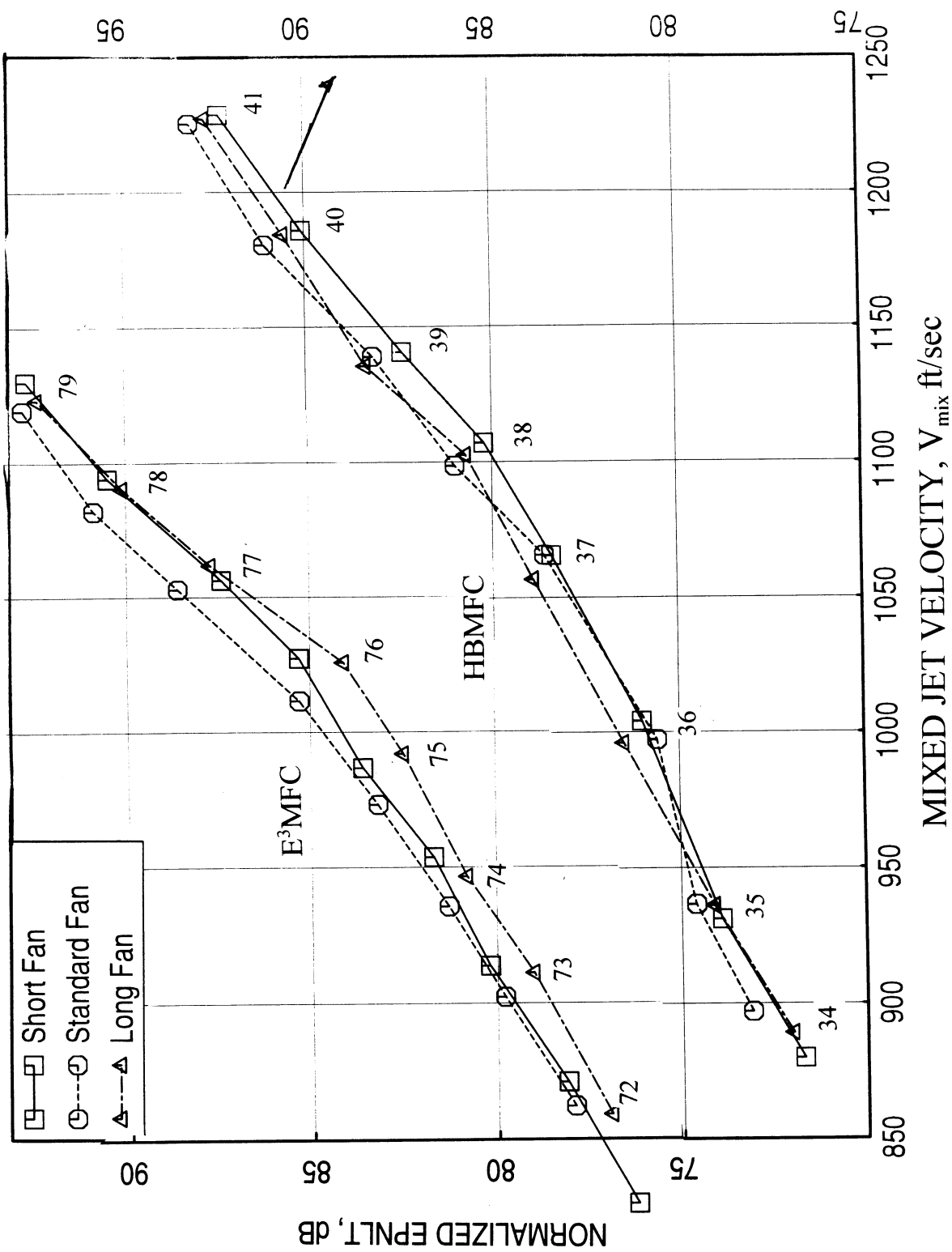


Figure 70. Effect of fan nozzle length on normalized EPNL for 22-lobed mixer with fan exit area of  $51.7 \text{ in}^2$  for different engine cycles at SAE  $77^\circ$  standard day conditions,  $A_8=3078 \text{ in}^2$ , Sideline Distance=1500 ft,  $M_f=0.28$ .

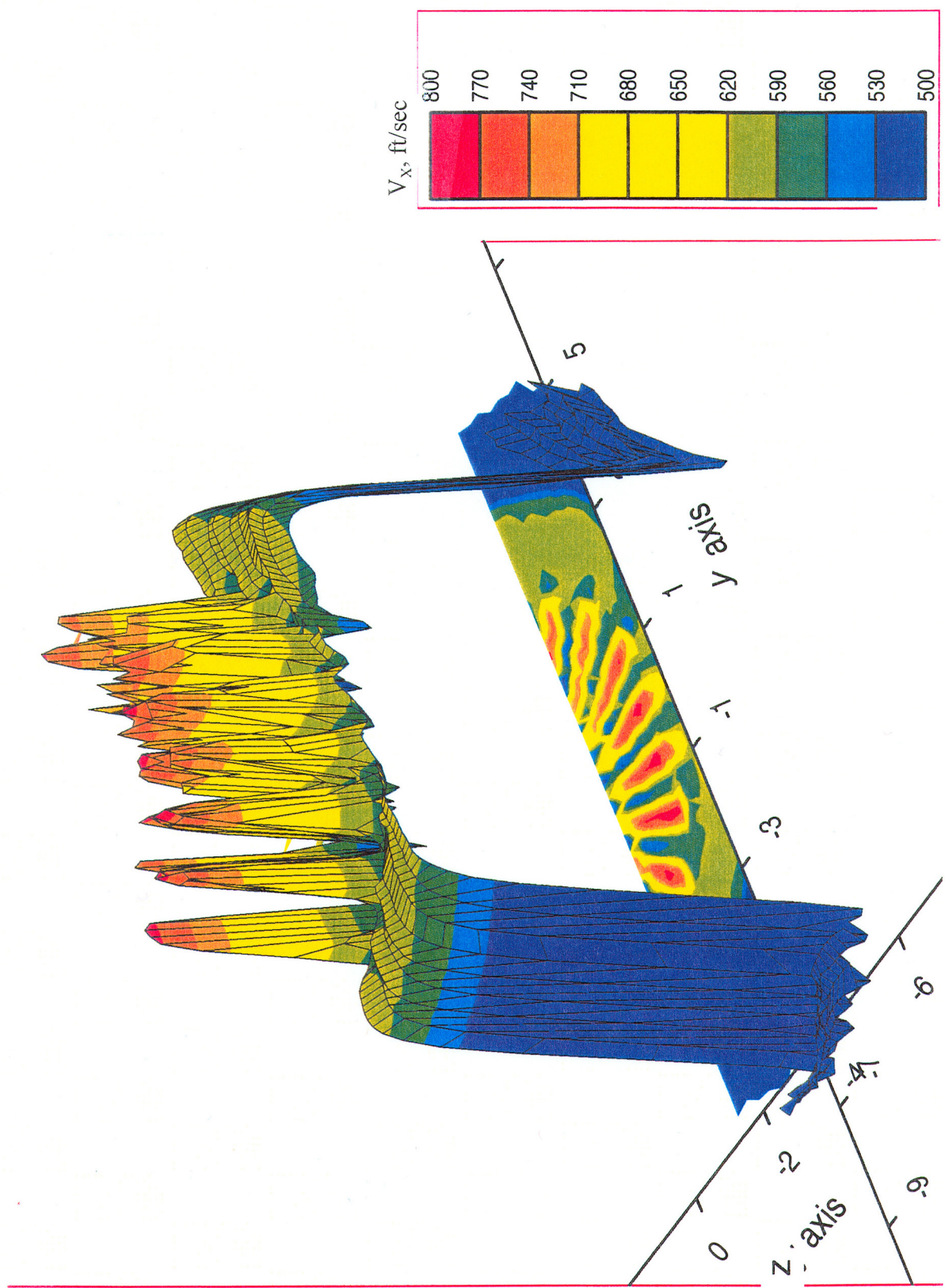


Figure 71. Axial velocity profile in 3-dimensional form at 0.47" downstream of the 22-lobe mixer without the fan nozzle,  $P_{r,s}=1.191$ ,  $T_{t,s}=640^{\circ}\text{R}$ ,  $V_{j,s}=612$  ft/sec,  $P_{r,p}=1.158$ ,  $T_{t,p}=1320^{\circ}\text{R}$ ,  $V_{j,p}=809$  ft/sec,  $M_F=0.28$ .

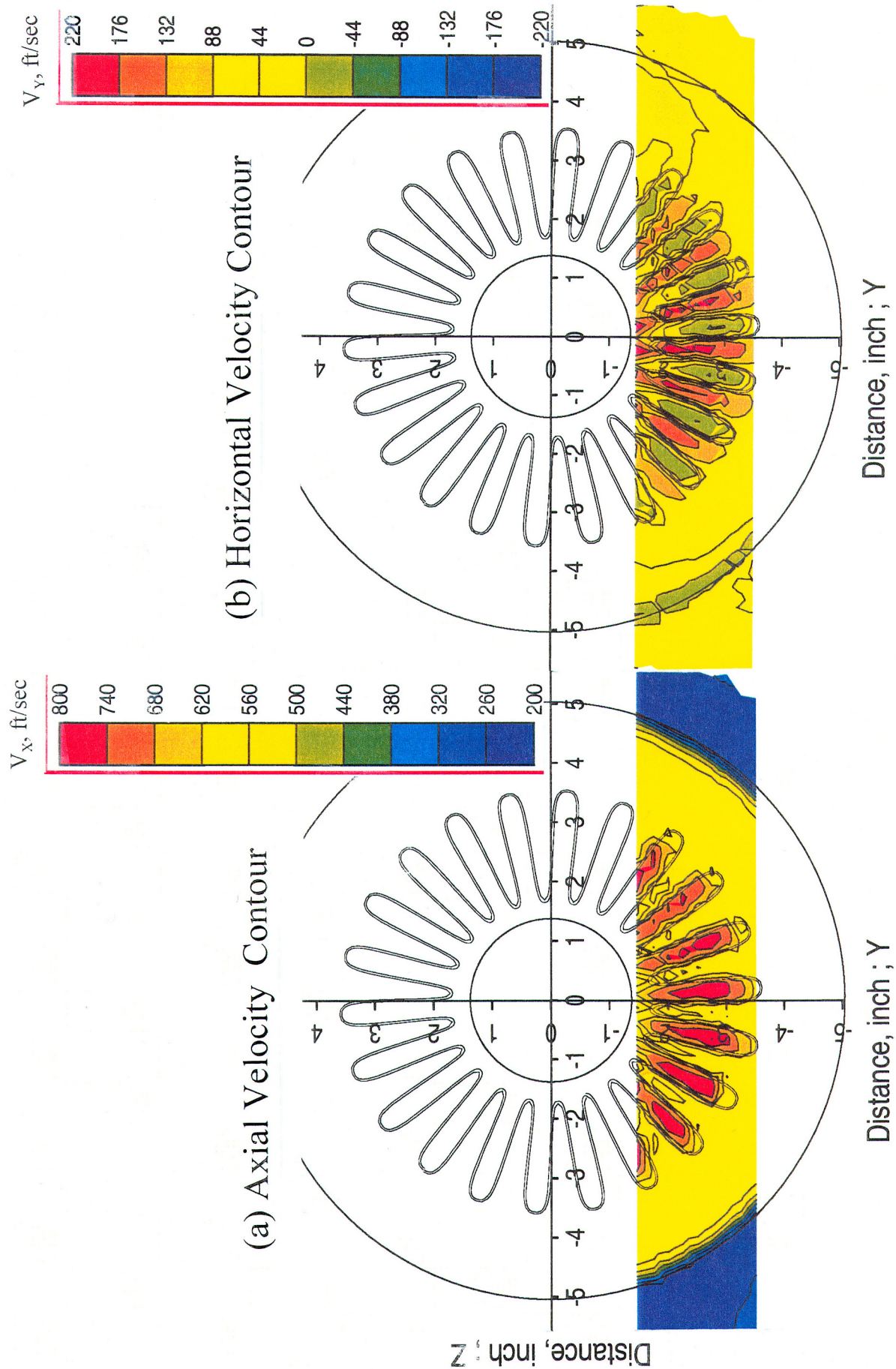
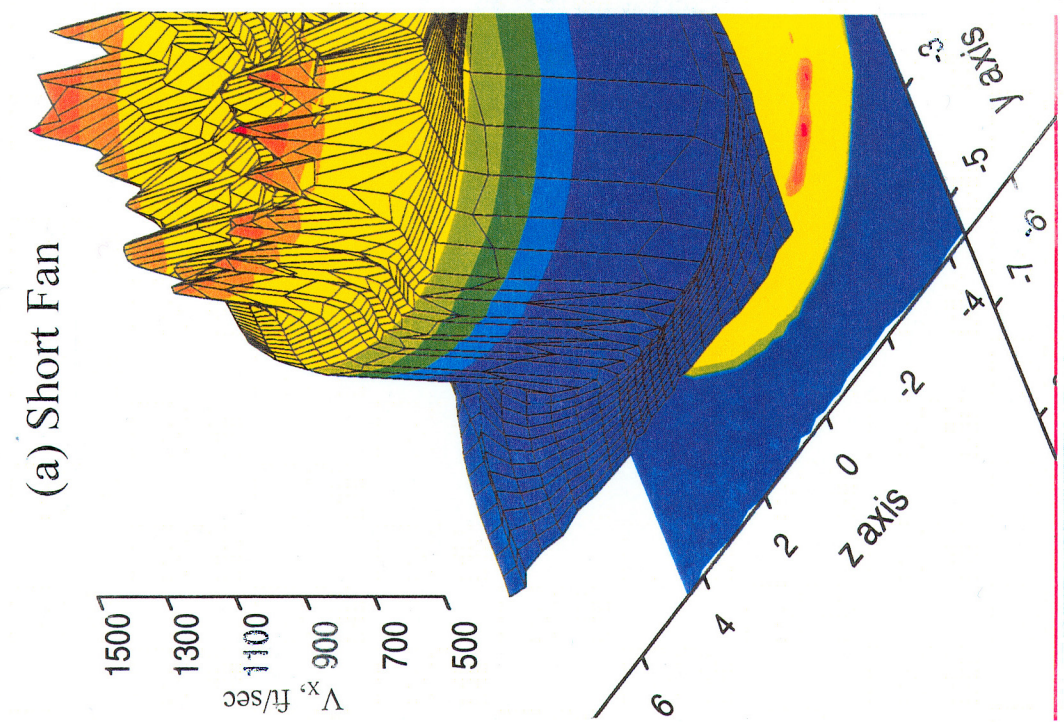


Figure 72. Axial and horizontal velocity contours for 22-lobed mixer without the fan nozzle at the mixer exit plane ( $X=0.47''$ ,  $Y=0$ ),  $P_{r,s}=1.191$ ,  $T_{t,s}=640^{\circ}\text{R}$ ,  $V_{j,p}=1320\text{ ft/sec}$ ,  $P_{r,p}=612 \text{ ft/sec}$ ,  $T_{t,p}=1.158$ ,  $V_{j,s}=809 \text{ ft/sec}$ ,  $M_F=0.28$ .



(b) Standard Fan

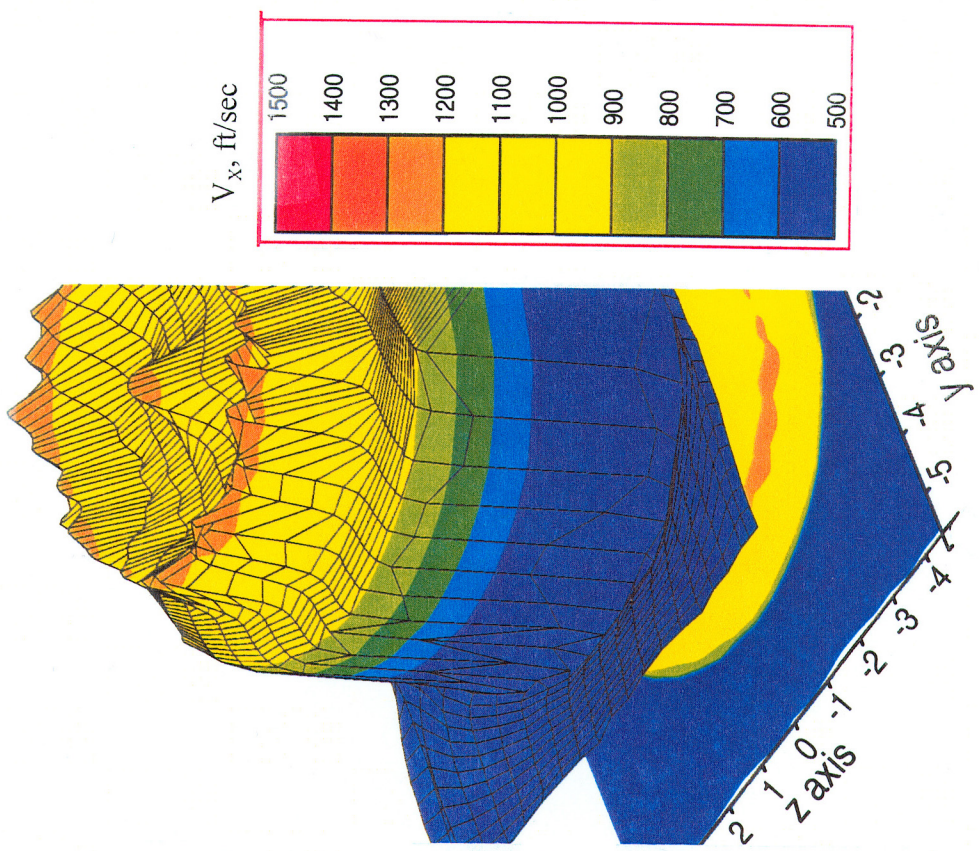


Figure 73. Effect of fan nozzle length on axial velocity profiles in 3-dimensional form at 0.5" downstream of the nozzle exit plane for model scale 22-lobed mixer with the fan exit area of 51.7 in<sup>2</sup> at a nominal  $V_{\text{mix}} = 1000$  ft/sec (TP75 of E<sup>3</sup>MFC),  $M_F = 0.28$ .

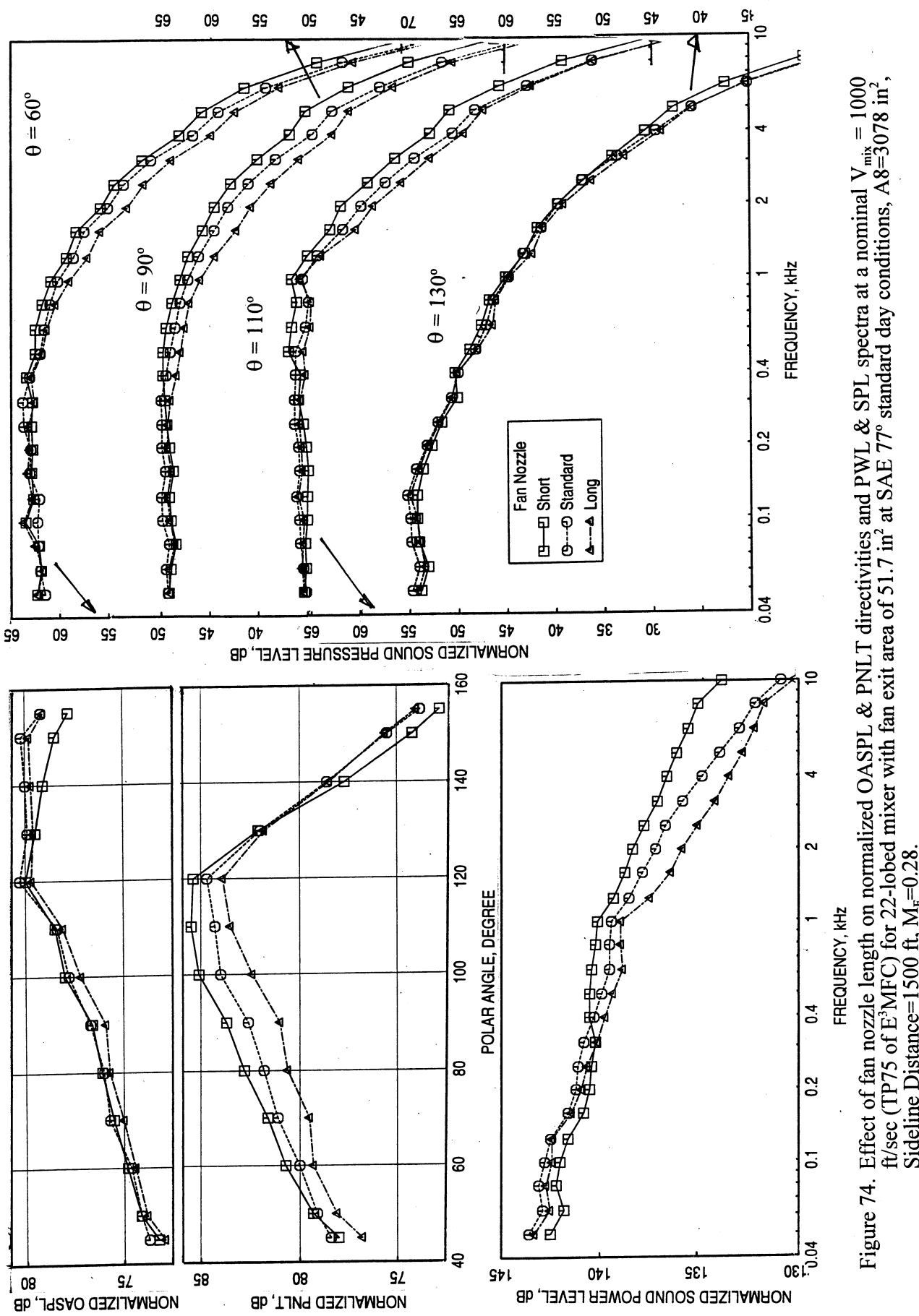


Figure 74. Effect of fan nozzle length on normalized OASPL & PNLT directivities and PWL & SPL spectra at a nominal  $V_{\text{mix}} = 1000$  ft/sec (TP75 of E<sup>3</sup>MFC) for 22-lobe mixer with fan exit area of 51.7 in<sup>2</sup> at SAE 77° standard day conditions,  $A_8 = 3078$  in<sup>2</sup>, Sideline Distance = 1500 ft,  $M_F = 0.28$ .

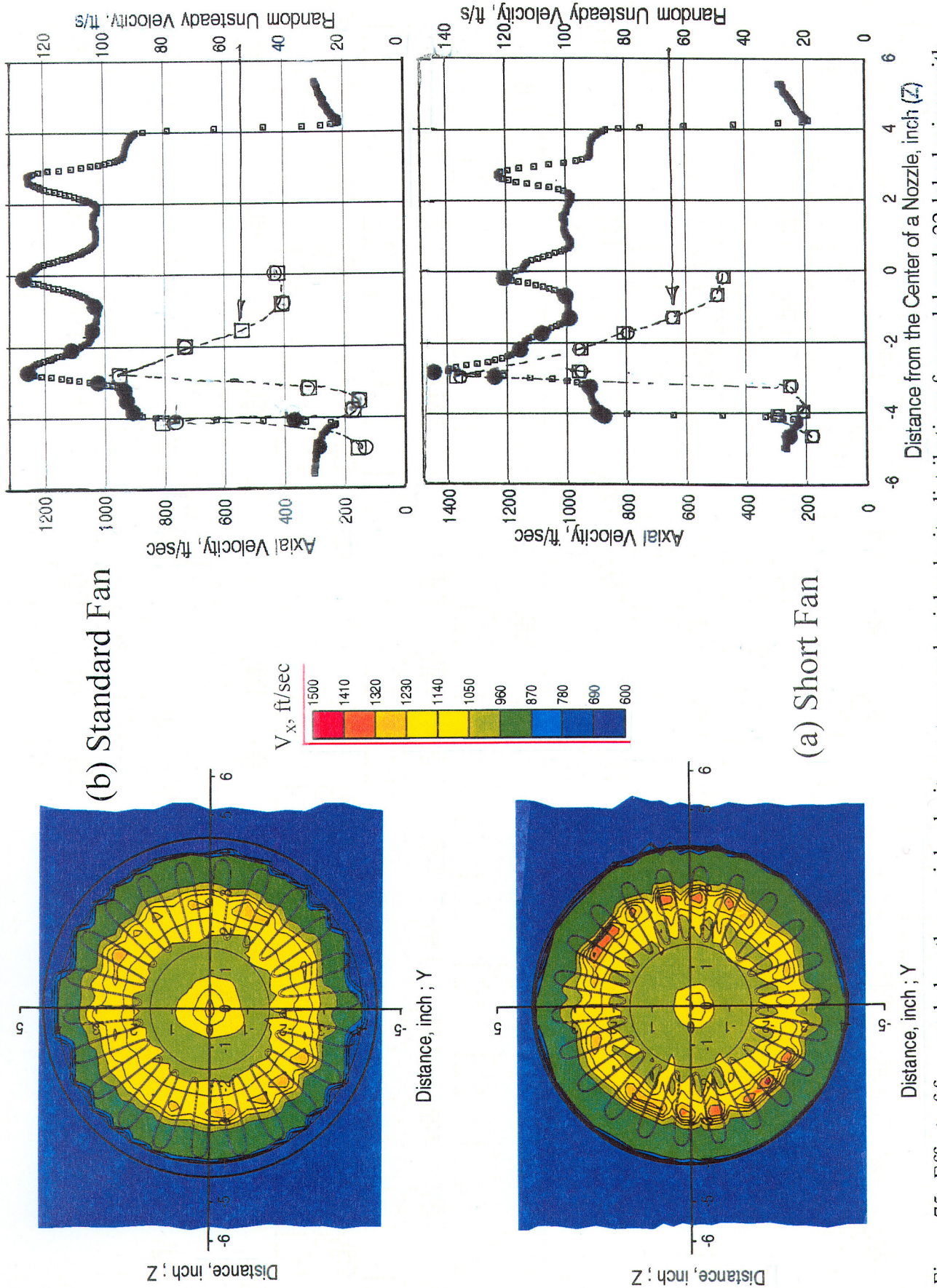


Figure 75. Effect of fan nozzle length on axial velocity contours and axial velocity distributions for model scale 22-lobed mixer with fan exit area of  $51.7 \text{ in}^2$  at the nozzle exit plane ( $X=0.57$ ;  $Y=0$ ) at a nominal  $V_{\text{mix}} = 1000 \text{ ft/sec}$  (TP75 of EMFC),  $M_F=0.28$ .

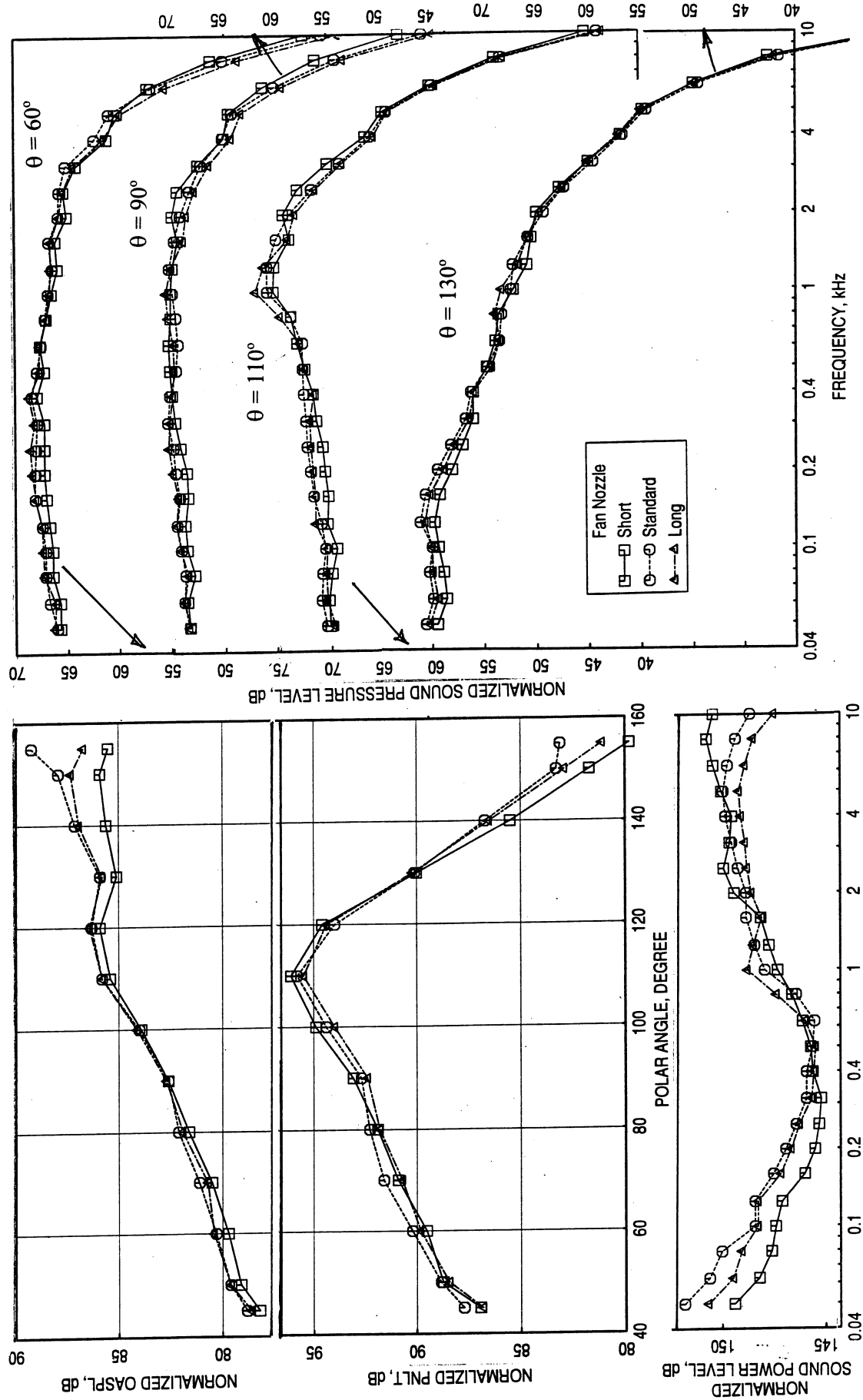


Figure 76. Effect of fan nozzle length on normalized OASPL & PNLT directivities and PWL & SPL spectra at a nominal  $V_{\text{mix}}^{\text{nom}} = 1100$  ft/sec (TP79 of E<sup>3</sup>MFC) for 22-lobe mixer with fan exit area of 51.7 in<sup>2</sup> at SAE 77° standard day conditions,  $A_8 = 3078$  in<sup>2</sup>, Sideline Distance = 1500 ft,  $M_F = 0.28$ .

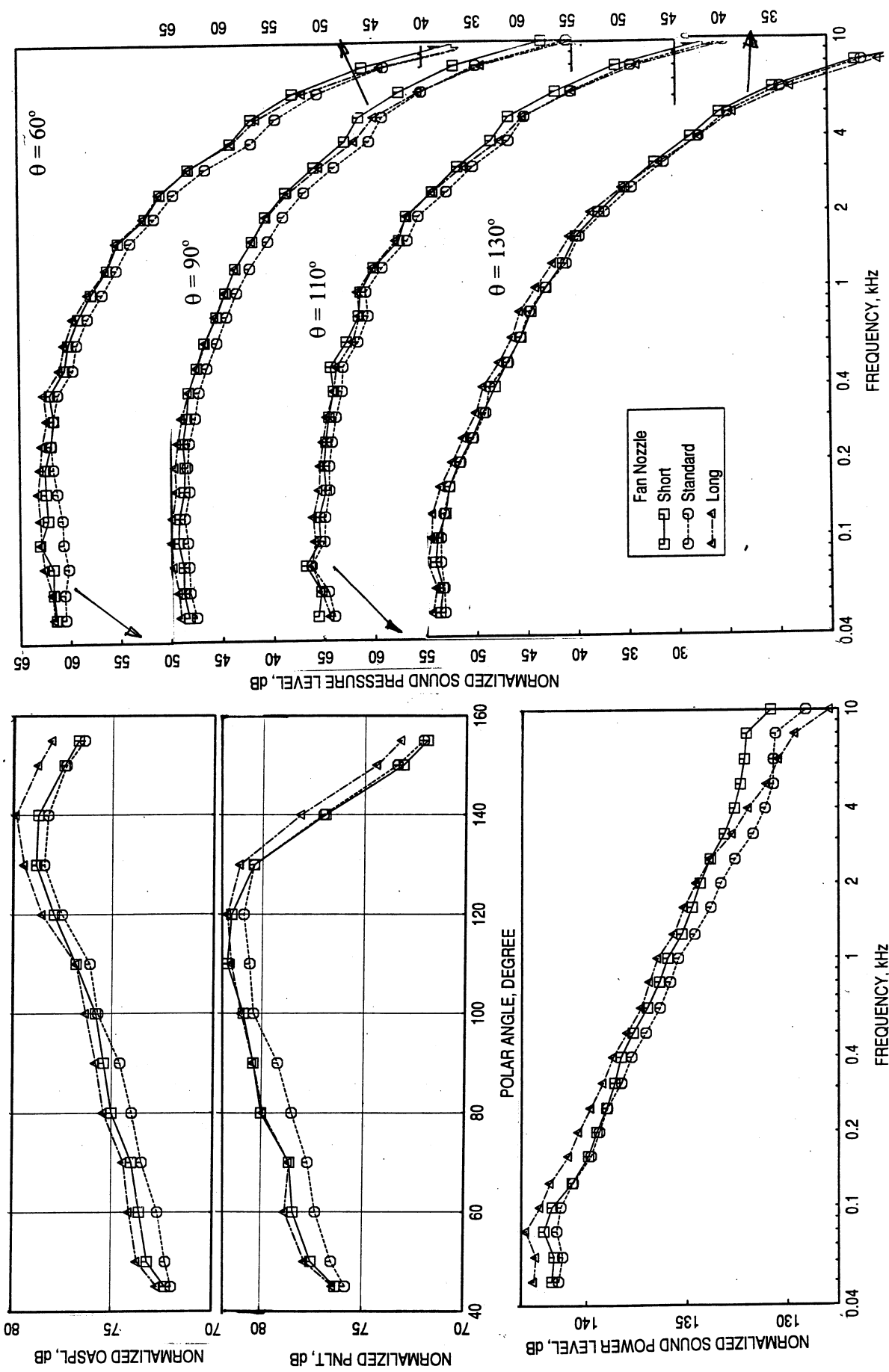
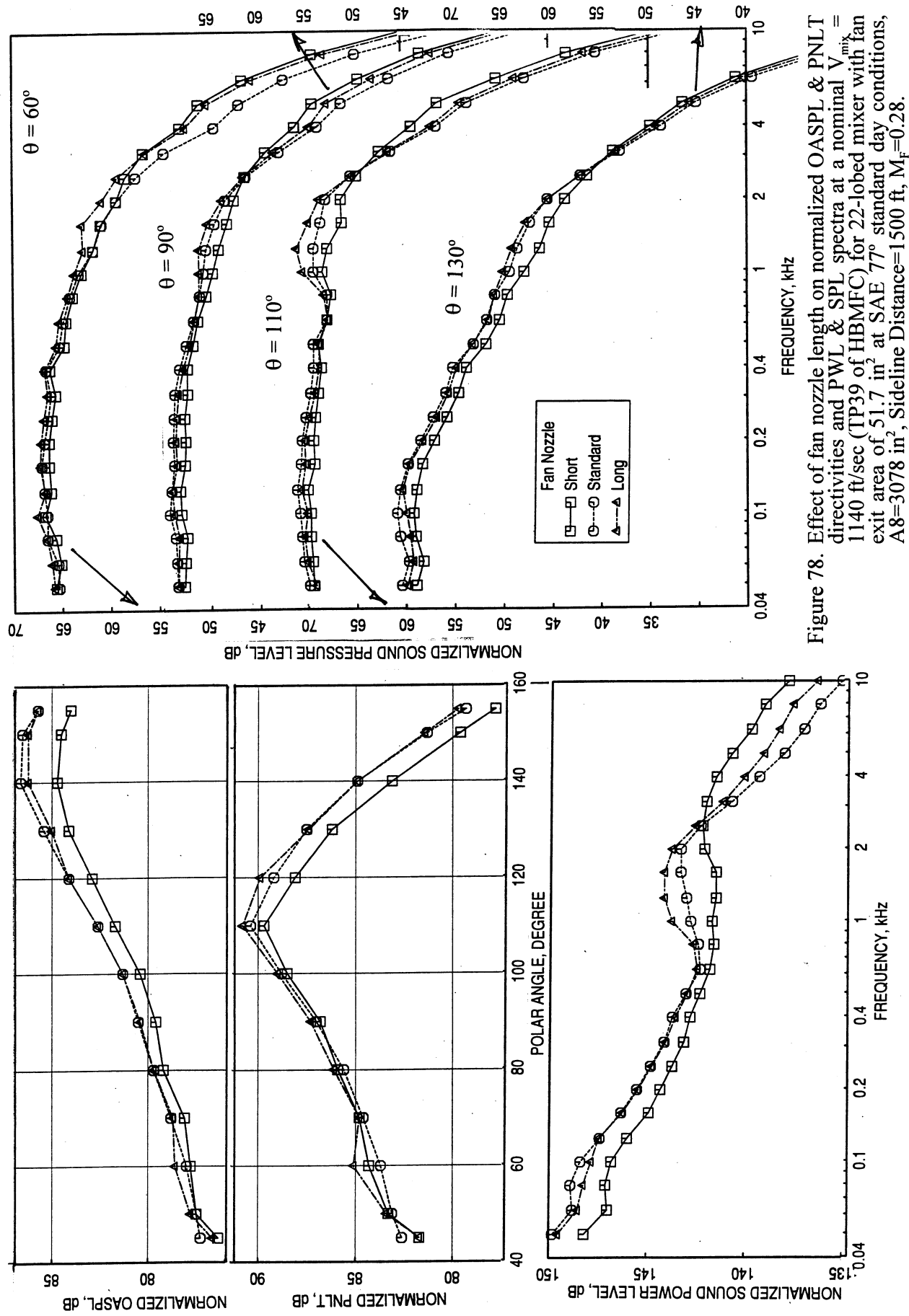


Figure 77. Effect of fan nozzle length on normalized OASPL & PNLT directivities and PWL & SPL spectra at a nominal  $V_{\text{mix}} = 1000 \text{ ft/sec}$  (TP36 of HBMFC) for 22-lobed mixer with fan exit area of  $51.7 \text{ in}^2$  at SAE  $77^\circ$  standard day conditions,  $A_8=3078 \text{ in}^2$ , Sideline Distance=1500 ft,  $M_F=0.28$ .



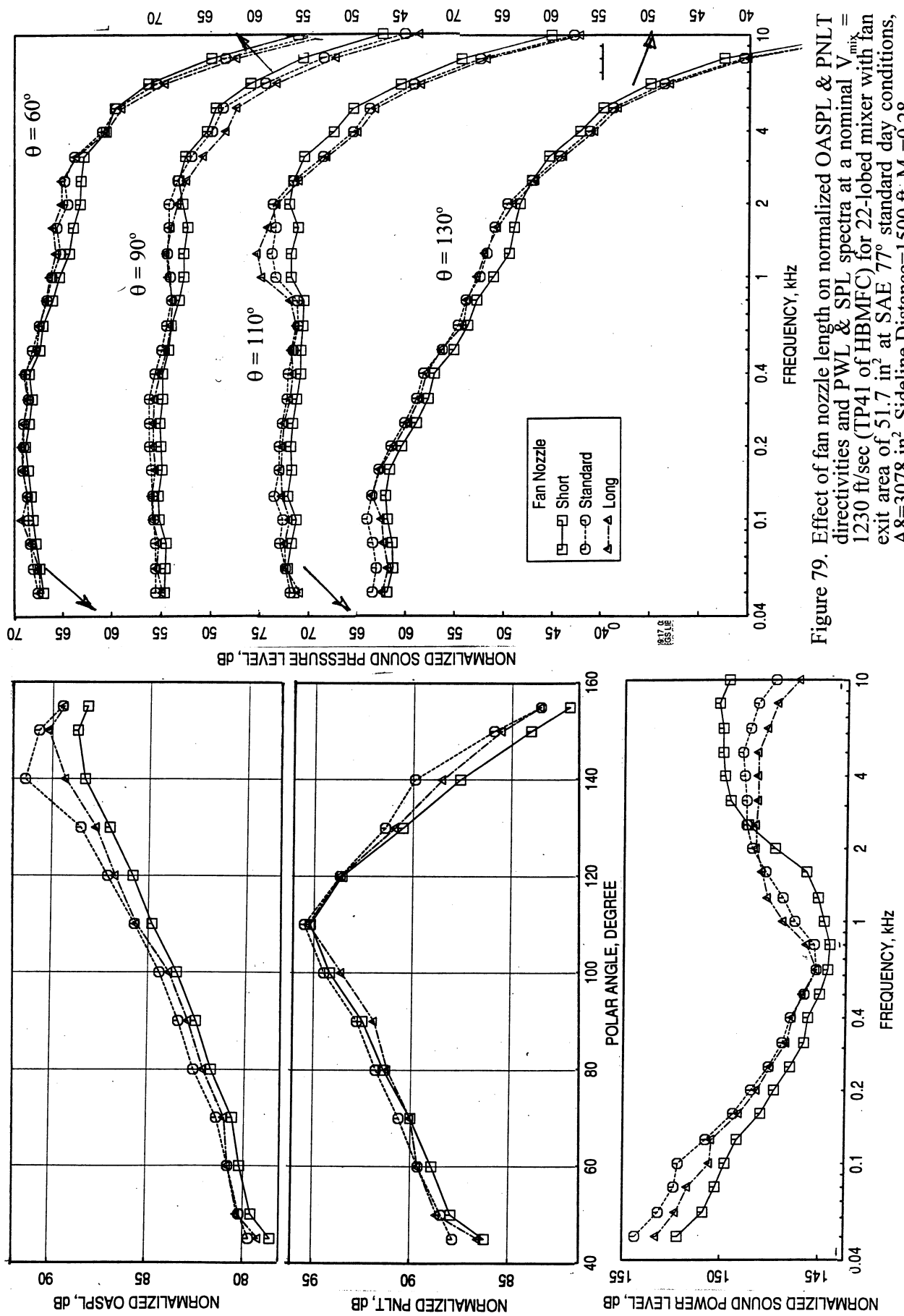


Figure 79. Effect of fan nozzle length on normalized OASPL & PNLT directivities and PWL & SPL spectra at a nominal  $V_{\text{mix}}^{\text{nom}} = 1230 \text{ ft/sec}$  (TP41 of HBMFC) for 22-lobed mixer with fan exit area of  $51.7 \text{ in}^2$  at SAE  $77^\circ$  standard day conditions,  $A_8 = 3078 \text{ in}^2$ , Sideline Distance = 1500 ft,  $M_F = 0.28$ .

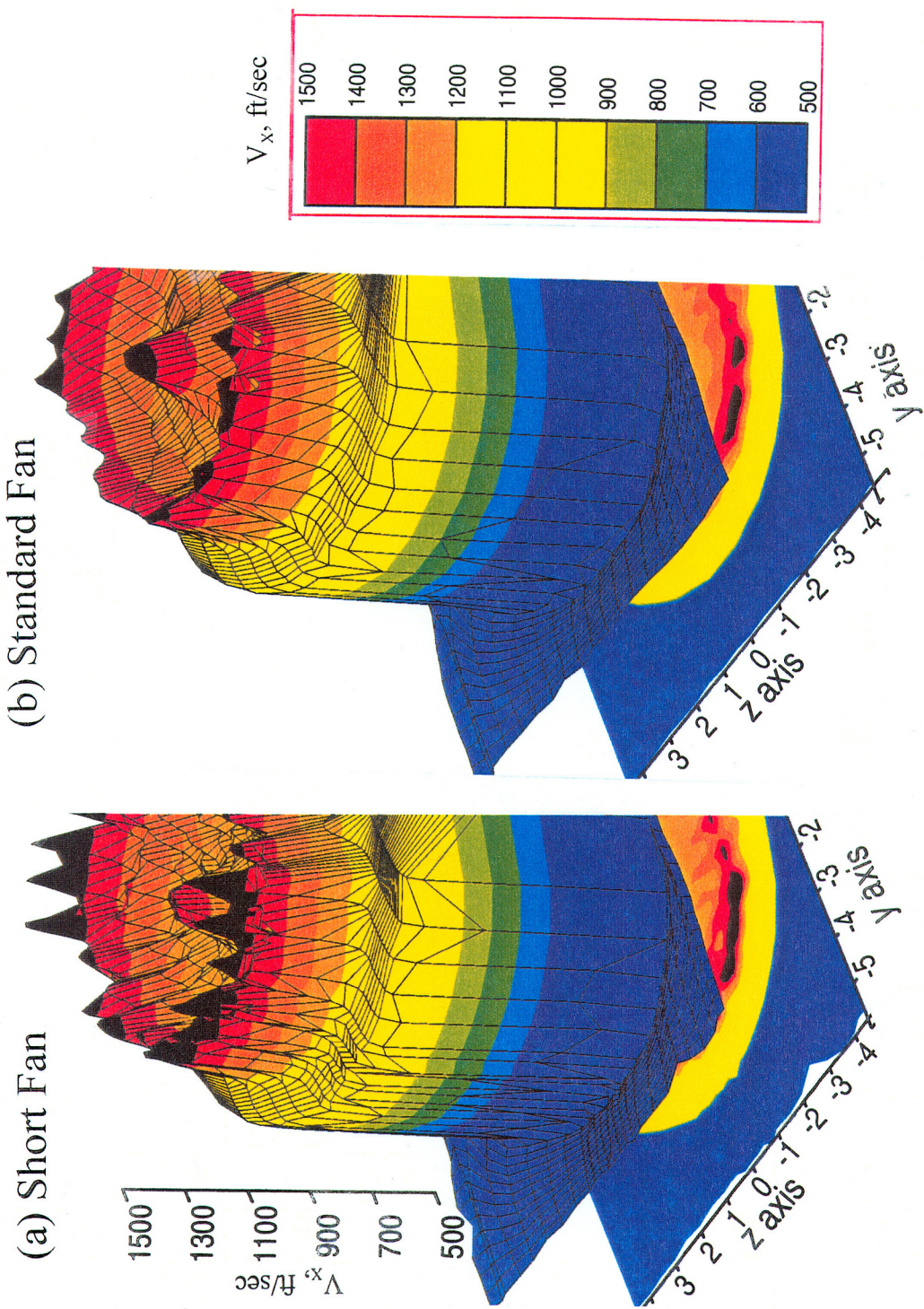


Figure 80. Effect of fan nozzle length on axial velocity profiles in 3-dimensional form at 0.5" downstream of the nozzle exit plane for model scale 22-lobed mixer with the fan exit area of 51.7 in<sup>2</sup> at a nominal  $V_{mix} = 1230$  ft/sec (TP41 of HBMFC),  $M_f=0.28$ .

profile due to the mixer lobes are less dominant for the standard fan compared to the short fan, indicating mixing enhancement due to longer fan nozzle. This effect on axial velocity contours and axial velocity distributions at 0.5" downstream of the nozzle exit plane is shown in Figure 81.

Increased fan nozzle length reduces noise level at all frequencies at lower velocity conditions due to improved mixing as indicated by LDV data. The trend is reversed at higher velocity conditions possibly due to increased turbulence level.

**Confluent Mixer:** Figure 82 shows the EPNL variation with respect to  $V_{mix}$  for the confluent mixer with fan nozzles of different lengths at two different cycle conditions. For E<sup>3</sup>MF Cycle the EPNL is higher for the standard fan compared to the short fan length for the entire velocity range. However, for HBMF cycle the effect is the same as the E<sup>3</sup>MF Cycle only at lower velocity conditions. At higher velocity conditions, above  $V_{mix}$  of 1000 ft/sec, the fan length has no measurable impact on the noise levels in terms of EPNL. This is further illustrated in Figures 83 and 84 for E<sup>3</sup>MF Cycle and HBMF cycle, respectively, showing the effect of fan nozzle length on PNLT & OASL directivities and PWL spectra at different  $V_{mix}$  conditions.

**6.5 Effect of Internal Pylon on Farfield Noise Level:** Acoustic measurements for the unique-lobed mixer with internal pylon are made at two azimuthal locations, 34° and 90°, to examine the assymetry introduced by the single unique lobe and the internal pylon. Figure 85 shows the EPNL variation with respect to  $V_{mix}$  for the unique-lobed mixer with standard fan nozzle and with the internal pylon at two azimuthal locations for HBMF and HBSF cycle conditions. EPNL for the 22-lobed mixer are also plotted in this figure. In general, the impact of internal pylon and the unique lobe on EPNL seems to be very small and is comparable to the 22-lobed mixer EPNL for most test conditions. For HBMFC the EPNdB for 22-lobed mixer is lower at mid  $V_{mix}$  conditions compared to unique-lobed mixer configuration. Also, the EPNLs are higher for unique-lobed mixer at 90° location compared to 34° levels at higher  $V_{mix}$ , above 1100 ft/sec for HBMF cycle conditions. These effects are further examined in terms of PNLT & OASL directivities and PWL and SPL spectra at different  $V_{mix}$  conditions in Figures 86 through 90. In general, the farfield noise is slightly impacted by the internal pylon and the unique lobe at higher frequencies and the noise levels are higher at the community compared to sideline for most conditions.

**6.6 Effect of Fan Nozzle Treatment on Farfield Noise Level and Plume Flowfield:** The acoustic treatment used for fan nozzle for the lobed-mixer configurations are designed using the data for several bulk materials. Two bulk absorbers, a stainless steel based foam, called Feltmetal and Astroquartz, are decided for the fan nozzle treatment. The hardware, showing the fan nozzle treatment installation, is shown in Figures 12 and 13.

**Treatment Design:** Preliminary acoustic treatment design for bulk absorber with perforated facesheet is carried out for the ~1/9-scale model high bypass exhaust nozzle applications. Based on the inner and outer flowlines for the standard long fan nozzle a

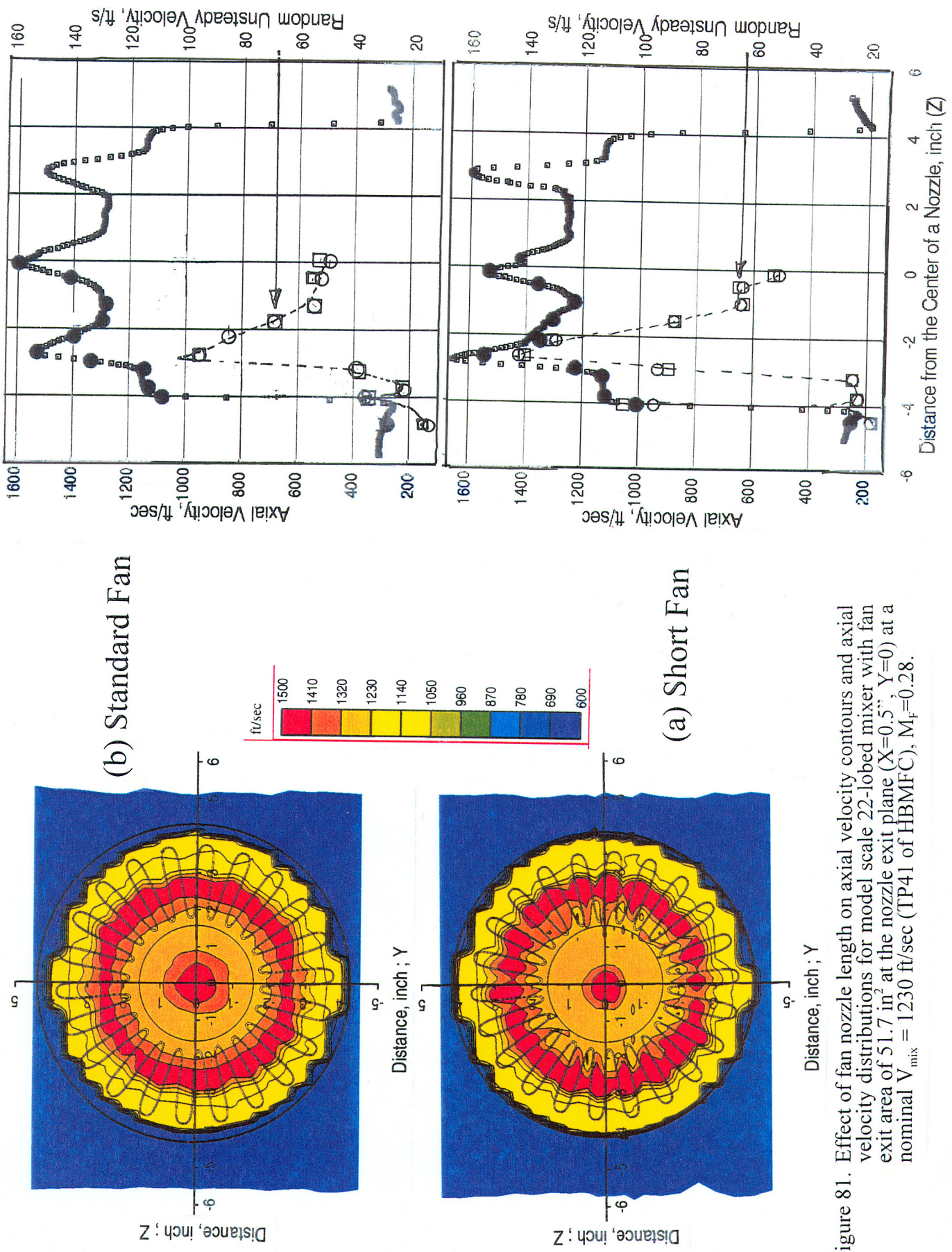


Figure 81. Effect of fan nozzle length on axial velocity contours and axial velocity distributions for model scale 22-lobed mixer with fan exit area of  $51.7 \text{ in}^2$  at the nozzle exit plane ( $X=0.5$ ,  $Y=0$ ) at a nominal  $V_{\text{mix}} = 1230 \text{ ft/sec}$  (TP41 of HBMFC),  $M_f = 0.28$ .

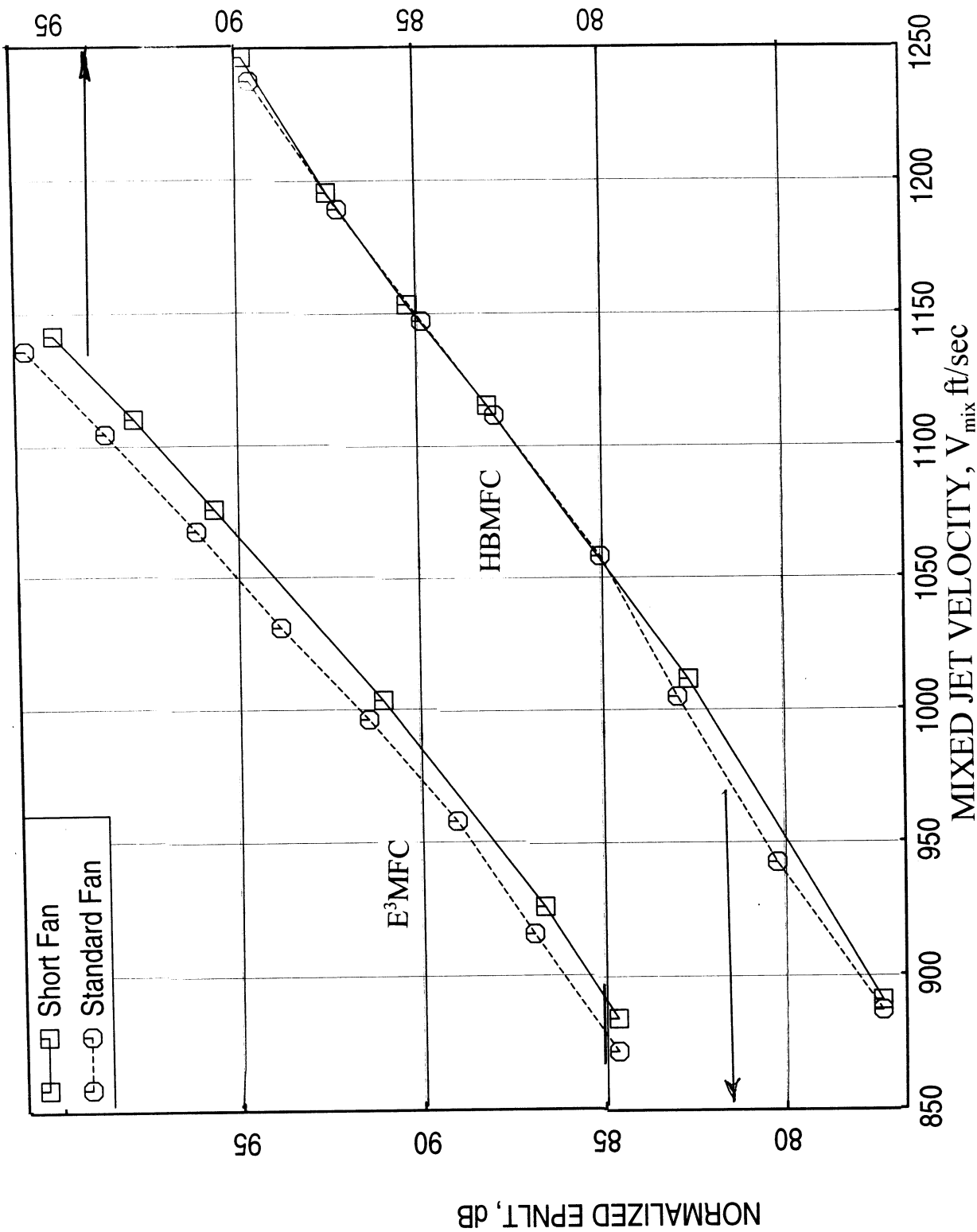


Figure 82. Effect of fan nozzle length on normalized EPNL for the confluent mixer with fan exit area of  $51.7 \text{ in}^2$  for different engine cycles at SAE 77° standard day conditions,  $A_8=3078 \text{ in}^2$ , Sideline Distance=1500 ft,  $M_p=0.28$ .

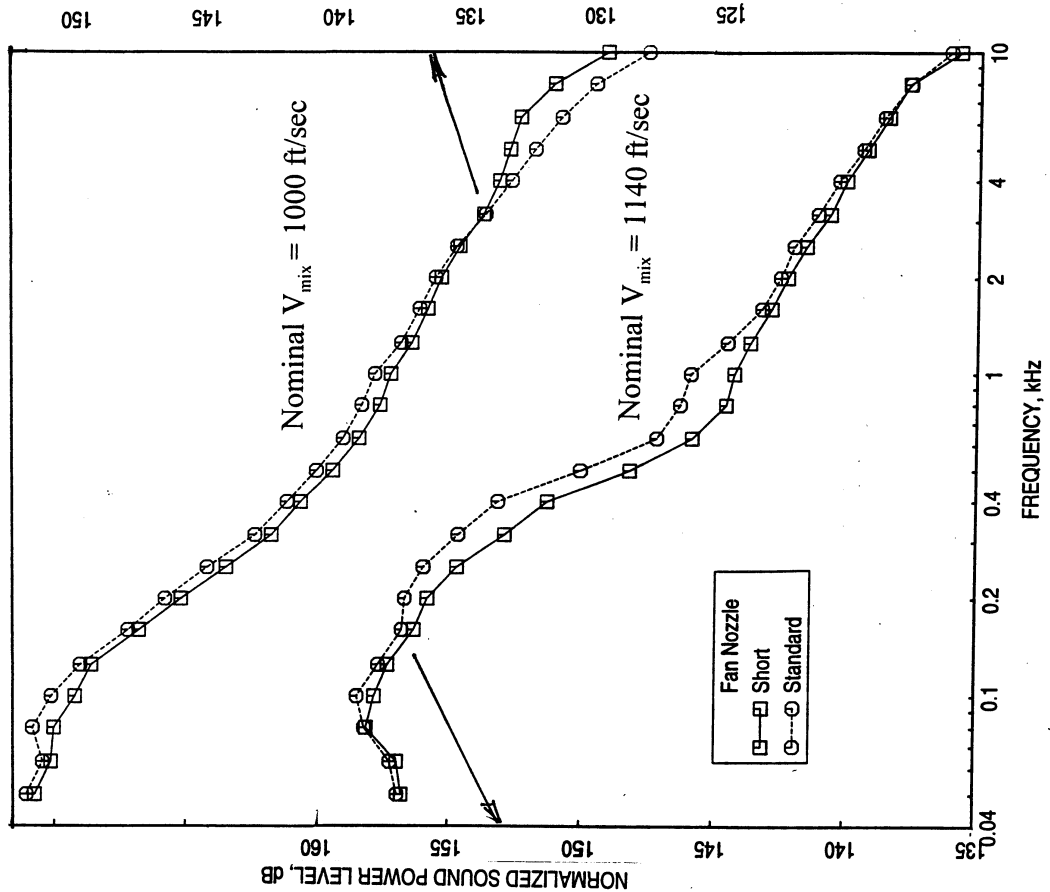
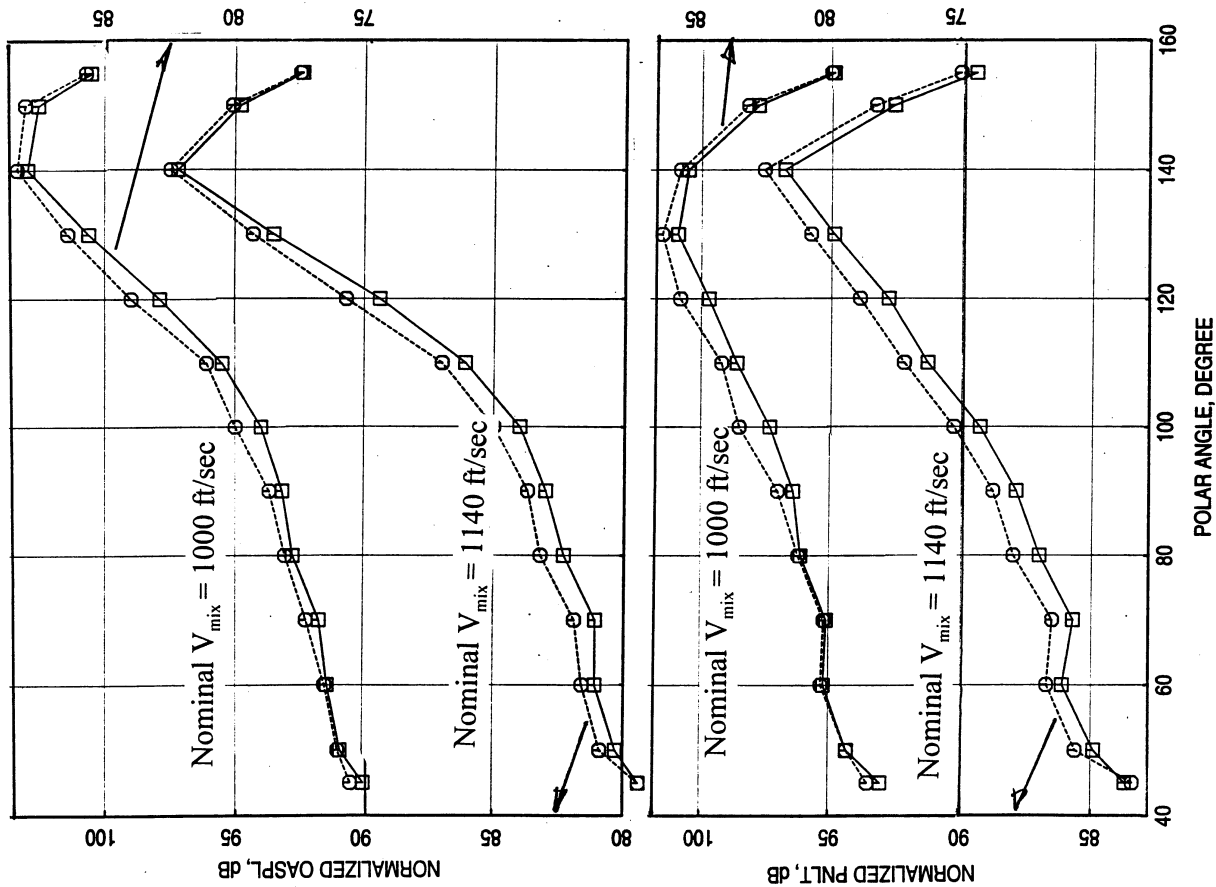


Figure 83. Effect of fan nozzle length on normalized OASPL & PNLT directivities and PWL spectra at different nominal mixed velocities for E<sup>3</sup>MFC for the confluent mixer with fan exit area of 51.7 in<sup>2</sup> at SAE 77° standard day conditions, A8=3078 in<sup>2</sup>, Sideline Distance=1500 ft,  $M_F=0.28$ .



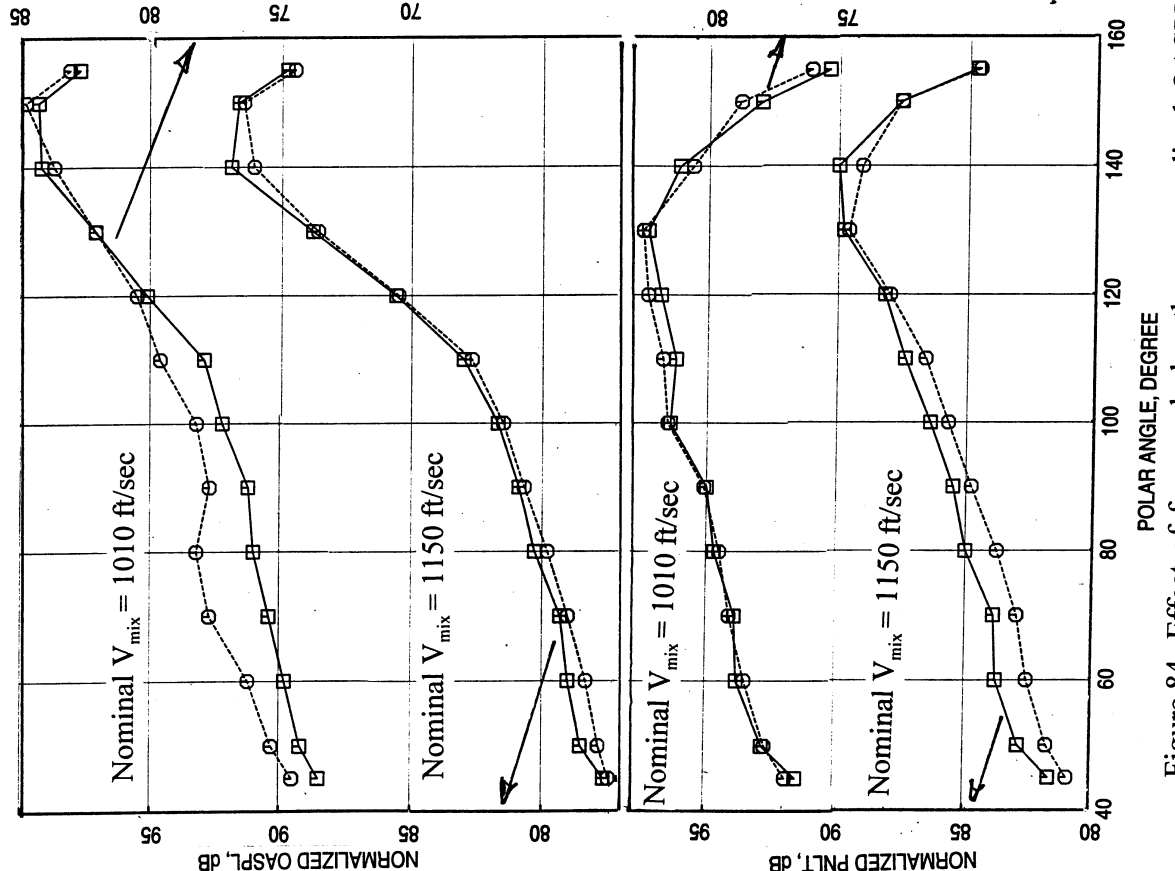
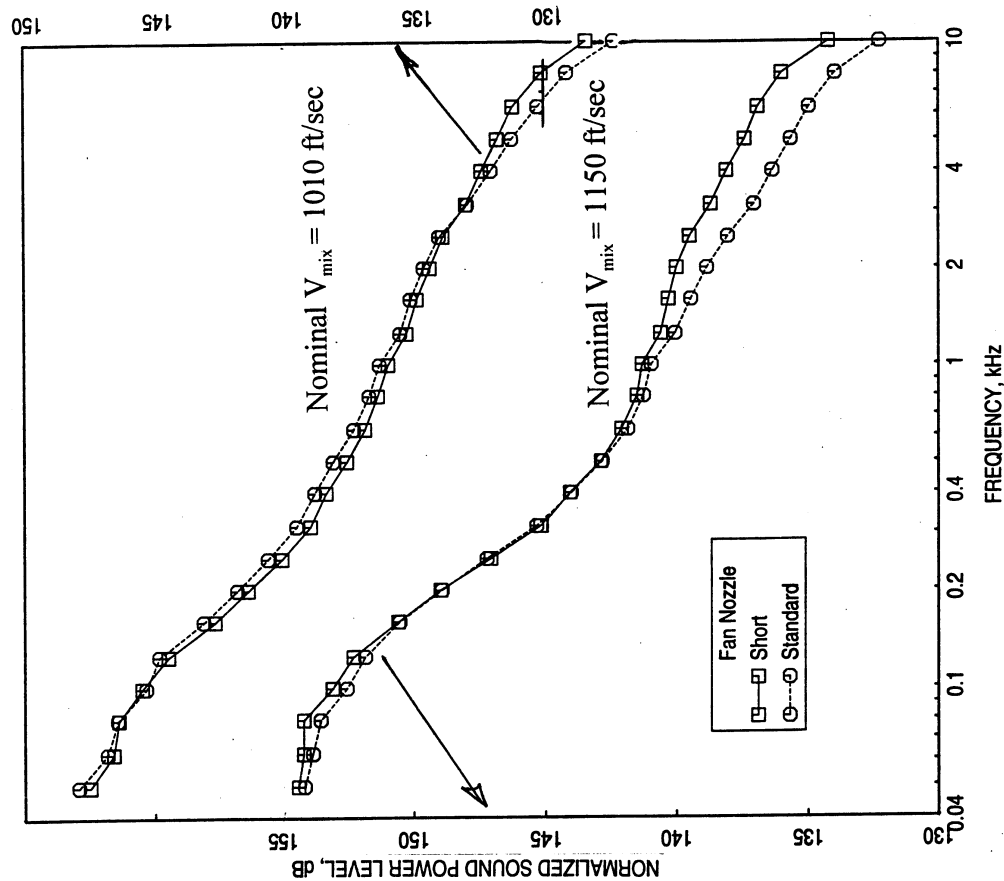


Figure 84. Effect of fan nozzle length on normalized OASPL & PNLT directivities and PWL spectra at different nominal mixed velocities for HBMFC for the confluent mixer with fan exit area of  $51.7 \text{ in}^2$  at SAE  $77^\circ$  standard day conditions,  $A8=3078 \text{ in}^2$ , Sideline Distance=1500 ft,  $M_F=0.28$ .

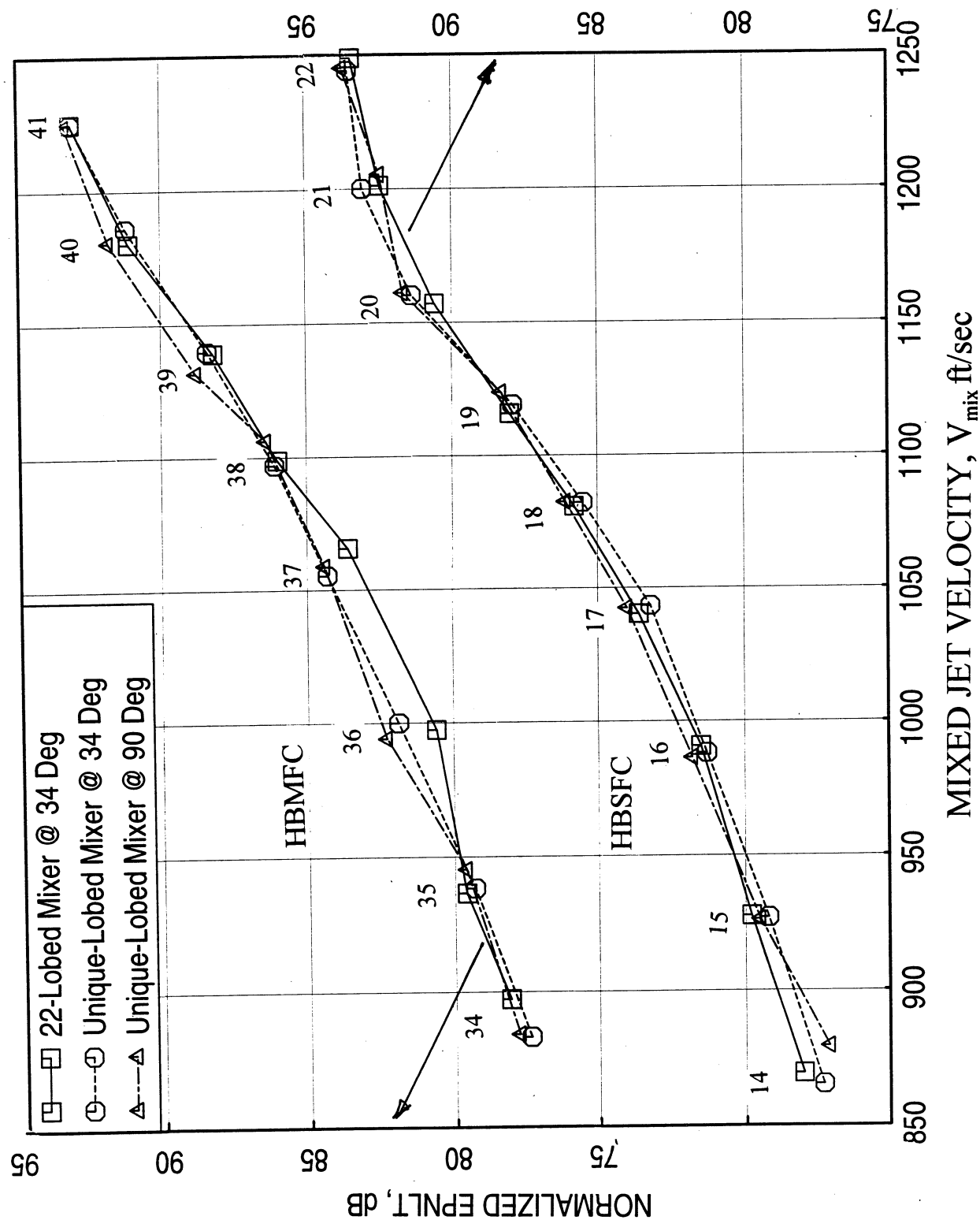


Figure 85. Effect of internal pylon on normalized EPNL for the unique-lobed mixer with standard fan of 51.7 in<sup>2</sup> exit area for different engine cycles at SAE 77° standard day conditions,  $A_8=3078$  in<sup>2</sup>, Sideline Distance=1500 ft,  $M_F=0.28$ .

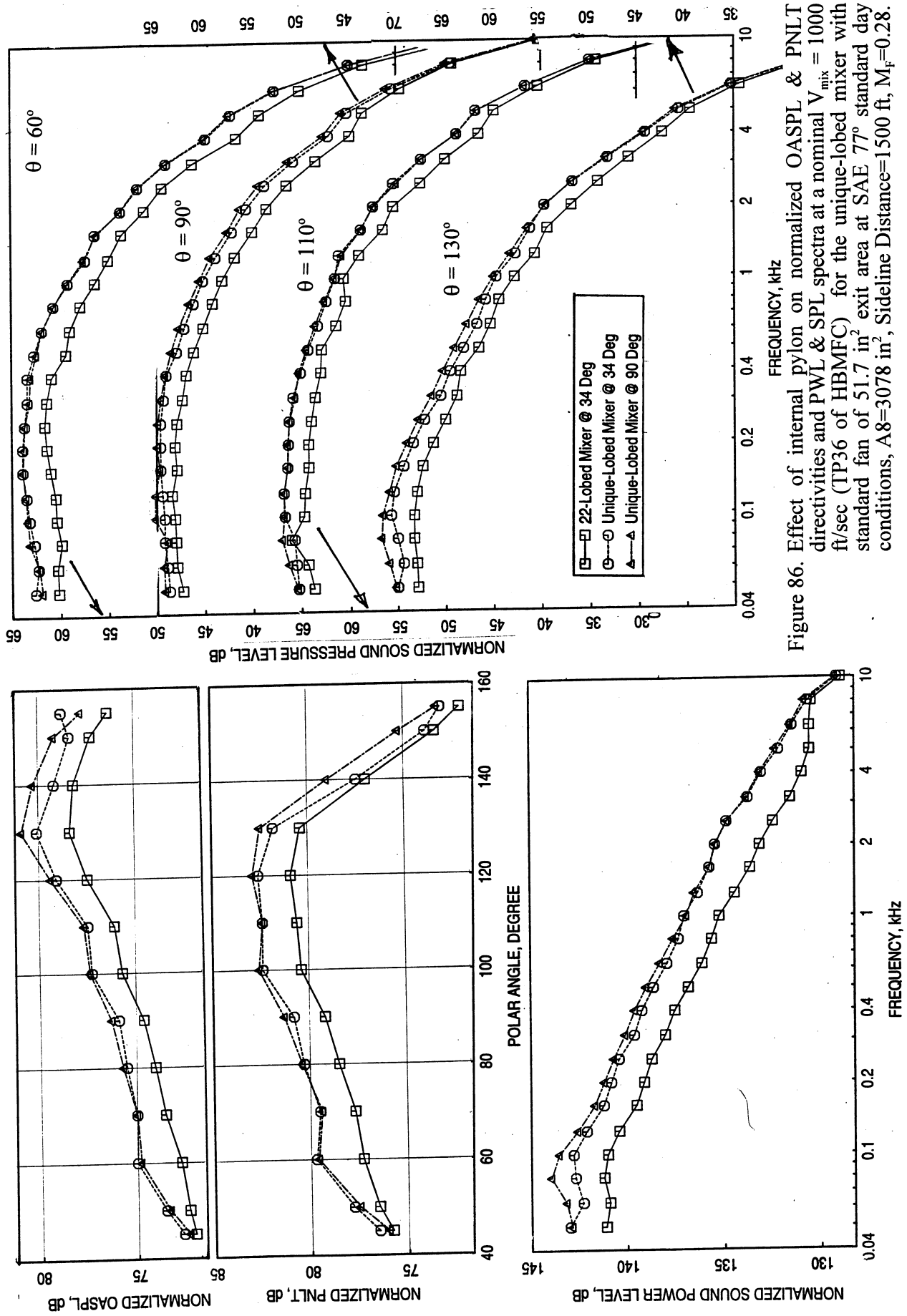


Figure 86. Effect of internal pylon on normalized OASPL & PNLT spectra at a nominal  $V_{mix} = 1000$  ft/sec (TP36 of HBMFC) for the unique-lobed mixer with standard fan of  $51.7 \text{ in}^2$  exit area at SAE  $77^\circ$  standard day conditions,  $A_8=3078 \text{ in}^2$ , Sideline Distance=1500 ft,  $M_F=0.28$ .

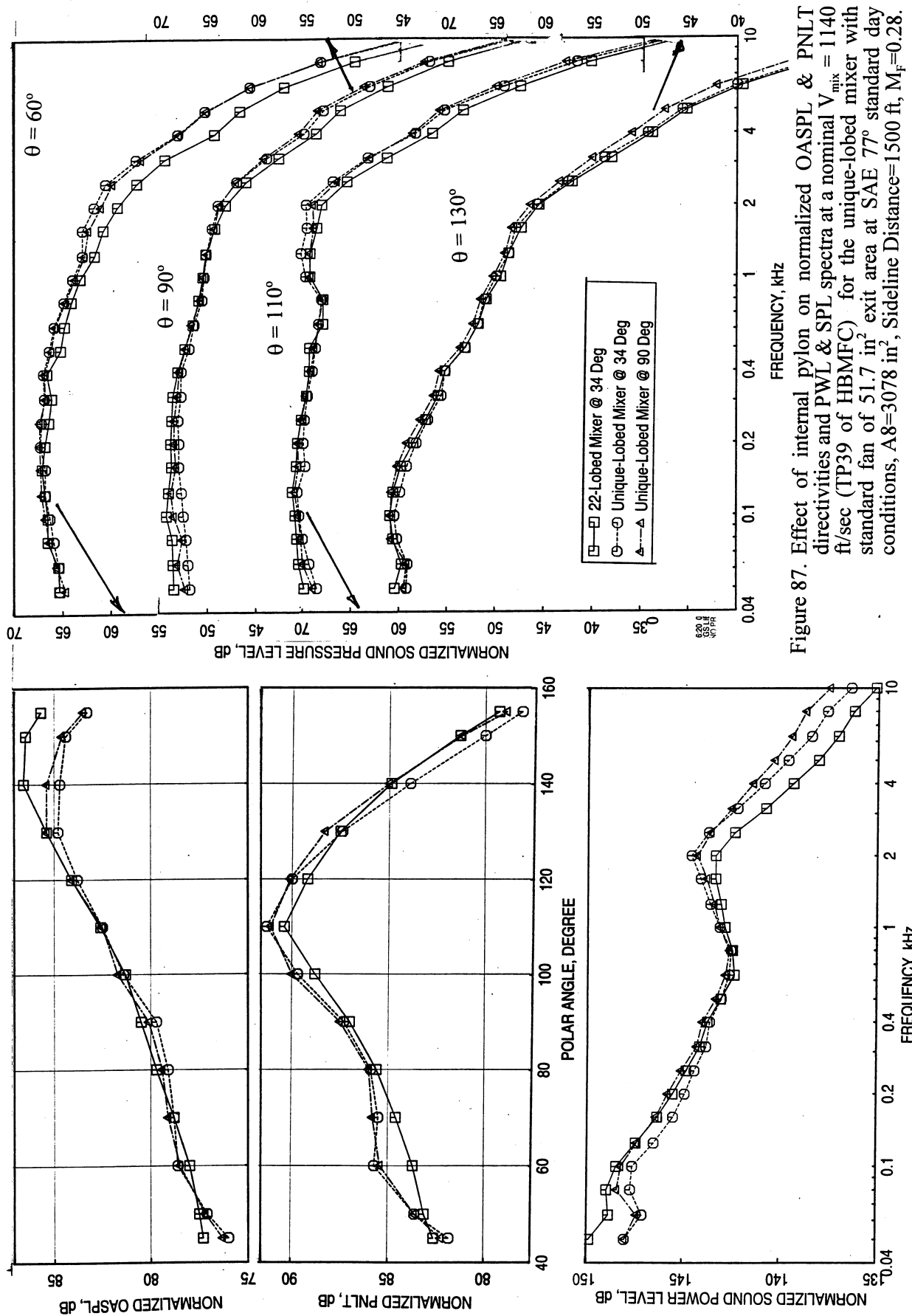


Figure 87. Effect of internal pylon on normalized OASPL & PNLT directivities and PWL & SPL spectra at a nominal  $V_{\text{mix}} = 1140 \text{ ft/sec}$  (TP39 of HBMFC) for the unique-lobed mixer with standard fan of  $51.7 \text{ in}^2$  exit area at SAE  $77^\circ$  standard day conditions,  $A_8=3078 \text{ in}^2$ , Sideline Distance=1500 ft,  $M_F=0.28$ .

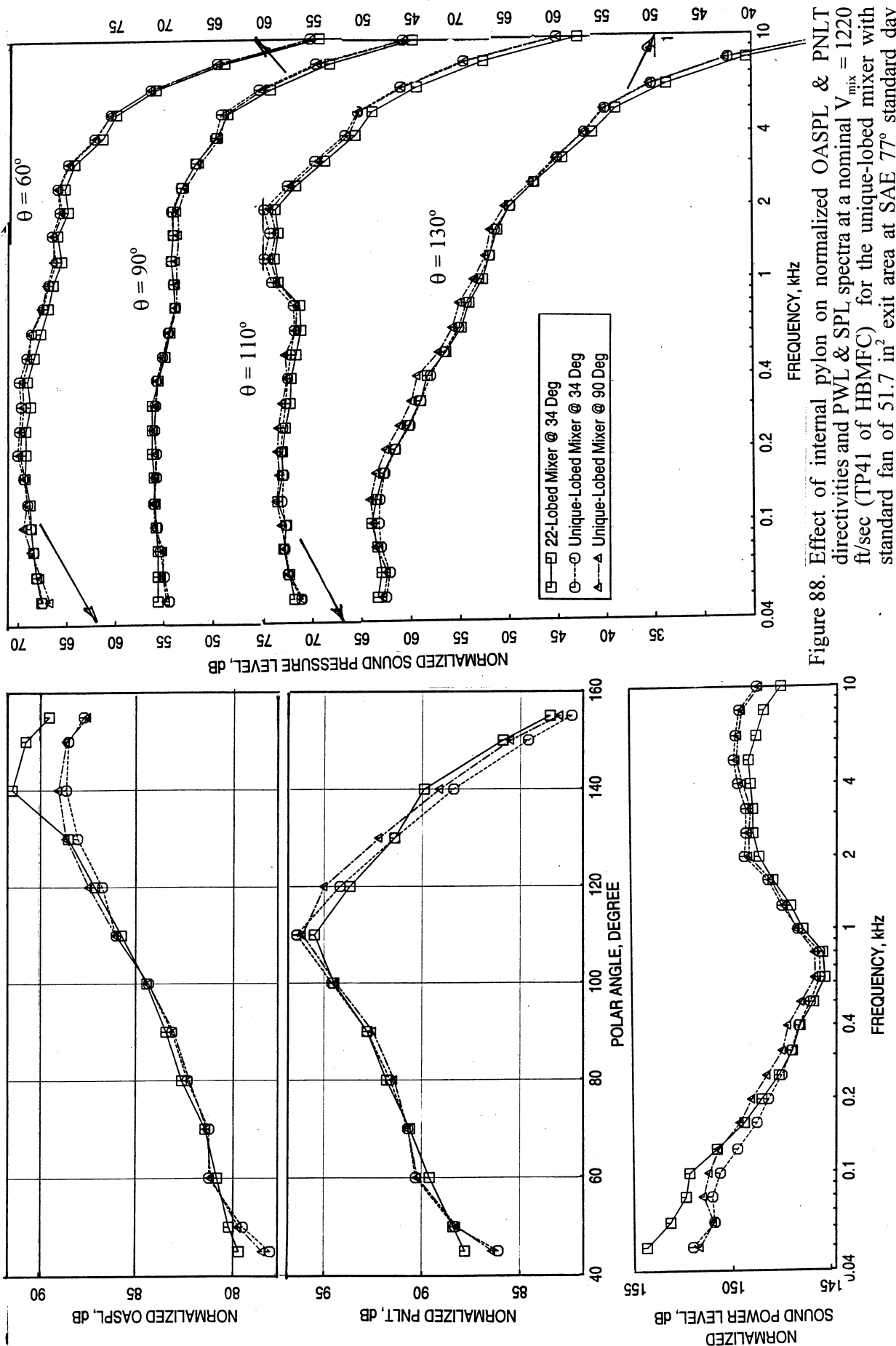


Figure 88. Effect of internal pylon on normalized OASPL & PNLT directivities and PWL & SPL spectra at a nominal  $V_{\text{mix}} = 1220$  ft/sec (TP41 of HBMFC) for the unique-lobed mixer with standard fan of  $51.7 \text{ in}^2$  exit area at SAE  $77^\circ$  standard day conditions,  $A_8=3078 \text{ in}^2$ , Sideline Distance=1500 ft,  $M_F=0.28$ .

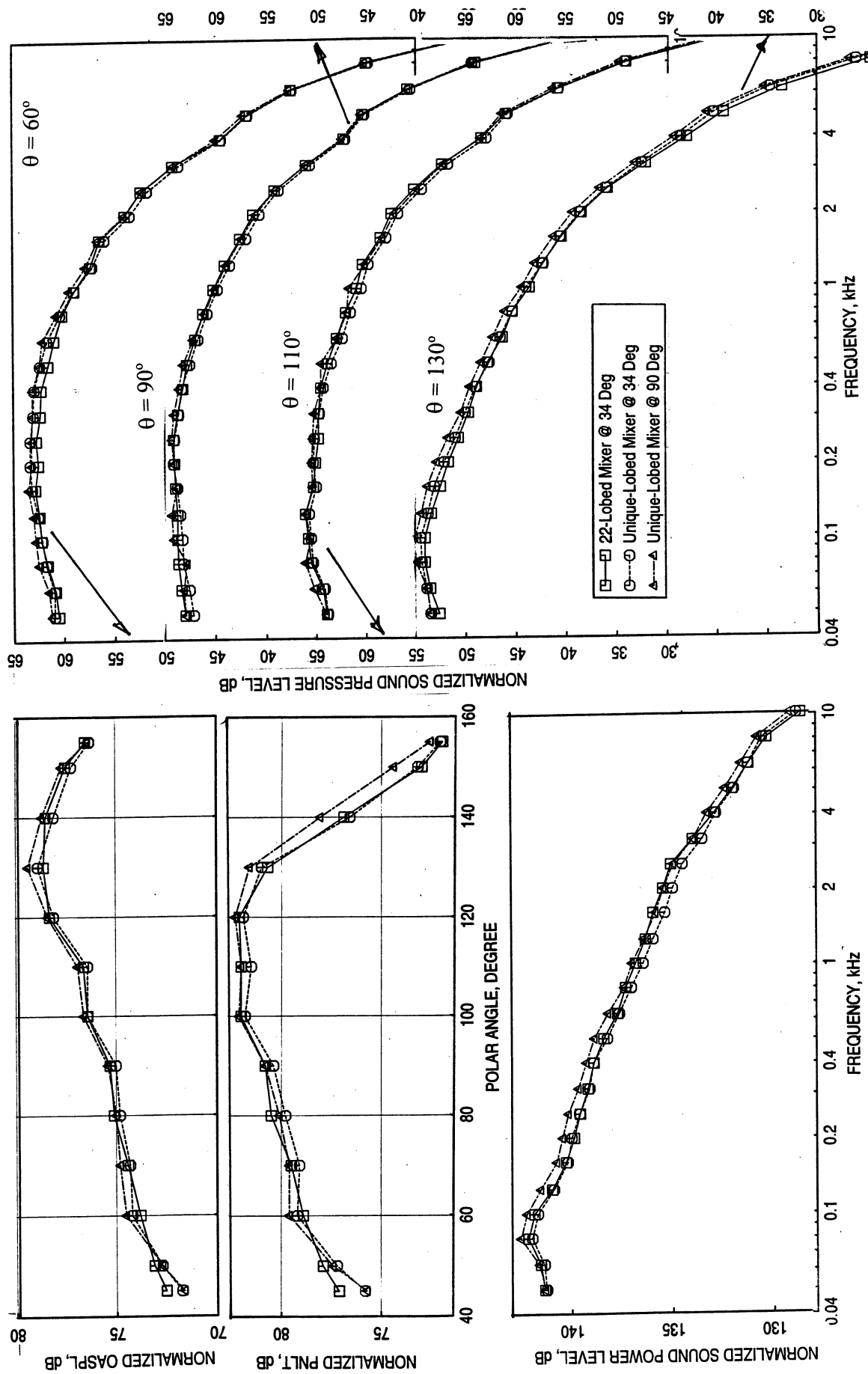


Figure 89. Effect of internal pylon on normalized OASPL & PNLT directivities and PWL & SPL spectra at a nominal  $V_{\text{mix}}^{1/2} = 1000 \text{ ft/sec}$  (TP16 of HBSFC) for the unique-lobed mixer with standard fan of  $51.7 \text{ in}^2$  exit area at SAE 7% standard day conditions,  $A_8 = 3078 \text{ in}^2$ , Sideline Distance = 1500 ft,  $M_F = 0.28$ .

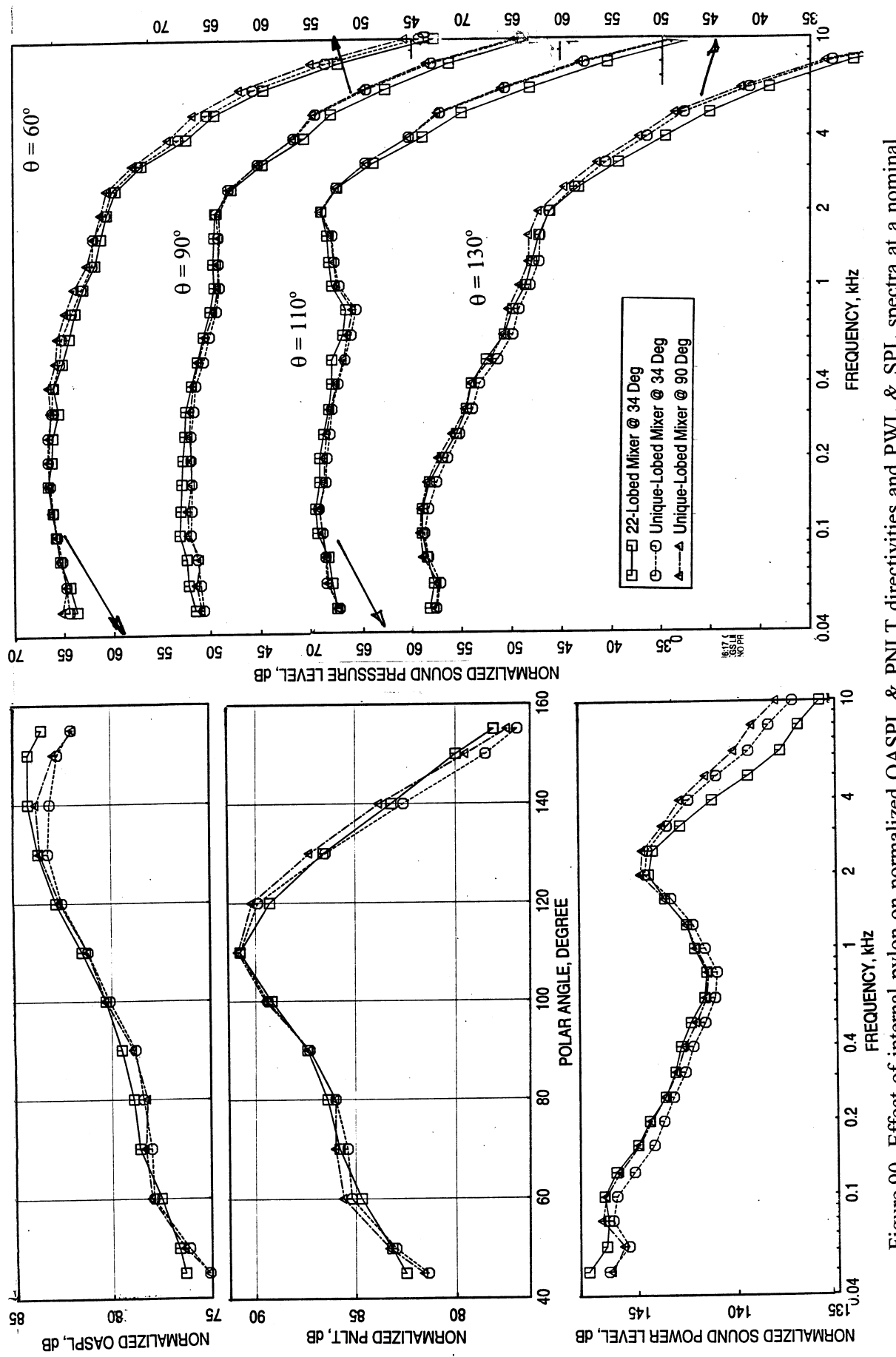


Figure 90. Effect of internal pylon on normalized OASPL & PNLT directivities and PWL & SPL spectra at a nominal  $V_{\text{mix}}^{77^\circ} = 1120 \text{ ft/sec}$  (TP19 of HBSF) for the unique-lobed mixer with standard fan of  $51.7 \text{ in}^2$  exit area at SAE  $77^\circ$  standard day conditions,  $A_8=3078 \text{ in}^2$ , Sideline Distance=1500 ft,  $M_r=0.28$ .

liner depth (i.e., bulk + facesheet) of 0.425" is decided with minimal outer flowline deviation. Based on the scale factor and previous data on E<sup>3</sup> mixers the critical frequencies impacting EPNL values would be about 20 to 30 kHz.

The objective of this design is to achieve desired optimum impedance at the critical frequencies. The optimum specific resistance and reactance ranges between 1.5 to 2 and -0.5 to 0.0, respectively, are chosen for the liner for maximum acoustic suppression on the basis of past experience.

Tests were conducted to measure the DC flow resistance and normal impedance for three available 0.4" deep bulk samples at room temperature conditions. Two perforated sheets of 0.025"-thick and 0.045" hole diameter with different porosities, namely 21% and 37%, were used in the impedance measurement tests. The normal impedance results for the bulk samples with and without facesheet are presented in Figure 91. The DC flow test results are listed below:

Material Description	Sample Depth Inches	A Rayls/cm	B Rayls. sec/cm <sup>2</sup>	R100 Rayls/cm
Silicon Carbide - 100 ppi	0.4	5.5	0.0320	8.70
Silicon Carbide - 200 ppi	0.4	23.0	0.1475	37.75
Felt Metal - 5% Dense	0.4	40.0	0.0800	48.00

The measured DC flow resistance and the facesheet properties are used in predicting the normal impedance for the bulk samples with and without facesheets and compared with the measured impedance data. The prediction code is based on Delany & Bezly method and assumes linear addition of reactance and resistance of the bulk and facesheet in the calculation of the combined values for the liner. Reasonably good agreement between data and prediction is observed on the limited range of frequencies up to 12 kHz (not shown here).

The liner design is carried out for a grazing flow Mach number of 0.4 and liner static temperature of 300°F. The boundary layer displacement thickness is assumed to be 0.05". A typical internal noise spectrum is assumed with an OASPL of 157 dB. Utilizing the above temperature, noise spectrum, and grazing flow conditions and using the set depths and boundary layer displacement thicknesses, the bulk resistivity and facesheet properties are varied to arrive at optimum liner design, such that the desired impedance values are attained at most frequencies of interest, especially at and around the critical frequencies.

A 0.01"-thick facesheet is required for the optimum liner. However, this thickness is not practical from the mechanical considerations. Thus, the impedance is predicted with a modified facesheet thickness of 0.025" (alternate design) and is compared with the optimum impedance in Figure 92. The reactance levels at higher frequencies are much higher for the alternate design compared to the optimum case. A bulk resistivity of 100 Rayls/cm is required for the optimum liner designs. However, it is necessary to predict the impedance deviations when available bulk materials are to be used in the liner. Thus,

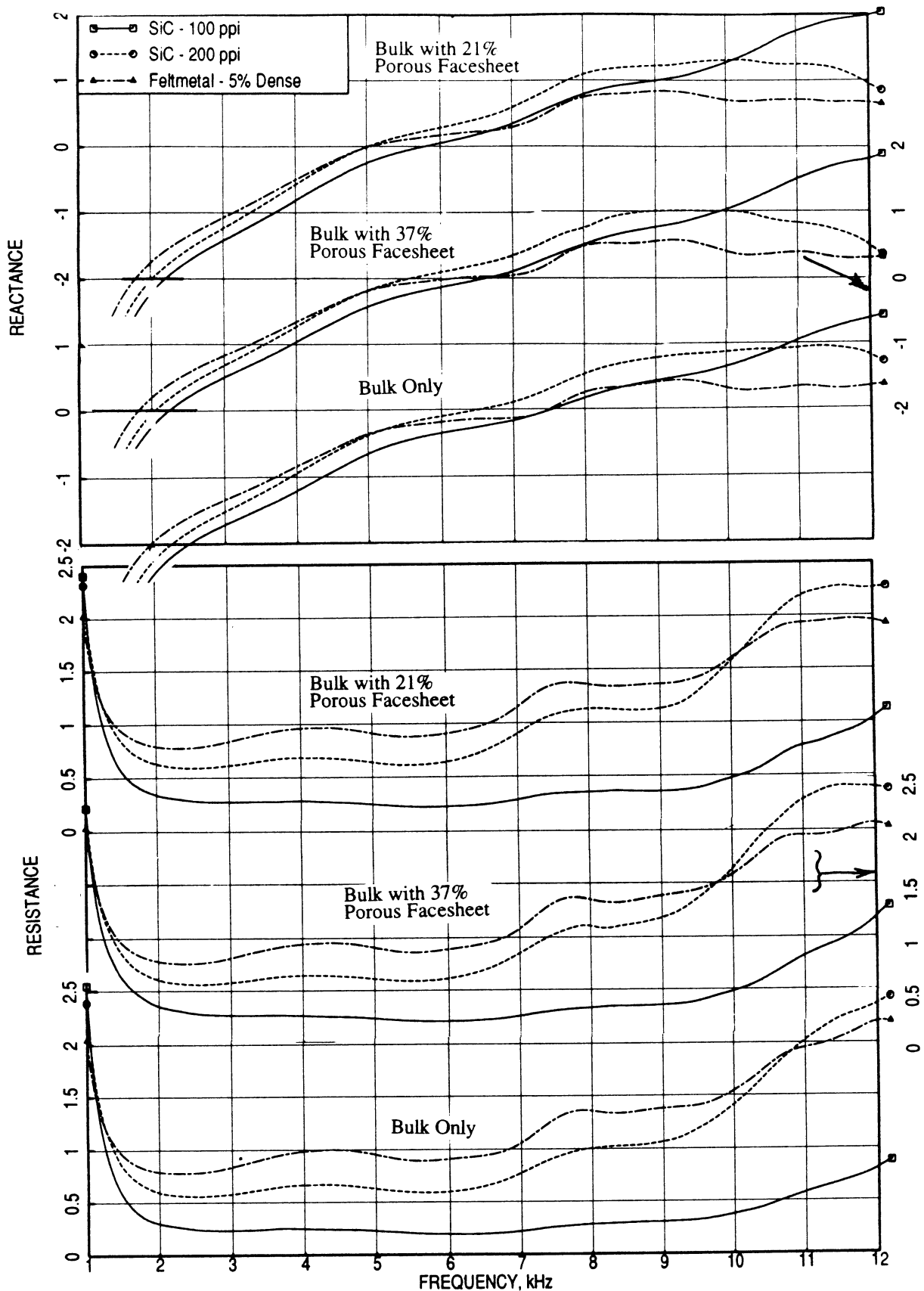


Figure 91. Effect of bulk resistivity on measured normal impedance for 0.4"-deep bulk samples with and without facesheet, facesheet thickness and hole diameters are 0.025" and 0.045", excitation OASPL=150 dB.

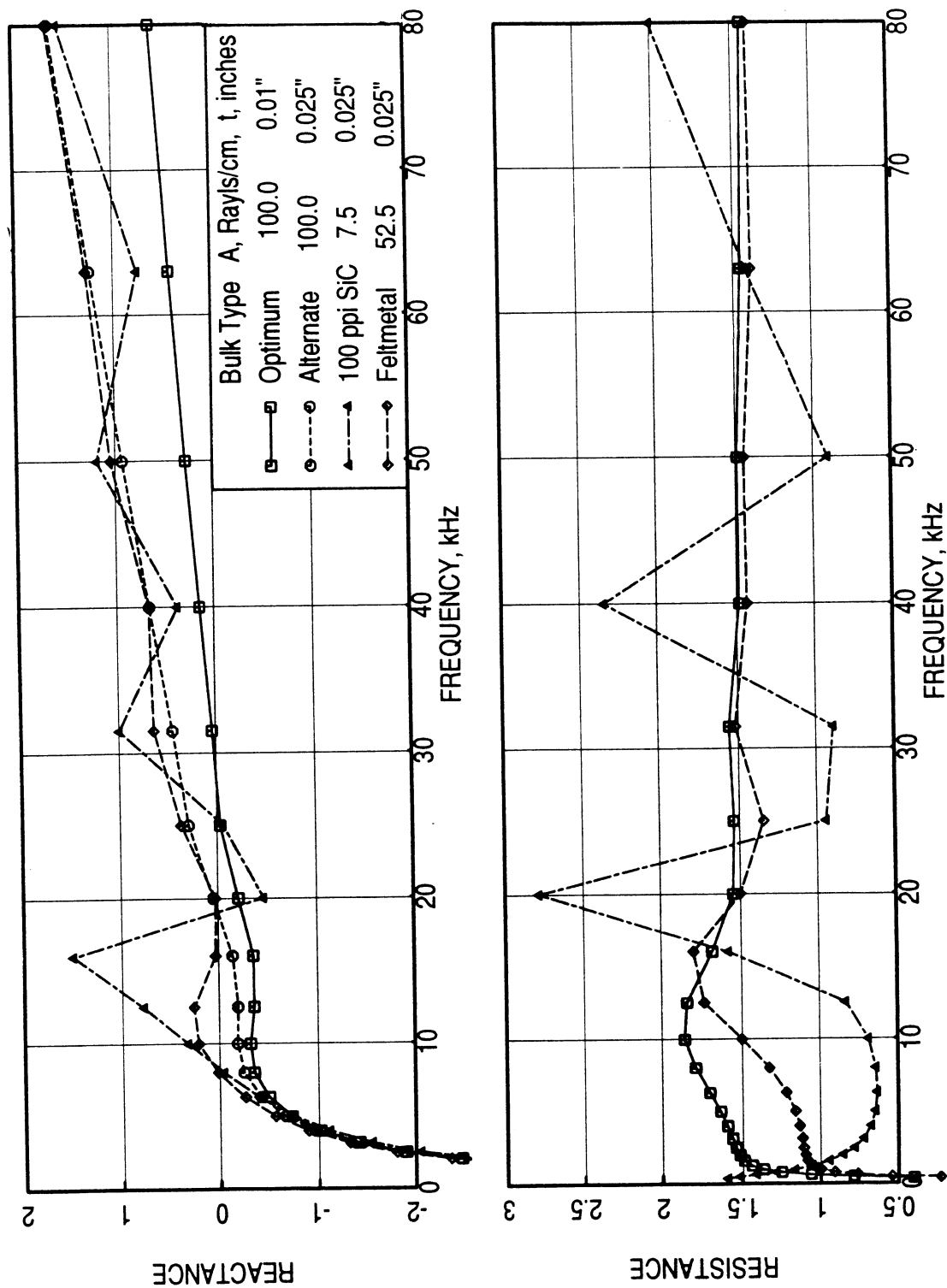


Figure 92. Effect of bulk resistivity and facesheet thickness on normal impedance compared to optimized normal impedance of 0.4" deep acoustic liners; facesheet porosity and hole diameters of 45% and 0.045", static temperature=300°F, static temperature=300°F, grazing flow Mach number=0.4, OASPL=157 dB.

the impedance is predicted for two different bulk materials (100 ppi SiC and 5% dense Feltmetal) and the impedance spectra are compared with optimum and alternate liner impedance spectra in Figure 92. In these predictions the bulk resistivities used for different materials are the values, appropriately modified for 300°F from measured resistivities at room temperature condition. The Feltmetal impedance seems to be very close to those of the alternate design case. Hence, 5% dense Feltmetal is selected for the current application.

The facesheet of the above specification (i.e., 0.025"-thick, 45% porous, and 0.045" hole diameter) is not a catalog item. However, the facesheet with the same specification, but with hole diameters of 0.038" and 0.078" are readily available as catalog items. Thus the impedance spectra for the liners with these facesheets are predicted and compared with the results of the facesheet with 0.045" hole diameter in Figure 93. Facesheet with 0.078" hole diameter seems to be very close to the design case. Thus the hole diameter of 0.078" is used for the current liner.

**Acoustic and Flowfield Results for 22-Lobed Mixer:** Figure 94 shows the EPNL and the peak PNLT levels with respect to mixed velocity for hardwalled and feltmetal treated long fan configurations with 22-lobed mixer. Significant acoustic suppression is achieved at all conditions in terms of EPNdB and peak PNLT. The acoustic suppression seems to be higher for E<sup>3</sup>MF cycle conditions compared to HBMF cycle. The effect of treatment with respect to acoustic suppression is further demonstrated in Figure 95 in terms of OASPL & PNLT directivities and PWL & SPL spectra for a nominal  $V_{mix}$  of 1125 ft/sec (TP79 of E<sup>3</sup>MFC) for the 22-lobed mixer configuration. Acoustic suppression is more significant at higher frequencies above 400 Hz.

The effect of fan nozzle treatment on the flowfield for E<sup>3</sup>MF cycle at a nominal  $V_{mix}$  of 1125 ft/sec (TP79) for the 22-lobed mixer configuration is shown in Figure 96 in the form of 3-dimensional velocity profiles measured at 0.5" downstream of the nozzle exit. This effect on axial velocity contours and axial velocity distributions at 0.5" downstream of the nozzle exit plane is shown in Figure 97. Effect of fan nozzle treatment is further examined in Figure 98 on axial velocity distributions at various axial locations from the nozzle exit plane. There is no measurable effect due to treated fan nozzle on the plume flowfield..

The effect of treatment with respect to acoustic suppression for HBMF cycle conditions is further demonstrated in Figures 99 through 101 in terms of OASPL & PNLT directivities and PWL & SPL spectra for nominal  $V_{mix}$  of 1000 ft/sec (TP36), 1055 ft/sec (TP37), and 1140 ft/sec (TP39) for the 22-lobed mixer configuration. Acoustic suppression is significant at higher frequencies and at higher mixed velocities.

**Acoustic Results for Unique-Lobed Mixer:** Unique-lobed mixer with internal pylon is a possible engine application. Thus the acoustic benefit due to treatment is examined for this configuration and is also compared with standard fan configuration without any acoustic treatment. Figure 102 shows the EPNL variation with respect to  $V_{mix}$

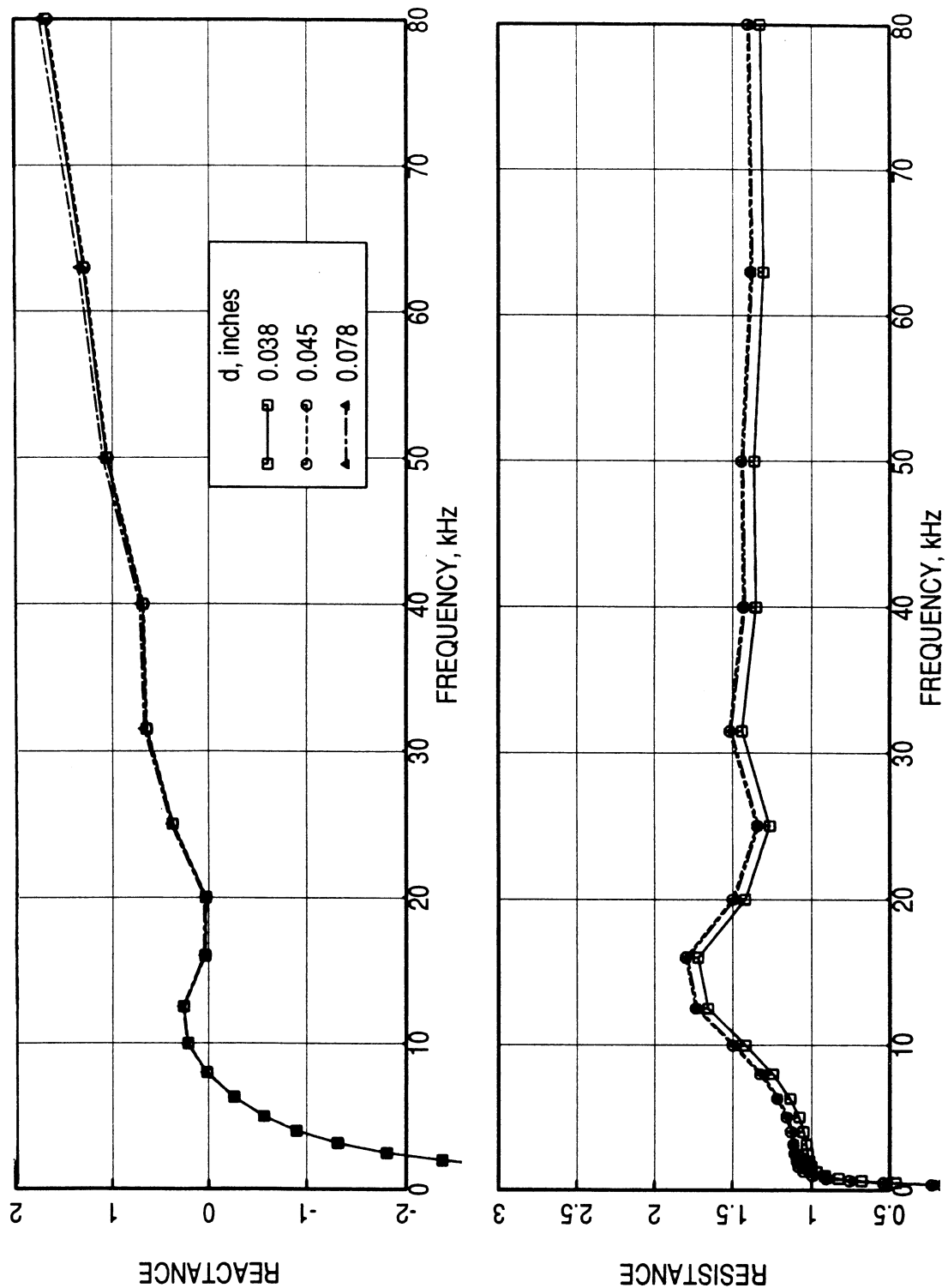


Figure 93. Effect of facesheet hole diameter on normal impedance of a 0.4" deep feltmetal acoustic liners; facesheet porosity and thickness of 45% and 0.025", static temperature=300°F, grazing flow Mach number=0.4, OASPL=157 dB, bulk resistivity at 300°F=52.5 Rayls/cm.

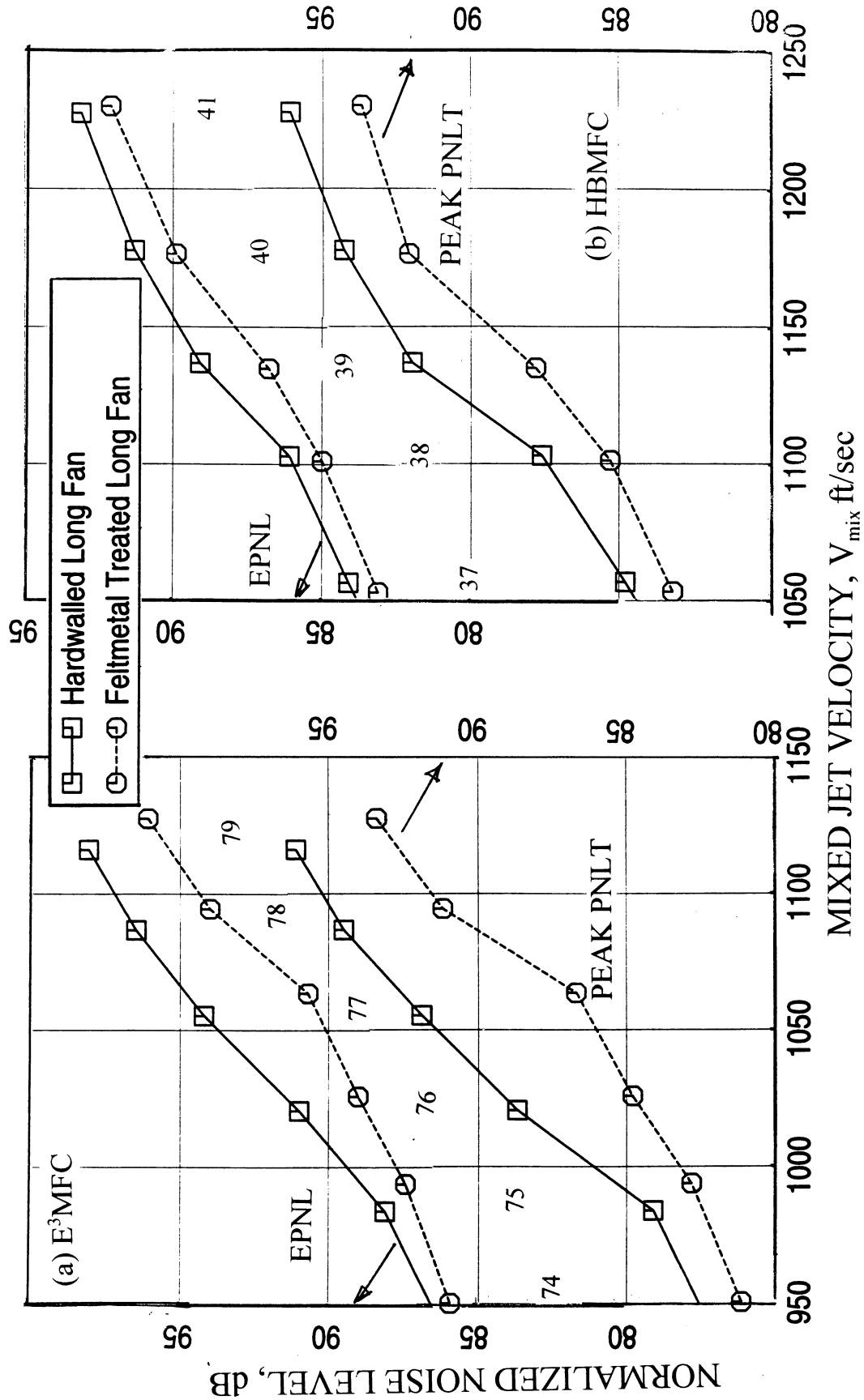


Figure 94. Effect of fan nozzle treatment on normalized EPNL and peak PNLT for the 22-lobed mixer with long fan of  $51.7 \text{ in}^2$  exit area for different engine cycles at SAE 77° standard day conditions,  $A_8 = 3078 \text{ in}^2$ , Sideline Distance = 1500 ft,  $M_f = 0.28$ .

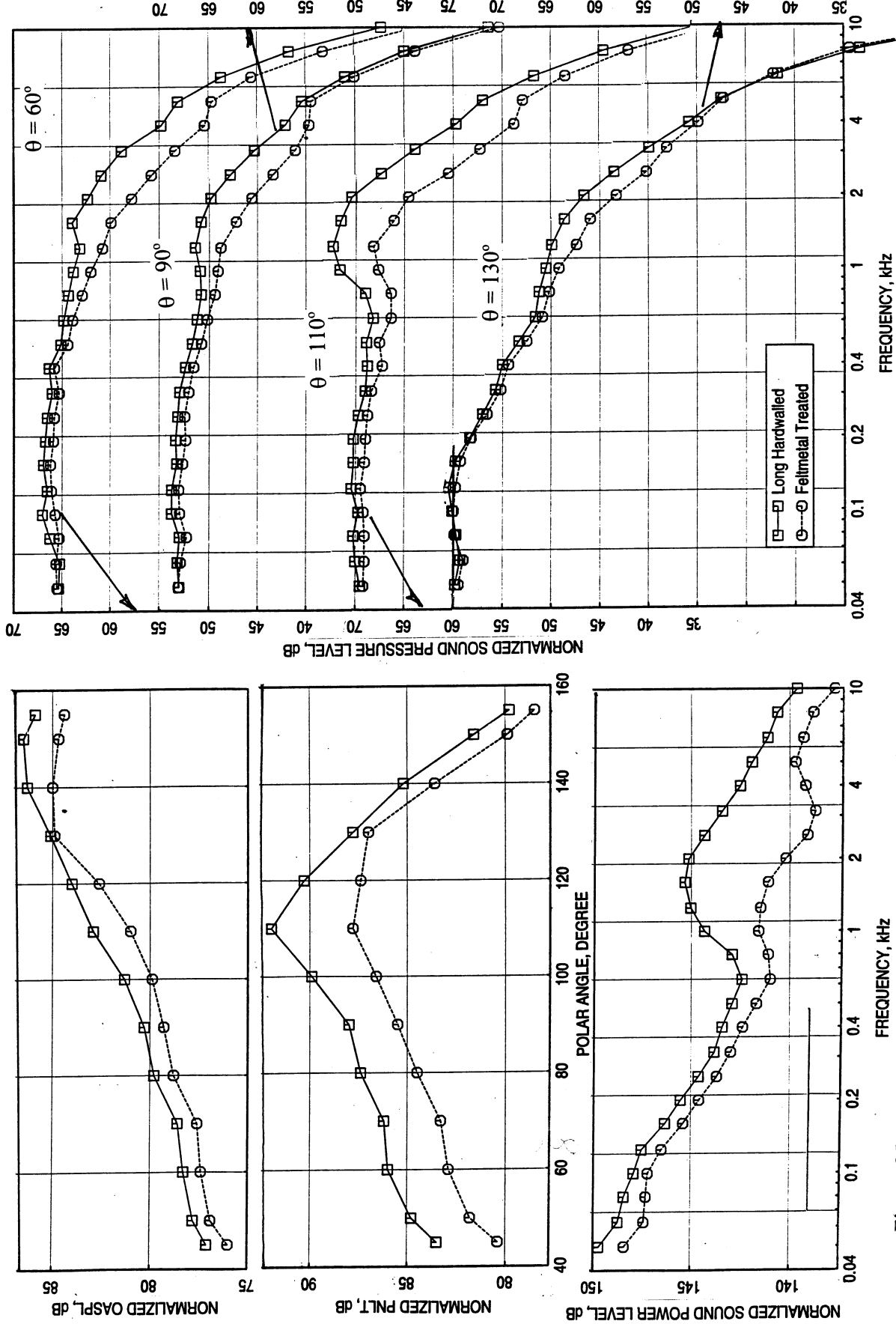


Figure 95. Effect of fan nozzle treatment on normalized OASPL & PNLT directivities and PWL & SPL spectra at a nominal  $V_{\text{mix}} = 1125 \text{ ft/sec}$  (TP79 of E-MFC) for the 22-lobed mixer with long fan of  $51.7 \text{ in}^2$  exit area at SAE 77° standard day conditions,  $A_8=3078 \text{ in}^2$ , Sideline Distance=1500 ft,  $M_F=0.28$ .

(a) Hardwalled

(b) Feltmetal Treated

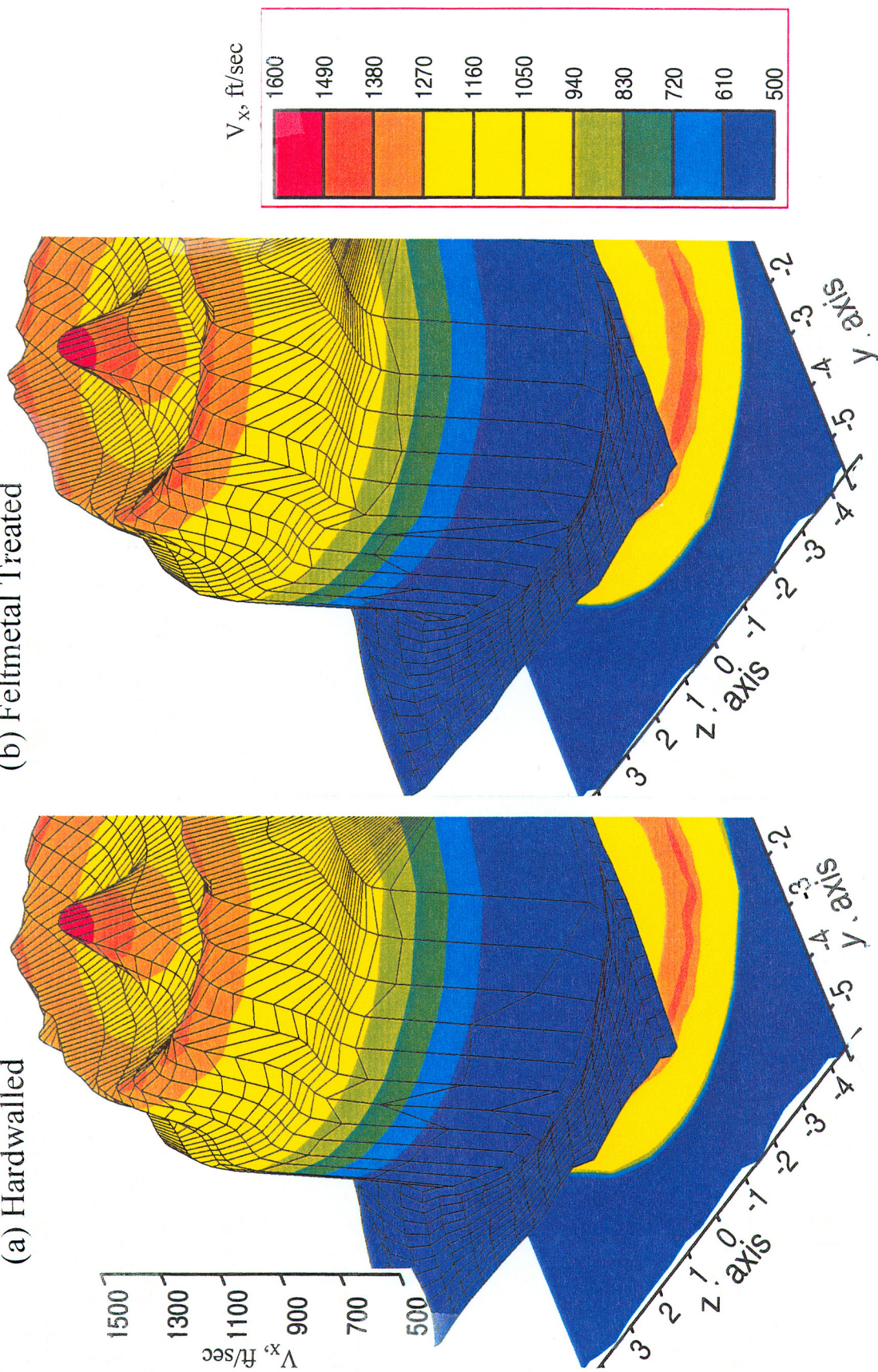


Figure 96. Effect of fan nozzle treatment on axial velocity profiles in 3-dimensional form at 0.5" downstream of the nozzle exit plane for model scale 22-lobed mixer with long fan of 51.7 in<sup>2</sup> exit area at a nominal  $V_{mix} = 1125$  ft/sec (TP79 of E<sup>3</sup>MFC),  $M_F = 0.28$ .

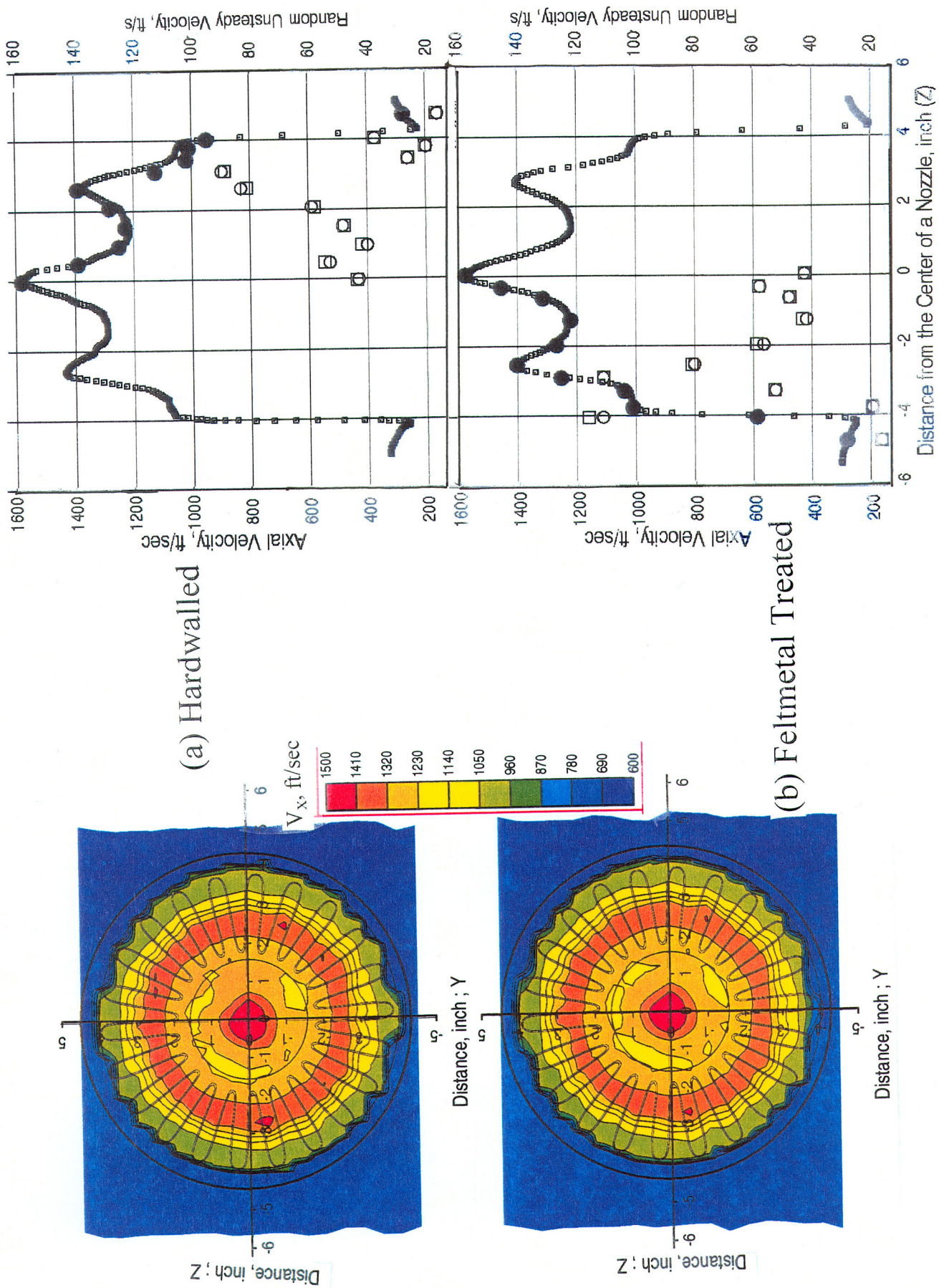


Figure 97. Effect of fan nozzle treatment on axial velocity contours and axial velocity distributions at 0.5" downstream of the nozzle exit plane for model scale 22-lobed mixer with long fan of 51.7 in<sup>2</sup> exit area at a nominal  $V_{mix} = 1125$  ft/sec (TP79 of E<sup>3</sup>MFC),  $M_F = 0.28$ .

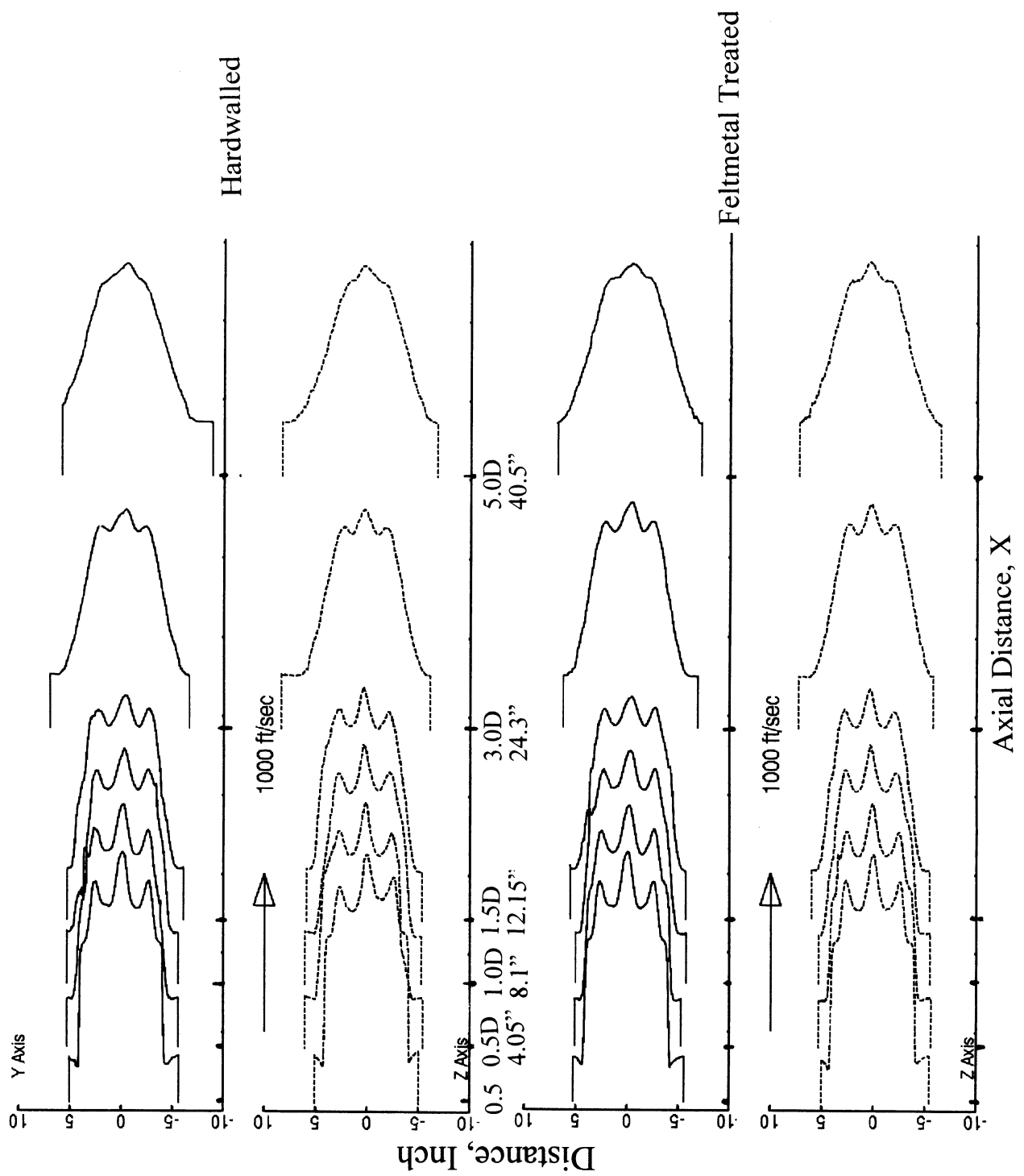


Figure 98.. Effect of fan nozzle treatment on axial velocity distribution at various axial downstream locations from the nozzle exit plane for model scale 22-lobed mixer with long fan of  $51.7 \text{ in}^2$  exit area at a nominal  $V_{\text{mix}} = 1125 \text{ ft/sec}$  (TP79 of  $E^3 \text{ MFC}$ ),  $M_f=0.28$

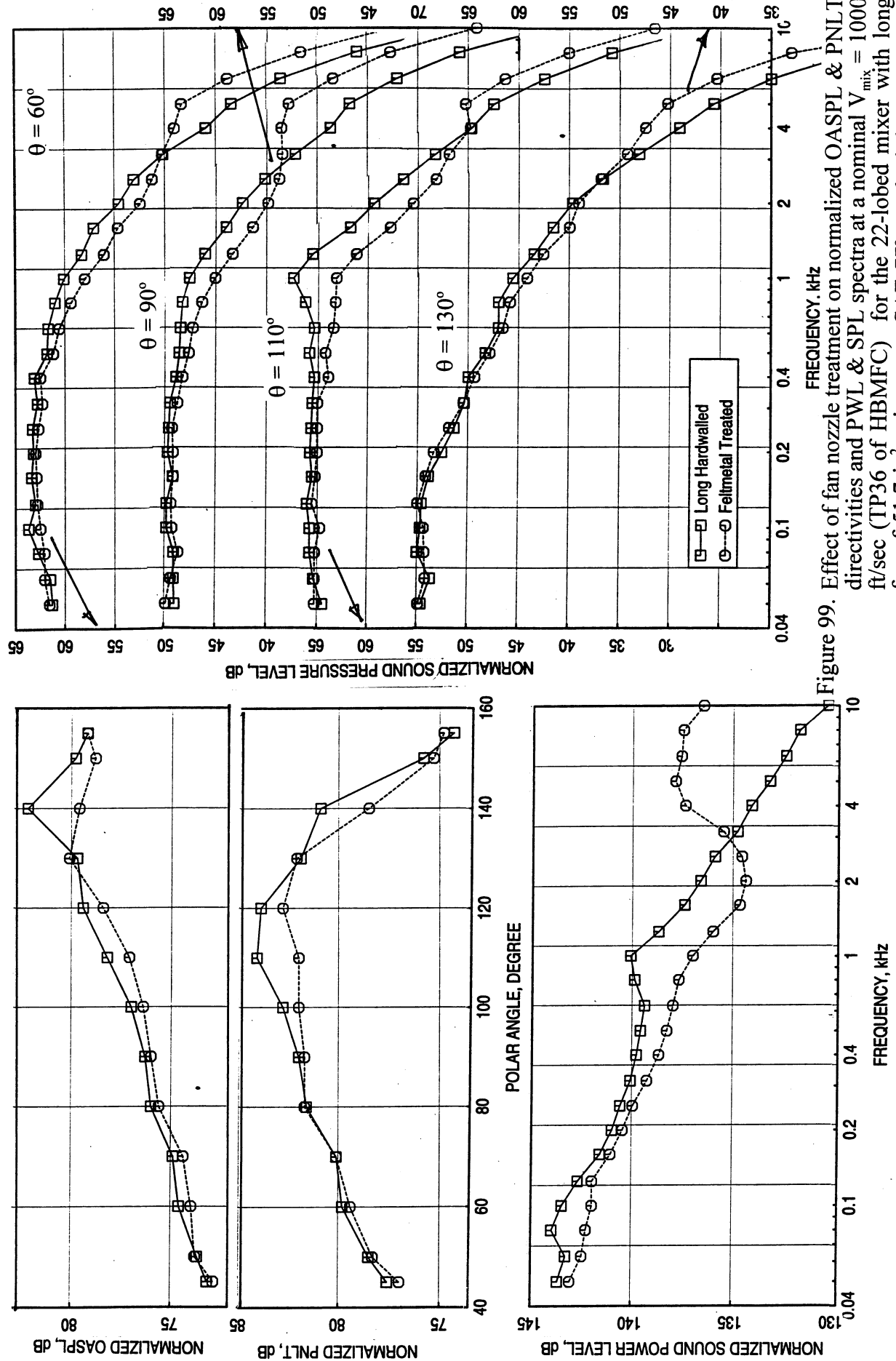


Figure 99. Effect of fan nozzle treatment on normalized OASPL & PNLT directivities and PWL & SPL spectra at a nominal  $V_{\text{mix}} = 1000 \text{ ft/sec}$  (TP36 of HBMFC) for the 22-lobed mixer with long fan of  $51.7 \text{ in}^2$  exit area at SAE  $77^\circ$  standard day conditions,  $A_8 = 3078 \text{ in}^2$ , Sideline Distance = 1500 ft,  $M_F = 0.28$ .

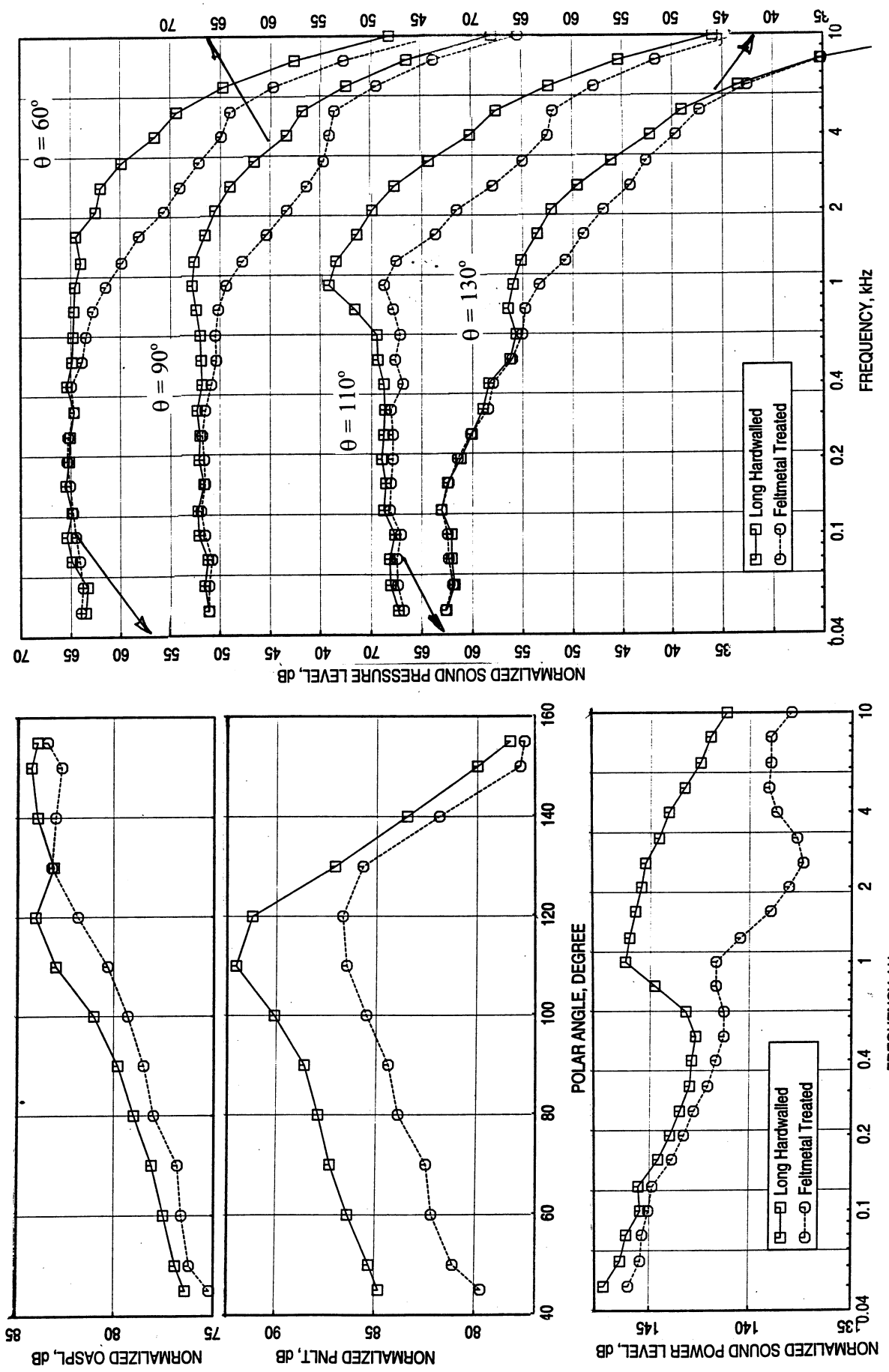


Figure 100. Effect of fan nozzle treatment on normalized OASPL & PNLT directivities and PWL & SPL spectra at a nominal  $V_{\text{mix}} = 1055 \text{ ft/sec}$  (TP37 of HBMFC) for the 22-lobe mixer with long fan of  $51.7 \text{ in}^2$  exit area at SAE  $77^\circ$  standard day conditions,  $A_8=3078 \text{ in}^2$ , Sideline Distance=1500 ft,  $M_F=0.28$ .

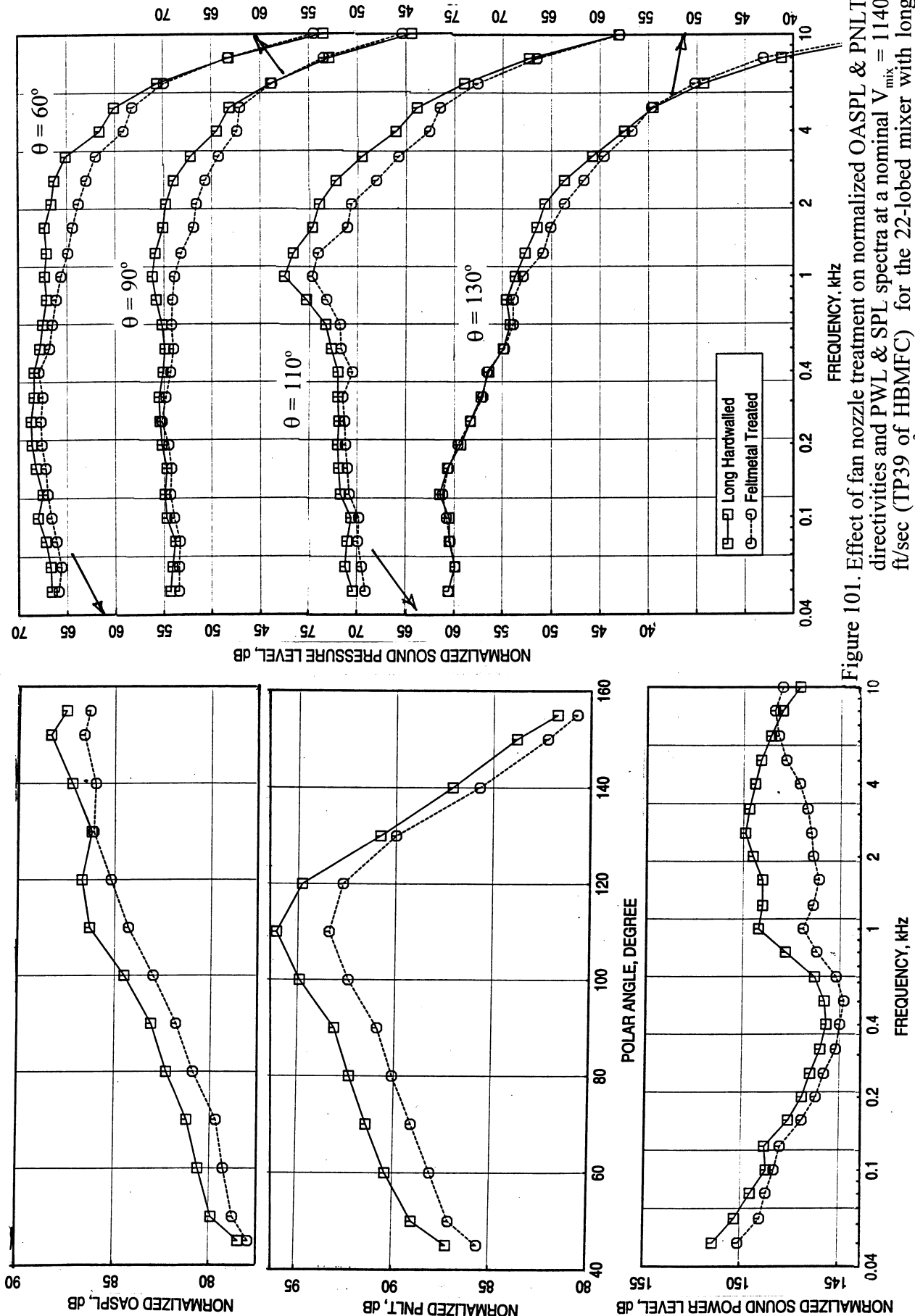


Figure 101. Effect of fan nozzle treatment on normalized OASPL & PNLT directivities and PWL & SPL spectra at a nominal  $V_{\text{mix}} = 1140 \text{ ft/sec}$  (TP39 of HBMFC) for the 22-lobed mixer with long fan of  $51.7 \text{ in}^2$  exit area at SAE  $77^\circ$  standard day conditions,  $A_8=3078 \text{ in}^2$ , Sideline Distance=1500 ft,  $M_F=0.28$ .

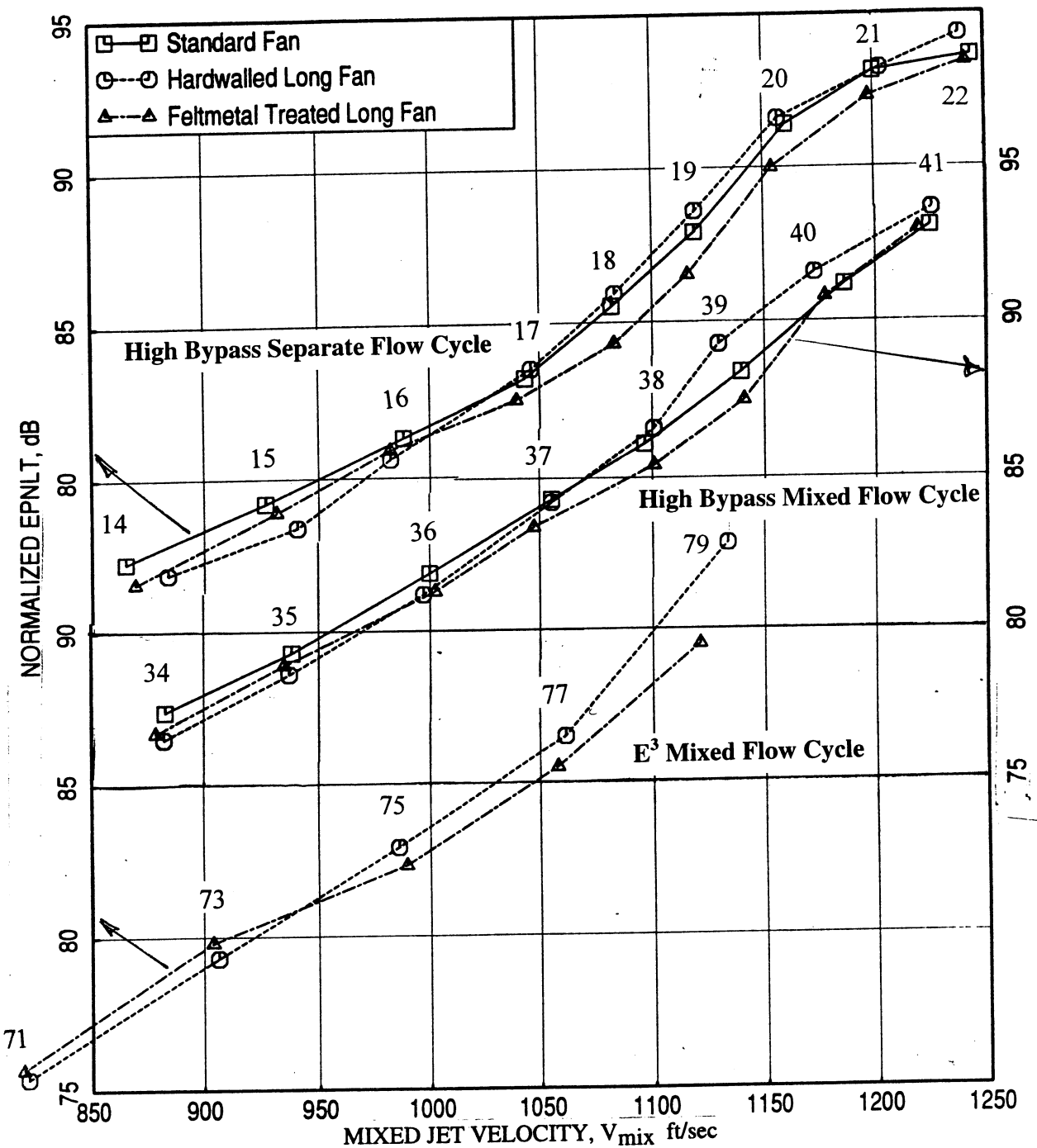


Figure 102. Effect of fan nozzle treatment and length on normalized EPNL for the unique-lobed mixer with fan of  $51.7 \text{ in}^2$  exit area at  $\phi=34^\circ$  for different engine cycles at SAE 77° standard day conditions,  $A_8=3078 \text{ in}^2$ , Sideline Distance=1500 ft,  $M_F=0.28$ .

comparing the treated configurations with hardwalled cases for three different cycle conditions. At higher mixed velocities the noise level is higher for long hardwalled fan nozzle configuration compared to the standard fan nozzle. However, with acoustic treatment, the noise level goes down significantly to give additional noise benefit over the long hardwalled fan nozzle. The effect of treatment with respect to acoustic suppression for different cycle conditions is further demonstrated in Figures 103 through 108 in terms of OASPL & PNLT directivities and PWL & SPL spectra for different nominal  $V_{mix}$ . For all three cycles the acoustic suppression is significant at higher frequencies, especially significant at higher mixed velocities. A noise increase due to treatment is observed at frequencies between 2 to 4 kHz at lower velocity conditions.

Acoustic treatment on fan nozzle is more effective in reducing noise compared to the hardwalled configuration at higher velocity conditions. Also, the treatment effectiveness is more for  $E^3$  mixed flow cycle conditions (for example, see Figure 108), possibly due to higher internal noise caused by higher core velocity. Treated configuration introduces excess noise at lower velocity conditions (see Figures 99, 103, 105, etc.) at higher frequencies (2 to 4 kHz) possibly due to increased small scale turbulence by liner perforations. However, these levels are small compared to noise reduction due to treatment at other frequencies at higher velocity conditions. Thus the treatment becomes more effective at higher velocity conditions. It should be clear that the acoustic treatment used is not representative of full scale design due to manufacturing limitations at 1/8-scale model. The acoustic suppression may be different for full scale engine when proper liner is used.

## **6.7 Farfield Noise for Multi-Lobed Mixer Configurations Compared to Confluent**

**Mixer & Conic Nozzle:** Figure 109 shows the EPNL variation with respect to  $V_{mix}$  comparing the 22-lobed mixer configuration with confluent mixer and conic nozzle cases for three different cycle conditions. A hardwalled standard fan nozzle is used for both the mixer configurations. For  $E^3MF$  cycle, the EPNL for 22-lobed mixer lies between the confluent mixer and conic nozzle EPNL for all velocity conditions. For  $HBMF$  cycle, the 22-lobed mixer data comes closer to conic nozzle EPNL at lower mixed velocities. At higher mixed velocities, above 1050 ft/sec, the EPNL for 22-lobed mixer becomes higher compared to conic nozzle, but remains lower than the confluent mixer data. However, for  $HBSF$  cycle, the 22-lobed mixer seems to be as noisier as the confluent mixer at lower mixed velocities and becomes more noisier than the confluent mixer at higher mixed velocities.

Figures 110 and 111 show the comparisons of OASPL & PNLT directivities and PWL & SPL spectra for  $HBSF$  cycle at nominal  $V_{mix} = 1000$  ft/sec (TP16) and 1120 ft/sec (TP19) between the 22-lobed mixer, confluent mixer, and conic nozzle configurations. At lower frequencies, up to about 1 kHz, SPL for 22-lobed mixer lies between those for confluent mixer and conic nozzle. Thus, the 22-lobed mixer improves the mixing and lowers the noise level at this frequency range. At higher frequencies for  $V_{mix}$  of 1000 ft/sec, SPL for all three configurations are very close to each other. However, at higher  $V_{mix}$  of 1120

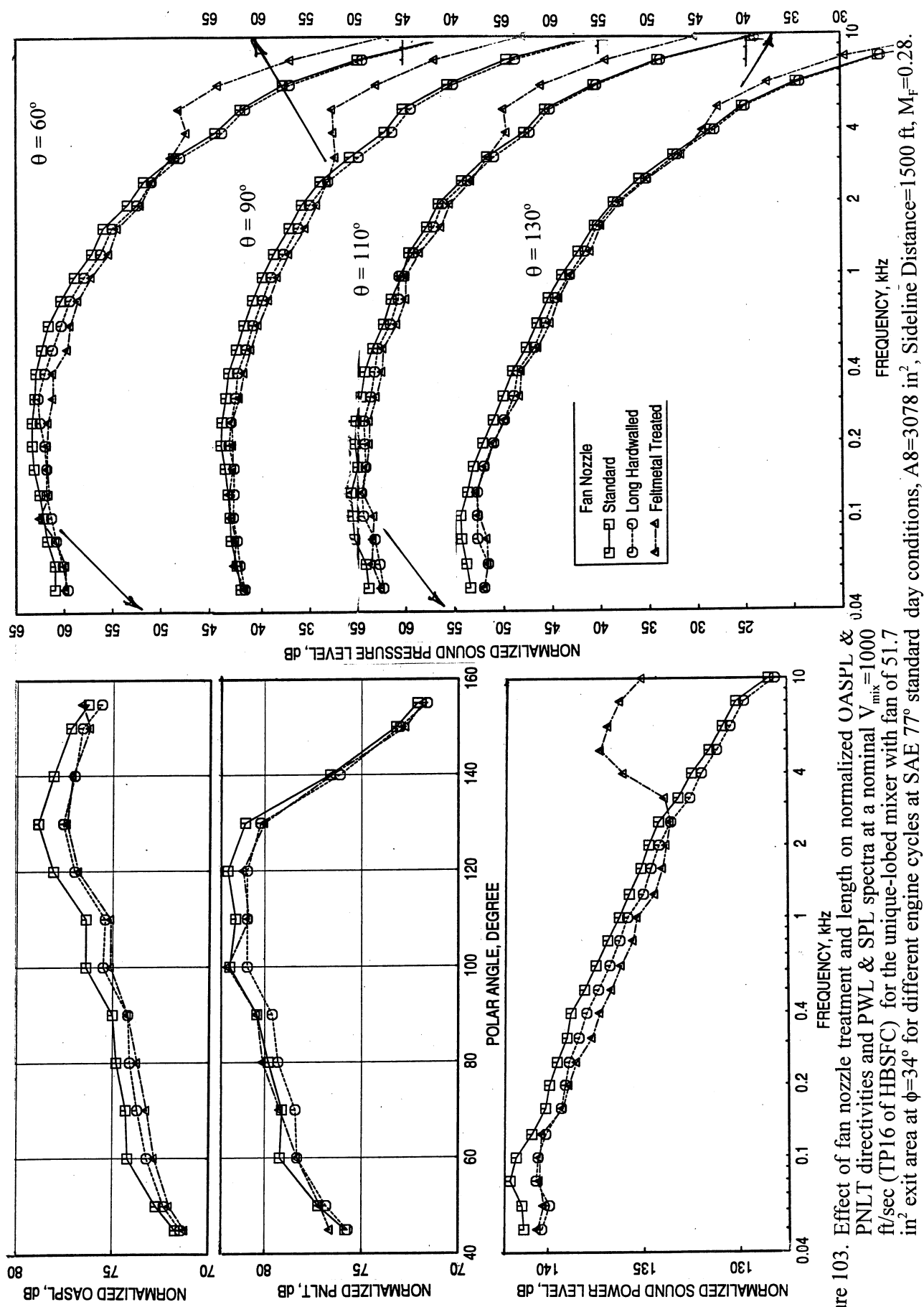


Figure 103. Effect of fan nozzle treatment and length on normalized OASPL & PNLT directivities and PWL & SPL spectra at a nominal  $V_{\text{mix}} = 1000$  ft/sec (TP16 of HBSFC) for the unique-lobe mixer with fan of 51.7 in $^2$  exit area at  $\phi = 34^\circ$  for different engine cycles at SAE 770 standard day conditions,  $A_8 = 3078 \text{ in}^2$ , Sideline Distance = 1500 ft,  $M_F = 0.28$ .

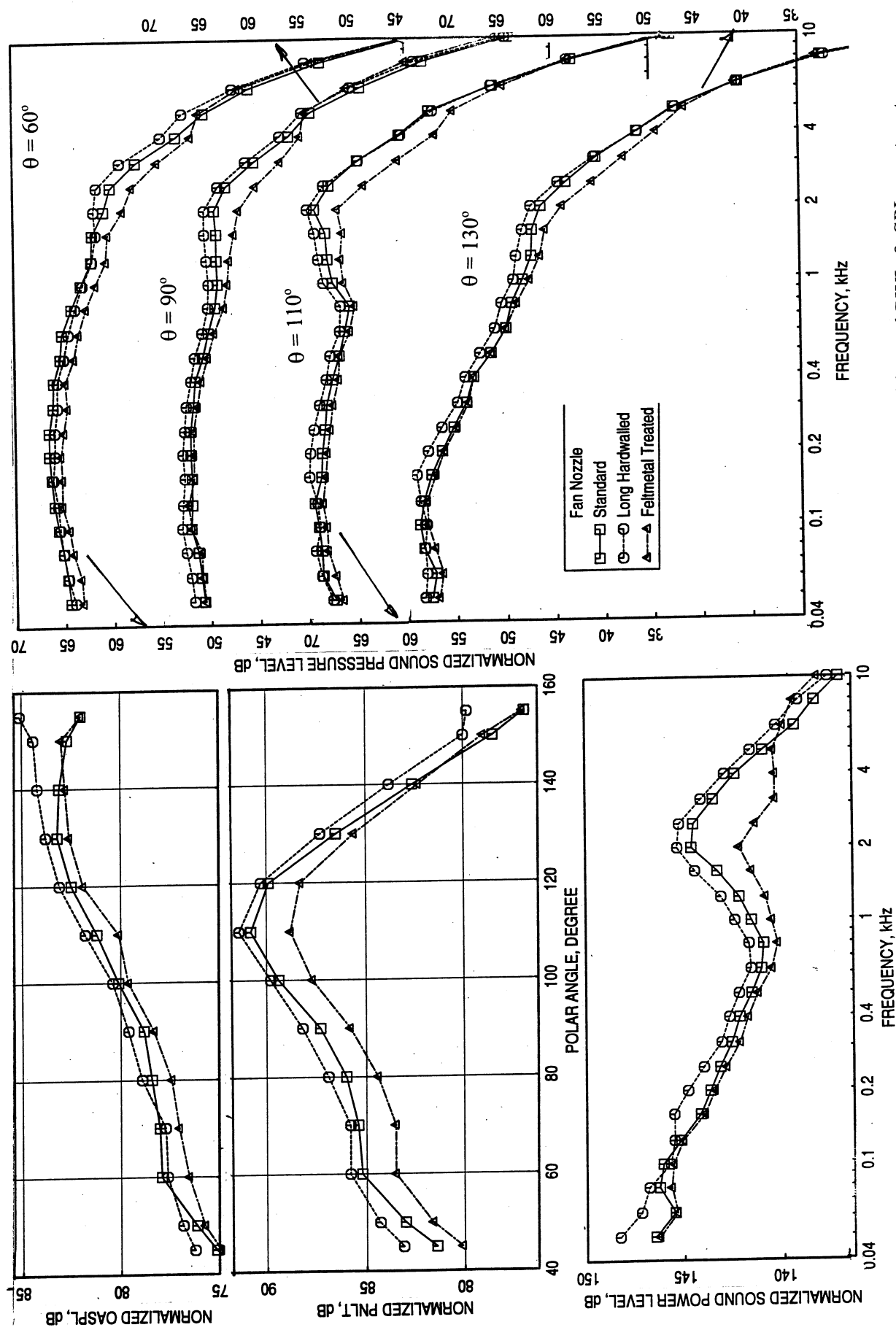


Figure 104. Effect of fan nozzle treatment and length on normalized OASPL & PNL & SPL spectra at a nominal  $V_{\text{mix}} = 1120 \text{ ft/sec}$  (TP19 of HBSFC) for the unique-lobe mixer with fan of  $51.7 \text{ in}^2$  exit area at  $\phi=34^\circ$  for different engine cycles at SAE  $77^\circ$  standard day conditions,  $A_8=3078 \text{ in}^2$ , Sideline Distance=1500 ft,  $M_f=0.28$ .

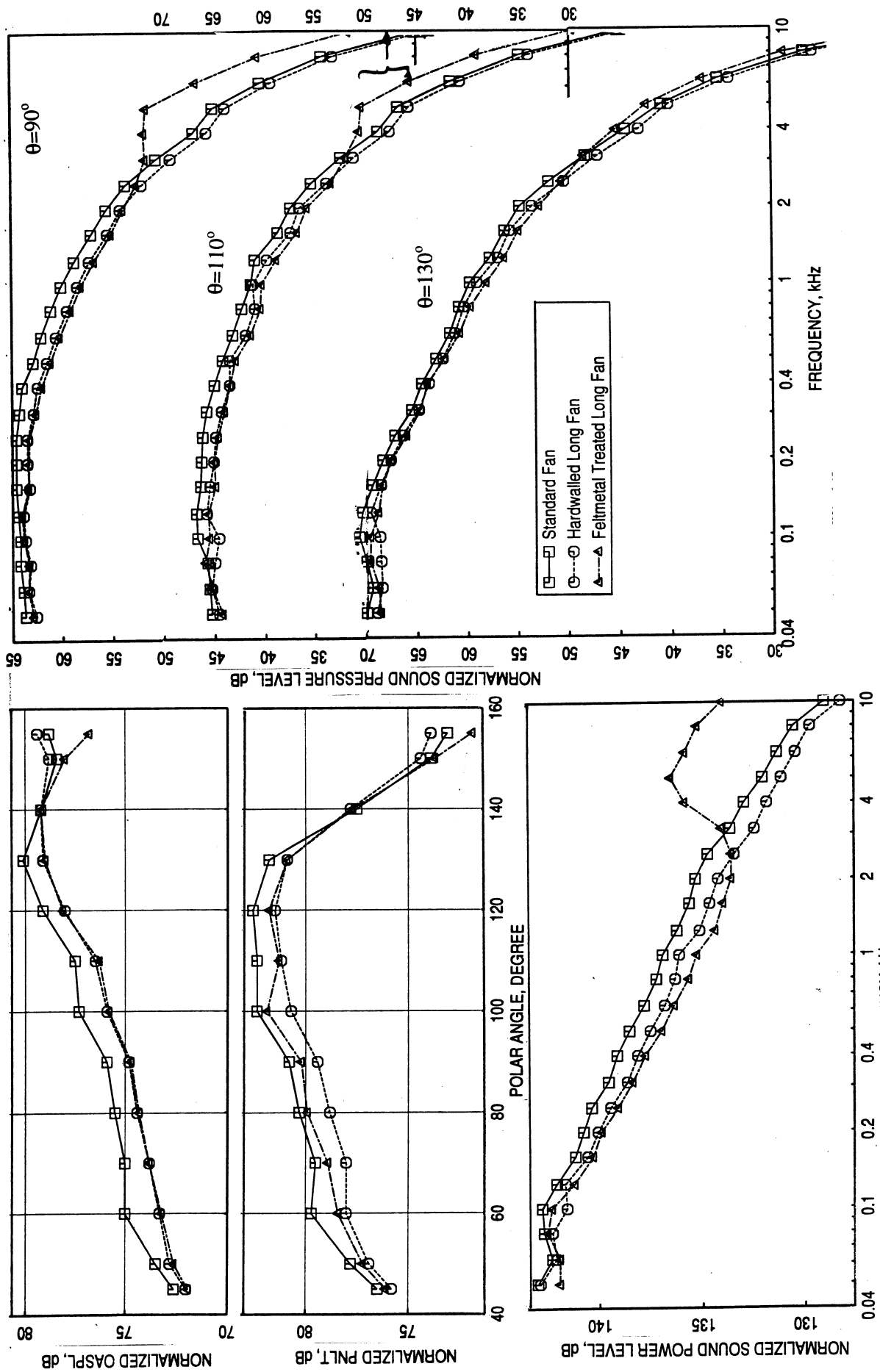


Figure 105. Effect of fan nozzle treatment and length on normalized OASPL & PNLT directivities and PWL & SPL spectra at a nominal  $V_{\text{mix}} = 1000 \text{ ft/sec}$  (TP36 of HBMFC) for the unique-lobed mixer with fan of  $51.7 \text{ in}^2$  exit area at  $\phi = 34^\circ$  for different engine cycles at SAE 77° standard day conditions,  $A_8 = 3078 \text{ in}^2$ , Sideline Distance = 1500 ft,  $M_F = 0.28$ .

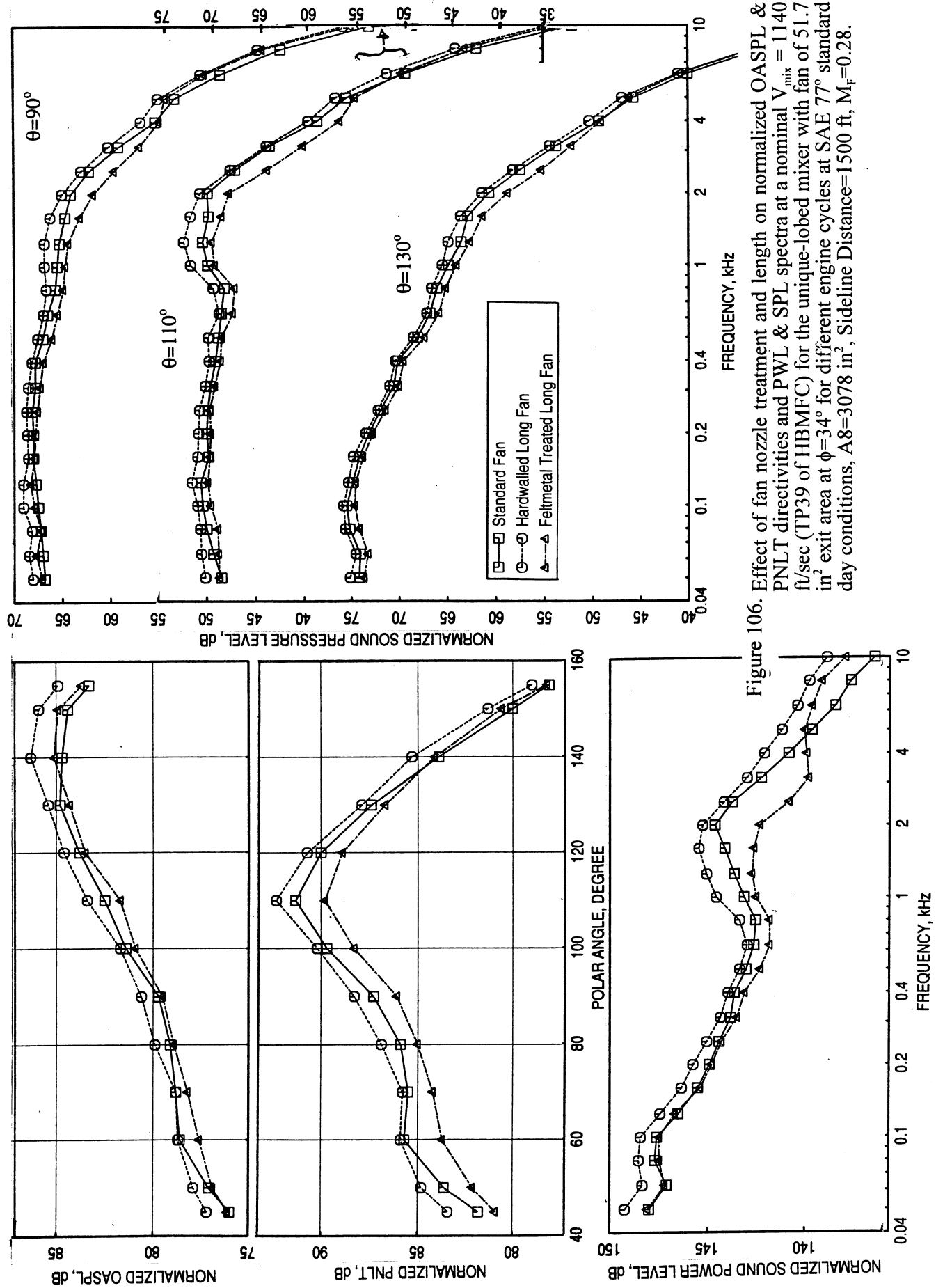


Figure 106. Effect of fan nozzle treatment and length on normalized OASPL & PNLT directivities and PWL & SPL spectra at a nominal  $V_{\text{mix}} = 1140 \text{ ft/sec}$  (TP39 of HBMFC) for the unique-lobed mixer with fan of  $51.7 \text{ in}^2$  exit area at  $\phi = 34^\circ$  for different engine cycles at SAE  $77^\circ$  standard day conditions,  $A_8 = 3078 \text{ in}^2$ , Sideline Distance = 1500 ft,  $M_F = 0.28$ .

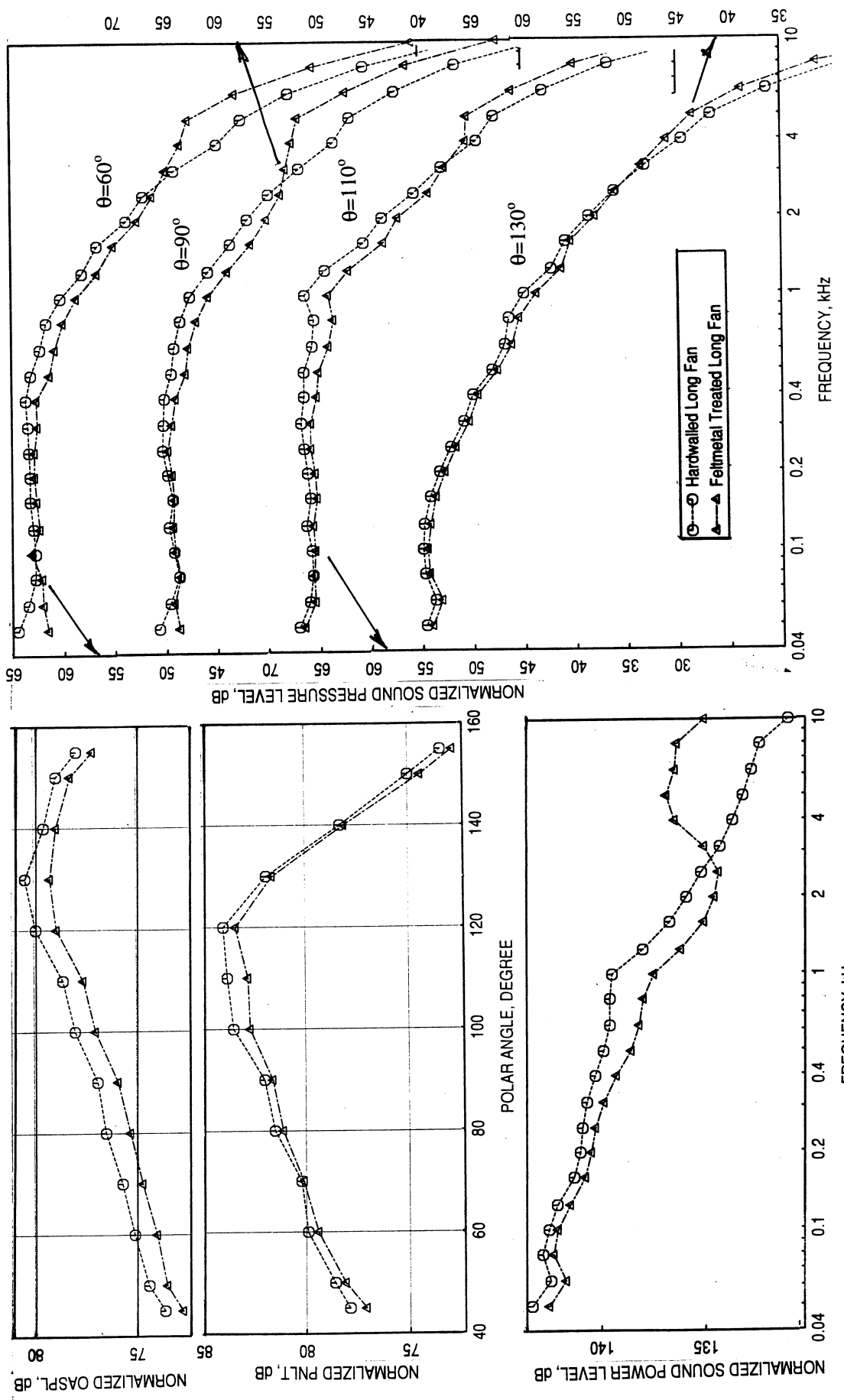


Figure 107. Effect of fan nozzle treatment on normalized OASPL & PNLT directivities and PWL & SPL spectra at a nominal  $V_{\text{mix}} = 1000 \text{ ft/sec}$  (TP75 of E'MFC) for the unique-lobed mixer with fan of  $51.7 \text{ in}^2$  exit area at  $\phi=34^\circ$  for different engine cycles at SAE 77° standard day conditions,  $A_8=3078 \text{ in}^2$ , Sideline Distance=1500 ft,  $M_f=0.28$ .

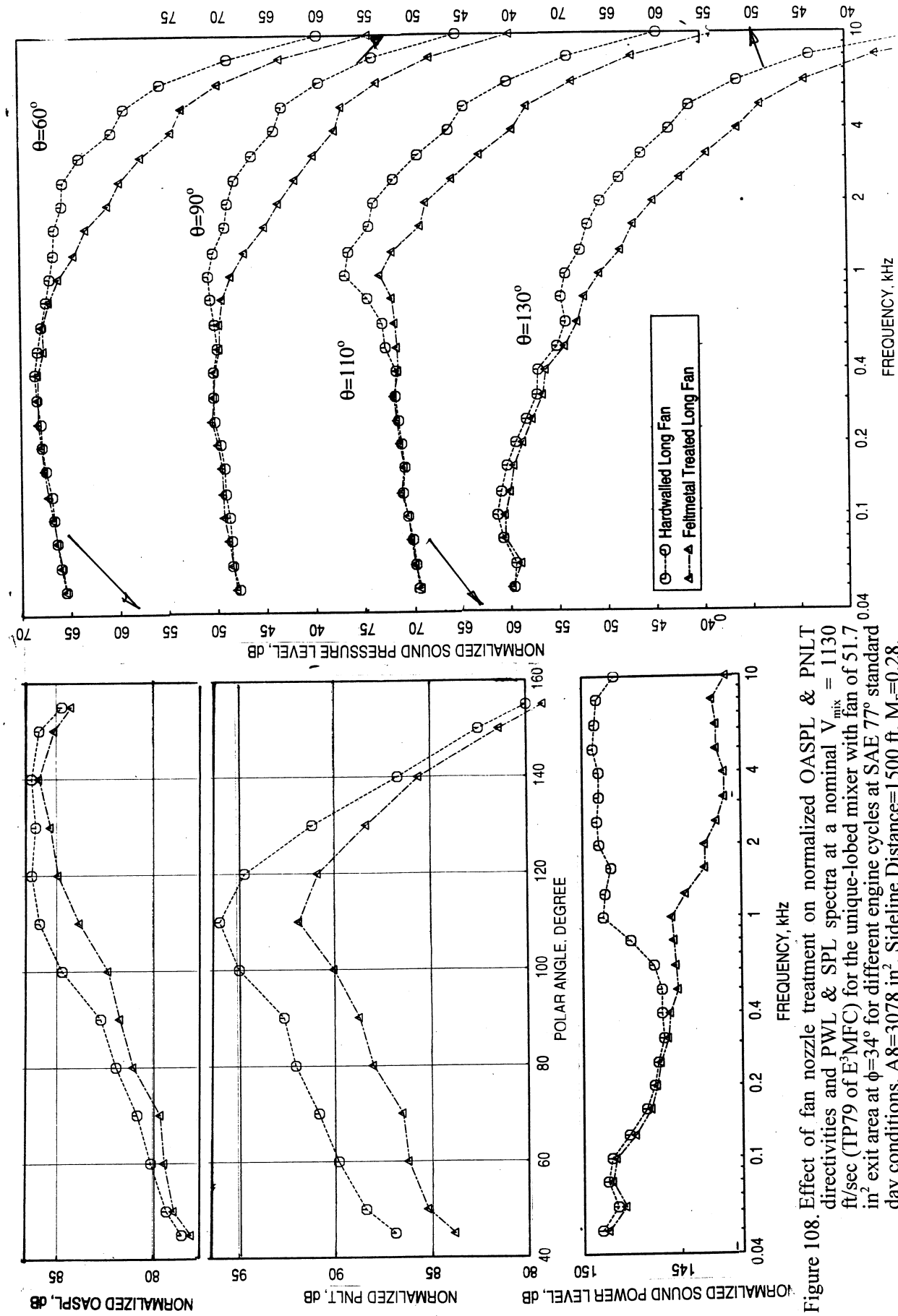


Figure 108. Effect of fan nozzle treatment on normalized OASPL & PNLT directivities and PWL & SPL spectra at a nominal  $V_{\text{mix}} = 1130 \text{ ft/sec}$  (TP79 of E'MFC) for the unique-lobed mixer with fan of  $51.7 \text{ in}^2$  exit area at  $\phi = 34^\circ$  for different engine cycles at SAE 77° standard day conditions,  $A_8 = 3078 \text{ in}^2$ , Sideline Distance = 1500 ft,  $M_F = 0.28$ .

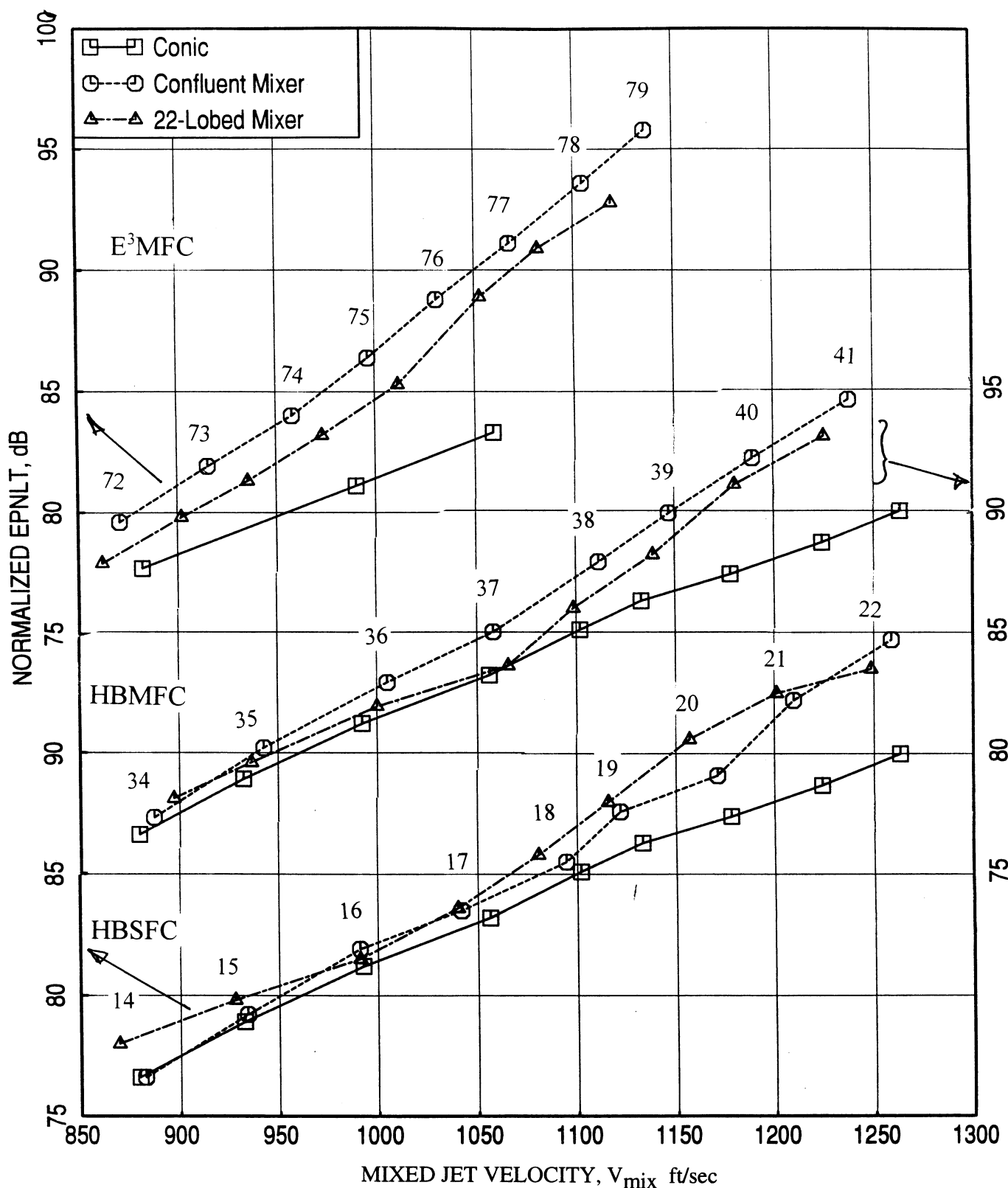


Figure 109. Normalized EPNL for the 22-lobed and confluent mixers with standard fan of 51.7 in<sup>2</sup> exit area compared to a conic nozzle for different engine cycles at SAE 77° standard day conditions, A<sub>8</sub>=3078 in<sup>2</sup>, Sideline Distance=1500 ft, M<sub>F</sub>=0.28.

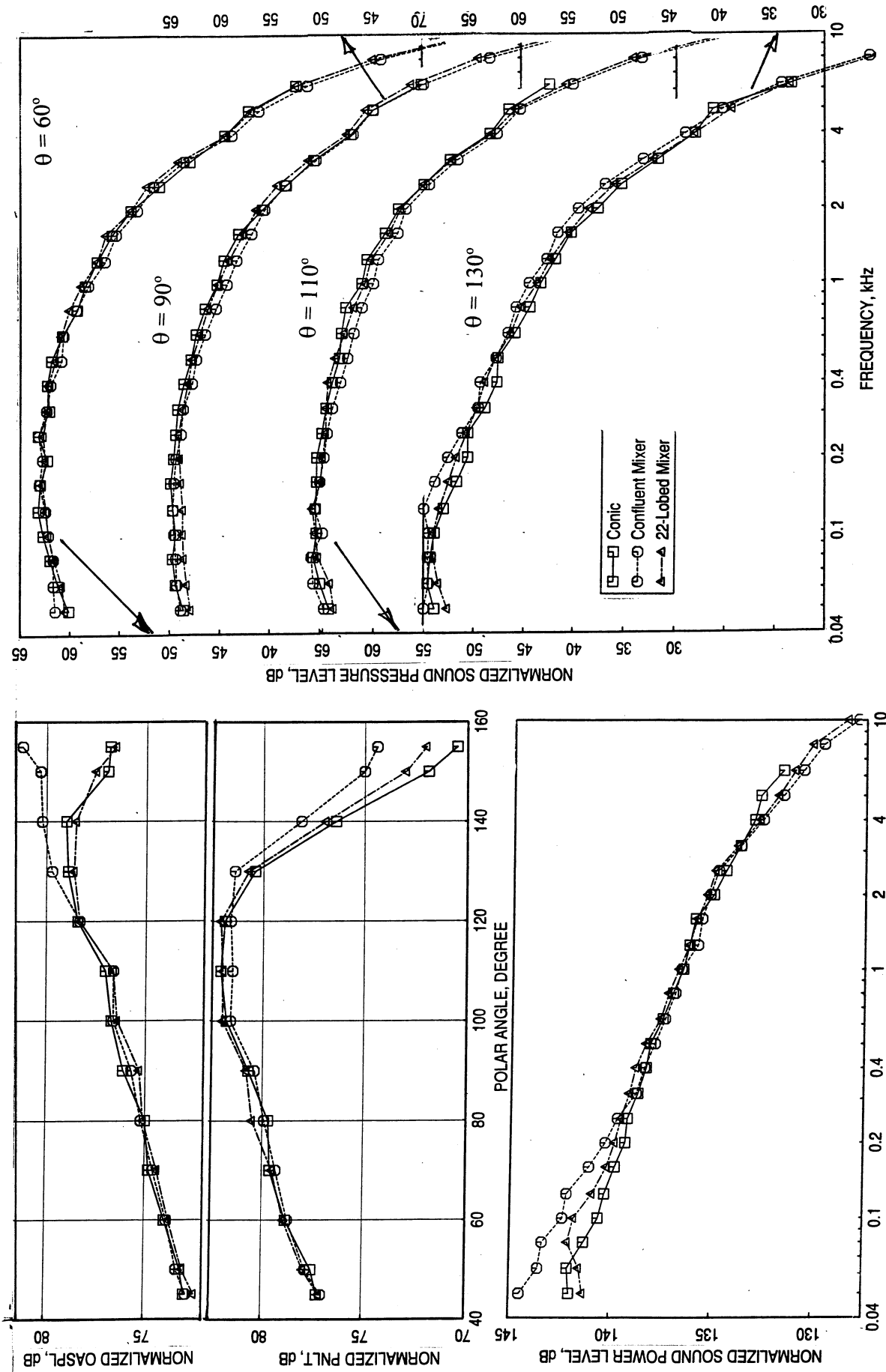


Figure 110. Normalized OASPL & PNLT directivities and PWL & SPL spectra at a nominal  $V_{\text{mix}} = 1000 \text{ ft/sec}$  (TP16 of HBSFC) for the 22-lobed and confluent mixers with standard fan of  $51.7 \text{ in}^2$  exit area at SAE 77° standard day conditions,  $A_8=3078 \text{ in}^2$ , Sideline Distance=1500 ft,  $M_F=0.28$ .

ft/sec (see Figure 111) the 22-lobed mixer is significantly noisier due to high frequency noise generation, resulting in higher EPNL compared to confluent mixer.

Similar results for HBMF cycle conditions are shown in Figures 112 and 113. The acoustic characteristics of 22-lobed mixer are similar to what is observed for HBSF cycle conditions. However, the high frequency noise increase for this cycle is relatively lower. Thus the EPNL for 22-lobed mixer, still remains lower than the confluent mixer at higher velocity conditions. Similar results for E<sup>3</sup>MF cycle conditions are shown in Figures 114 and 115. For this cycle conditions the confluent mixer noise levels at lower frequencies are much higher compared to the conic nozzle, possibly due to the higher core velocity. The noise reduction due to the 22-lobed mixer at lower frequencies are much greater compared to the other cycle conditions. Thus, the high frequency noise increase by the 22-lobed mixer does not significantly influence the total noise in terms of EPNdB. Thus, the EPNL remains lower than the confluent mixer level for all velocity conditions for this cycle.

**Acoustic Data Comparison for Unique-Lobed Mixer:** In this section the acoustic data comparisons are made between the unique-lobed mixer with treated long fan, confluent mixer with standard fan, and conic nozzle. The results presented in this section are for HBMF cycle conditions measured at an azimuthal location of 34°. Figure 116 shows the EPNL variation with respect to  $V_{mix}$  comparing the three configurations. The unique-lobed mixer data comes closer to the conic nozzle EPNL at lower mixed velocities up to about 1100 ft/sec, resulting into a decrease of about 2 EPNdB compared to the confluent mixer. At higher mixed velocities, above 1100 ft/sec, the EPNL for unique-lobed mixer becomes higher compared to the conic nozzle, but remains lower than the confluent mixer data.

Comparisons between the above three configurations in terms of OASPL & PNLT directivities and SPL spectra at nominal mixed velocities of 1000 ft/sec and 1175 ft/sec are shown in Figures 117 through 119. Significant noise reduction by the treated unique-lobed configuration is observed at frequencies below 1 kHz compared to confluent mixer. Adversely, noise increase by the treated unique-lobed configuration is observed at higher frequencies compared to confluent mixer. For lower mixed velocity conditions the low frequency noise reduction overcomes the contribution of high frequency noise increase due to the unique-lobed configuration, and thereby, the resulting EPNL remains lower (closer to those of conic nozzle) than the confluent mixer results. However, at higher mixed velocities the high frequency noise increase is substantial and the corresponding annoyance levels are also high (see Figures 118 and 119). Thus, the noise level for the unique-lobed mixer configuration, in terms of EPNL, increases significantly compared to the conic nozzle. Even though, the EPNL for the unique-lobed mixer configuration remains lower than the confluent mixer the difference becomes small.

The multi-lobed mixer configurations approach ideal mixer (i.e., conic nozzle) noise levels at velocities up to about 1050 ft/sec at a typical high bypass mixed flow cycle. At higher velocity conditions the noise reduction relative to a confluent mixer is moderate (~ 2 EPNdB at  $V_{mix} = 1150$  ft/sec), due to significantly higher high-frequency noise content with higher annoyance levels.

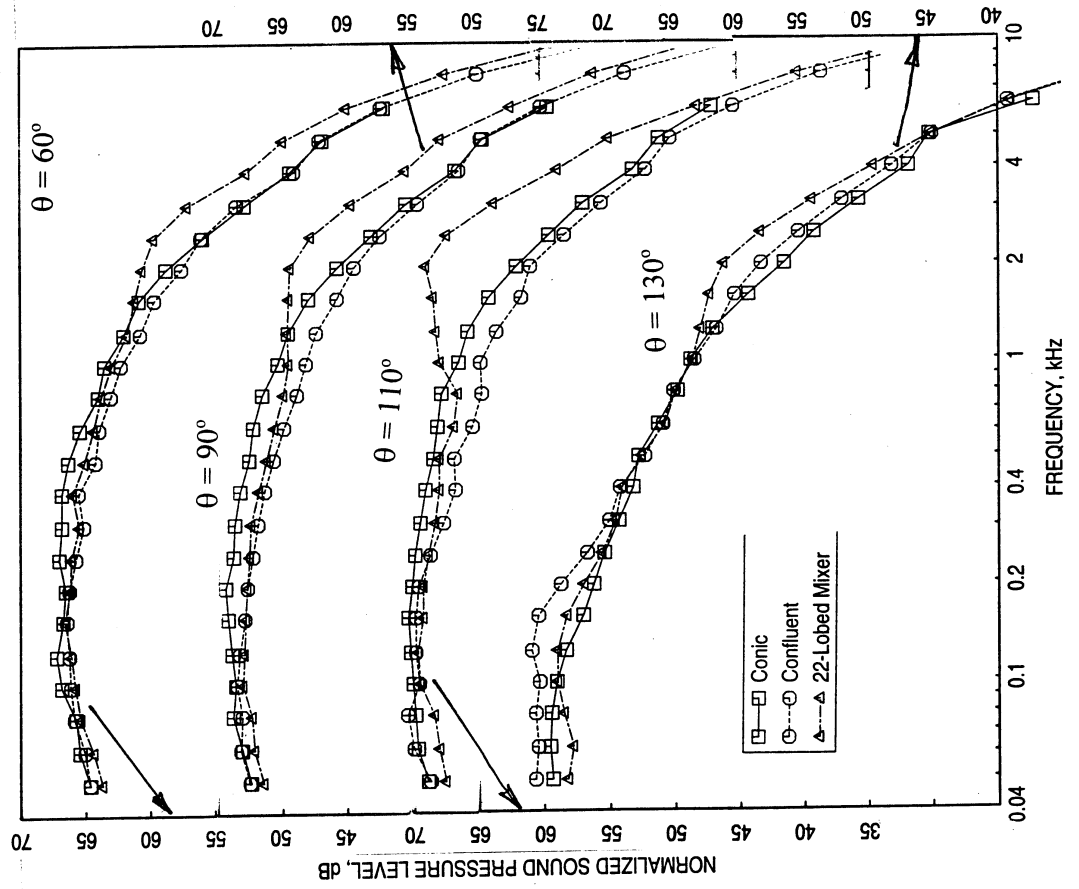
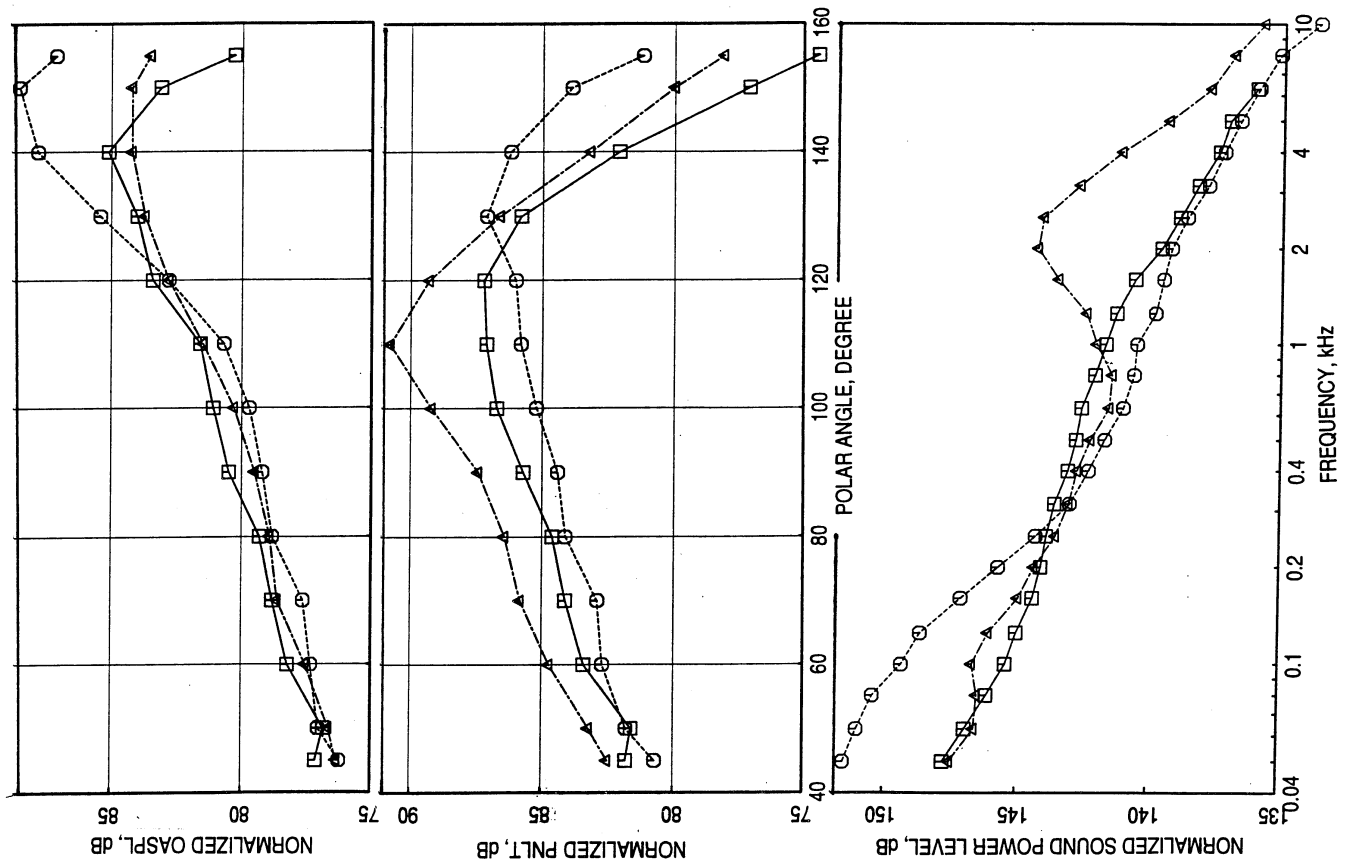


Figure 111. Normalized OASPL & PNLT directivities and PWL & SPL spectra at a nominal  $V_{\text{mix}} = 1120 \text{ ft/sec}$  (TP19 of HBSFC) for the 22-lobed and confluent mixers with standard fan of  $51.7 \text{ in}^2$  exit area at SAE 77° standard day conditions,  $A_8=3078 \text{ in}^2$ , Sideline Distance=1500 ft,  $M_F=0.28$ .



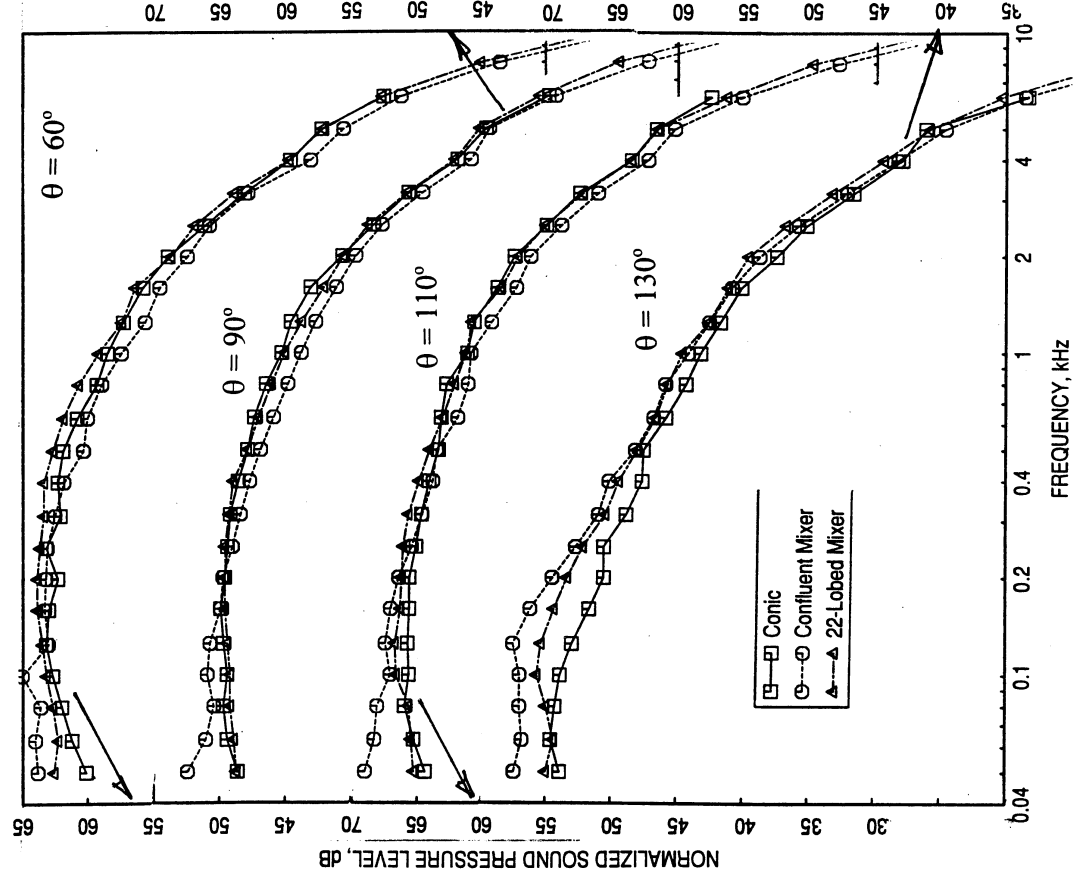
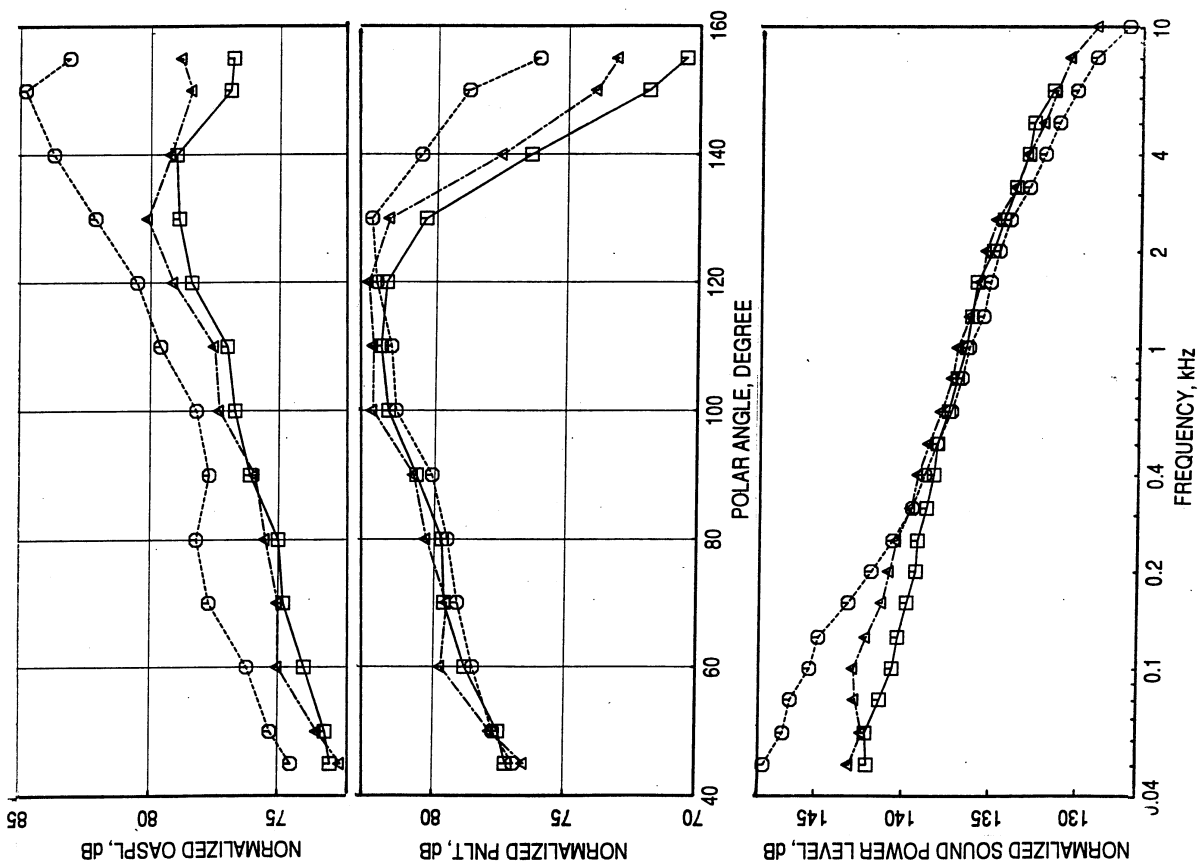


Figure 112. Normalized OASPL & PNLT directivities and PWL & SPL spectra at a nominal  $V_{\text{mix}}^{\text{nom}} = 1000 \text{ ft/sec}$  (TP36 of HBMFC) for the 22-lobed and confluent mixers with standard fan of  $51.7 \text{ in}^2$  exit area at SAE 77° standard day conditions,  $A_8=3078 \text{ in}^2$ , Sideline Distance=1500 ft,  $M_F=0.28$ .



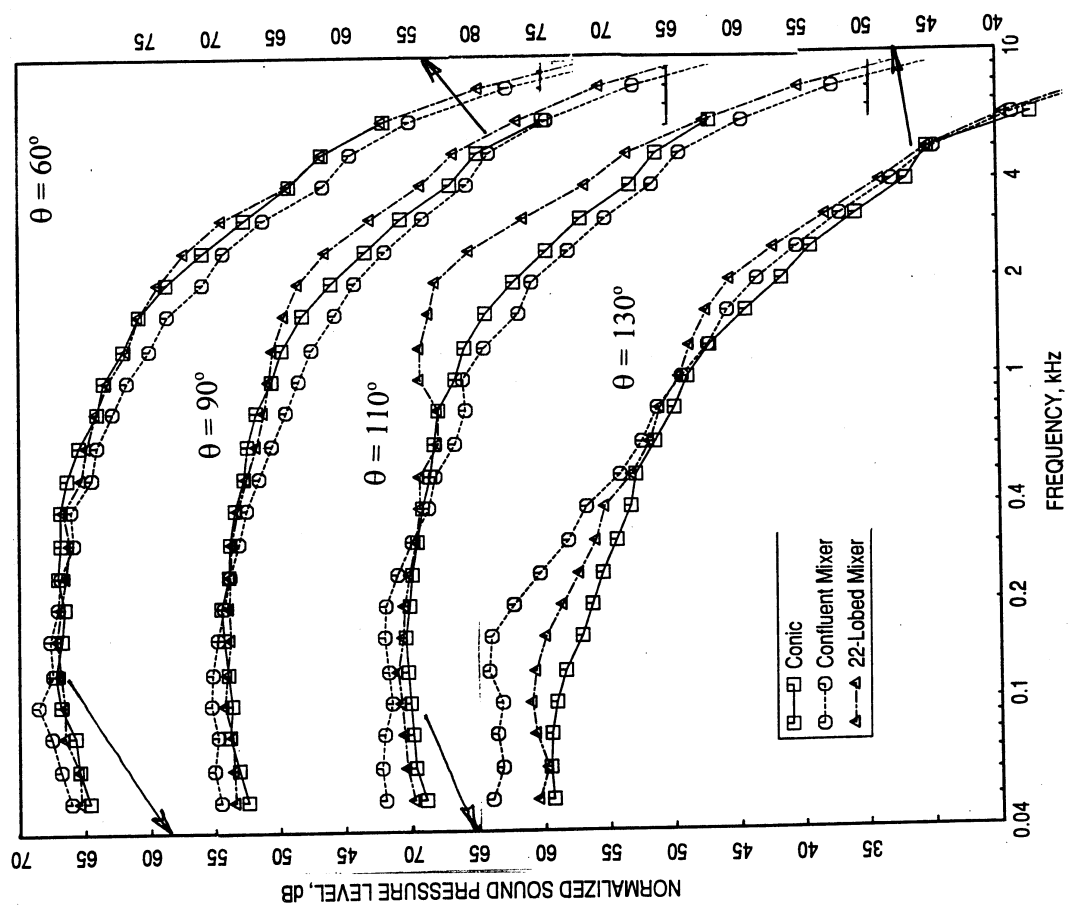
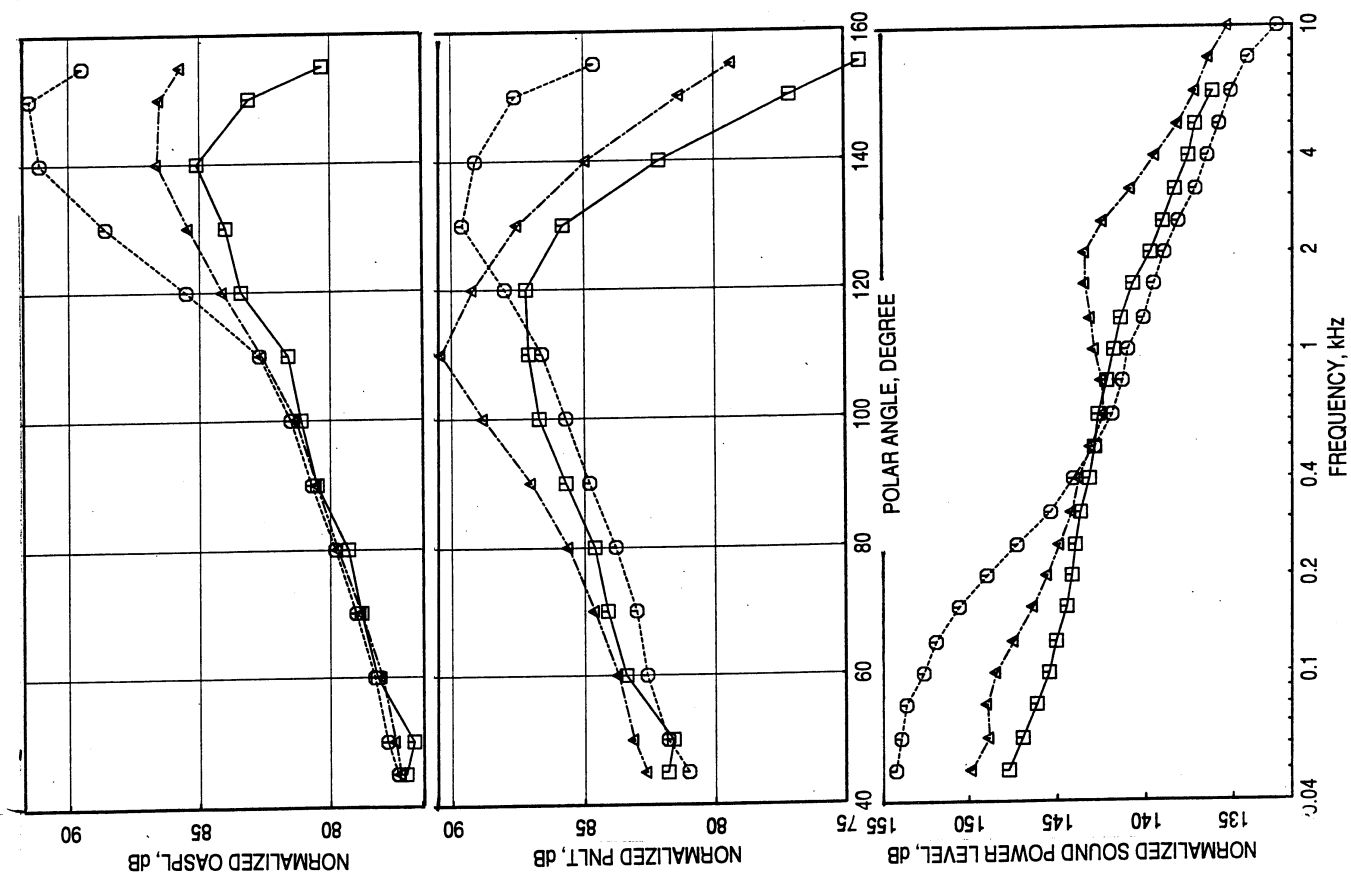


Figure 113. Normalized OASPL & PNLT directivities and PWL & SPL spectra at a nominal  $V_{\text{mix}}^{\text{nom}} = 1140 \text{ ft/sec}$  (TP39 of HBMFC) for the 22-lobed and confluent mixers with standard fan of  $51.7 \text{ in}^2$  exit area at SAE  $77^\circ$  standard day conditions,  $A_8=3078 \text{ in}^2$ , Sideline Distance=1500 ft,  $M_F=0.28$ .



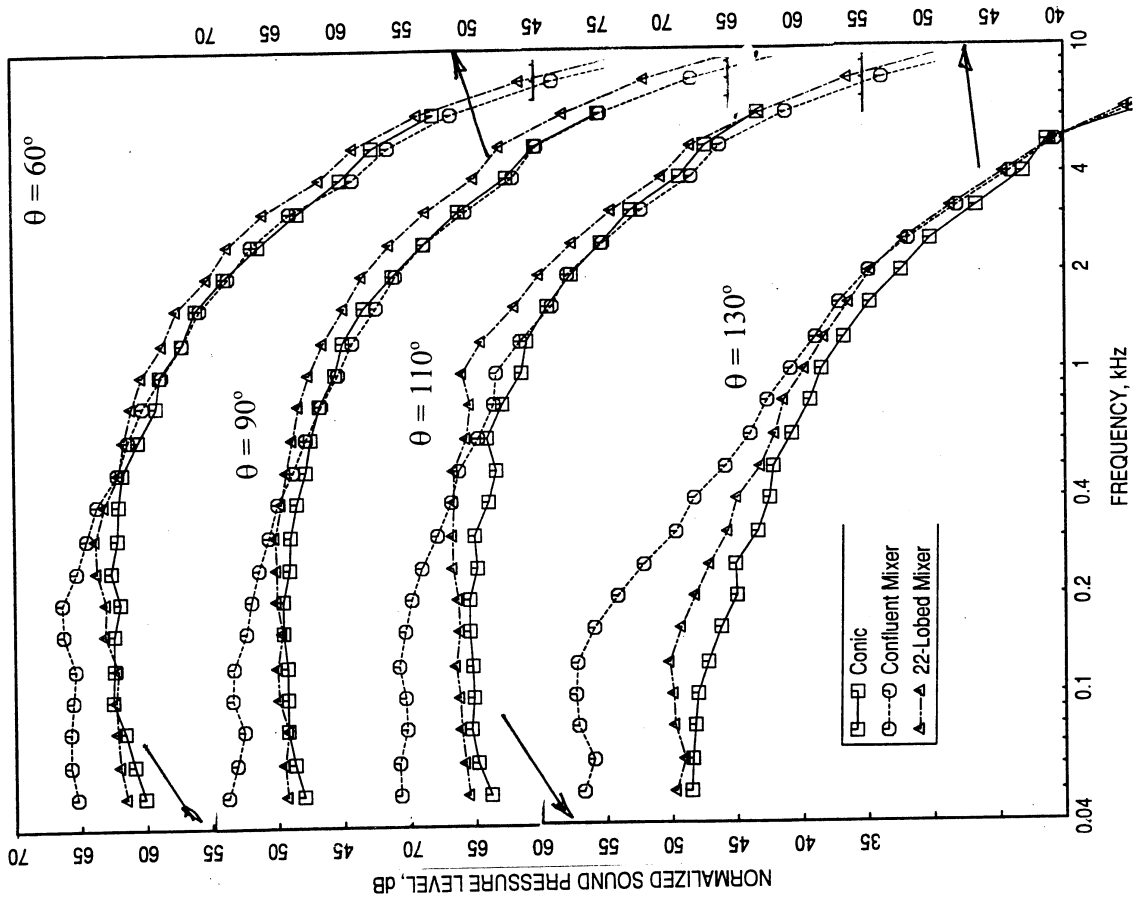
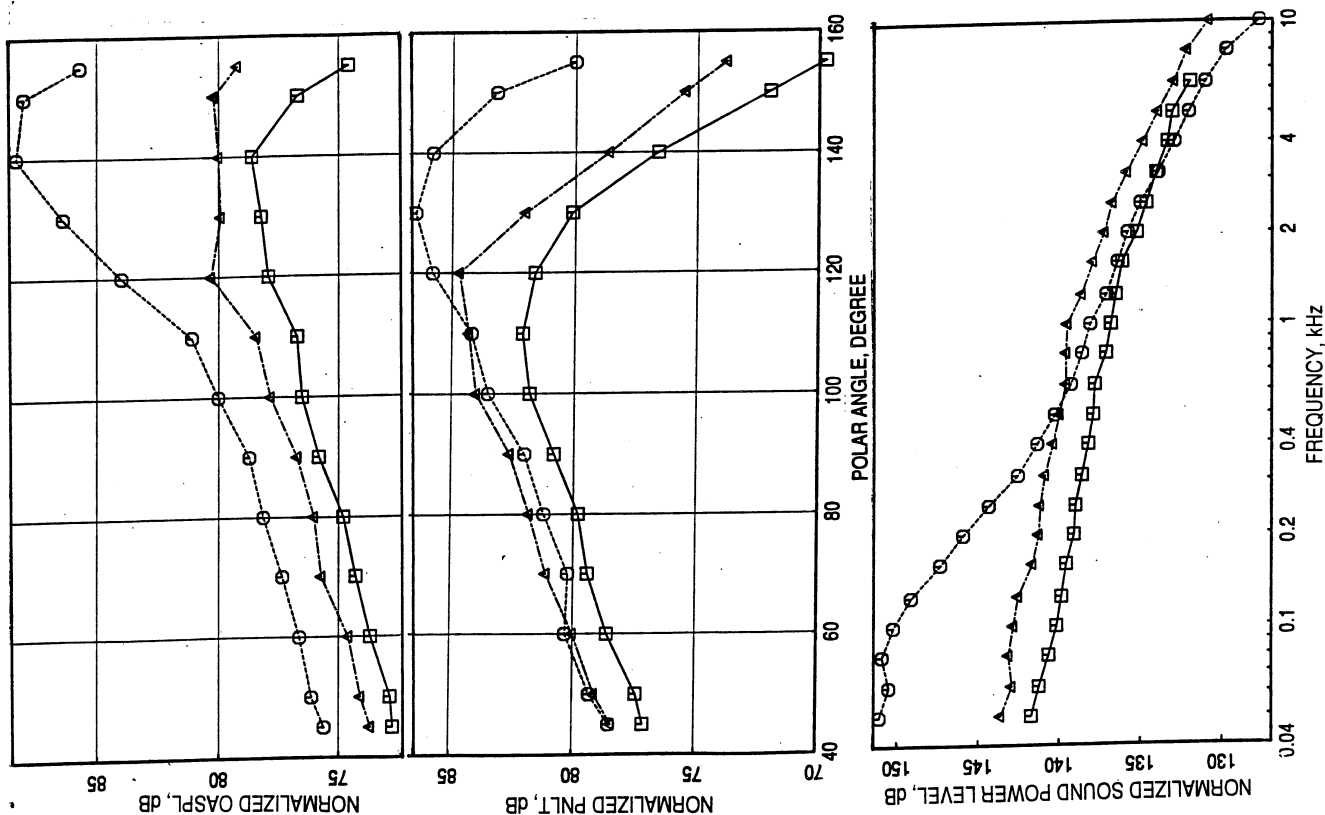


Figure 114. Normalized OASPL & PNLT directivities and PWL & SPL spectra at a nominal  $V_{mix} = 1000$  ft/sec (TP75 of EIMFC) for the 22-lobed and confluent mixers with standard fan of  $51.7 \text{ in}^2$  exit area at SAE 77° standard day conditions,  $A_8=3078 \text{ in}^2$ , Side-line Distance=1500 ft,  $M_F=0.28$ .



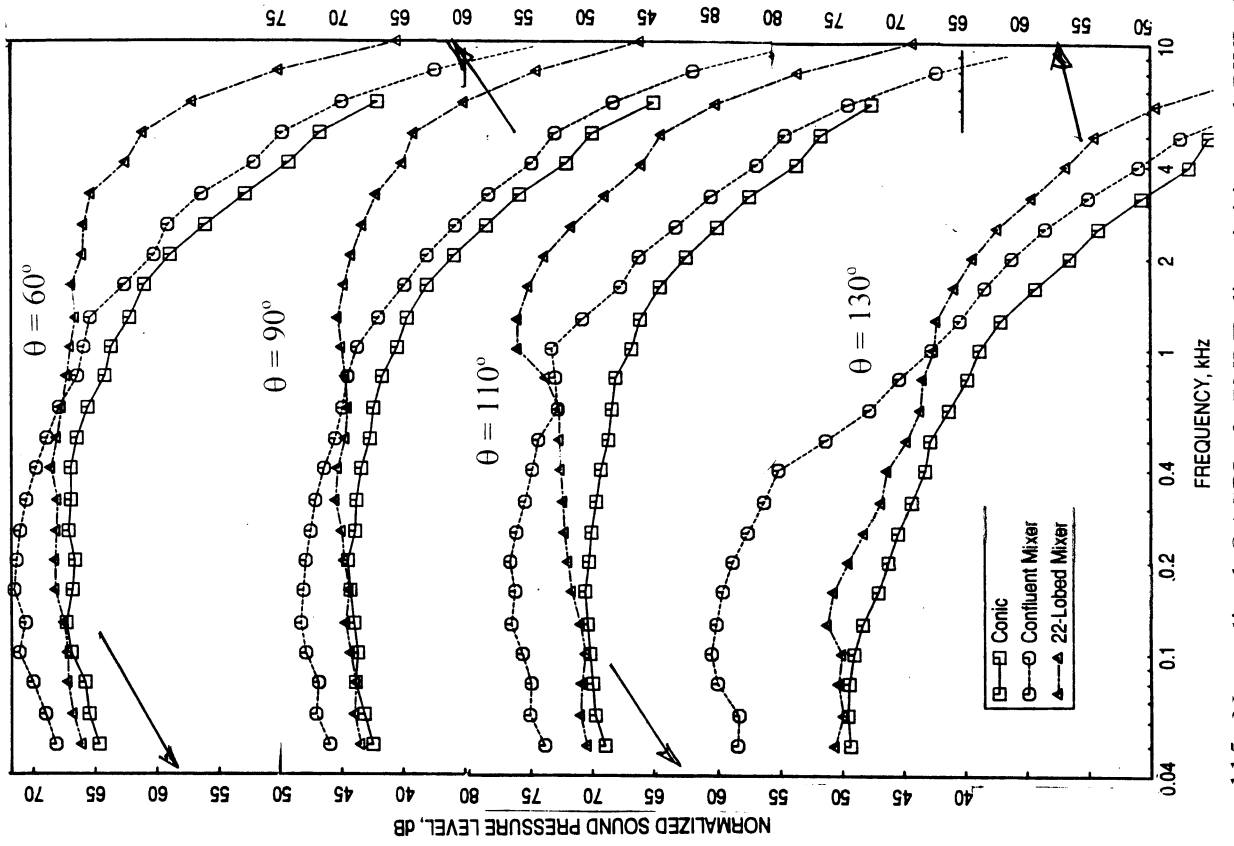
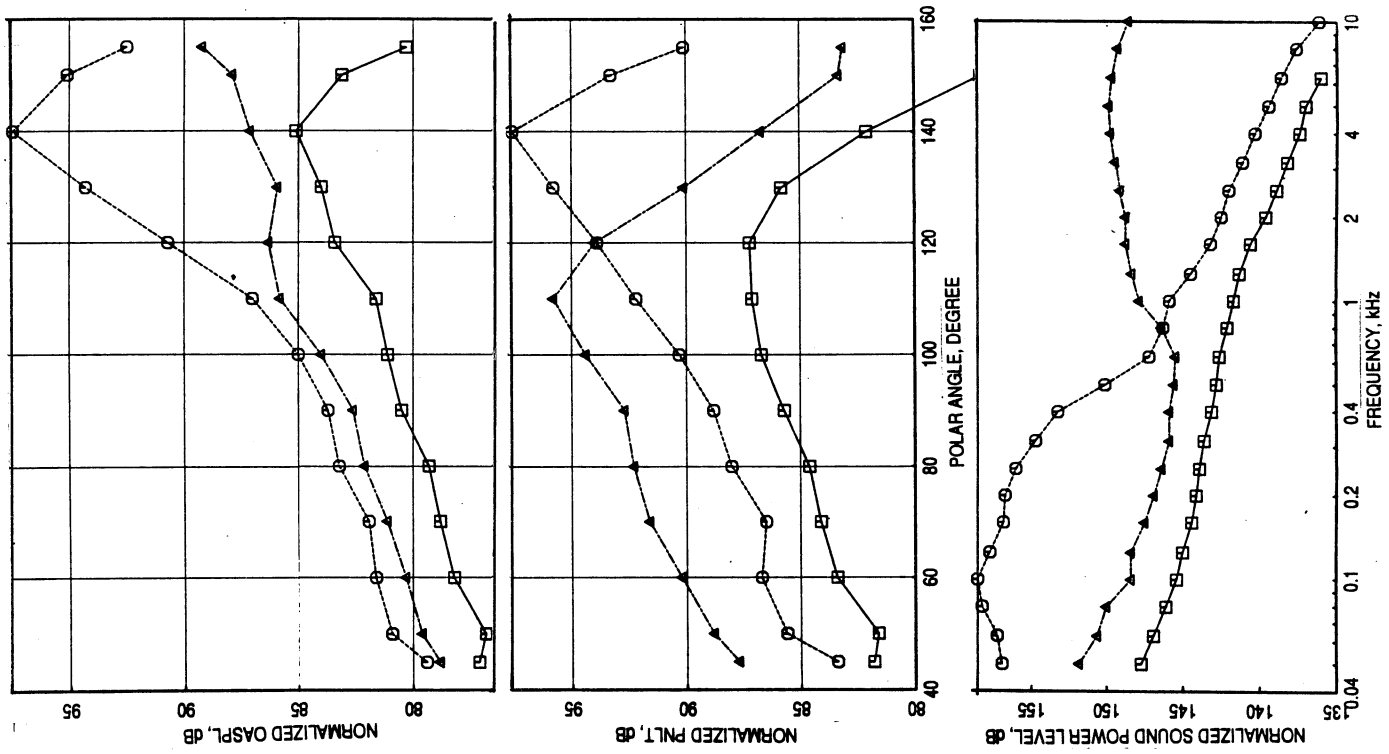


Figure 115. Normalized OASPL & PNLT directivities and PWL & SPL spectra at a nominal  $V_{\text{mix}} = 1125$  ft/sec (TP79 of E<sup>3</sup>MFC) for the 22-lobed and confluent mixers with standard fan of 51.7 in<sup>2</sup> exit area at SAE 77° standard day conditions,  $A_8=3078$  in<sup>2</sup>, Sideline Distance=1500 ft,  $M_F=0.28$ .



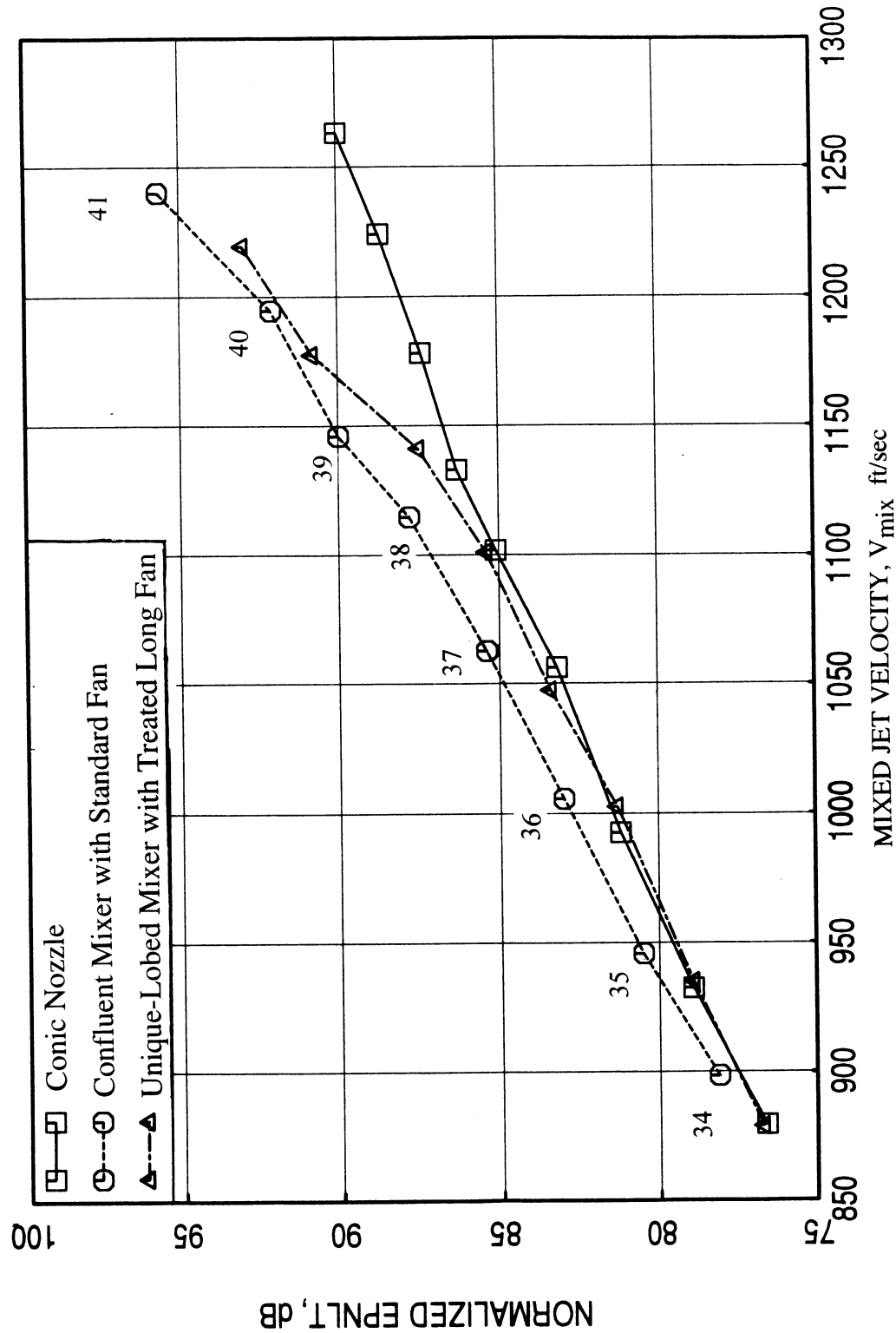


Figure 116. Normalized EPNL for the unique-lobed mixer with treated long fan and confluent mixer with internal pylon and standard fan of  $51.7 \text{ in}^2$  exit area compared to a conic nozzle for HBMFC at SAE 7° standard day conditions,  $A_8=3078 \text{ in}^2$ , Sideline Distance=1500 ft,  $M_F=0.28$ ,  $\phi=34^\circ$ .

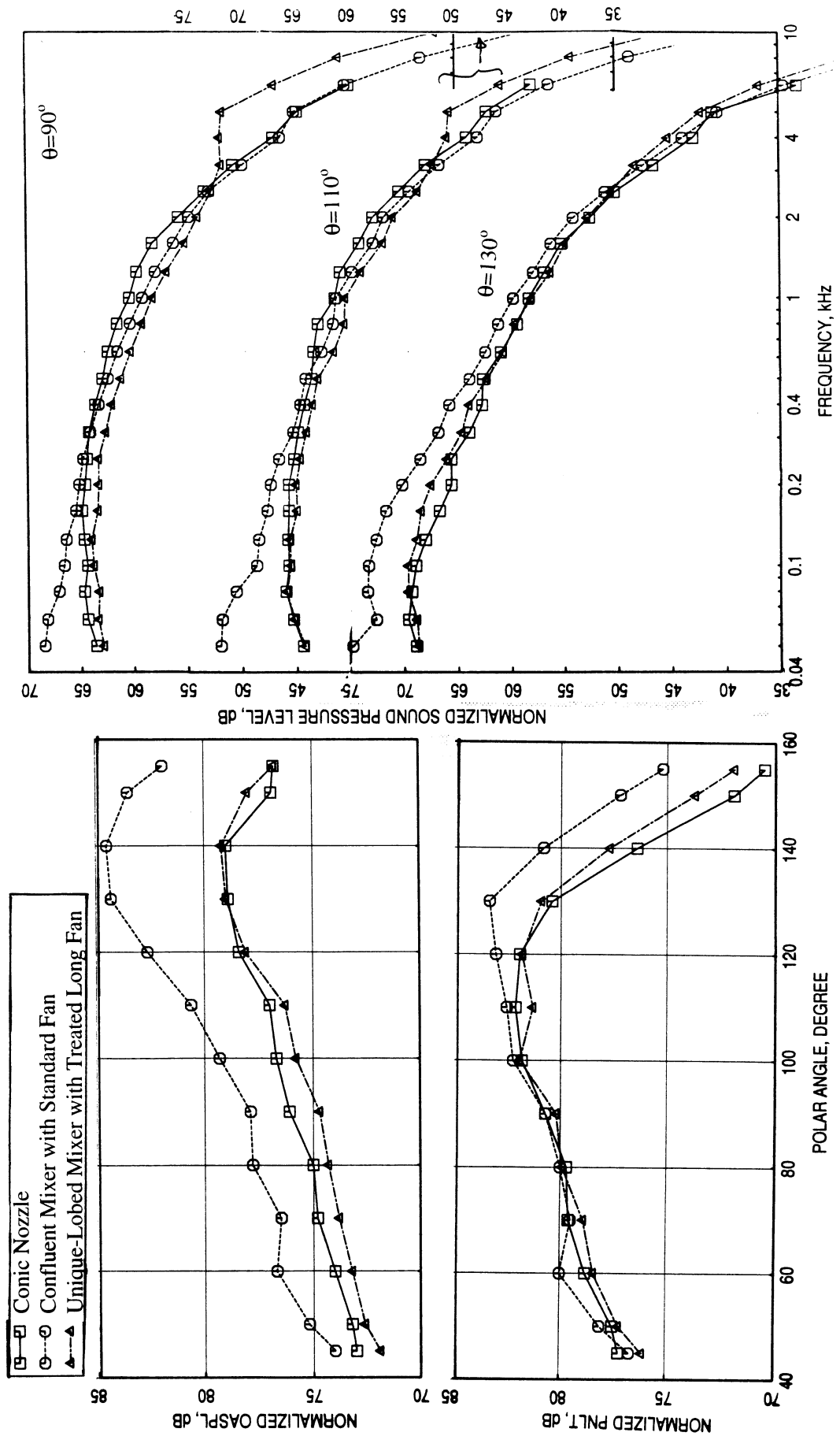


Figure 117. Normalized OASPL & PNL-T directivities and SPL spectra at a nominal  $V_{\text{mix}} = 1000 \text{ ft/sec}$  (TP36 of HBMFC) for the unique-lobed mixer with treated long fan and confluent mixer with internal pylon and standard fan of  $51.7 \text{ in}^2$  exit area compared to a conic nozzle at SAE 77° standard day conditions,  $A_8 = 3078 \text{ in}^2$ , Sideline Distance = 1500 ft,  $M_F = 0.28$ ,  $\phi = 34^\circ$ .

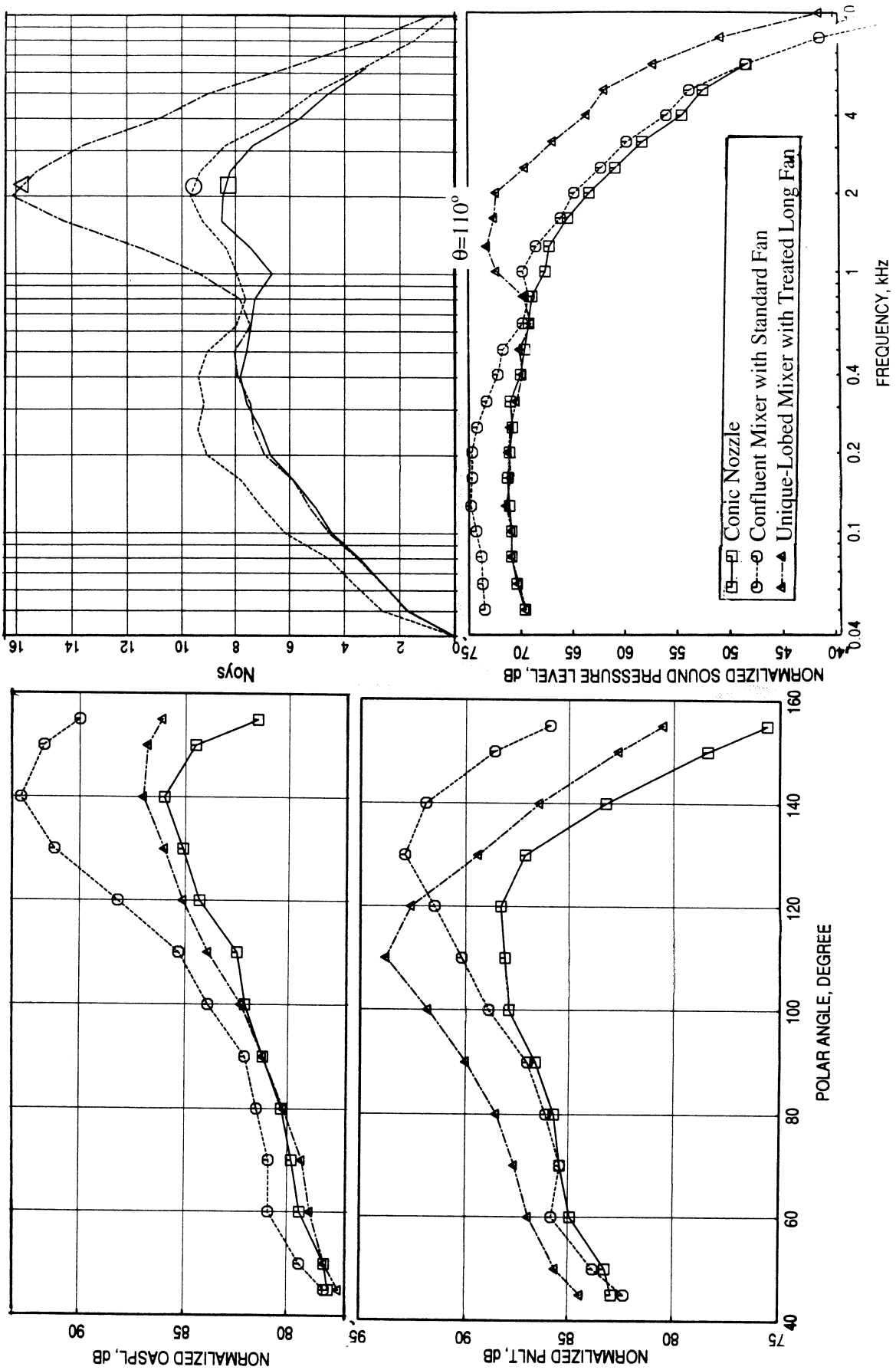


Figure 118. Normalized OASPL & PNLT directivities and SPL with NOY spectra at  $\theta=110^\circ$  at a nominal  $V_{mix}=1175 \text{ ft/sec}$  (TP40 of HBM/C) for the unique-lobed mixer with treated long fan and confluent mixer with internal pylon and standard fan of  $51.7 \text{ in}^2$  exit area compared to a conic nozzle at SAE  $77^\circ$  standard day conditions,  $A_8=3078 \text{ in}^2$ , Sideline Distance=1500 ft,  $M_p=0.28$ ,  $\phi=34^\circ$ .

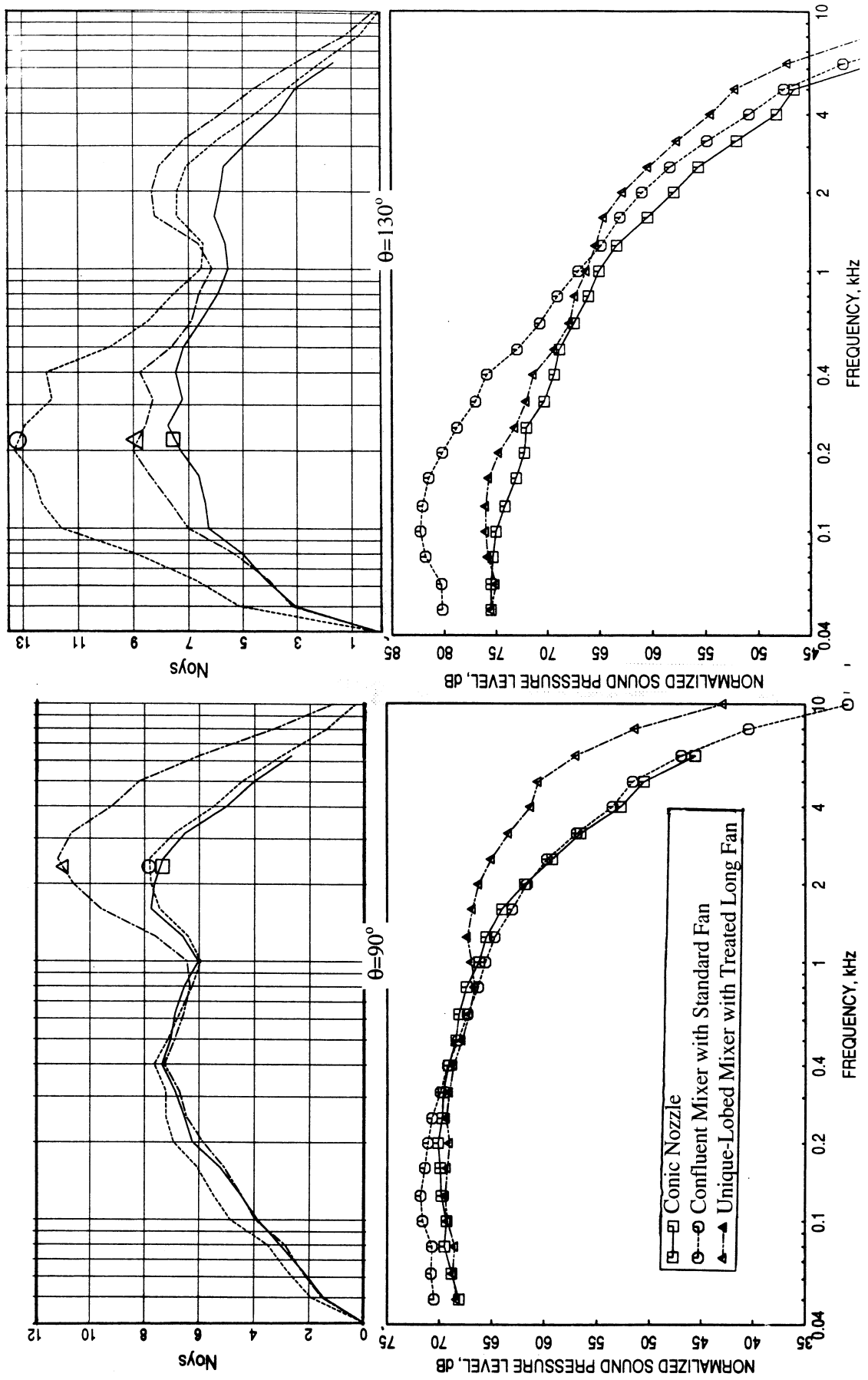


Figure 119. Normalized SPL with NOY spectra at a nominal  $V_{max} = 1175 \text{ ft/sec}$  (TP40 of HBMFC) for the unique-lobed mixer with treated long fan and confluent mixer with internal pylon and standard fan of  $51.7 \text{ in}^2$  exit area compared to a conic nozzle at SAE 77° standard day conditions,  $A_8 = 3078 \text{ in}^2$ , Sideline Distance = 1500 ft,  $M_F = 0.28$ ,  $\phi = 34^\circ$ .

## **6.8 Conclusions:**

- Significant noise reduction can be achieved by using a lower core velocity engine cycle for multi-lobed and confluent mixer exhaust systems.
- While 22- and unique-21-Lobed mixers compared to the confluent mixer significantly reduce the low frequency noise, high frequency noise increase is large.
- The Task objective of 3 EPNdB reduction relative to 1992 technology level was demonstrated in Task - A Tests: 12-lobed mixer configuration (F9B) resulted in a 3.5 EPNdB reduction compared to the confluent mixer at  $V_{mix}=1000$  ft/sec.
- 22- and unique-21-lobed mixer tests in Task - C along a reduced core velocity cycle (High Bypass Mixed Flow Cycle) resulted in an EPNdB lower than the F9B at  $V_{mix}=1000$  ft/sec due to a combination of cycle and mixer design, even though a 2 EPNdB reduction relative to confluent mixer is achieved.
- Increased fan nozzle length reduces noise level at all frequencies at lower velocity conditions due to improved mixing. The trend is reversed at higher velocity conditions possibly due to increased turbulence level.
- Internal pylon for unique-lobed mixer has very little effect on noise level compared to the 22-lobed axisymmetric mixer configuration.
- Acoustic treatment on fan nozzle is more effective in reducing noise at higher velocity conditions.
- Also, the treatment effectiveness is more for E<sup>3</sup> mixed flow cycle conditions, possibly due to higher internal noise caused by higher core velocity.
- Treated configuration introduces excess noise at lower velocity conditions at higher frequencies (2 to 4 kHz) possibly due to increased small scale turbulence by liner perforations. However, these levels are small compared to noise reduction due to treatment at other frequencies at higher velocity conditions.

## APPENDIX A

### TABULATED RESULTS FOR VARIOUS EXHAUST SYSTEM CONFIGURATIONS

Acoustic tests were conducted for 15 different scale model exhaust system configurations at static and simulated flight conditions at four different cycle points. In addition, measurements were made at different azimuthal locations. In total, about 1600 tests were conducted. Some of the results for all 15 configurations are listed in this appendix in tables 1 through 19. The nomenclature for various parameters included in these tables are defined as follows:

Config.=Defined in Table1 for different exhaust system configurations.

RDG=Numbers assigned to individual acoustic tests.

Test Point=Numbers assigned to test conditions along the engine cycles (Defined in Tables 2 through 4)

$P_{r,p}$  = Primary or core stream nozzle pressure ratio

$T_{t,p}$  = Primary or core stream nozzle total temperature in degree R

$W_p$  = Mass Flow Rate for primary or core stream in lbs/sec

$V_{j,p}$  = Ideal Nozzle Exhaust Velocity for primary (core) stream in ft/sec

$P_{r,s}$  = Secondary or fan stream nozzle pressure ratio

$T_{t,s}$  = Secondary or fan stream nozzle total temperature in degree R

$W_s$  = Mass Flow Rate for secondary stream in lbs/sec

$V_{j,s}$  = Ideal Nozzle Exhaust Velocity for secondary (fan) stream in ft/sec

$V_{mix} = (V_{j,p} \cdot W_p + V_{j,s} \cdot W_s) / (W_p + W_s)$  = Mass averaged mixed velocity in ft/sec

$Fg_{ref}$  = Total gross thrust in lb or klb

$P_{amb}$  = Ambient pressure in psi

$T_{amb}$  = Ambient temperature in degree R

$P_r$  = Nozzle pressure ratio for single stream nozzle

$T_t$  = Total temperature for single stream nozzle in degree R

$V_j$  = Ideal Exhaust Velocity or jet velocity for single stream nozzle in ft/sec

$Th_{cor}$  = Thrust Normalization factor in dB ( $10 \log_{10}(Fg_{tot}/Fg_{ref})$ ,  $Fg_{ref} = 60,000$  lbs.)

Table A-1. Conic Nozzle of 20.5 in<sup>2</sup> Exit Area (Config: 1000) at Static Condition

TOWER LOCATION=34. DEG

SCALED AREA = 3078.0 sq inches

EXTRAPOLATION DISTANCE = 1500.0 ft

RDG	Test Point	M <sub>F</sub>	P <sub>amb</sub> psi	T <sub>oF</sub> °F	P <sub>r</sub>	T <sub>i</sub> °R	V <sub>j</sub> ft/sec	F <sub>g<sub>tot</sub></sub> lb	EPNL dB	EPNL T dB	Th <sub>cor</sub> dB
Flight Velocity used for EPNdB Calculation=270 ft/sec											
320.	11	.022060	14.74	35.200	1.1692	607.14	564.51	14515.1	69.1	69.1	6.16
256.	11	.027722	14.76	32.100	1.1712	607.55	567.76	14661.2	68.7	69.4	6.12
321.	11	.37390	14.73	34.800	1.1790	606.43	578.62	15308.6	69.4	69.4	5.93
319.	12	.032954	14.74	35.000	1.2321	615.91	654.51	19527.4	74.6	74.6	4.88
318.	13	.042089	14.74	34.600	1.3039	625.55	740.83	25037.7	78.1	78.1	3.80
314.	14	.036057	14.73	34.600	1.3904	721.89	882.99	31374.7	85.5	85.5	2.82
Flight Velocity used for EPNdB Calculation=315 ft/sec											
314.	14	.036057	14.73	34.600	1.3904	721.89	882.99	31374.7	84.9	84.9	2.82
309.	15	.025767	14.75	32.800	1.4422	729.97	933.51	35034.4	87.3	87.3	2.34
308.	16	.038697	14.75	32.800	1.5121	736.81	993.34	39843.2	89.5	89.5	1.78
307.	17	.031804	14.75	32.800	1.5895	745.75	1054.3	44978.2	91.7	91.7	1.25
303.	18	.00000	14.75	32.300	1.6538	754.45	1101.9	49109.6	93.5	93.5	0.87
297.	19	.029407	14.76	32.300	1.7049	762.85	1138.5	52311.4	94.4	94.4	0.60
310.	19	.035089	14.75	33.600	1.7082	763.27	1140.8	52515.8	94.9	94.9	0.58
311.	20	.033130	14.74	34.300	1.7681	773.10	1181.7	56177.6	96.6	96.6	0.29
312.	21	.045016	14.74	34.600	1.8330	779.88	1220.7	60046.8	97.9	97.9	0.00
295.	21	.040751	14.76	31.400	1.8388	777.11	1221.5	60388.5	96.5	96.5	-0.03
294.	21	.038551	14.76	31.000	1.8454	776.24	1224.1	60775.8	98.0	98.0	-0.06
291.	22	.039805	14.76	33.300	1.9112	791.51	1267.8	64583.5	99.6	99.6	-0.32
313.	22	.046453	14.74	34.200	1.9140	790.12	1268.0	64744.9	99.3	99.4	-0.33
301.	72	.037800	14.76	32.200	1.4420	637.62	872.22	35033.0	85.1	85.1	2.34
300.	75	.030580	14.76	32.000	1.5944	654.37	990.56	45306.0	90.2	90.2	1.22
299.	77	.030366	14.76	32.000	1.7125	661.96	1064.6	52794.3	92.9	92.9	0.56
298.	77	.030961	14.76	31.900	1.7103	668.63	1068.8	52657.7	92.4	92.4	0.57
302.	86	.018911	14.76	32.200	1.6504	623.37	999.52	48906.4	90.6	90.6	0.89

Table A-2. Conic Nozzle of 20.5 in<sup>2</sup> Exit Area (Config: 1000) with Simulated Flight

TOWER LOCATION=34. DEG  
 SCALED AREA = 3078.0 sq inches  
 EXTRAPOLATION DISTANCE = 1500.0 ft

RDG	Test Point	M <sub>F</sub>	P <sub>amb</sub> psi	T <sub>amb</sub> °F	P <sub>r</sub>	T <sub>t</sub> °R	V <sub>j</sub> ft/sec	F <sub>b</sub> <sup>g<sub>tot</sub></sup>	EPNL dB	EPNLT dB	Th <sub>cor</sub> dB
Simulated Flight M <sub>F</sub> =0.24, Flight Velocity=270 ft/sec											
260.	13	.24577	14.75	34.300	1.2992	617.62	731.27	24676.8	67.0	67.2	3.86
261.	14	.24587	14.75	34.100	1.3807	720.12	872.93	30677.3	75.7	75.7	2.91
273.	14	.27883	14.76	33.600	1.3820	723.64	876.25	30770.7	75.0	75.1	2.90
270.	14	.23726	14.76	34.400	1.3834	724.79	878.29	30871.5	75.4	75.5	2.89
262.	14	.24594	14.75	34.100	1.3924	724.35	886.34	31517.9	75.1	75.2	2.80
Simulated Flight M <sub>F</sub> =0.28, Flight Velocity=315 ft/sec											
272.	14	.28148	14.76	34.700	1.3856	723.63	879.63	31029.9	73.5	73.7	2.86
274.	15	.28156	14.75	34.300	1.4414	729.19	932.36	34985.6	76.5	76.6	2.34
275.	16	.27959	14.76	34.400	1.5085	739.53	992.51	39599.5	79.3	79.6	1.80
276.	17	.27903	14.76	34.000	1.5927	745.63	1056.4	45186.7	81.8	82.0	1.23
277.	18	.28102	14.76	34.900	1.6511	757.01	1102.0	48938.1	84.0	84.2	0.89
285.	19	.28148	14.76	34.300	1.6985	760.34	1133.0	51914.4	85.5	85.7	0.63
286.	20	.28110	14.76	34.200	1.7643	771.17	1178.1	55948.2	86.9	87.1	0.30
287.	21	.28099	14.76	34.800	1.8419	778.52	1224.1	60570.2	88.6	88.8	-0.04
290.	22	.27957	14.76	35.900	1.8956	795.31	1263.5	63685.1	90.1	90.3	-0.26
284.	72	.27941	14.75	33.500	1.4501	642.99	882.23	35597.9	74.0	74.2	2.27
283.	75	.28107	14.76	34.400	1.5966	651.89	990.07	45449.2	79.7	79.9	1.21
281.	77	.28096	14.76	34.900	1.7021	662.29	1059.2	52149.9	82.6	82.8	0.61
282.	86	.27985	14.75	35.100	1.6500	627.91	1002.9	48880.8	80.4	80.6	0.89

Table A-3. Confluent Mixer with Standard Fan Nozzle (Config: 2100), Static Condition

TOWER LOCATION=34. DEG  
EXTRAPOLATION DISTANCE=1500.0 ft  
SCALED AREA = 3078.0 sq inches

RDG	Test Point	P <sub>r,p</sub>	T <sub>t,p</sub> <sup>o</sup> R	V <sub>ip</sub> <sup>ft/sec</sup>	W <sub>p</sub> <sup>lb/sec</sup>	P <sub>r,s</sub>	T <sub>R</sub> <sup>o</sup>	V <sub>is</sub> <sup>ft/sec</sup>	W <sub>s</sub> <sup>lb/sec</sup>	V <sub>mix</sub> <sup>ft/sec</sup>	F <sub>g</sub> <sup>ot</sup> klb	EPNL dB	EPNLT dB	Pamb psi	T <sub>amb</sub> °F	M <sub>f</sub>	Th <sub>cor</sub> dB
<b>High Bypass Separate Flow Cycle</b>																	
625	12	1.1115	1122.8	642.5	1.32	1.281	508.9	6446.6	16.46	6446.3	21.26	74.3	14.43	34.41	0.000	4.51	
626	12	1.116	1179.0	661.9	1.27	1.284	507.5	648.8	16.53	649.7	21.39	74.5	14.43	34.27	0.000	4.48	
628	13	1.150	1198.4	750.2	1.49	1.338	507.3	697.8	17.97	701.8	25.27	78.0	14.43	33.42	0.000	3.76	
663	14	1.2222	1261.3	920.0	1.85	1.443	636.7	872.1	18.31	876.5	32.69	85.5	14.55	25.42	0.000	2.64	
702	15	1.275	1275.5	1015.4	2.08	1.519	638.4	929.0	19.81	937.2	37.94	87.5	14.58	27.21	0.000	1.99	
675	16	1.340	1292.0	1117.2	2.41	1.585	637.2	971.6	20.92	986.7	42.58	91.1	11.2	14.56	24.70	0.000	1.49
704	17	1.425	1351.1	1251.4	2.70	1.667	637.9	1020.4	22.07	1045.7	47.92	93.3	14.57	27.84	0.000	0.98	
706	18	1.502	1394.1	1358.3	3.02	1.719	639.7	1049.6	22.51	1086.1	51.31	95.6	14.57	28.11	0.000	0.68	
715	19	1.571	1420.0	1439.9	3.26	1.772	635.6	1073.4	23.17	1118.6	54.71	97.0	14.55	28.86	0.000	0.40	
719	20	1.670	1498.2	1570.8	3.63	1.825	640.3	1102.3	23.42	1165.2	58.33	98.9	99.0	14.54	29.62	0.000	0.12
754	21	1.794	1521.1	1681.4	4.01	1.896	640.1	1133.4	23.25	1213.9	61.21	100.4	100.6	14.11	36.64	0.027	-0.09
752	22	1.921	1573.2	1799.2	4.47	1.950	639.4	1155.4	23.45	1258.4	64.98	102.2	102.4	14.10	36.98	0.039	-0.35
<b>High Bypass Mixed Flow Cycle</b>																	
627	32	1.169	1194.5	777.8	1.96	1.278	507.2	642.5	15.65	657.5	21.42	74.6	14.43	33.94	0.000	4.47	
629	33	1.227	903.5	903.7	2.30	1.345	508.3	704.1	17.30	727.5	26.38	78.7	78.8	14.43	33.50	0.000	3.57
701	34	1.325	1251.2	1078.9	2.89	1.424	638.7	858.9	17.06	890.8	32.87	86.3	86.3	14.59	26.80	0.000	2.61
703	35	1.389	1277.8	1173.9	3.14	1.492	640.7	912.0	18.27	950.4	37.65	89.7	89.8	14.58	27.64	0.000	2.02
674	36	1.461	1330.4	1283.0	3.39	1.558	640.4	956.6	19.28	1005.4	42.18	92.4	92.4	14.56	27.12	0.000	1.53
705	37	1.557	1366.3	1399.4	3.74	1.636	639.1	1003.8	20.41	1065.1	47.60	95.3	95.4	14.57	28.44	0.000	1.01
713	38	1.649	1412.8	1506.6	4.13	1.686	641.8	1033.8	20.93	1111.7	51.53	97.2	97.4	14.56	28.61	0.000	0.66
717	38	1.648	1396.1	1497.3	4.15	1.684	638.3	1030.1	20.95	1107.4	51.43	97.1	97.3	14.55	29.07	0.000	0.67
716	39	1.727	1421.4	1574.5	4.42	1.735	641.1	1059.1	21.39	1147.4	54.77	98.8	98.9	14.55	29.24	0.000	0.40
720	40	1.829	1460.2	1671.6	4.81	1.781	640.9	1082.2	21.72	1189.1	58.35	100.6	100.7	14.54	29.39	0.000	0.12
753	41	1.941	1505.0	1772.2	5.02	1.834	642.0	11107.8	21.43	1234.0	60.40	102.1	102.3	14.10	36.99	0.025	-0.03
<b>E<sup>3</sup> Mixed Flow Cycle</b>																	
633	71	1.364	1360.2	1179.5	3.05	1.419	519.8	771.1	18.22	829.7	32.65	86.0	86.0	14.44	32.98	0.000	2.64
634	72	1.429	1378.5	1268.9	3.40	1.454	520.2	796.0	18.77	868.5	35.63	88.8	88.9	14.44	32.28	0.000	2.26
636	73	1.493	1411.1	1356.5	3.64	1.508	519.5	831.3	19.84	912.7	39.65	91.0	91.1	14.45	32.10	0.000	1.80
637	74	1.565	1433.6	1441.8	3.89	1.572	518.7	869.4	20.99	958.9	44.14	93.6	93.8	14.45	31.68	0.000	1.33
638	75	1.640	1455.1	1521.7	4.21	1.610	518.4	890.5	21.54	993.7	47.35	95.6	95.8	14.45	31.51	0.000	1.03
639	76	1.702	1469.9	1582.2	4.39	1.665	520.8	921.0	22.31	1029.8	50.88	97.2	97.4	14.45	31.89	0.000	0.72
640	77	1.781	1498.5	1659.1	4.65	1.715	519.7	944.6	22.96	1064.9	54.39	99.0	99.1	14.45	31.99	0.000	0.43
641	78	1.856	1519.6	1725.0	4.84	1.781	519.8	974.3	23.80	1101.1	58.34	100.7	100.8	14.46	31.67	0.000	0.12
700	79	1.965	1549.6	1813.6	5.34	1.802	524.6	988.2	23.84	1139.2	61.49	103.0	103.1	14.59	27.76	0.000	-0.11
<b>E<sup>3</sup> Separate Flow Cycle</b>																	
630	82	1.292	1250.0	1030.0	2.32	1.495	510.1	815.5	21.11	836.7	36.26	85.0	85.0	14.44	33.63	0.009	2.19
631	84	1.387	1294.4	1179.3	2.69	1.600	511.4	878.8	23.05	910.2	43.34	89.0	89.0	14.44	33.13	0.000	1.41
632	86	1.509	1312.2	1324.8	3.12	1.725	514.4	944.4	24.99	986.7	51.31	92.7	92.9	14.44	32.89	0.000	0.68
<b>Mixed Conditions of Conic Nozzle</b>																	
748	18	1.653	756.3	1102.7	5.68	1.654	754.7	1102.0	18.18	1102.2	48.64	93.2	93.3	14.11	39.83	0.039	0.91
749	21	1.838	779.5	1223.1	6.31	1.827	778.1	1216.5	19.81	1218.1	58.85	98.0	98.1	14.10	37.37	0.048	0.08

Table A-4. Confluent Mixer with Standard Fan Nozzle (Config: 2100), Simulated Flight  $M_F = 0.28$ 

TOWER LOCATION=34. DEG  
SCALED AREA = 3078.0 sq inches

FLIGHT VELOCITY = 315.0 ft/sec  
EXTRAPOLATION DISTANCE = 1500.0 ft

RDG	Test Point	$P_{r,p}$	$T_{t,p}^o R$	$V_{i,p}$ ft/sec	$W_p$ lb/sec	$P_{r,s}$	$T_R^o$	$V_{i,s}$ ft/sec	$W_s$ lb/sec	$V_{mix}^o$ ft/sec	$F_{g,ot}^o$ klb	EPNL	EPNLT	$P_{amb}$ psi	$T_{amb}^o F$	$M_F$	$\text{Th}_{\text{cor}}$ dB
High Bypass Separate Flow Cycle																	
727	12	1.119	1167.6	665.9	1.15	1.299	507.7	662.4	16.58	662.6	21.74	-12.2	14.19	33.54	0.279	4.41	
681	13	1.152	1193.2	754.3	1.42	1.354	501.0	706.2	18.68	709.6	26.39	67.5	14.62	22.36	0.283	3.57	
666	14	1.221	1262.7	917.3	1.76	1.453	635.5	879.2	18.60	882.5	33.24	74.0	14.56	27.88	0.282	2.56	
669	15	1.266	1271.9	998.2	1.95	1.520	635.0	927.6	19.91	933.9	37.77	77.1	14.56	27.99	0.281	2.01	
672	16	1.342	1300.2	1124.1	2.37	1.590	638.3	975.5	20.90	990.6	42.64	80.4	14.56	28.17	0.281	1.48	
728	17	1.407	1350.9	1229.9	2.49	1.654	646.2	1019.9	21.09	1042.0	45.46	82.3	14.19	36.97	0.280	1.21	
730	18	1.505	1388.0	1357.8	2.91	1.742	638.3	1060.6	22.50	1094.7	51.45	84.7	14.17	37.25	0.283	0.67	
738	19	1.573	1426.5	1445.6	3.18	1.769	640.4	1075.7	22.33	1121.9	52.95	86.9	14.16	39.09	0.282	0.54	
740	20	1.682	1459.9	1559.8	3.57	1.844	640.1	1110.9	23.02	1171.1	57.62	88.8	14.15	39.64	0.281	0.18	
742	21	1.785	1523.7	1676.2	3.99	1.887	639.9	1129.5	23.18	1209.8	60.81	92.2	14.14	40.46	0.280	-0.06	
745	22	1.921	1555.1	1789.3	4.46	1.962	638.5	1159.0	23.66	1259.1	65.51	95.0	14.12	40.36	0.279	-0.38	
High Bypass Mixed Flow Cycle																	
680	32	1.172	1157.5	785.8	1.90	1.290	500.9	650.3	16.16	664.5	22.20	68.5	14.63	21.11	0.281	4.32	
684	33	1.220	1197.6	892.6	2.18	1.352	503.6	706.6	17.74	727.0	26.79	67.3	14.61	22.80	0.282	3.50	
667	34	1.305	1216.9	1035.7	2.68	1.428	641.0	863.7	17.06	887.1	32.40	74.6	14.56	28.36	0.282	2.68	
671	35	1.378	1285.7	1163.7	3.04	1.484	639.6	905.3	18.05	942.6	36.78	78.0	14.56	28.23	0.281	2.13	
673	36	1.464	1303.4	1272.9	3.41	1.560	639.2	957.5	19.28	1005.0	42.19	81.4	14.56	27.91	0.281	1.53	
729	37	1.546	1357.1	1384.0	3.63	1.621	642.5	997.7	19.58	1058.2	45.43	83.7	14.18	37.49	0.281	1.21	
737	38	1.646	1409.3	1502.1	3.96	1.697	637.8	1036.7	20.64	1111.7	50.59	87.0	14.16	38.80	0.282	0.74	
739	39	1.736	1427.2	1585.1	4.37	1.726	640.7	1054.4	20.62	1147.2	53.03	89.3	14.15	39.50	0.282	0.54	
741	40	1.834	1455.5	1672.7	4.72	1.779	641.1	1081.1	21.06	1189.4	56.73	91.8	14.15	39.96	0.280	0.24	
744	41	1.954	1503.5	1779.6	5.14	1.829	643.7	1107.2	21.37	1237.6	60.69	94.6	14.13	40.43	0.279	-0.05	
$E^3$ Mixed Flow Cycle																	
689	71	1.364	1374.2	1185.1	3.05	1.419	520.3	771.0	18.31	830.1	32.80	74.2	14.43	21.11	0.281	2.62	
690	72	1.426	1389.2	1271.4	3.38	1.460	520.2	800.1	19.06	871.0	36.15	77.3	14.62	26.95	0.281	2.20	
691	73	1.490	1413.8	1355.2	3.62	1.513	520.9	836.0	20.08	915.4	40.14	80.2	14.62	27.32	0.281	1.75	
692	74	1.563	1418.3	1431.7	3.93	1.569	520.8	869.2	21.04	957.8	44.25	82.7	14.62	27.85	0.281	1.32	
693	75	1.633	1445.2	1510.2	4.20	1.617	522.2	897.1	21.75	996.2	47.83	85.4	14.62	28.15	0.279	0.98	
694	76	1.710	1471.3	1588.7	4.49	1.659	521.8	918.8	22.32	1031.0	51.15	88.1	14.61	28.54	0.281	0.69	
695	77	1.780	1493.4	1655.3	4.69	1.717	523.2	948.4	23.13	1067.6	54.94	90.6	14.61	29.37	0.280	0.38	
696	78	1.868	1523.9	1735.4	5.00	1.760	525.6	970.3	23.47	1104.6	58.18	93.4	14.60	29.74	0.280	0.13	
698	79	1.961	1545.9	1808.8	5.35	1.791	524.9	983.5	23.61	1136.0	60.86	95.8	14.60	29.65	0.278	-0.06	
$E^3$ Separate Flow Cycle																	
685	82	1.292	1254.5	1032.7	2.26	1.505	507.0	819.8	21.64	839.9	37.14	74.1	14.62	24.47	0.282	2.08	
686	84	1.390	1288.3	1180.2	2.64	1.626	509.6	891.2	23.99	919.8	45.31	79.1	14.62	24.25	0.281	1.22	
687	86	1.504	1318.9	1322.4	3.10	1.728	514.6	945.6	25.39	986.7	51.99	82.0	14.62	25.88	0.281	0.62	
Mixed Conditions of Conic Nozzle																	
747	18	1.656	751.9	1101.1	5.72	1.649	756.3	1100.0	17.97	1100.3	48.22	83.4	14.11	41.83	0.280	0.95	
746	21	1.837	781.3	1223.6	6.24	1.838	780.0	1223.3	19.95	1223.4	59.28	88.3	14.11	41.94	0.279	0.05	

Table A-5. Confluent Mixer with Standard Fan Nozzle with Internal Pylon (Config: 2110), Simulated Flight  $M_F=0.28$

TOWER LOCATION=34. DEG

SCALED AREA = 3078.0 sq inches

FLIGHT VELOCITY = 315.0 ft/sec

EXTRAPOLATION DISTANCE = 1500.0 ft

RDG	Test Point	$P_{r,p}$	$T_{t,p}^{\circ R}$	$V_{i,p}$ ft/sec	$W_p$ lb/sec	$P_{r,s}$	$T_{t,s}^{\circ R}$	$V_{i,s}$ ft/sec	$W_s$ lb/sec	$V_{mix}$ ft/sec	$F_{tot}$ klb	EPNL dB	EPNL T	Pamb psi	$T_{amb}$ °F	$M_F$	$Th_{cor}$ dB
High Bypass Separate Flow Cycle																	
56	14	1.213	1245.1	897.5	1.96	1.439	640.0	871.4	18.60	873.8	33.23	74.2	14.50	38.28	0.283	2.57	
60	15	1.265	1279.4	1000.2	2.19	1.516	637.8	926.7	20.24	933.9	38.74	77.3	14.52	38.36	0.283	1.90	
64	16	1.336	1307.1	1118.8	2.52	1.599	637.9	980.9	21.74	995.2	44.67	80.4	14.54	38.69	0.282	1.28	
71	17	1.405	1351.2	1228.0	2.85	1.653	638.3	1012.6	22.53	1036.7	48.69	82.3	14.56	38.92	0.282	0.91	
82	18	1.504	1392.0	1359.3	3.25	1.729	639.0	1054.3	23.48	1091.4	53.96	85.3	14.57	37.80	0.280	0.46	
87	19	1.580	1430.6	1454.4	3.53	1.780	638.3	1079.6	24.06	1127.6	57.55	87.1	14.58	38.01	0.280	0.18	
91	20	1.678	1474.5	1564.5	3.92	1.831	640.6	1105.3	24.39	1168.9	61.22	89.8	14.58	38.18	0.280	-0.09	
95	21	1.798	1524.8	1686.1	4.35	1.899	637.4	1132.6	25.09	1214.3	66.13	92.5	14.59	39.23	0.280	-0.42	
137	22	1.939	1545.0	1794.8	5.01	1.950	639.0	1154.9	25.51	1260.0	71.16	96.1	14.73	35.05	0.282	-0.74	
High Bypass Mixed Flow Cycle																	
59	34	1.315	1247.4	1063.5	2.87	1.439	640.8	871.8	17.84	898.4	34.42	75.7	14.51	38.66	0.282	2.41	
63	35	1.373	1288.6	1158.8	3.13	1.494	636.8	910.5	18.98	945.7	38.68	78.5	14.53	38.09	0.280	1.91	
67	36	1.456	1321.5	1273.2	3.51	1.561	639.9	958.6	20.03	1005.5	43.80	81.6	14.54	38.78	0.282	1.37	
73	37	1.555	1357.0	1393.0	3.94	1.630	639.9	1000.9	21.08	1062.7	49.20	84.5	14.56	39.00	0.280	0.86	
84	38	1.650	1405.9	1503.8	4.28	1.698	640.4	1039.4	22.05	1114.8	54.30	87.3	14.58	37.95	0.279	0.43	
88	39	1.733	1433.3	1586.2	4.64	1.725	640.8	1054.1	22.15	1146.2	56.81	89.7	14.58	38.62	0.281	0.24	
92	40	1.835	1463.7	1677.7	4.96	1.794	642.7	1089.9	22.90	1194.5	61.57	92.2	14.59	38.27	0.280	-0.11	
136	41	1.957	1503.0	1781.2	5.45	1.849	642.7	1115.2	23.59	1240.2	66.64	96.1	14.73	35.92	0.281	-0.46	

Table A-6. Confluent Mixer with Short Fan Nozzle (Config: 2200)  
 TOWER LOCATION=34, DEG  
 SCALED AREA = 3078.0 sq inches  
 EXTRAPOLATION DISTANCE = 1500.0 ft

RDG	Test Point	P <sub>r,p</sub>	T <sub>r,p</sub>	T <sub>i,p</sub> <sup>o</sup> R	V <sub>i,p</sub> <sup>o</sup> C	W <sub>i,p</sub>	P <sub>r,s</sub>	T <sub>r,s</sub> <sup>o</sup>	V <sub>i,s</sub> <sup>o</sup> C	W <sub>s</sub>	V <sub>mix</sub> <sup>ft/sec</sup>	F <sub>g, tot</sub> Klb	EPNL dB	EPNL T dB	Pamb psi	M <sub>F</sub>	T <sub>amb</sub> °F	Th <sub>cor</sub> dB
-----	------------	------------------	------------------	---------------------------------	---------------------------------	------------------	------------------	-------------------------------	---------------------------------	----------------	------------------------------------	----------------------------	------------	--------------	-------------	----------------	------------------------	-------------------------

(a) Static Condition, Flight Velocity for EPNdB = 315.0 ft/sec

E <sup>3</sup> Mixed Flow Cycle																	
1129	72	1.431	1386.4	1276.0	3.56	1.458	528.1	805.3	18.27	882.2	35.63	88.8	88.9	14.35	40.04	0.028	2.26
1138	77	1.779	1501.6	1659.0	4.73	1.727	529.7	959.2	22.31	1081.5	54.10	98.8	99.0	14.33	41.79	0.043	0.45
1137	78	1.857	1514.4	1722.8	5.04	1.751	530.3	970.7	22.39	1108.9	56.27	100.3	100.5	14.33	41.37	0.046	0.28
1136	79	1.971	1551.2	1818.3	5.43	1.792	530.1	989.0	22.78	1148.7	59.96	102.0	102.1	14.34	42.83	0.040	0.00
High Bypass Mixed Flow Cycle																	
1117	34	1.315	1279.7	1076.8	2.95	1.429	636.5	861.3	16.53	894.0	32.21	86.1	86.1	14.37	36.75	0.023	2.70
1128	36	1.455	1310.8	1267.2	3.56	1.562	641.1	959.7	18.58	1009.2	41.33	92.0	92.1	14.35	39.76	0.027	1.62
1127	38	1.649	1395.1	1497.5	4.31	1.689	640.7	1034.5	20.23	1115.8	50.66	97.0	97.2	14.35	39.47	0.029	0.73
1126	39	1.732	1434.9	1586.7	4.60	1.729	640.1	1055.5	20.60	1152.5	53.75	98.5	98.7	14.35	38.94	0.016	0.48
1125	40	1.840	1459.2	1679.0	4.97	1.795	639.9	1087.9	21.30	1199.7	58.31	100.4	100.6	14.35	39.41	0.023	0.12
1124	41	1.954	1497.3	1775.6	5.33	1.850	643.3	1116.2	21.59	1246.8	62.09	102.3	102.5	14.35	39.73	0.025	-0.15

(b) Simulated Flight M<sub>F</sub>=0.28, Flight Velocity= 315.0 ft/sec

E <sup>3</sup> Mixed Flow Cycle																	
1130	72	1.428	1396.8	1277.0	3.47	1.469	523.9	809.0	18.41	883.3	35.76	77.2	77.3	14.35	42.31	0.279	2.25
1131	73	1.494	1410.5	1357.7	3.75	1.522	521.8	842.1	19.44	925.5	39.70	79.8	79.8	14.34	44.28	0.279	1.79
1132	75	1.626	1451.2	1507.0	4.22	1.628	522.1	902.8	21.10	1003.4	46.99	84.8	84.9	14.34	44.95	0.279	1.06
1133	77	1.776	1492.9	1652.2	4.73	1.725	524.8	953.9	22.35	1075.9	53.89	90.0	90.1	14.34	44.99	0.281	0.47
1134	78	1.863	1516.1	1727.6	5.03	1.769	525.0	974.2	22.81	1110.3	57.17	92.5	92.6	14.34	46.99	0.281	0.21
1135	79	1.958	1553.7	1812.0	5.38	1.781	527.7	982.0	22.59	1141.6	59.07	94.8	94.9	14.34	46.30	0.281	0.07
High Bypass Mixed Flow Cycle																	
1118	34	1.318	1263.5	1074.6	2.95	1.420	640.8	857.0	16.00	890.9	31.25	74.5	74.5	14.37	38.06	0.281	2.83
1119	36	1.456	1331.8	1277.8	3.51	1.568	638.2	961.8	18.74	1011.6	41.63	81.0	81.0	14.37	42.12	0.281	1.59
1120	38	1.638	1415.3	1498.8	4.19	1.693	640.1	1036.2	20.26	1115.4	50.45	87.2	87.3	14.36	43.14	0.279	0.75
1121	39	1.741	1420.7	1584.9	4.68	1.725	641.8	1054.7	20.45	1153.4	53.62	89.7	89.8	14.36	42.79	0.281	0.49
1122	40	1.827	1468.2	1674.7	4.90	1.782	642.6	1083.8	20.97	1195.7	57.23	92.2	92.3	14.36	43.08	0.279	0.21
1123	41	1.952	1514.0	1784.3	5.30	1.849	642.2	1115.0	21.64	1246.6	62.12	94.8	94.9	14.35	42.46	0.279	-0.15

TOWER LOCATION=34. DEG  
SCALED AREA = 3078.0 sq inches

Table A-7. 22-Lobed Mixer with Standard Fan Nozzle (Config: 3100), Static Condition

FLIGHT VELOCITY FOR EPNdB= 315.0 ft/sec  
EXTRAPOLATION DISTANCE = 1500.0 ft

RDG	Test Point	P <sub>r,p</sub>	T <sub>t,p</sub> <sup>°</sup> R	V <sub>i,p</sub> <sup>ip</sup>	W <sub>p</sub>	P <sub>r,s</sub>	T <sub>t,R</sub> <sup>°</sup>	V <sub>i,s</sub>	W <sub>s</sub>	V <sub>mix</sub>	EPNL	EPNL T	Pamb	T <sub>amb</sub>	M <sub>f</sub>	Th <sub>cor</sub>	
High Bypass Separate Flow Cycle																	
763	12	1.113	1164.2	650.1	0.99	1.304	501.1	662.7	17.32	662.0	22.43	74.7	14.24	21.92	0.019	4.27	
761	13	1.153	1198.8	758.6	1.27	1.361	505.3	715.5	18.69	718.2	26.52	78.4	14.24	21.86	0.000	3.55	
823	14	1.220	1252.6	913.0	1.63	1.450	636.8	877.6	19.02	880.4	33.64	85.7	14.74	6.20	0.034	2.51	
825	15	1.270	1279.9	1008.0	1.78	1.525	636.9	932.5	20.55	938.6	38.77	88.3	14.75	6.78	0.014	1.90	
827	16	1.340	1313.4	1127.1	2.15	1.587	638.4	973.8	21.44	987.8	43.11	90.4	14.75	7.54	0.000	1.44	
829	17	1.417	1352.8	1243.6	2.40	1.662	638.1	1017.9	22.52	1039.6	47.94	92.9	14.75	8.54	0.000	0.97	
832	18	1.504	1392.1	1359.5	2.75	1.728	637.3	1052.8	23.36	1085.1	52.42	94.4	14.74	9.55	0.000	0.59	
859	19	1.575	1424.0	1445.8	2.98	1.780	635.5	1076.7	23.83	1117.8	55.45	95.9	96.0	14.72	9.12	0.012	0.34
854	20	1.681	1453.3	1555.4	3.36	1.837	639.8	1107.2	23.99	1162.3	58.83	97.8	97.9	14.71	17.85	0.015	0.09
862	21	1.795	1514.1	1678.2	3.79	1.885	636.3	1125.2	24.22	1200.1	62.20	99.7	99.9	14.73	10.17	0.004	-0.16
864	22	1.915	1566.8	1792.1	4.17	1.946	638.4	1152.9	24.55	1245.8	66.20	101.4	101.5	14.72	10.77	0.014	-0.43
High Bypass Mixed Flow Cycle																	
762	32	1.169	1163.9	782.1	1.70	1.284	502.9	645.8	15.86	659.0	21.41	74.8	14.24	22.04	0.000	4.47	
791	33	1.221	1201.3	895.2	1.94	1.356	510.2	715.1	17.61	732.9	26.50	78.2	78.3	14.25	22.12	0.012	3.55
824	34	1.323	1249.5	1075.4	2.59	1.425	639.4	859.5	17.36	887.6	32.76	85.7	14.74	6.03	0.042	2.63	
826	35	1.374	1288.0	1160.5	2.76	1.479	643.0	904.0	18.38	937.6	36.67	88.1	88.1	14.74	7.41	0.026	2.14
828	36	1.469	1315.9	1284.2	3.12	1.571	636.5	962.4	20.11	1005.7	43.22	90.8	90.8	14.75	8.04	0.010	1.42
831	37	1.563	1361.9	1402.4	3.45	1.636	638.8	1003.6	20.85	1060.2	47.66	93.4	93.5	14.74	9.30	0.007	1.00
858	38	1.650	1403.6	1502.8	3.76	1.687	639.4	1032.6	21.40	1102.9	51.33	95.1	95.2	14.72	8.28	0.000	0.68
860	39	1.745	1423.6	1590.1	4.12	1.738	636.6	1057.2	21.94	1141.5	55.04	96.0	96.1	14.73	8.69	0.007	0.37
861	40	1.831	1471.0	1679.6	4.33	1.791	641.5	1087.5	22.26	1183.9	58.23	98.7	98.9	14.73	9.53	0.007	0.13
863	41	1.962	1502.3	1783.4	4.83	1.842	641.0	1110.4	22.61	1228.8	62.38	100.9	101.0	14.72	10.45	0.016	-0.17
E <sup>3</sup> Mixed Flow Cycle																	
787	71	1.362	1372.2	1182.2	2.64	1.425	511.9	769.3	18.31	821.4	31.85	82.9	82.9	14.25	21.80	0.000	2.75
786	72	1.408	1391.6	1249.5	2.76	1.476	515.7	807.8	19.20	863.2	35.06	85.7	85.7	14.24	22.76	0.000	2.33
776	73	1.498	1407.8	1361.0	3.19	1.522	508.3	831.1	19.96	904.1	38.72	87.4	87.5	14.23	23.27	0.024	1.90
779	74	1.567	1421.5	1437.0	3.46	1.564	510.9	857.8	20.50	941.4	41.73	89.3	89.4	14.25	21.86	0.000	1.58
780	75	1.647	1441.7	1520.2	3.70	1.627	510.6	892.7	21.48	984.8	45.86	91.1	91.2	14.24	21.23	0.022	1.17
781	76	1.710	1480.5	1594.0	3.83	1.686	514.8	925.9	22.31	1023.8	49.51	93.2	93.3	14.24	21.79	0.020	0.83
783	77	1.796	1494.1	1667.9	4.14	1.730	514.5	946.5	22.80	1057.5	52.71	94.5	94.6	14.24	21.78	0.000	0.56
784	78	1.866	1519.5	1731.7	4.34	1.765	514.0	962.2	23.02	1084.3	54.89	96.6	96.7	14.24	21.57	0.021	0.39
785	79	1.969	1553.8	1818.6	4.63	1.822	514.8	987.2	23.57	1123.8	58.64	98.5	98.7	14.24	22.08	0.000	0.10
E <sup>3</sup> Separate Flow Cycle																	
790	82	1.284	1258.8	1021.6	1.88	1.518	511.1	831.3	21.70	846.4	36.92	84.4	84.4	14.25	22.88	0.015	2.11
789	83	1.398	1273.1	1183.1	2.39	1.622	509.9	889.1	23.34	916.4	43.61	87.6	87.6	14.24	22.45	0.000	1.39
788	84	1.499	1323.6	1320.5	2.71	1.713	509.4	933.8	24.65	972.1	49.20	90.9	90.9	14.23	22.17	0.035	0.86

Table A-8. 22-Lobed Mixer with Standard Fan Nozzle (Config: 3100), Simulated Flight  $M_F=0.28$

TOWER LOCATION=34. DEG  
SCALED AREA = 3078.0 sq inches

FLIGHT VELOCITY = 315.0 ft/sec  
EXTRAPOLATION DISTANCE = 1500.0 ft

RDG	Test Point	$P_{r,p}$	$T_{t,p}^{\circ}\text{R}$	$V_{j,p}$ ft/sec	$W_p$ lb/sec	$P_{r,s}$	$T_{t,s}^{\circ}$ $R$	$V_{j,s}$ ft/sec	$W_s$ lb/sec	$V_{mix}$ ft/sec	$F_{g_{tot}}$ klb	EPNL dB	EPNL T dB	Pamb psi	$T_{amb}$ °F	$M_F$	$TH_{cor}$
High Bypass Separate Flow Cycle																	
764	12	1.115	1175.9	658.3	0.99	1.299	501.6	659.0	17.06	659.0	22.00	65.9	66.0	14.24	23.13	0.282	4.36
767	13	1.156	1209.7	768.8	1.20	1.368	503.7	720.0	18.77	722.9	26.72	68.3	68.3	14.24	25.93	0.281	3.51
806	14	1.218	1247.1	907.1	1.61	1.434	637.4	866.1	18.21	869.4	31.88	75.1	75.2	14.50	13.74	0.280	2.75
808	15	1.258	1291.1	993.3	1.65	1.513	634.5	922.2	19.94	927.6	37.06	77.7	77.7	14.49	14.28	0.280	2.09
810	16	1.336	1305.8	1118.0	1.99	1.595	638.2	978.8	21.15	990.8	42.42	80.0	80.0	14.49	15.88	0.280	1.51
812	17	1.412	1351.7	1236.3	2.35	1.641	637.7	1005.4	21.55	1028.1	45.46	82.3	82.4	14.49	17.68	0.280	1.21
813	17	1.419	1354.9	1246.7	2.32	1.665	636.9	1018.7	22.10	1040.3	46.99	82.5	82.5	14.49	17.34	0.280	1.06
849	18	1.499	1393.5	1354.6	2.67	1.718	638.1	1048.2	22.91	1080.2	51.12	84.8	84.8	14.71	17.49	0.283	0.70
815	18	1.502	1388.7	1355.1	2.67	1.719	637.5	1048.4	22.61	1080.8	50.56	85.1	85.1	14.49	17.90	0.280	0.74
851	19	1.578	1417.1	1445.3	3.03	1.771	636.5	1073.4	23.57	1115.8	54.92	87.6	87.6	14.71	18.31	0.279	0.38
853	20	1.675	1466.1	1557.6	3.36	1.820	640.4	1100.3	23.71	1157.1	57.95	90.4	90.4	14.71	19.40	0.280	0.15
866	21	1.794	1511.6	1676.1	3.81	1.883	638.4	1126.6	24.20	1201.3	62.25	92.6	92.7	14.73	17.58	0.280	-0.16
865	22	1.923	1561.1	1793.6	4.23	1.954	638.1	1155.7	24.75	1248.8	66.95	93.7	94.0	14.73	13.29	0.280	-0.48
High Bypass Mixed Flow Cycle																	
766	32	1.168	1163.9	780.5	1.61	1.290	503.4	651.5	15.90	663.4	21.49	64.4	64.6	14.24	25.89	0.280	4.46
768	33	1.219	1199.9	890.9	1.86	1.349	504.0	704.8	17.29	722.9	25.61	67.3	67.3	14.24	25.62	0.280	3.70
807	34	1.319	1249.0	1068.9	2.44	1.444	636.6	873.4	17.61	897.2	33.28	75.6	75.6	14.48	14.48	0.282	2.56
809	35	1.369	1301.4	1159.6	2.60	1.486	636.8	904.6	18.23	936.5	36.10	77.4	77.4	14.49	14.87	0.281	2.21
1026	36	1.454	1303.1	1262.4	2.95	1.561	638.0	956.7	19.21	997.4	40.88	78.8	78.9	14.34	54.36	0.271	1.67
814	37	1.565	1377.0	1412.4	3.40	1.627	650.1	1006.9	20.04	1065.7	46.21	82.5	82.5	14.49	16.99	0.280	1.13
850	38	1.643	1412.0	1501.7	3.70	1.680	638.7	1028.2	21.14	1098.8	50.50	85.2	85.2	14.71	18.37	0.280	0.75
852	39	1.740	1427.3	1588.5	4.11	1.730	638.0	1054.1	21.75	1139.0	54.49	87.8	87.8	14.70	18.15	0.281	0.42
869	40	1.830	1471.8	1679.0	4.35	1.783	640.5	1082.5	22.12	1180.4	57.81	90.9	91.0	14.73	17.67	0.280	0.16
866	41	1.952	1501.8	1777.0	4.76	1.842	639.2	1109.3	22.63	1225.3	62.08	93.2	93.3	14.73	15.84	0.281	-0.15
$E^3$ Mixed Flow Cycle																	
773	71	1.361	1371.4	1179.8	2.61	1.419	510.0	763.3	17.98	816.2	31.09	72.7	72.7	14.24	25.36	0.282	2.86
774	72	1.419	1404.1	1269.1	2.80	1.476	509.5	802.5	19.12	862.1	34.96	75.6	75.5	14.24	24.89	0.283	2.35
775	73	1.497	1399.9	1356.3	3.19	1.517	509.2	828.9	19.73	902.2	38.26	77.8	77.8	14.24	25.04	0.283	1.95
798	74	1.559	1451.2	1444.8	3.37	1.586	494.6	856.4	21.67	935.5	43.33	79.9	79.9	14.47	11.23	0.282	1.41
799	75	1.625	1464.8	1513.7	3.58	1.636	498.5	886.4	22.36	973.1	46.70	82.1	82.2	14.48	10.87	0.282	1.09
802	76	1.707	1471.8	1586.9	3.88	1.684	502.4	913.6	22.78	1011.5	49.89	84.4	84.5	14.49	11.14	0.281	0.80
803	77	1.778	1501.5	1658.8	4.02	1.760	505.2	951.7	24.03	1052.9	54.65	88.0	88.2	14.48	11.81	0.283	0.41
804	78	1.861	1520.5	1728.8	4.34	1.783	508.5	964.5	23.85	1082.1	56.44	90.6	90.7	14.50	13.12	0.281	0.27
805	79	1.964	1543.3	1809.3	4.71	1.826	510.8	984.7	24.17	1119.2	59.80	92.7	92.8	14.50	13.12	0.281	0.01
$E^3$ Separate Flow Cycle																	
769	82	1.295	1269.0	1043.1	1.93	1.514	503.4	821.9	21.53	840.2	36.48	73.6	73.6	14.25	25.68	0.279	2.16
770	84	1.389	1285.1	1177.5	2.17	1.645	504.4	896.4	24.05	919.7	44.60	77.8	77.9	14.24	25.85	0.280	1.29
772	86	1.508	1322.1	1328.1	2.63	1.745	506.1	945.8	25.40	981.6	50.90	82.7	82.7	14.25	25.95	0.282	0.71

Table A-9. 22-Lobed Mixer with Short Fan Nozzle (Config: 3200), Simulated Flight  $M_F=0.28$ 

TOWER LOCATION=34. DEG  
SCALED AREA = 3078.0 sq inches  
FLIGHT VELOCITY = 315.0 ft/sec  
EXTRAPOLATION DISTANCE = 1500.0 ft

RDG	Test Point	$P_{r,p}$	$T_{t,p}^o R$	$V_{j,p}$ ft/sec	$W_p$ lb/sec	$P_{r,s}$	$T_{t,s}^o$ $R$	$V_{j,s}$ ft/sec	$W_s$ lb/sec	$V_{mix}$ ft/sec	$Fg_{tot}$ klb	EPNL dB	EPNLT dB	Pamb psi	$T_{amb}$ °F	$M_F$	$TH_{cor}$
High Bypass Mixed Flow Cycle																	
972	32	1.172	1166.8	788.6	1.79	1.288	508.7	653.0	15.44	667.1	21.27	66.5	67.0	14.46	40.08	0.280	4.50
973	33	1.217	1197.1	886.0	2.02	1.352	509.3	711.3	17.14	729.7	25.87	67.5	67.6	14.46	40.49	0.280	3.65
1005	34	1.305	1243.1	1046.4	2.55	1.416	642.1	854.3	16.48	880.0	30.99	73.8	73.8	14.56	44.51	0.281	2.87
1006	35	1.369	1286.1	1153.6	2.84	1.471	638.8	895.3	17.51	931.3	35.06	76.5	76.5	14.55	48.43	0.281	2.33
1007	36	1.461	1321.2	1278.5	3.16	1.565	637.1	959.0	19.18	1004.3	41.52	79.4	79.4	14.55	50.38	0.280	1.60
1008	37	1.560	1367.2	1403.0	3.52	1.640	639.9	1007.0	20.23	1065.6	46.81	82.3	82.3	14.55	51.38	0.273	1.08
1009	38	1.649	1401.9	1500.6	3.85	1.686	641.5	1034.0	20.67	1107.2	50.22	84.3	84.4	14.53	52.57	0.272	0.77
1010	39	1.730	1418.8	1575.7	4.13	1.730	639.4	1055.3	21.09	1140.6	53.22	86.8	86.8	14.53	52.47	0.274	0.52
1011	40	1.829	1462.6	1673.1	4.42	1.793	640.0	1087.1	21.76	1185.9	57.42	89.8	89.9	14.53	53.09	0.272	0.19
1012	41	1.944	1506.8	1775.2	4.78	1.836	642.8	1109.4	21.88	1228.8	60.61	92.3	92.4	14.53	53.30	0.274	-0.04
$E^3$ Mixed Flow Cycle																	
974	71	1.365	1375.5	1188.0	2.78	1.426	512.6	770.2	17.99	826.2	31.76	73.4	73.4	14.46	42.09	0.279	2.76
976	72	1.424	1398.1	1272.7	3.02	1.476	515.0	806.9	18.90	871.0	35.32	75.8	75.8	14.45	42.39	0.272	2.30
985	73	1.494	1413.0	1358.9	3.30	1.523	516.6	838.7	19.62	913.6	38.73	78.3	78.3	14.44	44.04	0.272	1.90
986	74	1.554	1440.8	1434.5	3.47	1.581	517.0	873.1	20.72	953.7	42.68	80.2	80.2	14.44	43.62	0.272	1.48
987	75	1.625	1446.1	1503.2	3.76	1.620	518.3	895.2	21.17	986.8	45.51	82.3	82.4	14.44	44.66	0.272	1.20
988	76	1.706	1468.6	1584.3	4.03	1.673	520.3	924.8	21.89	1027.3	49.27	84.4	84.4	14.44	45.29	0.272	0.86
989	77	1.778	1501.8	1658.4	4.23	1.717	517.4	943.2	22.52	1056.3	52.27	86.8	86.8	14.44	45.55	0.272	0.60
990	78	1.867	1525.4	1735.4	4.50	1.771	518.7	969.0	23.07	1094.1	55.80	90.2	90.2	14.44	46.52	0.271	0.32
991	79	1.973	1545.2	1816.0	4.85	1.808	519.9	986.2	23.18	1129.9	58.60	92.5	92.6	14.44	46.92	0.271	0.10

Table A-10. 22-Lobed Mixer with Long Fan Nozzle (Config: 3300), Simulated Flight  $M_F=0.28$ 

TOWER LOCATION=34. DEG  
SCALED AREA = 3078.0 sq inches  
FLIGHT VELOCITY = 315.0 ft/sec  
EXTRAPOLATION DISTANCE = 1500.0 ft

RDG	Test Point	$P_{r,p}$	$T_{t,p} \text{ } ^\circ R$	$V_{j,p}$ ft/sec	$W_p$ lb/sec	$P_{r,s}$	$T_{t,s} \text{ } ^\circ R$	$V_{j,s}$ ft/sec	$W_s$ lb/sec	$V_{mix}$ ft/sec	$F_{g_{tot}}$ k/lb	EPNL dB	EPNLT dB	Pamb psi	$T_{amb}$ $^{\circ}F$	$M_F$	$TH_{cor}$
High Bypass Mixed Flow Cycle																	
1031	32	1.168	1158.3	778.1	1.58	1.286	507.8	650.9	16.25	662.2	21.84	65.6	65.7	14.54	35.82	0.280	4.39
1032	33	1.220	1193.9	890.8	1.83	1.348	508.0	706.5	17.73	723.7	26.19	67.2	67.3	14.53	37.58	0.282	3.60
1053	34	1.321	1241.6	1069.7	2.47	1.428	642.0	863.8	17.50	889.3	32.86	74.4	74.4	14.66	27.58	0.278	2.61
1054	35	1.378	1284.7	1164.1	2.66	1.482	638.4	903.3	18.51	936.2	36.67	77.0	77.0	14.65	26.92	0.278	2.14
1055	36	1.457	1326.5	1276.7	2.92	1.556	639.0	924.5	19.64	996.2	41.59	79.9	79.9	14.65	27.28	0.280	1.59
1056	37	1.553	1375.7	1400.7	3.25	1.633	640.3	1003.1	20.78	1056.8	46.97	82.8	82.8	14.66	27.54	0.279	1.06
1057	38	1.653	1407.3	1507.0	3.65	1.692	638.0	1034.2	21.55	1102.8	51.42	84.9	85.0	14.65	28.09	0.280	0.67
1058	39	1.726	1423.3	1575.4	3.93	1.730	640.6	1056.2	21.76	1135.6	53.97	87.9	87.9	14.66	27.83	0.280	0.46
1060	40	1.842	1463.0	1682.6	4.31	1.791	641.9	1087.6	22.21	1184.3	58.11	90.4	90.4	14.67	27.97	0.279	0.14
1061	41	1.954	1504.4	1779.9	4.68	1.847	641.3	1113.2	22.73	1227.1	62.22	92.8	92.9	14.67	27.83	0.279	-0.16
$E^3$ Mixed Flow Cycle																	
1034	71	1.367	1373.1	1189.2	2.63	1.428	511.9	771.5	18.75	822.9	32.54	72.3	72.3	14.55	38.70	0.281	2.66
1035	72	1.418	1390.6	1261.5	2.82	1.469	513.4	800.8	19.49	859.1	35.46	74.6	74.6	14.55	38.17	0.281	2.28
1036	73	1.495	1406.2	1356.2	3.10	1.535	514.8	844.4	20.70	911.0	40.12	77.2	77.2	14.56	38.60	0.281	1.75
1037	74	1.559	1442.9	1440.9	3.35	1.572	517.6	868.2	21.11	946.6	42.83	79.3	79.4	14.56	39.60	0.280	1.46
1038	75	1.641	1459.5	1524.9	3.65	1.635	519.0	904.2	22.20	991.9	47.44	81.5	81.5	14.56	38.68	0.281	1.02
1039	76	1.709	1476.0	1591.2	3.84	1.684	520.6	930.3	22.77	1025.7	50.51	83.3	83.4	14.57	38.91	0.281	0.75
1040	77	1.785	1496.6	1661.2	4.04	1.747	520.0	959.3	23.66	1061.8	54.41	87.2	87.2	14.57	39.65	0.281	0.42
1041	78	1.866	1516.8	1730.3	4.33	1.785	518.5	974.8	23.99	1090.3	57.12	89.9	89.9	14.57	39.19	0.281	0.21
1042	79	1.958	1552.2	1810.9	4.66	1.807	523.0	988.6	23.82	1123.1	59.18	92.3	92.4	14.57	38.58	0.281	0.06

Table A-11. 22-Lobed Mixer with Hardwalled Long Fan Nozzle (Config: 3401), Simulated Flight  $M_f=0.28$ 

TOWER LOCATION=34. DEG  
SCALED AREA = 3078.0 sq inches  
FLIGHT VELOCITY = 315.0 ft/sec  
EXTRAPOLATION DISTANCE = 1500.0 ft

RDG	Test Point	$P_{r,p}$	$T_{t,p}^{\circ R}$	$V_{j,p}$ ft/sec	$W_p$ lb/sec	$P_{r,s}$	$T_{t,s}^{\circ R}$	$V_{j,s}$ ft/sec	$W_s$ lb/sec	$V_{mix}$ ft/sec	$F_{g,ot}$ klb	EPNL dB	EPNLT dB	Pamb psi	$T_{amb}$ °F	$M_f$	$TH_{cor}$
High Bypass Mixed Flow Cycle																	
891	32	1.172	1156.2	784.7	1.60	1.281	499.8	640.9	15.89	654.0	21.17	66.5	66.6	14.37	26.31	0.280	4.52
892	33	1.217	1195.2	885.5	1.80	1.345	499.8	698.7	17.65	716.0	25.77	67.0	67.2	14.37	27.31	0.278	3.67
871	34	1.324	1238.0	1071.3	2.46	1.433	639.4	866.4	17.64	891.5	33.15	74.8	74.8	14.71	20.24	0.280	2.58
872	35	1.377	1286.3	1163.8	2.65	1.486	638.7	905.9	18.63	938.0	36.94	77.4	77.4	14.71	22.25	0.280	2.11
873	36	1.466	1324.4	1285.5	2.99	1.566	639.3	961.1	19.96	1003.3	42.60	80.2	80.2	14.70	23.94	0.282	1.49
874	37	1.558	1370.4	1401.9	3.32	1.631	640.1	1001.6	20.80	1056.8	47.16	83.0	83.0	14.70	24.89	0.280	1.05
875	38	1.646	1407.7	1502.0	3.65	1.690	641.2	1035.6	21.56	1103.0	51.45	85.4	85.5	14.70	24.32	0.280	0.67
876	39	1.735	1425.0	1583.3	4.00	1.731	638.8	1055.2	21.86	1136.9	54.38	88.7	88.7	14.69	24.69	0.280	0.43
877	40	1.828	1457.8	1670.0	4.29	1.781	641.3	1082.6	22.19	1177.7	57.68	91.1	91.1	14.69	25.57	0.280	0.17
878	41	1.958	1506.4	1783.8	4.72	1.843	641.8	1111.7	22.63	1227.6	62.10	93.2	93.2	14.69	25.36	0.281	-0.15
$E^3$ Mixed Flow Cycle																	
894	71	1.362	1393.9	1191.4	2.54	1.426	502.3	762.9	18.69	814.2	31.98	72.3	72.3	14.38	28.23	0.280	2.73
896	72	1.424	1399.2	1273.4	2.84	1.469	504.6	794.0	19.41	855.2	35.21	75.1	75.1	14.39	26.66	0.281	2.32
897	73	1.489	1411.2	1352.5	3.08	1.521	507.1	829.8	20.32	898.6	38.90	77.1	77.1	14.40	26.55	0.280	1.88
898	74	1.558	1428.5	1432.2	3.36	1.561	507.7	853.6	20.84	934.0	41.83	79.2	79.2	14.40	25.63	0.280	1.57
905	75	1.632	1465.8	1520.3	3.47	1.659	503.7	902.6	22.86	984.0	47.93	82.1	82.2	14.43	20.70	0.280	0.98
906	76	1.710	1473.8	1590.3	3.74	1.715	504.5	930.5	23.61	1020.7	51.65	85.4	85.4	14.43	22.18	0.281	0.65
919	77	1.772	1485.0	1644.8	3.97	1.760	513.1	958.9	24.27	1055.4	55.15	88.8	88.8	14.59	10.85	0.280	0.37
918	78	1.863	1509.7	1724.2	4.29	1.805	510.2	975.8	24.66	1086.7	58.20	91.3	91.3	14.59	10.78	0.281	0.13
917	79	1.960	1534.4	1801.4	4.67	1.822	512.6	984.9	24.38	1116.2	59.99	93.0	93.1	14.59	8.89	0.281	0.00

Table A-12. 22-Lobed Mixer with Feltmetal Treated Long Fan Nozzle (Config: 3402), Simulated Flight  $M_F=0.28$ 

TOWER LOCATION=34. DEG  
SCALED AREA = 3078.0 sq inches  
FLIGHT VELOCITY = 315.0 ft/sec  
EXTRAPOLATION DISTANCE = 1500.0 ft

RDG	Test Point	$P_{r,p}$	$T_{t,p} \text{ } ^\circ\text{R}$	$V_{j,p} \text{ ft/sec}$	$W_p \text{ lb/sec}$	$P_{r,s}$	$T_{t,s} \text{ } ^\circ\text{R}$	$V_{j,s} \text{ ft/sec}$	$W_s \text{ lb/sec}$	$V_{mix} \text{ ft/sec}$	$F_{g_{tot}} \text{ klb}$	EPNL dB	EPNL dB	$T_{amb} \text{ } ^\circ\text{F}$	$M_F$	$TH_{cor}$	
High Bypass Mixed Flow Cycle																	
921	32	1.167	1173.7	781.0	1.52	1.285	496.8	642.8	16.31	654.6	21.60	69.3	14.57	14.17	0.279	4.44	
922	33	1.219	1194.8	890.1	1.74	1.367	497.6	714.5	18.55	729.5	27.38	70.7	14.57	15.33	0.280	3.41	
951	34	1.325	1236.1	1072.5	2.46	1.429	642.4	865.2	17.27	891.0	32.52	75.3	14.56	11.99	0.279	2.66	
952	35	1.375	1270.8	1153.7	2.59	1.486	640.7	907.4	18.32	937.9	36.29	78.2	14.57	14.26	0.282	2.18	
953	36	1.459	1308.7	1270.0	2.89	1.561	638.0	957.0	19.57	997.3	41.45	81.0	81.1	14.56	14.44	0.281	
954	37	1.557	1360.0	1395.7	3.27	1.630	640.2	1001.0	20.49	1055.4	46.39	83.6	83.7	14.56	15.16	0.282	
955	38	1.645	1408.4	1501.0	3.53	1.696	639.6	1037.9	21.34	1103.6	50.77	85.8	85.9	14.56	15.25	0.281	
956	39	1.746	1405.7	1580.7	4.04	1.732	643.1	1059.2	21.50	1141.7	53.95	88.1	88.2	14.56	15.74	0.281	
957	40	1.840	1464.5	1681.8	4.24	1.811	639.3	1095.1	22.62	1187.7	59.01	91.0	91.1	14.56	16.31	0.281	
958	41	1.959	1500.8	1781.1	4.67	1.845	640.6	1111.8	22.42	1227.3	61.51	93.4	93.5	14.56	16.58	0.280	
$E^3$ Mixed Flow Cycle																	
923	71	1.358	1393.0	1185.8	2.47	1.438	500.4	770.2	19.21	817.5	32.80	74.4	14.56	16.14	0.280	2.62	
925	72	1.435	1378.0	1276.1	2.87	1.492	503.2	808.5	20.15	866.8	36.92	76.7	14.55	17.11	0.280	2.11	
926	73	1.503	1400.9	1362.1	3.13	1.543	504.1	840.4	20.97	908.1	40.48	78.7	78.8	14.55	18.10	0.278	1.71
927	74	1.562	1428.8	1435.8	3.33	1.584	507.0	866.3	21.52	942.6	43.34	80.4	80.5	14.55	18.73	0.278	1.41
928	75	1.646	1449.7	1524.2	3.59	1.657	506.8	904.4	22.72	989.0	48.13	82.4	82.4	14.54	19.13	0.278	0.96
929	76	1.709	1469.5	1586.8	3.74	1.712	508.7	932.8	23.48	1022.7	51.51	84.3	84.4	14.54	20.16	0.278	0.66
930	77	1.781	1480.2	1649.1	3.96	1.768	511.3	960.9	24.19	1057.8	55.09	87.9	88.0	14.54	20.26	0.279	0.37
931	78	1.870	1516.5	1732.5	4.27	1.805	513.9	979.3	24.32	1091.7	57.73	91.0	91.1	14.54	19.62	0.278	0.17
932	79	1.982	1535.9	1815.9	4.76	1.821	515.0	986.7	24.00	1123.9	59.80	92.8	92.9	14.54	19.93	0.280	0.01

Table A-13. 22-Lobed Mixer with Astroquartz Treated Long Fan Nozzle (Config: 3403), Simulated Flight  $M_F=0.28$

TOWER LOCATION=34. DEG  
SCALED AREA = 3078.0 sq inches

RDG	Test Point	$P_{r,p}$	$T_{t,p}^{\circ R}$	$V_{j,p}$ ft/sec	$W_p$ lb/sec	$P_{r,s}$	$T_{t,s}^{\circ}$ $R$	$V_{j,s}$ ft/sec	$W_s$ lb/sec	$V_{mix}$ ft/sec	$Fg_{tot}$ klb	EPNL dB	EPNLT dB	Pamb psi	$T_{amb}$ °F	$M_F$	$TH_{cor}$
<b>High Bypass Mixed Flow Cycle</b>																	
1086	34	1.313	1246.6	1060.3	2.38	1.417	640.5	854.4	17.17	879.5	31.81	77.9	78.2	14.72	19.58	0.281	2.76
1088	36	1.455	1326.1	1274.1	2.88	1.555	642.9	956.8	19.55	997.6	41.41	82.0	82.0	14.71	22.33	0.283	1.61
1089	38	1.638	1410.9	1496.7	3.52	1.691	639.2	1034.5	21.42	1099.8	50.74	86.2	86.2	14.71	23.05	0.281	0.73
1090	39	1.741	1421.1	1585.6	3.99	1.731	640.3	1056.4	21.61	1138.9	53.96	87.6	87.7	14.70	23.59	0.282	0.46
1108	40	1.831	1467.8	1677.7	4.16	1.795	639.9	1087.9	22.02	1181.6	57.25	90.3	90.3	14.49	38.00	0.280	0.20
1109	41	1.950	1506.5	1778.6	4.58	1.840	642.5	1110.9	22.14	1225.4	60.58	92.6	92.7	14.49	39.58	0.281	-0.04
<b>E<sup>3</sup> Mixed Flow Cycle</b>																	
1092	72	1.414	1400.7	1260.9	2.72	1.478	524.2	815.6	19.53	870.1	35.82	79.3	79.5	14.72	25.90	0.280	2.24
1110	73	1.491	1418.0	1358.5	3.06	1.521	528.4	846.6	19.81	915.2	38.72	80.3	80.4	14.48	42.35	0.281	1.90
1111	75	1.634	1460.9	1519.1	3.58	1.615	526.8	900.3	21.20	989.6	45.37	83.3	83.3	14.47	42.51	0.281	1.21
1112	77	1.776	1501.8	1657.1	4.03	1.716	529.7	954.0	22.57	1060.4	52.19	85.9	85.9	14.47	43.30	0.280	0.61
1113	78	1.875	1515.4	1735.6	4.37	1.773	527.9	978.5	23.28	1098.1	56.17	88.4	88.4	14.47	43.59	0.280	0.29
1114	79	1.960	1557.2	1814.8	4.67	1.783	529.4	984.1	22.89	1124.8	57.34	91.3	91.3	14.47	43.39	0.281	0.20

Table A-14. Unique-Lobed Mixer with Standard Fan Nozzle & Internal Pylon (Config: 4110), Simulated Flight  $M_F=0.28$ 

TOWER LOCATION=34. DEG  
SCALED AREA = 3078.0 sq inches

FLIGHT VELOCITY = 315.0 ft/sec  
EXTRAPOLATION DISTANCE = 1500.0 ft

RDG	Test Point	$P_{r,p}$	$T_{t,p}^o R$	$V_{j,p}$	$W_p$	$P_{r,s}$	$T_{t,s}^o$	$V_{j,s}$	$W_s$	$V_{mix}$	$F_{g_{tot}}$	EPNL	EPNL T	$T_{amb}$	$M_F$	$TH_{cor}$	
High Bypass Separate Flow Cycle																	
232	14	1.213	1242.9	896.5	1.71	1.426	641.6	862.5	18.64	865.3	32.58	74.6	14.54	36.98	0.281	2.65	
238	15	1.271	1266.8	1004.2	1.97	1.507	636.4	919.5	20.42	926.9	38.40	77.2	77.3	14.54	37.38	0.281	1.94
242	16	1.342	1308.7	1128.0	2.23	1.591	635.7	974.1	21.93	988.2	44.17	79.9	79.9	14.54	39.30	0.281	1.33
246	17	1.414	1355.5	1241.1	2.44	1.675	635.2	1022.8	23.39	1043.4	49.86	82.3	82.4	14.53	40.07	0.281	0.80
185	18	1.498	1386.0	1350.5	2.77	1.722	638.5	1050.6	23.58	1082.2	52.76	84.9	85.0	14.44	51.81	0.277	0.56
250	18	1.501	1394.4	1357.0	2.78	1.725	639.6	1052.8	23.73	1084.7	53.19	84.7	84.7	14.53	40.93	0.280	0.52
292	18	1.510	1375.5	1357.3	2.82	1.728	637.5	1052.8	23.46	1085.5	52.77	84.1	84.2	14.32	60.67	0.278	0.56
189	19	1.578	1416.8	1445.3	3.05	1.778	637.8	1078.1	24.22	1119.1	56.46	87.6	87.6	14.44	52.42	0.279	0.26
253	20	1.682	1447.8	1553.3	3.42	1.841	636.6	1106.5	24.94	1160.3	60.86	91.3	91.5	14.53	40.02	0.281	-0.06
257	21	1.789	1511.8	1672.7	3.80	1.887	639.2	1128.7	25.15	1200.1	64.28	93.4	93.4	14.53	40.28	0.280	-0.30
286	21	1.790	1517.0	1675.8	3.69	1.903	640.3	1136.8	25.10	1205.9	64.22	92.6	92.6	14.35	58.14	0.279	-0.30
281	22	1.919	1557.3	1788.8	4.15	1.947	639.8	1154.2	25.15	1244.1	67.44	94.1	94.1	14.36	53.84	0.279	-0.51
High Mixed Separate Flow Cycle																	
233	34	1.323	1245.5	1073.7	2.62	1.419	639.5	855.0	17.66	883.2	33.14	74.8	74.8	14.54	36.86	0.281	2.58
241	35	1.373	1280.8	1155.2	2.76	1.482	644.0	906.6	18.94	938.3	37.67	77.3	77.3	14.54	39.26	0.281	2.02
245	36	1.458	1320.8	1274.9	3.06	1.564	638.1	958.9	20.49	1000.0	43.58	80.5	80.5	14.54	40.09	0.281	1.39
291	37	1.556	1364.8	1398.1	3.37	1.625	642.6	1000.1	20.92	1055.4	47.45	82.5	82.5	14.33	60.88	0.278	1.02
249	37	1.554	1364.1	1395.7	3.41	1.630	639.9	1001.2	21.40	1055.4	48.45	83.3	83.3	14.53	40.67	0.280	0.93
290	38	1.646	1376.6	1485.1	3.73	1.676	643.4	1029.7	21.51	1096.9	51.22	85.0	85.0	14.33	61.66	0.279	0.69
251	38	1.646	1402.9	1498.7	3.73	1.680	643.1	1031.9	21.86	1099.9	52.06	85.7	85.7	14.53	40.75	0.280	0.62
186	38	1.645	1404.4	1498.7	3.67	1.694	641.3	1037.7	22.08	1103.3	52.55	85.3	85.4	14.44	52.13	0.280	0.58
252	39	1.727	1423.2	1576.2	4.05	1.716	641.7	1050.1	22.31	1130.8	55.14	88.2	88.3	14.53	40.22	0.280	0.37
289	39	1.731	1430.3	1583.0	3.96	1.728	642.3	1056.7	22.15	1136.5	54.89	88.0	88.1	14.33	60.60	0.279	0.39
190	39	1.744	1422.2	1588.0	4.05	1.739	638.8	1059.2	22.56	1139.7	56.10	87.5	87.6	14.44	52.32	0.279	0.29
256	40	1.829	1456.1	1669.2	4.35	1.771	641.7	1078.0	22.82	1172.7	58.95	91.9	92.0	14.53	40.28	0.281	0.08
288	40	1.830	1463.1	1674.1	4.28	1.780	643.5	1083.8	22.69	1177.5	58.76	91.1	91.1	14.34	59.74	0.279	0.09
259	40	1.846	1457.5	1682.1	4.38	1.786	648.4	1090.8	22.84	1186.0	59.73	91.7	91.7	14.53	41.00	0.280	0.02
285	41	1.941	1503.7	1771.5	4.57	1.843	642.1	1111.9	23.22	1220.4	62.74	93.3	93.4	14.35	57.77	0.279	-0.19
260	41	1.955	1503.2	1779.5	4.65	1.854	641.2	1116.1	23.66	1225.0	64.17	94.1	94.1	14.52	40.70	0.280	-0.29

Table A-15. Unique-Lobed Mixer with Standard Fan Nozzle & Internal Pylon (Config: 4110), Simulated Flight  $M_F = 0.28$ 

TOWER LOCATION=90. DEG  
SCALED AREA = 3078.0 sq inches

RDG	Test Point	$P_{r,p}$	$T_{t,p}^{\circ R}$	$V_{j,p}$ ft/sec	$W_p$ lb/sec	$P_{r,s}$	$T_{t,s}^{\circ}$ $R$	$V_{i,s}$ ft/sec	$W_s$ lb/sec	$V_{mix}$ ft/sec	$F_{g_{tot}}$ klb	EPNL	EPNLT	Pamb psi	$T_{amb}$ °F	$M_F$	$TH_{cor}$
<b>High Bypass Separate Flow Cycle</b>																	
231	14	1.225	1240.1	917.5	1.79	1.441	643.3	875.8	19.00	879.4	33.82	74.6	74.7	14.54	36.36	0.281	2.49
239	15	1.273	1271.6	1010.2	1.98	1.504	637.3	918.1	20.30	926.3	38.18	77.5	77.5	14.54	37.93	0.281	1.96
243	16	1.345	1319.1	1135.6	2.26	1.582	639.0	970.9	21.62	986.5	43.58	80.4	80.4	14.54	39.71	0.281	1.39
247	17	1.416	1343.9	1238.0	2.46	1.669	638.3	1021.7	23.11	1042.5	49.33	83.1	83.2	14.53	39.52	0.281	0.85
179	18	1.507	1380.3	1356.4	2.85	1.720	638.4	1049.3	23.50	1082.5	52.76	85.5	85.6	14.45	49.85	0.276	0.56
188	19	1.587	1429.7	1460.0	3.10	1.787	636.6	1081.3	24.50	1123.8	57.39	88.0	88.1	14.44	53.12	0.278	0.19
254	20	1.680	1455.9	1555.9	3.40	1.842	637.2	1107.4	24.97	1161.2	60.95	91.7	91.7	14.53	40.05	0.280	-0.07
287	21	1.799	1516.1	1682.1	3.75	1.896	640.0	1133.6	24.89	1205.4	63.86	92.6	92.8	14.34	59.11	0.279	-0.27
282	22	1.921	1557.7	1790.5	4.15	1.950	639.6	1155.5	25.22	1245.2	67.66	94.2	94.3	14.35	55.53	0.280	-0.52
<b>High Bypass Mixed Flow Cycle</b>																	
234	34	1.324	1251.4	1078.2	2.62	1.419	640.2	855.5	17.66	884.2	33.18	75.2	75.2	14.54	37.14	0.281	2.57
240	35	1.381	1328.3	1187.4	2.76	1.485	645.5	910.0	18.93	945.3	37.94	77.5	77.6	14.54	39.42	0.281	1.99
244	36	1.452	1338.6	1276.7	3.02	1.553	638.3	952.0	20.22	994.2	42.75	80.8	80.9	14.54	39.67	0.281	1.47
248	37	1.566	1353.2	1401.0	3.46	1.640	636.3	1003.9	21.56	1058.9	49.01	83.5	83.5	14.53	40.62	0.281	0.88
187	38	1.651	1402.3	1503.2	3.70	1.699	640.6	1040.1	22.19	1106.2	52.98	85.8	85.8	14.44	52.14	0.280	0.54
191	39	1.727	1427.8	1578.3	3.98	1.724	638.8	1052.0	22.30	1131.6	55.01	88.3	88.4	14.44	53.03	0.278	0.38
255	40	1.837	1465.4	1680.6	4.34	1.786	643.4	1086.7	23.05	1180.8	59.83	91.6	91.7	14.53	40.95	0.281	0.01
284	41	1.943	1509.0	1776.0	4.53	1.858	641.1	1117.9	23.49	1224.3	63.45	93.4	93.6	14.35	57.03	0.280	-0.24

Table A-16. Unique-Lobed Mixer with Hardwalled Long Fan Nozzle & Internal Pylon (Config: 4111), Simulated Flight  $M_F=0.28$ 

TOWER LOCATION=34. DEG  
SCALED AREA = 3078.0 sq inches  
FLIGHT VELOCITY = 315.0 ft/sec  
EXTRAPOLATION DISTANCE = 1500.0 ft

RDG	Test Point	$P_{r,p}$	$T_{t,p}^o R$	$V_{j,p}$	$W_p$	$P_{r,s}$	$T_{t,s}^o$	$V_{j,s}$	$W_s$	$V_{mix}$	$F_{g_{tot}}$	EPNL	EPNLT	Pamb	$T_{amb}$	$M_F$	$TH_{cor}$
				lb/sec	ft/sec	lb/sec	R	ft/sec	lb/sec	ft/sec	klb	dB	dB	psi	°F		
<b>High Bypass Separate Flow Cycle</b>																	
482	14	1.217	1251.0	906.4	1.54	1.452	641.5	882.4	19.42	884.2	34.29	74.5	74.5	14.35	43.14	0.280	2.43
488	15	1.275	1286.0	1019.0	1.78	1.525	638.5	933.7	20.84	940.5	39.36	76.6	76.6	14.36	41.99	0.282	1.83
492	16	1.338	1310.8	1122.2	2.05	1.583	635.3	969.2	21.80	982.3	43.34	79.2	79.2	14.36	42.38	0.282	1.41
510	17	1.417	1357.3	1244.7	2.34	1.674	640.5	1026.6	23.65	1046.2	50.29	82.7	82.7	14.61	19.49	0.283	0.77
520	18	1.503	1392.3	1357.9	2.70	1.728	637.7	1052.8	24.26	1083.4	54.05	85.4	85.4	14.62	19.14	0.281	0.45
524	19	1.581	1419.2	1449.3	2.98	1.780	638.7	1079.7	24.75	1119.4	57.42	88.4	88.4	14.63	21.50	0.281	0.19
528	20	1.669	1464.7	1552.0	3.25	1.836	638.5	1105.9	25.27	1156.8	61.03	91.6	91.7	14.63	22.60	0.282	-0.07
532	21	1.791	1510.6	1673.2	3.66	1.904	639.8	1136.6	25.73	1203.3	65.41	93.5	93.5	14.62	21.74	0.281	-0.38
536	22	1.902	1550.7	1773.9	4.04	1.954	638.4	1155.9	26.04	1239.0	68.95	94.8	94.9	14.62	21.53	0.281	-0.60
<b>High Bypass Mixed Flow Cycle</b>																	
483	34	1.318	1233.5	1061.2	2.48	1.425	636.6	857.9	17.91	882.7	33.31	73.9	74.0	14.35	42.48	0.281	2.56
491	35	1.368	1285.1	1151.9	2.60	1.487	640.0	908.0	19.10	937.2	37.62	76.5	76.6	14.36	42.04	0.283	2.03
495	36	1.457	1314.8	1270.5	2.93	1.558	641.3	957.4	20.18	997.1	42.64	79.7	79.7	14.37	43.19	0.283	1.48
512	37	1.559	1345.8	1390.3	3.38	1.641	635.7	1003.9	22.00	1055.4	49.55	83.3	83.3	14.62	19.08	0.282	0.83
521	38	1.645	1413.9	1503.9	3.63	1.694	639.2	1036.1	22.60	1100.9	53.42	86.1	86.1	14.62	21.62	0.282	0.50
525	39	1.727	1432.3	1581.3	3.97	1.720	640.2	1050.6	22.66	1129.7	55.65	88.9	88.9	14.63	21.78	0.282	0.33
531	40	1.826	1464.8	1672.2	4.27	1.770	644.4	1079.7	22.97	1172.6	59.07	91.5	91.5	14.62	21.63	0.281	0.07
535	41	1.963	1507.3	1507.3	4.66	1.853	641.8	1116.2	23.83	1225.9	64.62	94.0	94.0	14.62	21.42	0.281	-0.32
<b>E<sup>3</sup> Mixed Flow Cycle</b>																	
570	71	1.367	1364.1	1185.6	2.75	1.402	532.1	766.8	18.56	820.8	32.35	72.7	72.7	14.54	51.89	0.280	2.68
572	73	1.493	1409.6	1356.3	3.23	1.499	531.8	835.5	20.46	906.5	39.73	77.5	77.6	14.54	52.73	0.281	1.79
575	75	1.633	1446.0	1510.8	3.71	1.600	534.1	898.3	22.20	985.9	47.26	81.8	81.8	14.55	52.76	0.279	1.04
576	77	1.776	1500.8	1656.7	4.08	1.716	536.5	960.0	23.99	1061.3	55.12	86.1	86.2	14.55	52.95	0.280	0.37
579	79	1.973	1554.9	1822.0	4.68	1.813	537.0	1004.3	24.89	1133.6	62.01	92.9	92.9	14.55	52.96	0.279	-0.14

Table A-17. Unique-Lobed Mixer with Feltmetal Treated Long Fan & Internal Pylon (Config: 4112), Simulated Flight  $M_F=0.28$ 

TOWER LOCATION=34. DEG  
SCALED AREA = 3078.0 sq inches  
FLIGHT VELOCITY = 315.0 ft/sec  
EXTRAPOLATION DISTANCE = 1500.0 ft

RDG	Test Point	$P_{r,p}$	$T_{t,p}^o R$	$V_{j,p}$ ft/sec	$W_p$ lb/sec	$P_{r,s}$	$T_{t,s}^o$ $R$	$V_{j,s}$ ft/sec	$W_s$ lb/sec	$V_{mix}$ ft/sec	$F_{g_{tot}}$ klb	EPNL dB	EPNL T dB	Pamb psi	$T_{amb}$ °F	$M_F$	$TH_{cor}$
High Bypass Separate Flow Cycle																	
325	14	1.219	1244.7	907.5	1.60	1.433	639.9	866.3	18.81	869.5	32.84	73.8	74.0	14.35	54.78	0.281	2.62
360	15	1.273	1281.6	1014.1	1.79	1.510	640.0	924.5	20.65	931.7	38.69	76.7	77.0	14.56	47.97	0.281	1.91
419	16	1.341	1311.7	1126.9	2.05	1.582	635.6	968.4	21.77	982.1	43.28	79.4	79.5	14.46	42.96	0.281	1.42
423	17	1.409	1345.1	1230.3	2.25	1.667	638.8	1021.1	23.19	1039.6	48.91	81.5	81.7	14.46	44.87	0.281	0.89
407	18	1.507	1375.4	1353.7	2.72	1.727	638.2	1052.6	24.02	1083.2	53.58	83.7	83.8	14.57	49.42	0.281	0.49
403	19	1.582	1421.3	1451.8	2.98	1.773	637.3	1075.1	24.45	1116.0	56.64	86.2	86.3	14.56	49.70	0.281	0.25
398	20	1.667	1453.4	1543.7	3.24	1.832	638.3	1103.6	25.02	1154.0	60.33	90.0	90.1	14.56	49.28	0.281	-0.02
394	21	1.796	1516.4	1680.6	3.71	1.890	635.9	1127.4	25.38	1197.9	64.46	92.6	92.6	14.56	48.24	0.281	-0.31
390	22	1.917	1557.9	1788.1	4.11	1.944	640.5	1153.6	25.56	1241.6	68.17	93.9	94.0	14.57	44.92	0.280	-0.55
High Bypass Mixed Flow Cycle																	
326	34	1.321	1224.6	1062.1	2.50	1.414	641.9	852.7	17.34	879.1	32.26	73.9	74.0	14.35	54.32	0.281	2.70
361	35	1.380	1283.0	1165.2	2.70	1.481	638.0	902.4	19.05	935.0	37.62	76.7	76.9	14.56	47.50	0.281	2.03
422	36	1.465	1323.0	1283.6	2.96	1.566	640.0	961.7	20.37	1002.5	43.27	79.8	79.9	14.46	44.56	0.281	1.42
415	37	1.559	1367.1	1402.1	3.38	1.610	641.0	990.2	20.99	1047.4	47.22	82.3	82.4	14.56	50.07	0.282	1.04
406	38	1.653	1392.5	1499.1	3.66	1.695	638.0	1035.8	22.36	1101.0	53.02	84.8	84.8	14.56	49.78	0.281	0.54
401	39	1.732	1448.0	1593.6	3.88	1.742	642.7	1064.2	22.81	1141.1	56.34	87.1	87.2	14.56	49.72	0.281	0.27
397	40	1.830	1463.5	1674.6	4.22	1.792	640.9	1087.4	23.27	1177.5	59.88	90.6	90.8	14.56	49.31	0.281	0.01
393	41	1.945	1489.2	1765.1	4.60	1.840	644.4	1112.7	23.49	1219.5	63.38	93.1	93.2	14.56	48.29	0.281	-0.24
$E^3$ Mixed Flow Cycle																	
601	71	1.368	1365.0	1186.5	2.68	1.403	527.6	764.6	18.21	818.7	31.64	72.9	72.9	14.33	59.40	0.275	2.78
602	73	1.493	1403.3	1353.3	3.17	1.498	529.7	833.2	20.03	904.2	38.81	77.8	77.9	14.33	60.09	0.277	1.89
605	75	1.639	1443.4	1514.2	3.66	1.603	535.5	901.0	21.70	989.5	46.41	81.1	81.2	14.33	60.46	0.279	1.11
606	77	1.773	1486.7	1646.8	4.04	1.703	538.2	955.2	23.17	1057.9	53.26	85.0	85.0	14.33	61.13	0.279	0.52
609	79	1.962	1552.3	1813.5	4.59	1.793	530.8	989.9	24.15	1121.3	59.62	89.4	89.5	14.33	61.45	0.279	0.03

Table A-18. Confluent Mixer (Exit Area = 45.7 in<sup>2</sup>) with Standard Fan (Config: V1 of Task A), Simulated Flight M<sub>F</sub>=0.28  
 TOWER LOCATION=34. DEG  
 EXTRAPOLATION DISTANCE = 1500.0 ft  
 FLIGHT VELOCITY = 315.0 ft/sec  
 SCALED AREA = 3078.0 sq inches

RDG	Test Point	P <sub>r,p</sub>	T <sub>t,p</sub> <sup>o</sup> R	V <sub>j,p</sub>	W <sub>p</sub>	P <sub>r,s</sub>	T <sub>t,s</sub> <sup>o</sup> R	V <sub>j,s</sub>	W <sub>s</sub>	V <sub>mix</sub>	F <sub>g<sub>tot</sub></sub>	EPNL	EPNL T	Pamb	T <sub>amb</sub>	M <sub>F</sub>	TH <sub>cor</sub>
<b>High Bypass Separate Flow Cycle</b>																	
1499	16	1.365	1318.2	1162.6	0.80	1.597	641.0	981.8	22.57	988.0	48.33	78.7	14.52	47.60	0.282	0.94	
1500	18	1.508	1400.8	1367.9	1.27	1.722	639.4	1051.4	24.26	1067.1	57.01	82.9	83.0	14.52	50.70	0.283	0.22
1501	19	1.580	1431.6	1454.9	1.65	1.762	639.7	1071.9	24.53	1096.0	60.05	84.7	84.8	14.54	51.39	0.279	0.00
1502	20	1.679	1447.4	1550.6	2.00	1.829	638.6	1102.6	25.24	1135.4	64.74	86.9	87.0	14.53	51.10	0.282	-0.33
1503	21	1.787	1516.3	1673.2	2.39	1.903	637.6	1134.4	26.14	1179.6	70.46	89.6	89.6	14.52	51.34	0.283	-0.70
1505	22	1.920	1550.9	1785.8	2.81	1.953	640.2	1157.3	26.26	1218.1	74.13	92.5	92.6	14.52	51.22	0.281	-0.92
<b>High Bypass Mixed Flow Cycle</b>																	
1476	36	1.465	1330.4	1287.9	1.85	1.563	640.5	960.0	20.31	987.4	45.80	78.9	78.9	14.52	48.93	0.282	1.17
1477	37	1.565	1337.3	1391.5	2.16	1.645	639.3	1009.0	21.63	1043.7	51.99	82.2	82.3	14.52	50.47	0.283	0.62
1478	38	1.647	1432.9	1516.0	2.38	1.696	638.6	1037.0	22.31	1083.2	55.99	84.4	84.5	14.52	50.79	0.280	0.30
1479	39	1.730	1434.8	1585.0	2.65	1.734	640.6	1058.5	22.65	1113.8	59.00	86.6	86.7	14.52	50.56	0.280	0.07
1480	40	1.844	1455.6	1679.5	3.09	1.780	639.8	1080.7	23.07	1151.3	63.05	89.8	89.9	14.52	50.69	0.280	-0.22
1481	41	1.956	1503.9	1780.9	3.33	1.850	641.5	1114.7	24.00	1195.9	68.41	92.7	92.8	14.52	50.46	0.280	-0.57
<b>E<sup>3</sup> Mixed Flow Cycle</b>																	
1488	75	1.646	1433.3	1515.2	2.62	1.619	530.9	905.5	22.54	969.0	51.05	83.3	83.3	14.53	48.61	0.280	0.70
1489	76	1.699	1465.1	1577.1	2.71	1.674	529.1	932.8	23.63	999.2	55.11	85.5	85.5	14.53	49.67	0.279	0.37
1490	77	1.771	1495.3	1649.4	2.83	1.723	526.2	953.9	24.47	1026.0	58.62	87.9	88.0	14.53	50.00	0.282	0.10
1491	78	1.866	1518.2	1730.7	3.18	1.771	526.4	976.2	25.11	1061.1	62.85	91.6	91.7	14.52	50.31	0.282	-0.20
1492	79	1.975	1538.5	1813.3	3.53	1.796	527.6	988.0	25.19	1089.4	65.49	94.4	94.6	14.53	50.38	0.281	-0.38

Table A-19. 12-Lobed Mixer (Exit Area = 45.7 in<sup>2</sup>) with Standard Fan (Config: F9B of Task A), Simulated Flight M<sub>F</sub>=0.28  
 TOWER LOCATION=34. DEG  
 SCALED AREA = 3078.0 sq inches  
 FLIGHT VELOCITY = 315.0 ft/sec  
 EXTRAPOLATION DISTANCE = 1500.0 ft

RDG	Test Point	P <sub>r,p</sub>	T <sub>t,p</sub> <sup>o</sup> R	V <sub>i,p</sub>	W <sub>p</sub>	P <sub>r,s</sub>	T <sub>t,s</sub> <sup>o</sup> R	V <sub>j,s</sub>	W <sub>s</sub>	V <sub>mix</sub>	F <sub>g<sub>tot</sub></sub>	EPNL	EPNLT	Pamb	T <sub>amb</sub>	M <sub>F</sub>	TH <sub>cor</sub>
<b>High Bypass Separate Flow Cycle</b>																	
1434	15	1.305	1275.5	1060.0	0.70	1.522	637.1	930.4	17.86	935.3	36.34	75.7	14.47	51.37	0.281	2.18	
1437	16	1.344	1321.3	1135.6	0.69	1.590	636.1	974.1	19.18	979.7	40.74	78.1	78.3	14.45	51.75	0.282	1.68
1439	17	1.420	1359.6	1249.6	0.97	1.660	636.9	1015.6	19.96	1026.4	44.96	80.7	80.8	14.44	51.70	0.281	1.25
1442	18	1.518	1385.3	1371.0	1.46	1.724	639.3	1051.9	20.33	1073.4	48.96	82.3	82.4	14.43	51.08	0.282	0.88
1444	19	1.590	1436.2	1466.8	1.65	1.767	637.5	1072.5	20.62	1101.7	51.35	83.4	83.4	14.42	51.33	0.282	0.68
1462	20	1.680	1447.7	1551.6	1.90	1.832	637.2	1102.9	21.46	1139.3	55.70	85.9	85.9	14.55	43.03	0.280	0.32
1464	21	1.781	1492.2	1655.8	2.25	1.900	636.2	1131.8	22.11	1180.2	60.20	88.1	88.2	14.55	44.29	0.282	-0.01
1466	22	1.927	1522.1	1773.7	2.87	1.941	644.9	1156.7	21.81	1228.4	63.46	89.7	89.8	14.55	45.20	0.281	-0.24
<b>High Bypass Mixed Flow Cycle</b>																	
1435	34	1.321	1232.0	1064.2	1.40	1.422	639.2	857.5	14.88	875.3	29.82	73.0	73.1	14.47	51.89	0.280	3.04
1436	35	1.382	1267.7	1161.5	1.61	1.482	639.5	903.8	15.87	927.5	33.93	75.0	75.2	14.46	51.65	0.281	2.48
1438	36	1.462	1315.4	1277.1	1.77	1.565	640.6	961.7	17.18	991.2	39.32	78.2	78.4	14.44	51.85	0.283	1.84
1441	37	1.559	1358.2	1397.5	2.03	1.644	636.8	1006.7	18.23	1045.8	44.34	81.0	81.1	14.44	51.66	0.281	1.31
1443	38	1.650	1398.1	1499.7	2.37	1.685	640.2	1032.5	18.45	1085.7	47.34	83.2	83.3	14.44	51.53	0.280	1.03
1445	39	1.737	1419.2	1581.5	2.68	1.728	638.0	1053.0	18.80	1118.9	50.31	84.6	84.7	14.43	51.52	0.279	0.76
1463	40	1.841	1460.4	1680.2	3.04	1.789	639.5	1084.6	19.56	1164.8	55.11	87.1	87.2	14.55	44.24	0.281	0.37
1465	41	1.947	1496.3	1770.8	3.24	1.843	642.3	1112.4	19.94	1204.4	58.44	89.3	89.3	14.54	44.32	0.283	0.11
<b>E<sup>3</sup> Mixed Flow Cycle</b>																	
1419	72	1.422	1397.2	1270.1	1.85	1.462	529.3	808.7	16.56	854.9	32.93	73.3	73.6	14.54	49.35	0.280	2.61
1420	73	1.496	1415.1	1362.4	2.09	1.517	528.8	844.7	17.47	900.1	36.85	76.1	76.1	14.53	50.41	0.282	2.12
1422	74	1.561	1431.5	1437.0	2.29	1.564	528.7	872.9	18.18	936.0	40.11	78.0	78.2	14.51	51.33	0.282	1.75
1423	75	1.629	1444.3	1506.2	2.45	1.621	530.6	906.5	19.10	974.7	43.98	80.2	80.5	14.51	51.25	0.282	1.35
1426	76	1.706	1479.8	1590.6	2.67	1.664	534.6	932.5	19.42	1012.1	46.81	82.3	82.6	14.50	51.78	0.281	1.08
1428	77	1.774	1497.6	1653.2	2.82	1.715	531.8	955.5	20.29	1040.8	50.37	83.9	84.0	14.51	51.82	0.279	0.76
1431	78	1.864	1513.0	1726.5	3.14	1.747	534.1	972.2	20.23	1073.6	52.53	86.1	86.2	14.48	51.25	0.281	0.58
1432	79	1.969	1533.5	1806.3	3.47	1.775	536.2	987.2	20.27	1106.9	55.00	88.4	88.5	14.47	52.02	0.282	0.38
<b>E<sup>3</sup> Separate Flow Cycle</b>																	
1415	82	1.310	1256.3	1059.2	0.70	1.517	517.0	835.2	19.70	842.9	36.00	73.0	73.0	14.55	45.67	0.280	2.22
1416	84	1.401	1253.5	1177.9	1.11	1.609	523.6	894.2	20.95	908.4	41.95	76.6	76.7	14.54	49.77	0.282	1.55
1421	86	1.506	1308.0	1319.6	2.05	1.569	528.6	875.9	18.77	919.6	40.08	76.4	76.6	14.52	50.75	0.283	1.75

## APPENDIX B

### DEVELOPMENT OF NOISE PREDICTION CODE FOR INTERNAL MIXER NOZZLE SYSTEMS

The problems involved in the design of the exhaust nozzle system for large subsonic aircraft engines include tradeoffs between performance of the various components to obtain the best overall economic performance in the customer's aircraft. Further complications occur when noise considerations are important, as they now are for both civil and military aircrafts. To facilitate the complicated trades required in the design process, relatively simple and easy to use aerodynamic and acoustic prediction methods are needed to link with engine cycle and mission analysis. Thus, a semi-empirical method for predicting the noise from internal mixer nozzle systems is developed utilizing the experimental results obtained in the current task. J. R. Stone and B. J. Clark of Modern Technologies Corporation, Aerospace Propulsion Division perform this work for GE Aircraft Engines as subcontractor.

There are three noise-generating regions and mechanisms, shown in Figure B-1, are considered in the current methodology. The first source region is from the mixing plane of the nozzle exit plane. The internal region is characterized by intense small scale mixing, which produces high frequency noise. The second source region, the premerged, extends from the nozzle exit plane to a distance where the primary and secondary flow regions can no longer be distinguished. For extremely long nozzles the premerged region may approach the fully mixed limit, but because of weight considerations this is unlikely to occur in practice. The premerged region is characterized by residual elements of the primary and secondary flows mixing with each other and the ambient air at small to moderate length scales, producing mid-to-high frequency noise. The third region, the merged, extends downstream with significant low frequency noise generated downstream for a distance of several nozzle exit diameters. The detail formulation of the method and the results are presented in a report, "Development of a Noise Prediction Code for Internal Mixer Nozzle System," by J. R. Stone and B. J. Clark, 1997.

Typical results for the confluent mixer with standard fan nozzle are shown in Figures B-2 through B-4. Similar results for the 22-lobed mixer with standard fan nozzle are shown in Figures B-5 through B-8. The test points and reading numbers (i.e., RDG) referred in the figures are listed in Tables 2 through 4 of main text and tables from the Appendix A, respectively. Following observations are made on the basis of the results presented here and the results not shown here;

- Premerged noise is predicted reasonably well, but there appear to be cycle effects, especially for the confluent mixer nozzles, which may imply that the degree of mixing should be related to cycle conditions as well as the geometry. The internal mixing noise is also significantly under-predicted
- For the lobed mixers, merged and premerged predictions agree quite well with the experimental data in all cases, but the internal mixing noise is greatly under-predicted and the peak frequency is far from predicted.

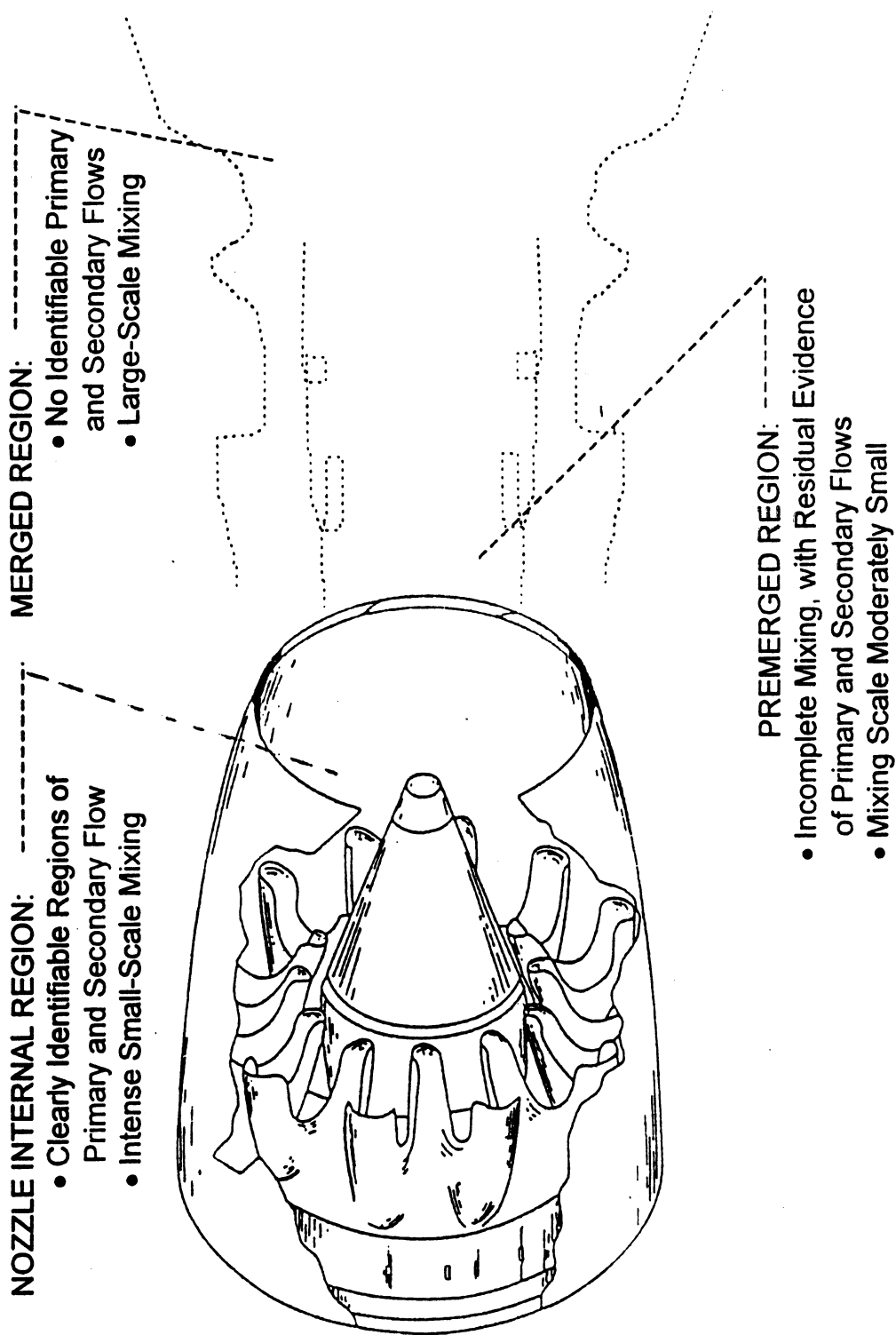


Figure B-1. Internal mixer nozzle noise generating regions and mechanisms.

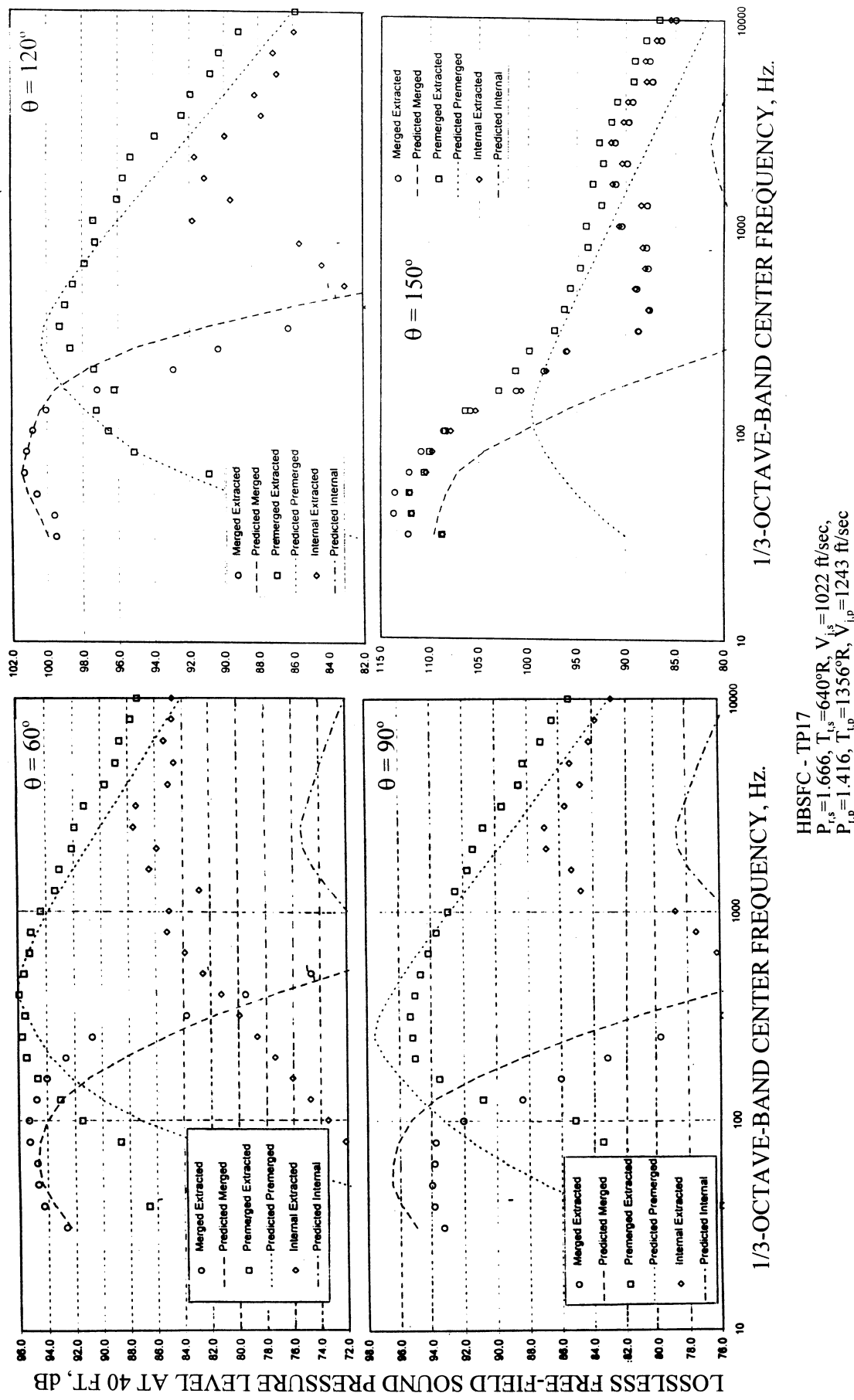


Figure B-2. Comparison of experimental/extracted and predicted spectra for confluent mixer with standard fan nozzle for High Bypass Separated Flow Cycle, Nominal  $V_{\text{mix}} = 1055 \text{ ft/sec}$  (TP17),  $M_F = 0.28$  (RDG. 728).

HBSFC - TP17  
 $P_{r,s} = 1.666$ ,  $T_{t,s} = 640^\circ\text{R}$ ,  $V_i^s = 1022 \text{ ft/sec}$ ,  
 $P_{i,p} = 1.416$ ,  $T_{i,p} = 1356^\circ\text{R}$ ,  $V_{j,p} = 1243 \text{ ft/sec}$

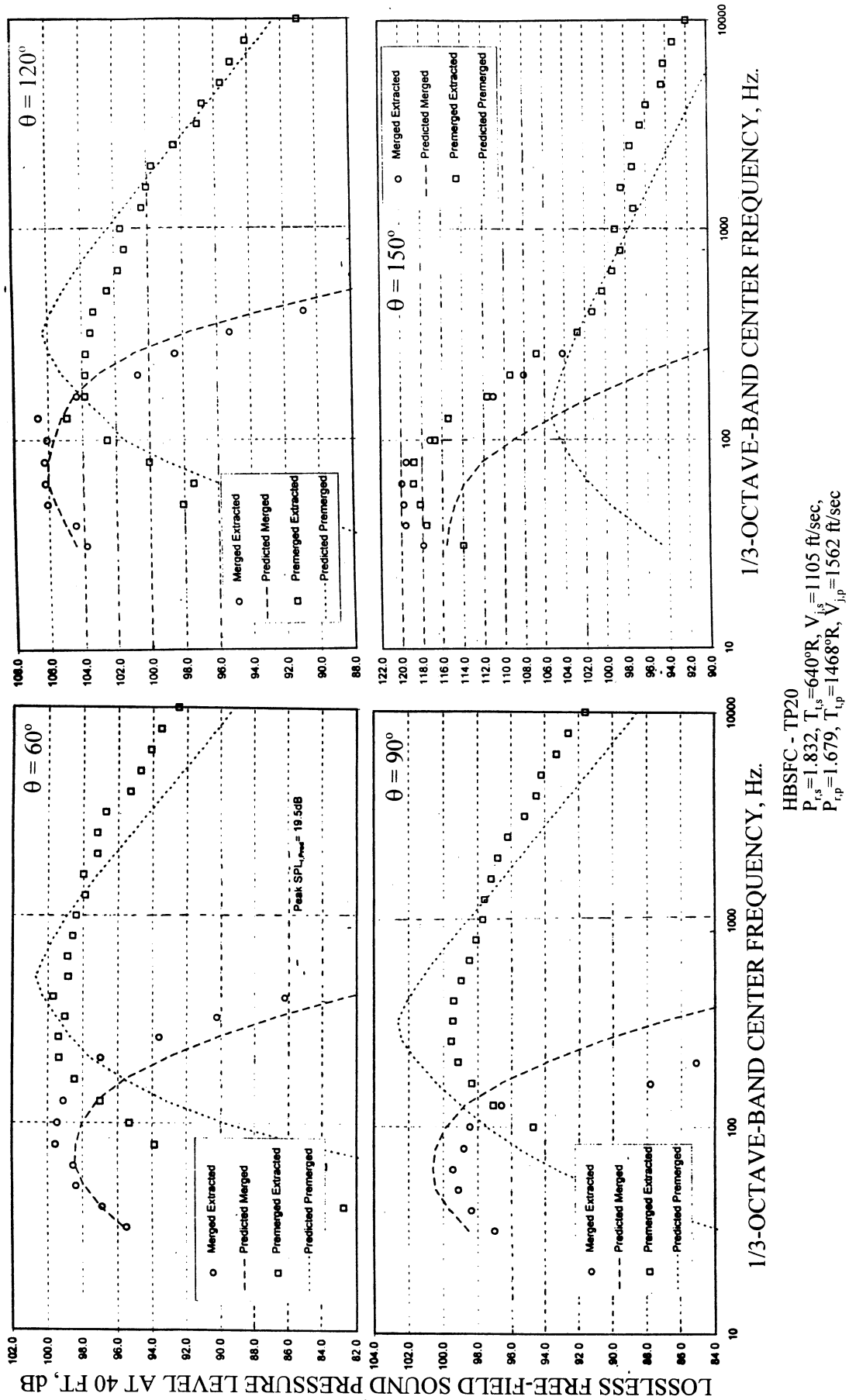


Figure B-3. Comparison of experimental/extracted and predicted spectra for confluent mixer with standard fan nozzle for High Bypass Separated Flow Cycle, Nominal  $V_{\text{mix}} = 1180 \text{ ft/sec}$  (TP20),  $M_F = 0.28$  (RDG. 740).

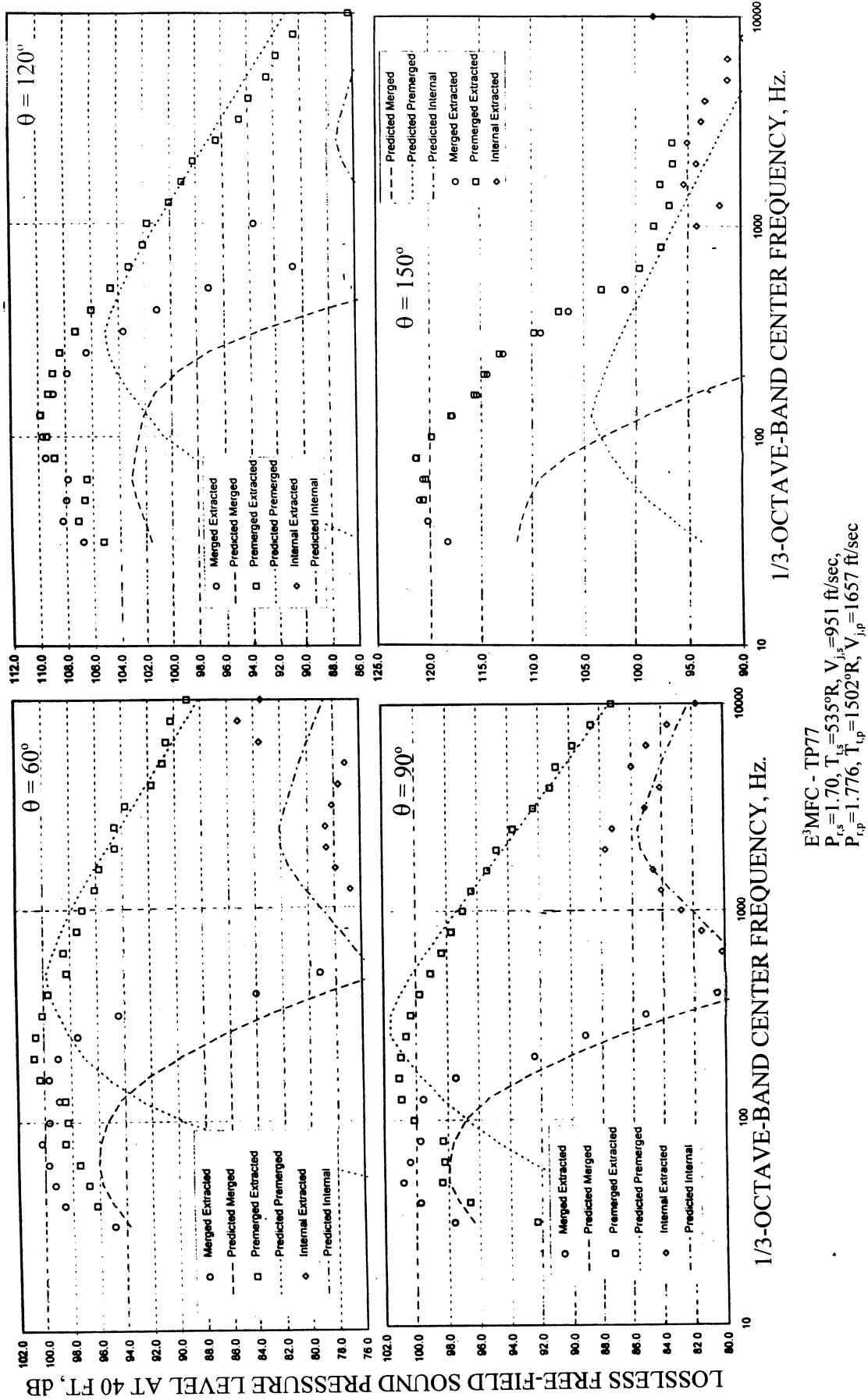


Figure B-4. Comparison of experimental/extracted and predicted spectra for confluent mixer with standard fan nozzle for E<sup>3</sup> Mixed Flow Cycle, Nominal  $V_{mix} = 1071 \text{ ft/sec}$  (TP77),  $M_F = 0.28$  (RDG. 695).

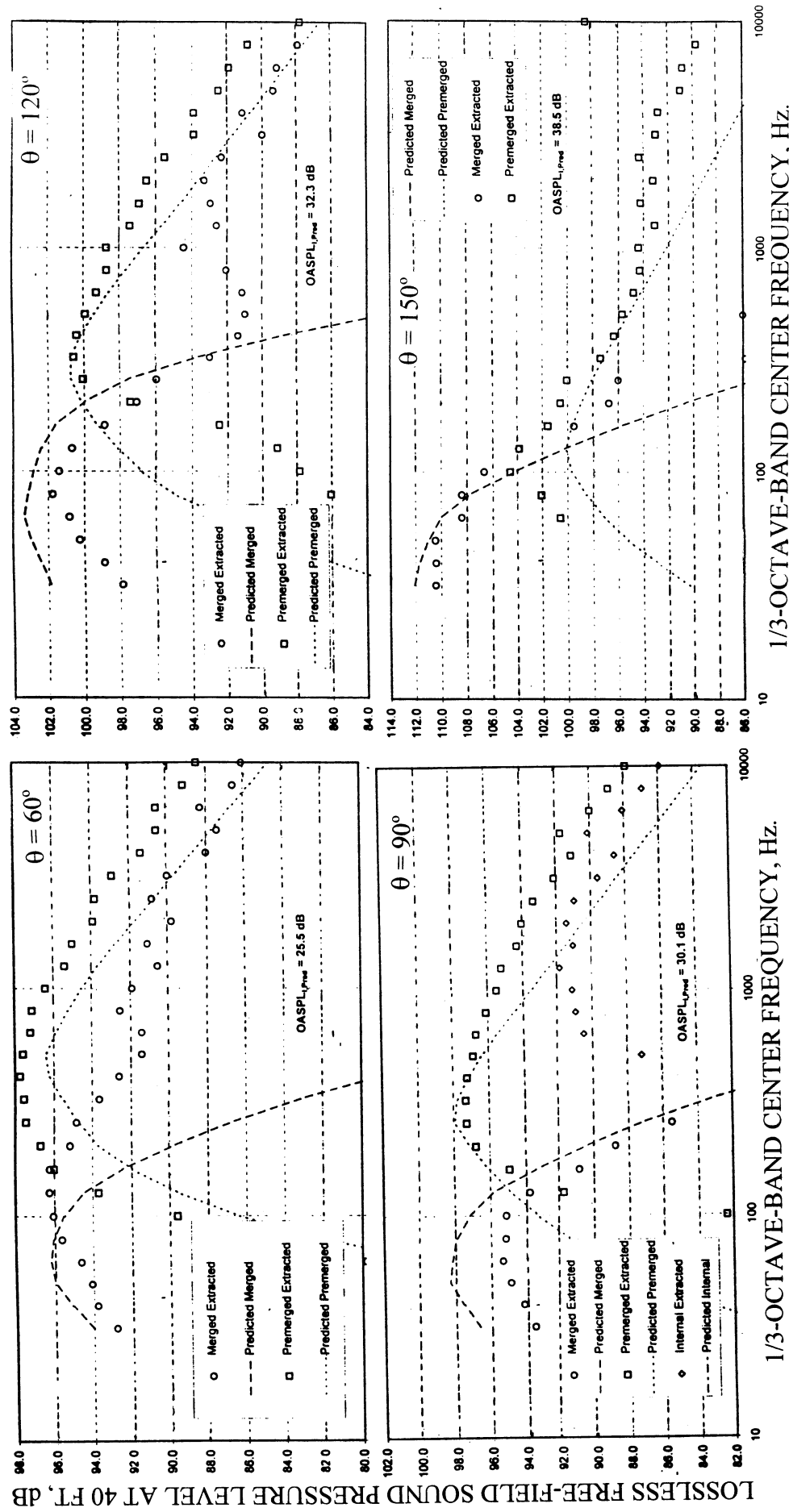
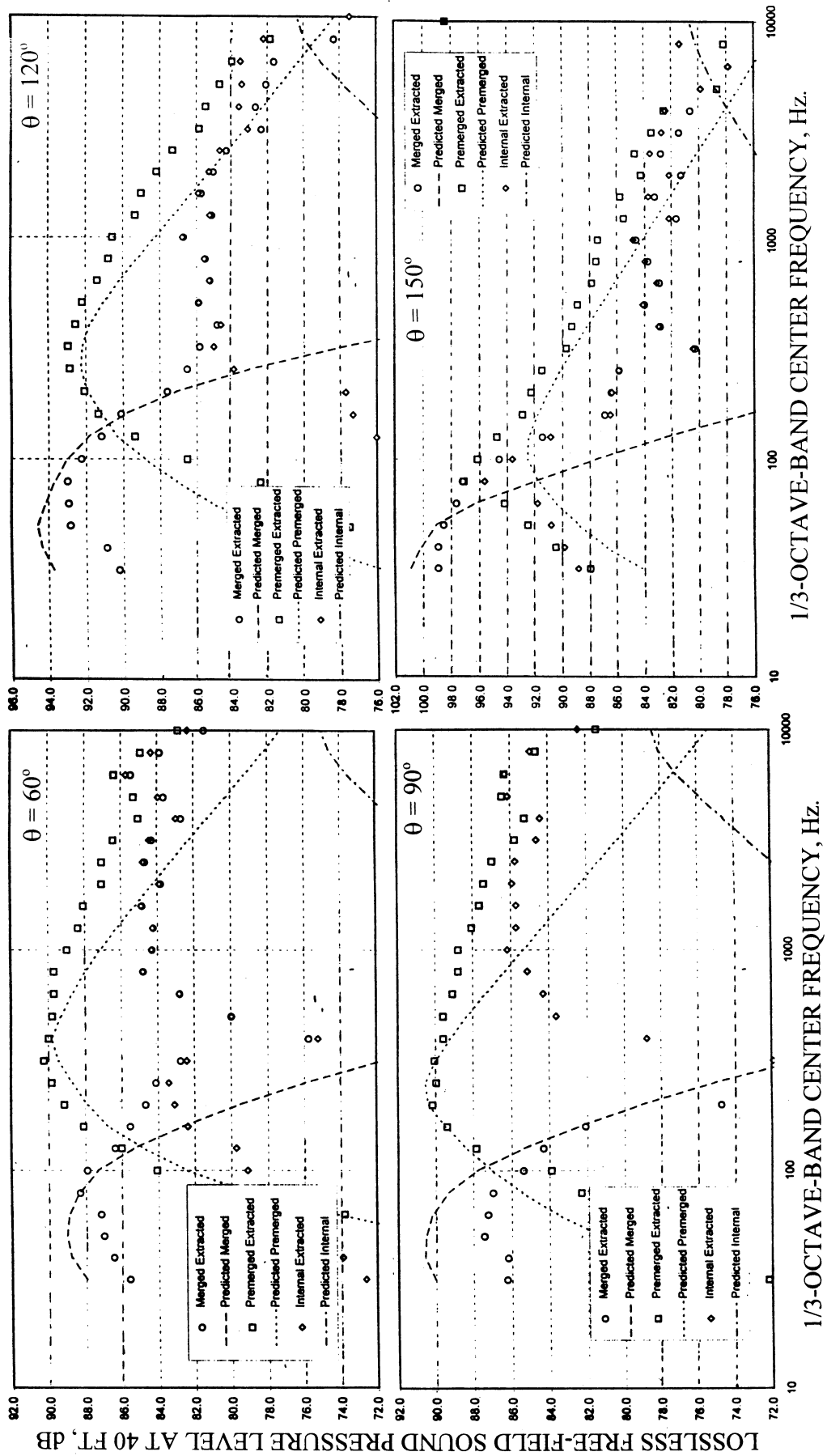
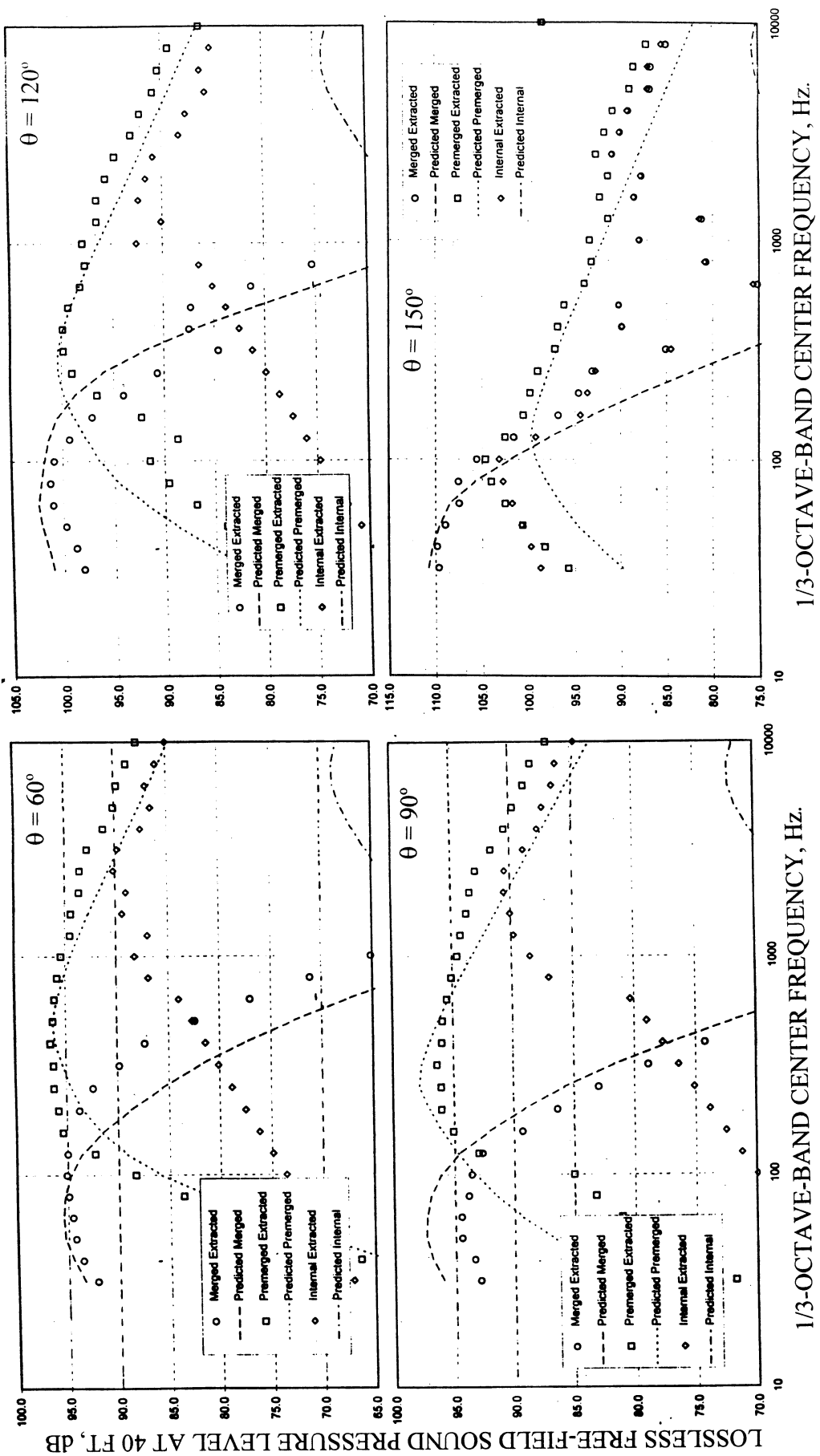


Figure B-5. Comparison of experimental/extracted and predicted spectra for confluent mixer with standard fan nozzle for equal fan and core pressure and temperature (Mixed Condition of Conic Nozzle, TP18), Nominal  $V_{\text{mix}} = 1105 \text{ ft/sec}$ ,  $M_F = 0.28$  (RDG. 747).



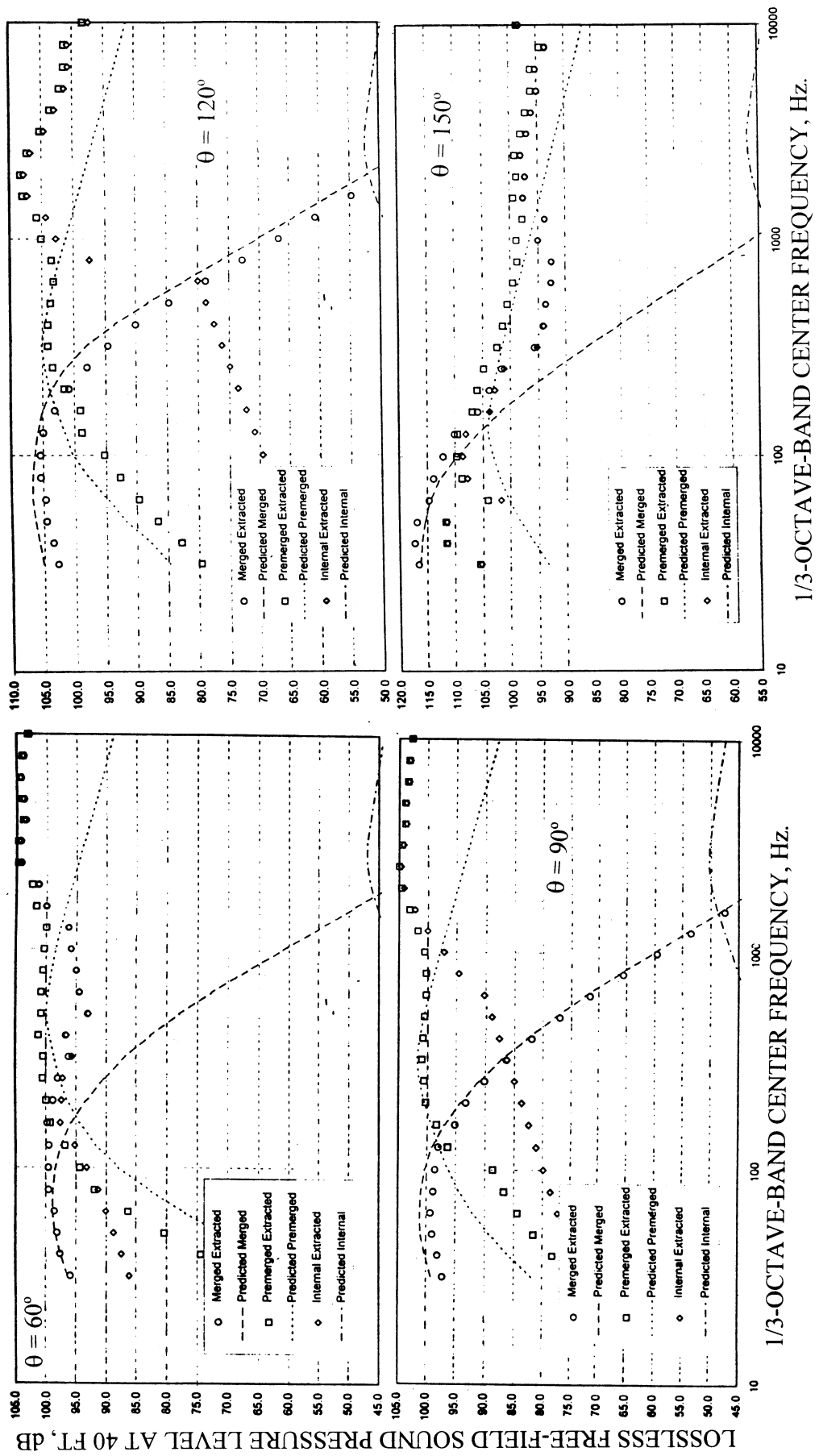
HBSFC - TP14  
 $P_{i,s} = 1.442$ ,  $T_{i,s} = 640^\circ R$ ,  $V_{i,s} = 874 \text{ ft/sec}$ ,  
 $P_{i,p} = 1.219$ ,  $T_{i,p} = 1248^\circ R$ ,  $V_{j,p} = 909 \text{ ft/sec}$

Figure B-6. Comparison of experimental/extracted and predicted spectra for 221-lobed mixer with standard fan nozzle for High Bypass Separated Flow Cycle, Nominal  $V_{\text{mix}} = 879 \text{ ft/sec}$  (TP14),  $M_f = 0.28$  (RDG. 806).



HBSFC - TP17  
 $P_{r,s} = 1.666$ ,  $T_{i,s} = 640^\circ R$ ,  $V_{i,s} = 1022 \text{ ft/sec}$ ,  
 $P_{r,p} = 1.416$ ,  $T_{i,p} = 1356^\circ R$ ,  $V_{j,p} = 1243 \text{ ft/sec}$

Figure B-7. Comparison of experimental/extracted and predicted spectra for 22-lobe mixer with standard fan nozzle for High Bypass Separated Flow Cycle, Nominal  $V_{mix} = 1055 \text{ ft/sec}$  (TP17),  $M_F = 0.28$  (RDG. 813).



HBSFC - TP20  
 $P_{r,s} = 1.832$ ,  $T_{ls} = 640^\circ R$ ,  $V_{ls} = 1105 \text{ ft/sec}$ ,  
 $P_{r,p} = 1.679$ ,  $T_{lp} = 1468^\circ R$ ,  $V_{lp} = 1562 \text{ ft/sec}$

Figure B-8. Comparison of experimental/extracted and predicted spectra for 22-lobed mixer with standard fan nozzle for High Bypass Separated Flow Cycle, Nominal  $V_{\text{mix}} = 1180 \text{ ft/sec}$  (TP20),  $M_f = 0.28$  (RDG. 853).

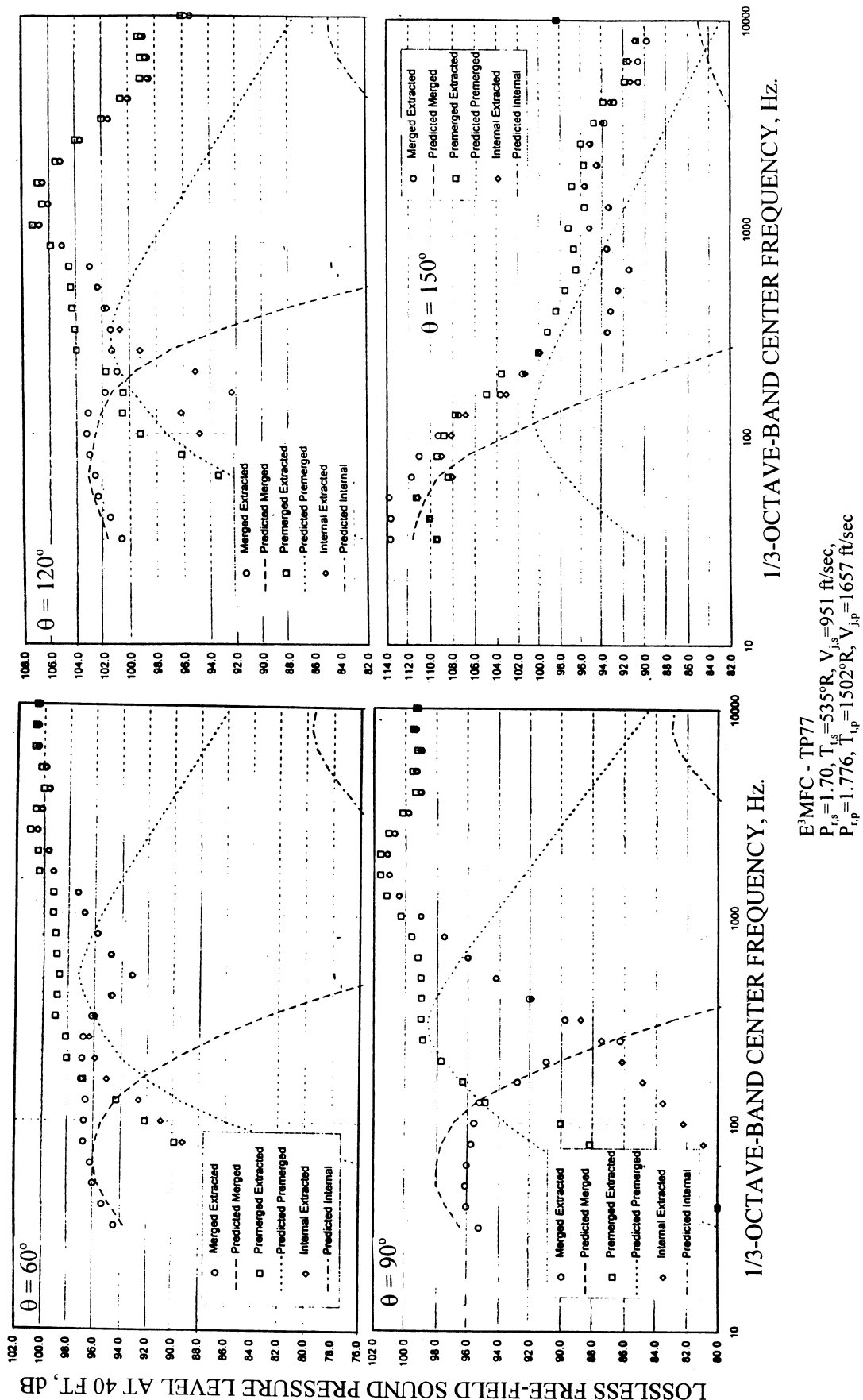


Figure B-9. Comparison of experimental/extracted and predicted spectra for 22-lobed mixer with short fan nozzle for E<sup>3</sup> Mixed Flow Cycle, Nominal  $V_{mix} = 1071 \text{ ft/sec}$  (TP77),  $M_F = 0.28$  (RDG. 803).

## APPENDIX C

### IMPLEMENTATION AND IMPROVEMENT OF MGB CODE TO PREDICT FARFIELD NOISE USING CFD PREDICTED/MEASURED FLOWFIELD DATA

Significant effort is being made to implement measured flowfield data to the MGB code to predict farfield jet noise. Dr. Nathan Messersmith, a professor from Purdue University, worked on this task at GEAE as an employee of AS&M during the summer of 1996. Since flowfield measurements are limited, interpolation/extrapolation of measured data is required for this application. However, noise contribution by a slice of jet could still be computed using measured flowfield data. In this effort, measured Kiel probe stagnation temperature and pressure data of the E<sup>3</sup> mixer nozzles are used to compute density and axial velocity. The computed axial velocities are compared with LDV data. Typical examples are shown in Figures C-1 and C-2 for a confluent mixer (V1) and a 12-lobed scalloped mixer (V2), hardware tested under Task A. All the results presented in this appendix are for E3 Mixed Flow Cycle, Test Point 75 (see Table 3 of main text). Velocities computed using Kiel probe data seem to be slightly higher than the LDV results. The cause for noted velocity differences are yet to be identified.

The major flowfield inputs to the MGB for farfield noise prediction code are the velocity, density, and the rms velocity of the plume. The Kiel probe data is useful for MGB code, since the measured temperature and pressure data can be readily utilized to compute density (see Figure C-3 as examples), an important input for MGB code. LDV data is equally important, since the rms velocities are obtained only from LDV measurements. The mean velocity can be used either from Kiel probe data or from LDV measurements. Utilization of Kiel probe data for density and mean velocity and rms velocity from LDV measurement as the flowfield input to the MGB code is currently being carried out.

**Measured Scale Model Acoustic Data:** Measured spectral directivity of various mixer nozzles are used to generate surface spectral contours to be compared with prediction. Figures C-4 through C-6 show the surface spectral contour plots of the measured sound pressure level (SPL) of the confluent mixer V1, the Scalloped mixer V2, and the skewed mixer F12A, respectively. Several items are of note, the increased SPL of the V1 mixer compared to the various lobed mixers at low frequencies and high angles relative to the inlet, and the increased bulge in SPL of the F12A mixer at a high frequency range and for a wide range of angles. The surface contour plots help to quickly identify regions of noticeable difference in the spectral content and directivity of the SPL for the various mixers. A comparison plot, Figure C-7, of the mixer spectra at 90 degrees directivity clearly shows the low frequency contribution of the V1 mixer and that of the F12A mixer in comparison to the other mixers, namely V2, scalloped mixer with extended tailpipe V2L, and scalloped & staggered mixer F9B.

**Acoustic prediction of Modified MGB Model Using Experimental Data :** The MGB code has been modified into a version, that uses nth order polynomial curve fits for the radial profiles of the mean velocity, RMS velocity, and density.

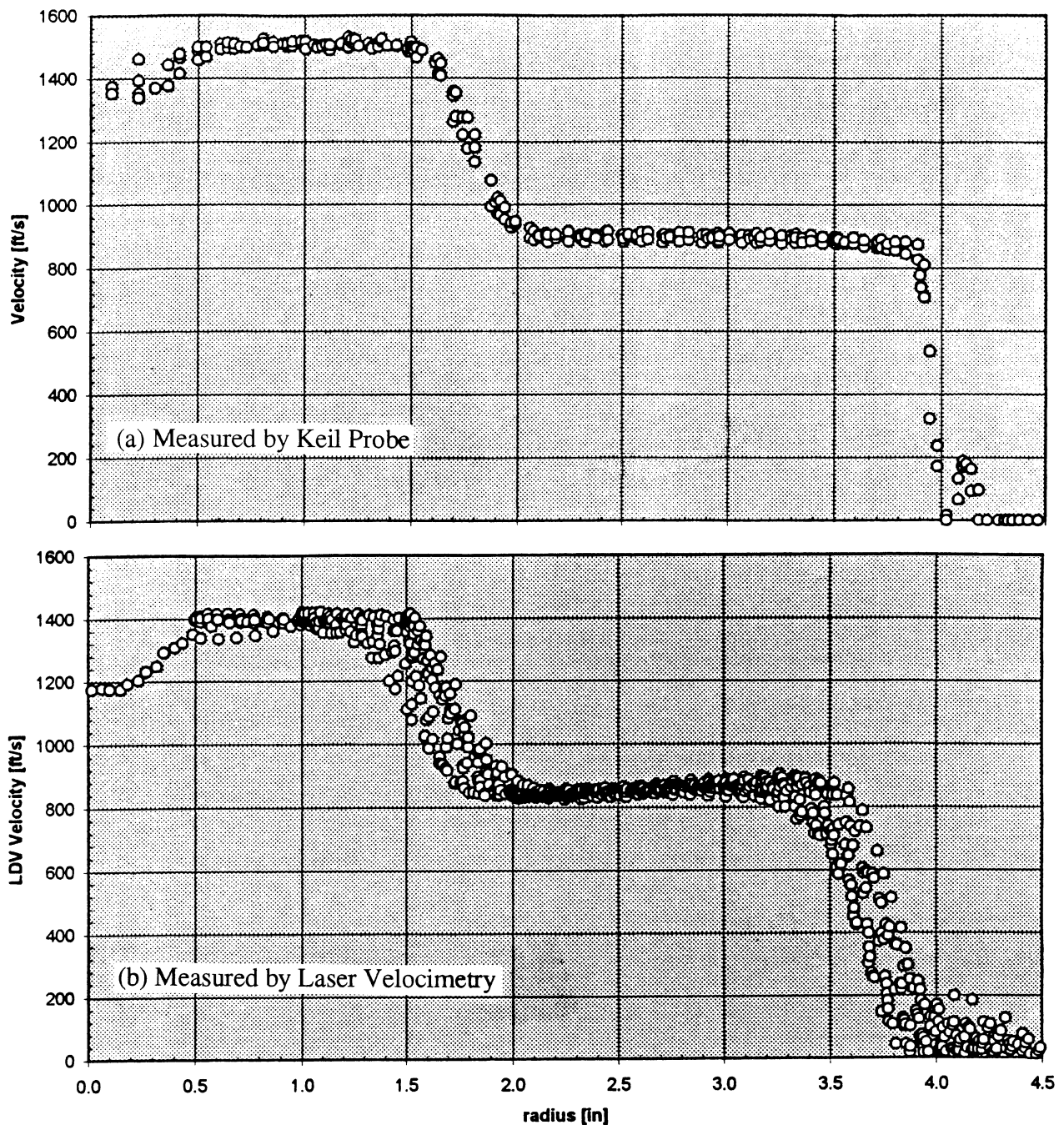


Figure C-1. Radial distribution of axial velocity at the nozzle exit plane for a confluent mixer (V1) measured by (a) Keil probe and (b) laser velocimetry (LDV) at static condition; nozzle pressure ratios and total temperatures are 1.6 & 540°R for fan stream and 1.631 & 1454°R for core stream (E<sup>3</sup>MFC - TP75).

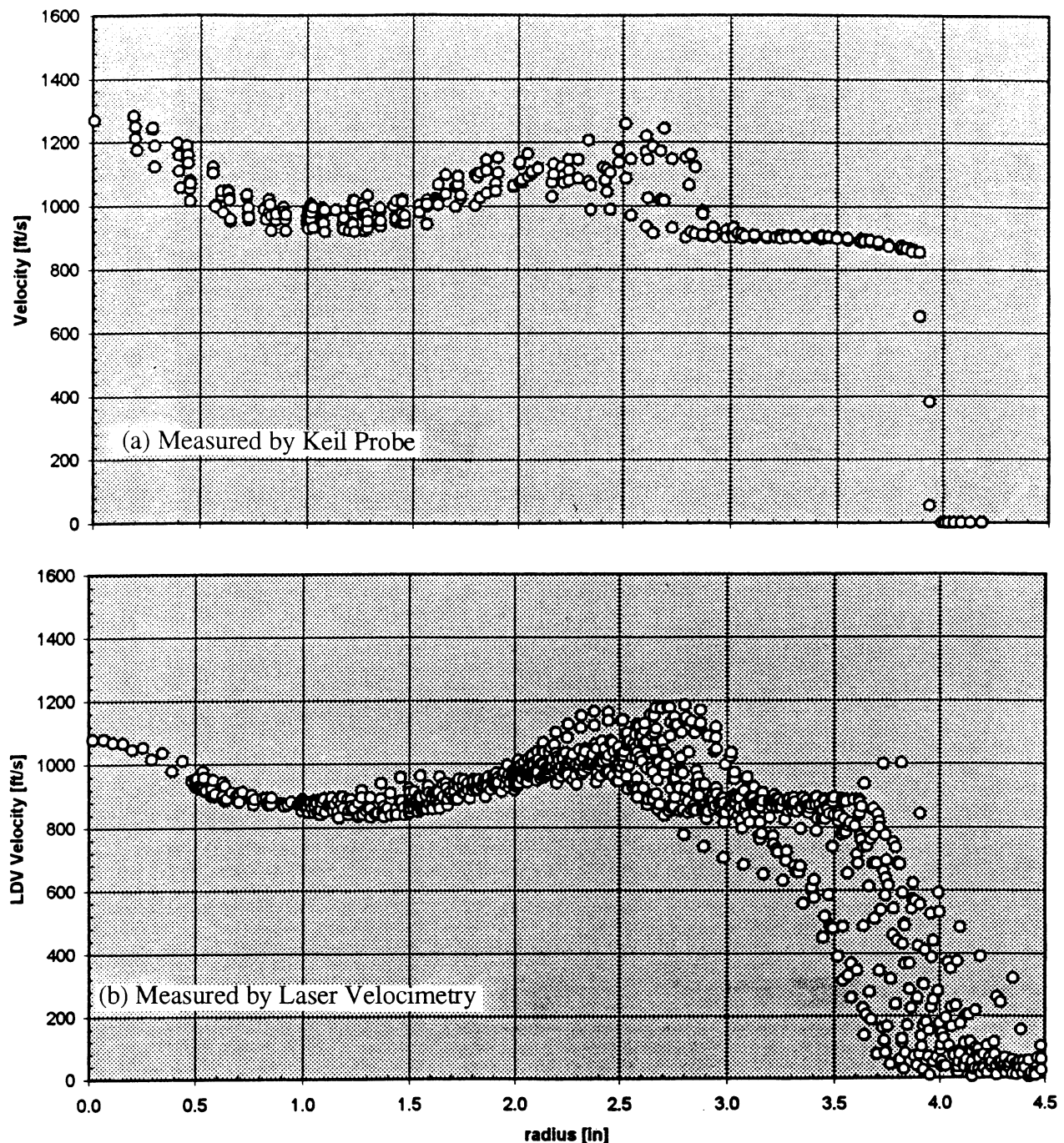


Figure C-2. Radial distribution of axial velocity at the nozzle exit plane for a 12-lobed scalloped mixer (V2) measured by (a) Keil probe and (b) laser velocimetry (LDV) at static condition; nozzle pressure ratios and total temperatures are 1.6 & 540°R for fan stream and 1.631 & 1454°R for core stream (E<sup>3</sup>MFC - TP75).

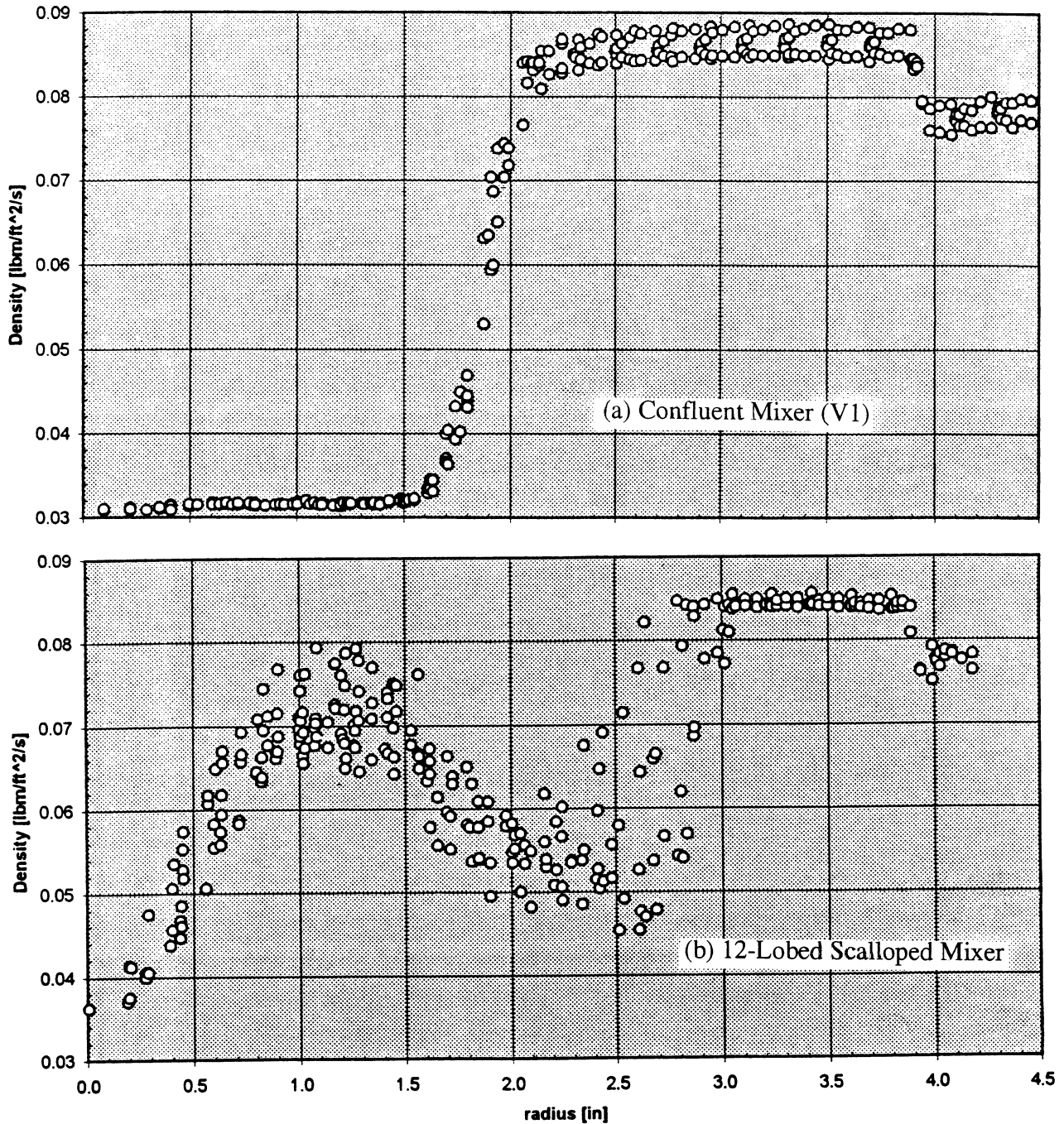


Figure C-3. Radial distribution of density at the nozzle exit plane for (a) a confluent mixer (V1) and (b) a 12-lobed scalloped mixer (V2) computed using measured Keil probe total temperature and pressure at static condition; nozzle pressure ratios and total temperatures are 1.6 & 540°R for fan stream and 1.631 & 1454°R for core stream (E<sup>3</sup>MFC - TP75).

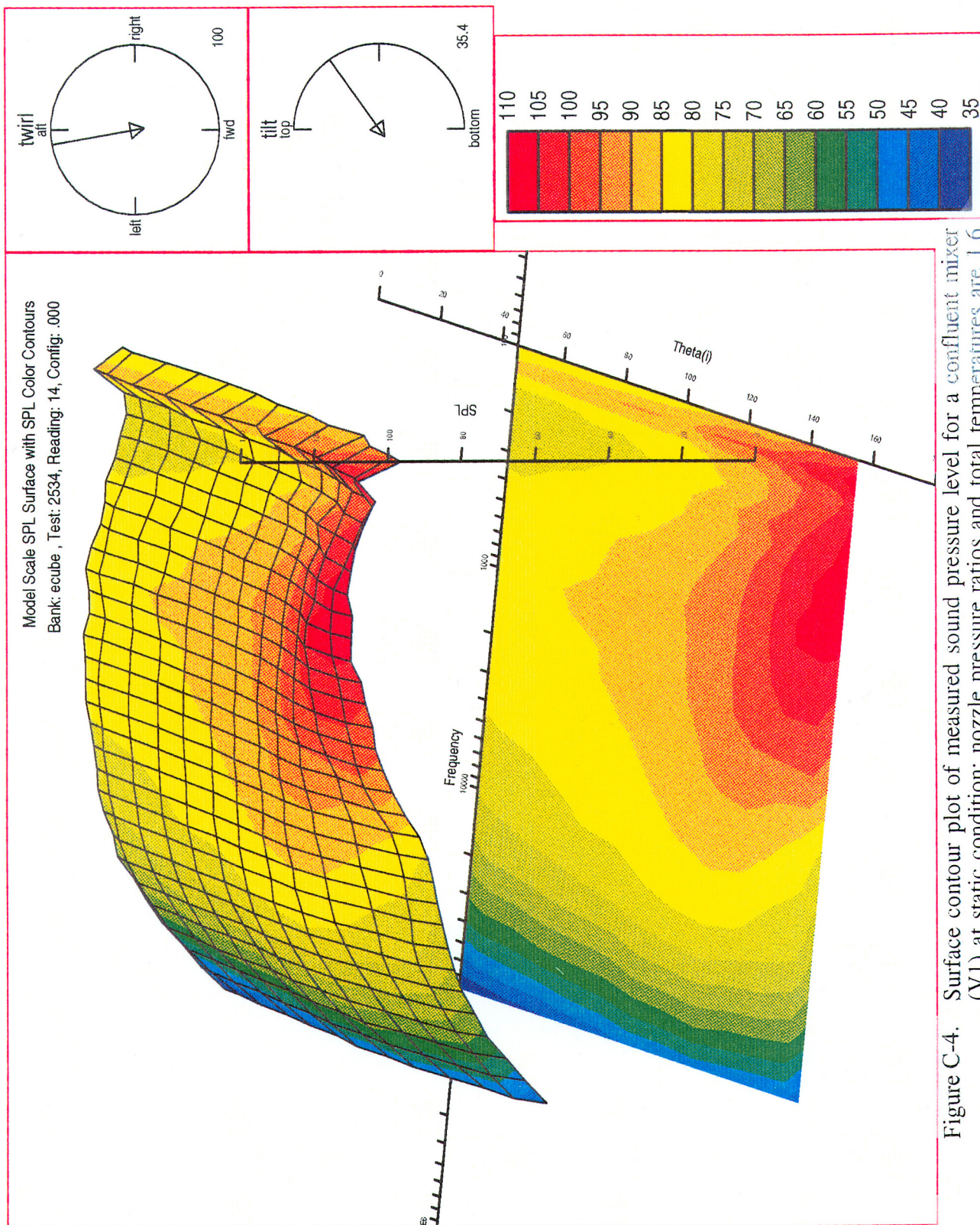


Figure C-4. Surface contour plot of measured sound pressure level for a confluent mixer (V1) at static condition; nozzle pressure ratios and total temperatures are 1.6 & 540°R for fan stream and 1.631 & 1454°R for core stream (E'MFC - TP75).

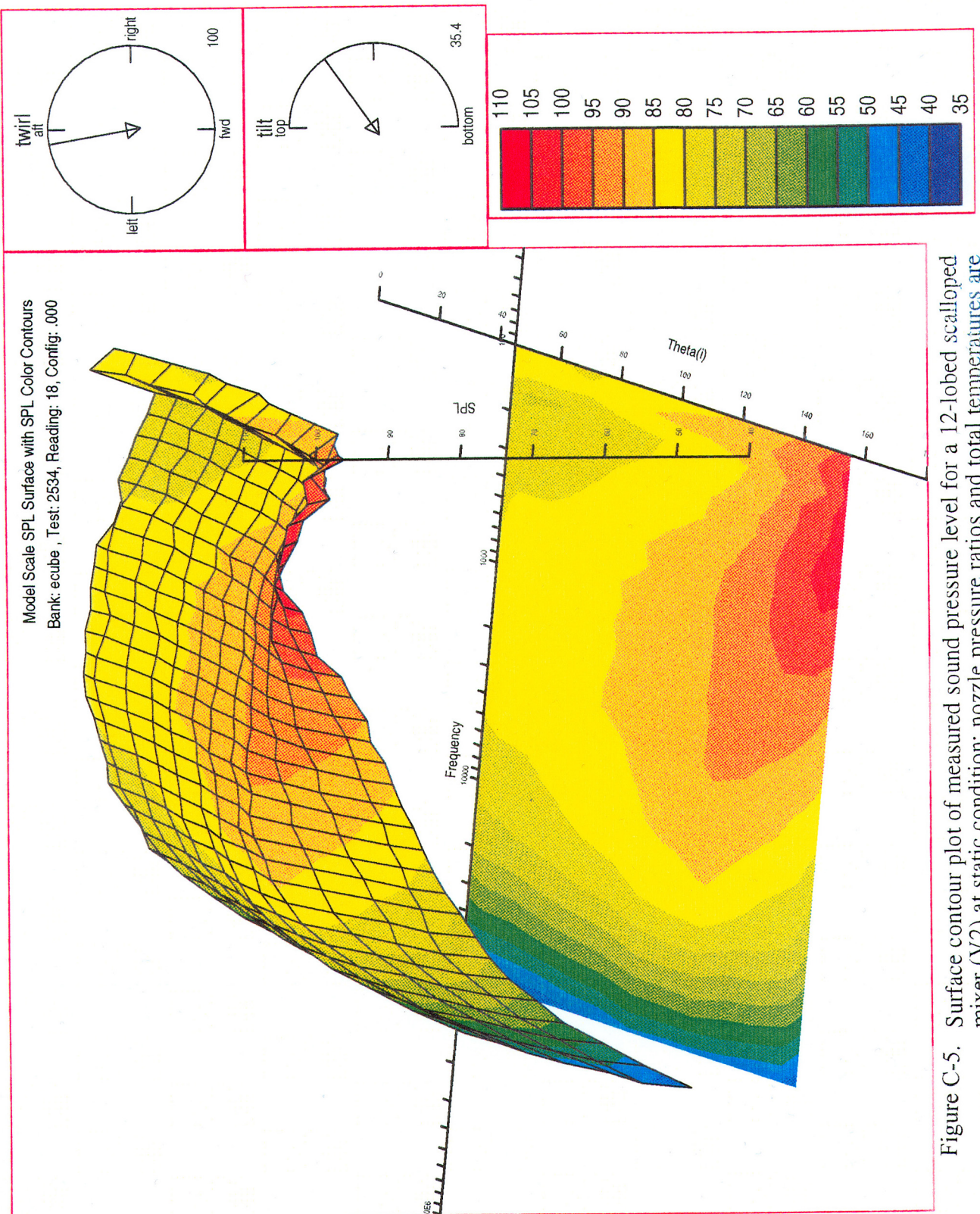


Figure C-5. Surface contour plot of measured sound pressure level for a 12-lobed scalloped mixer (V2) at static condition; nozzle pressure ratios and total temperatures are 1.6 & 540°R for fan stream and 1.631 & 1454°R for core stream (E<sup>3</sup>MFC - TP75).

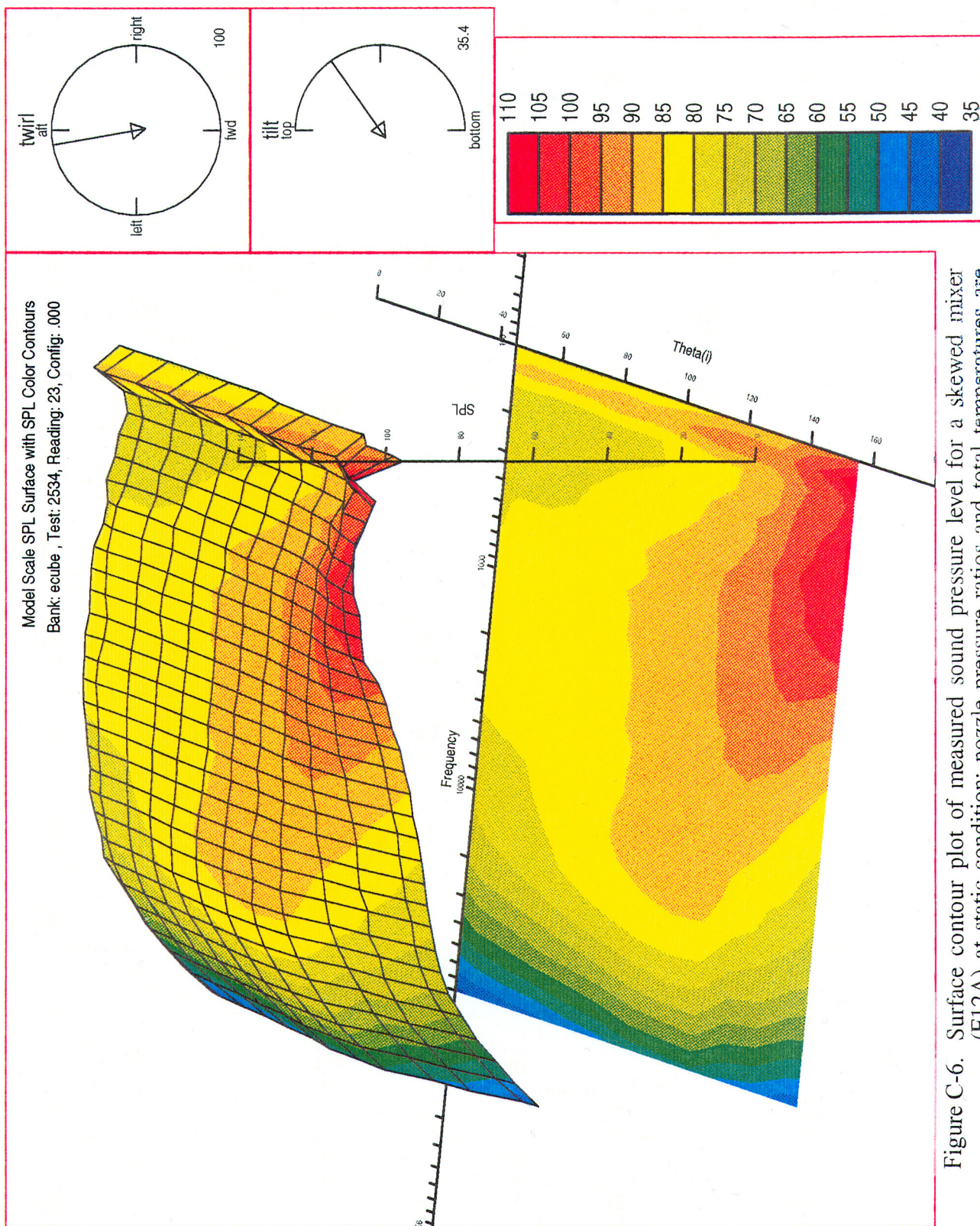
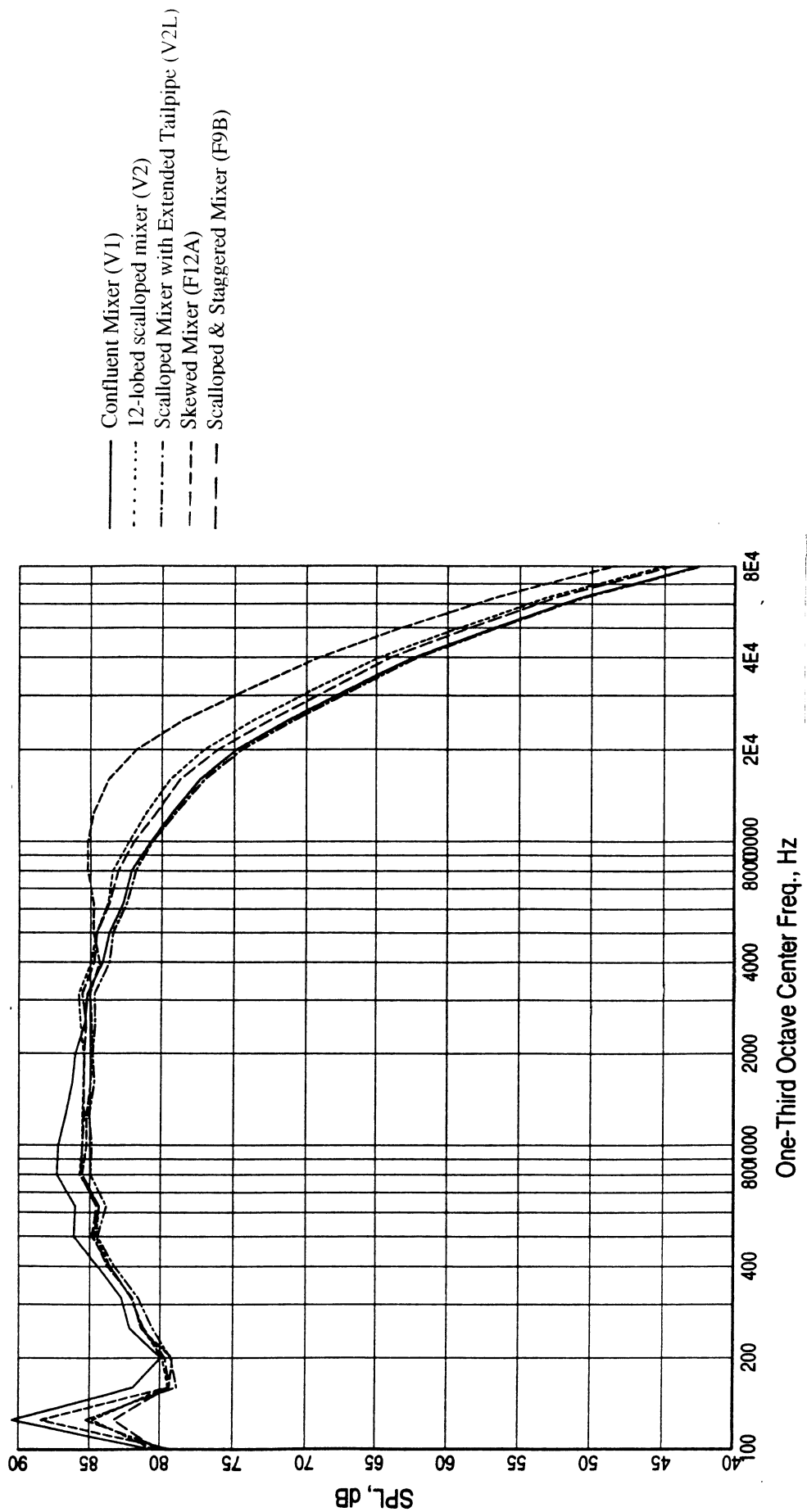


Figure C-6. Surface contour plot of measured sound pressure level for a skewed mixer (F12A) at static condition; nozzle pressure ratios and total temperatures are 1.6 & 540°R for fan stream and 1.631 & 1454°R for core stream (E<sup>3</sup>MFC - TP75).



**Figure C-7.** Measured sound pressure level spectra of the various mixers at 90° at static condition; nozzle pressure ratios and total temperatures are 1.6 & 540°R for fan stream and 1.631 & 1454°R for core stream ( $E^3MFC - TP75$ ).

Figures C-8 through C-10 illustrate the SPL surface contour plots of the predicted farfield noise for the V1, V2, and F12A mixers, respectively, using the experimental data at the nozzle exit plane. In all cases, the predicted high frequency spectra fills the data more than the low frequency spectra, as expected from the data at a single plane close to nozzle exit. Nevertheless, key features are noted, such as a bulge at about 1000 Hz that is attributed to the mass averaged jet exhaust noise, and another peak region at higher frequencies that is attributed to the mixing noise. This is less clearly defined for the V1 mixer compared to the V2 mixer, while the high frequency content of the F12A mixer is seen to dominate the noise pattern for this flow. The F12A mixer also seems to exhibit less attenuation due to shielding effects at large angles compared to both the V1 and V2 mixers.

Figure C-11 shows a direct comparison of the E<sup>3</sup> acoustic data with the predictions of the V1 mixer. Good agreement is found at the high frequencies, with a large discrepancy at the lower frequencies that is again attributed to the single plane of data used for the predictions. It is expected that better agreement at the low frequencies would be found if more data were available. It is not known how much more data would affect the present agreement at the high frequencies.

Figure C-12 shows another comparison of data with prediction with full plume calculation for an equivalent coannular nozzle. A clear deficiency is observed in the prediction of the high frequency noise, and a slight overprediction of the noise is found in the intermediate frequency range; however, the agreement is reasonably good in the intermediate frequency range. Figure C-13 shows the noise spectra comparisons for observer angles of 60, 90, 120, and 150 degrees relative to the inlet, respectively. The above mentioned differences are clearly seen in these plots, with a reasonable agreement occurring for the 150 degree observation angle, but much less so for all other angles.

For the study of subsonic exhausts jets, the Kiel probe provides total pressure and total temperature, which yield jet density, if jet static pressure is assumed to be equal to ambient static pressure. LDV yields accurate mean velocity and turbulence data. For the conditions considered in the present work, there seems to be some agreement in the measured acoustic data and the predicted acoustic field (using the V1 mixer experimental data) at high frequencies. The large discrepancies observed at the lower frequencies are attributed at present to the availability of experimental data only at the nozzle exit, which lies in a region that is biased towards high frequency noise production. Whether the agreement with the predictions and the measurements remains as more experimental data becomes available at greater distances within the jet plume remains for future investigations.

The effort of flowfield data implementation to MGB is described in detail in the report "Correlation Between the Aerodynamics and Aeroacoustics of the E<sup>3</sup> Mixer Nozzles," by Nathan Messersmith, 1996.

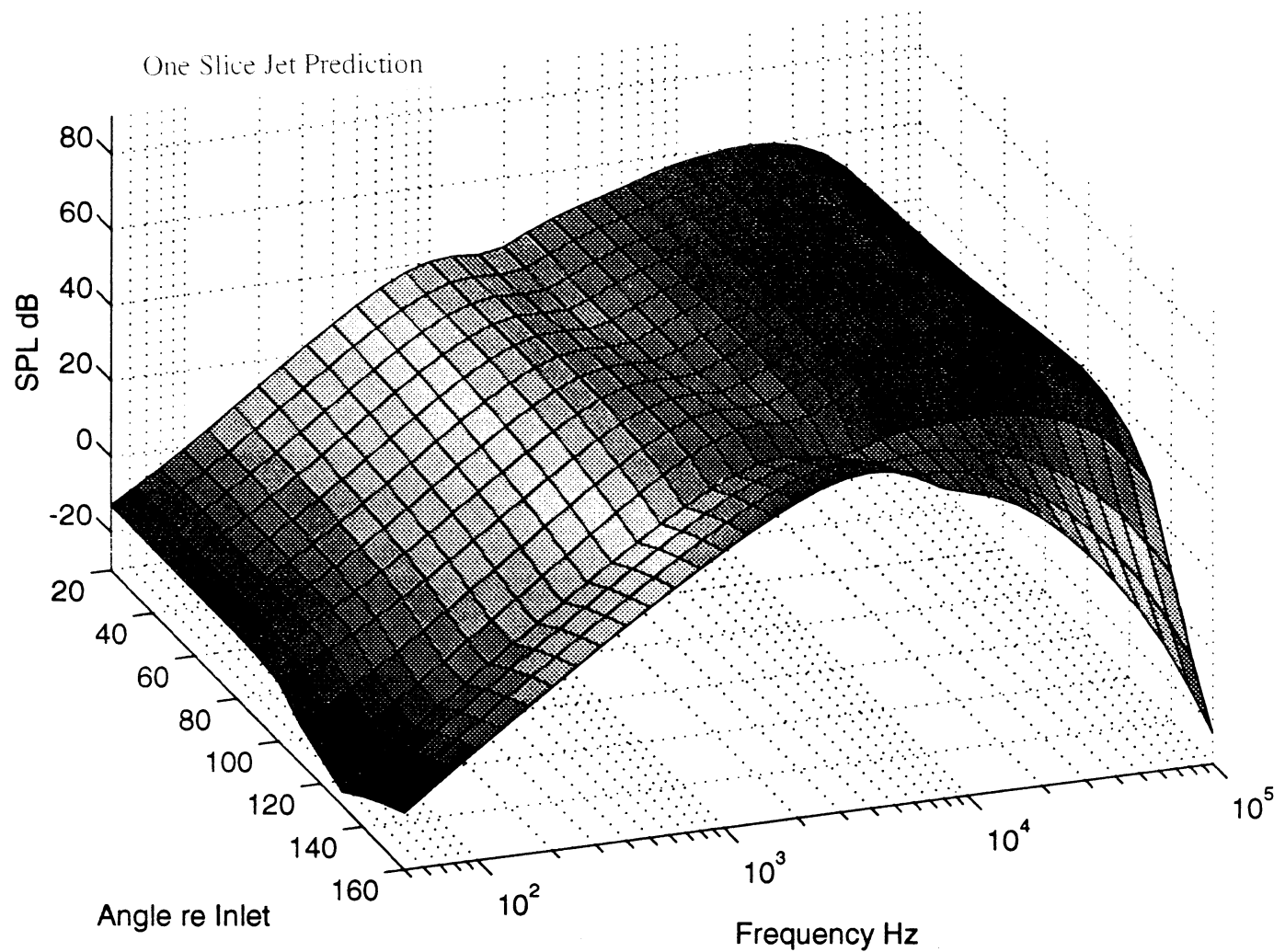


Figure C-8. Predicted sound pressure level surface contour plot for a confluent mixer (V1) at static condition; nozzle pressure ratios and total temperatures are 1.6 & 540°R for fan stream and 1.631 & 1454°R for core stream (E<sup>3</sup>MFC - TP75).

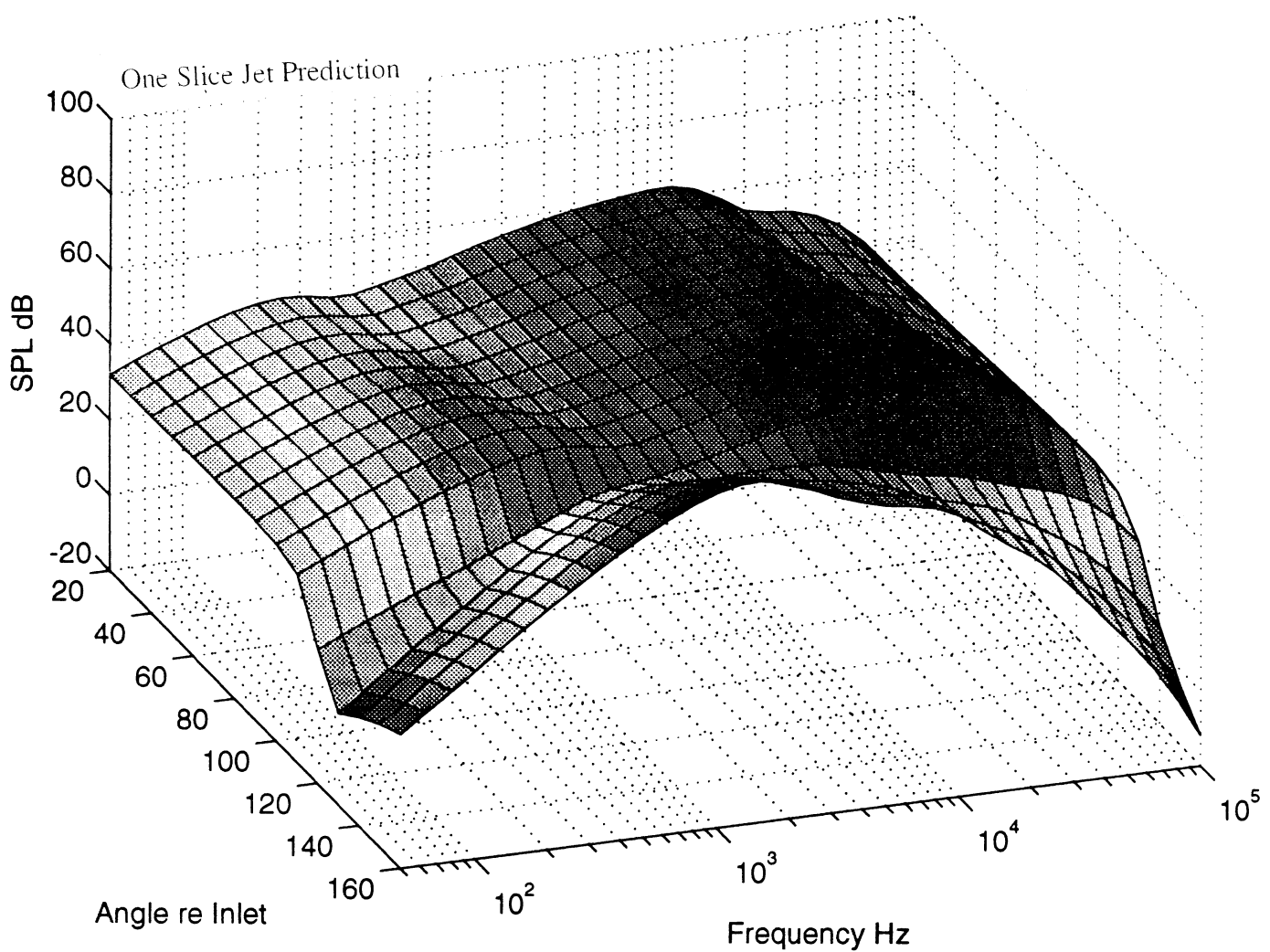


Figure C-9. Predicted sound pressure level surface contour plot for a 12-lobed scalloped mixer (V2) at static condition; nozzle pressure ratios and total temperatures are 1.6 & 540°R for fan stream and 1.631 & 1454°R for core stream (E<sup>3</sup>MFC - TP75).

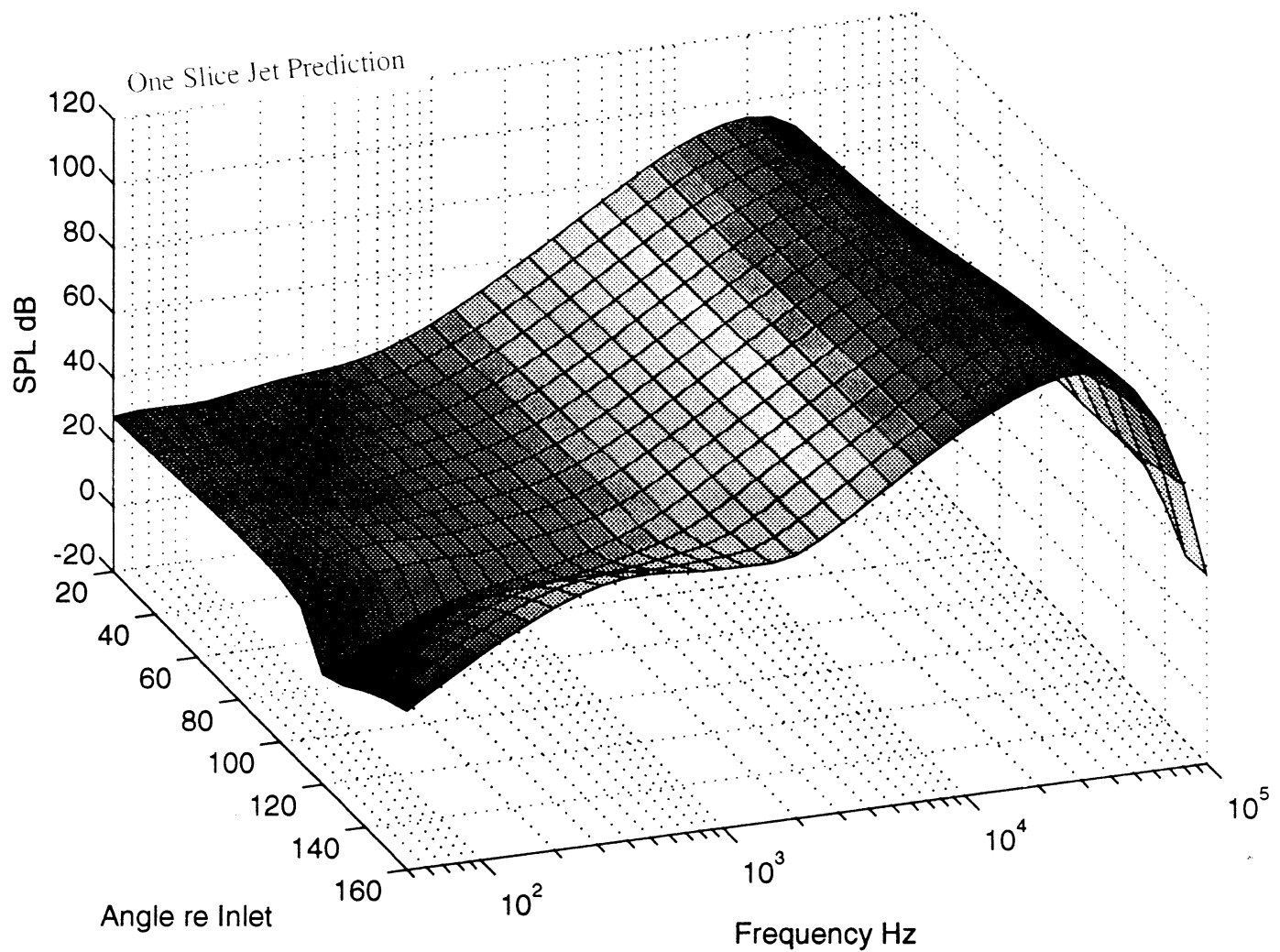


Figure C-10. Predicted sound pressure level surface contour plot for a skewed mixer (F12A) at static condition; nozzle pressure ratios and total temperatures are 1.6 & 540°R for fan stream and 1.631 & 1454°R for core stream (E<sup>3</sup>MFC - TP75).

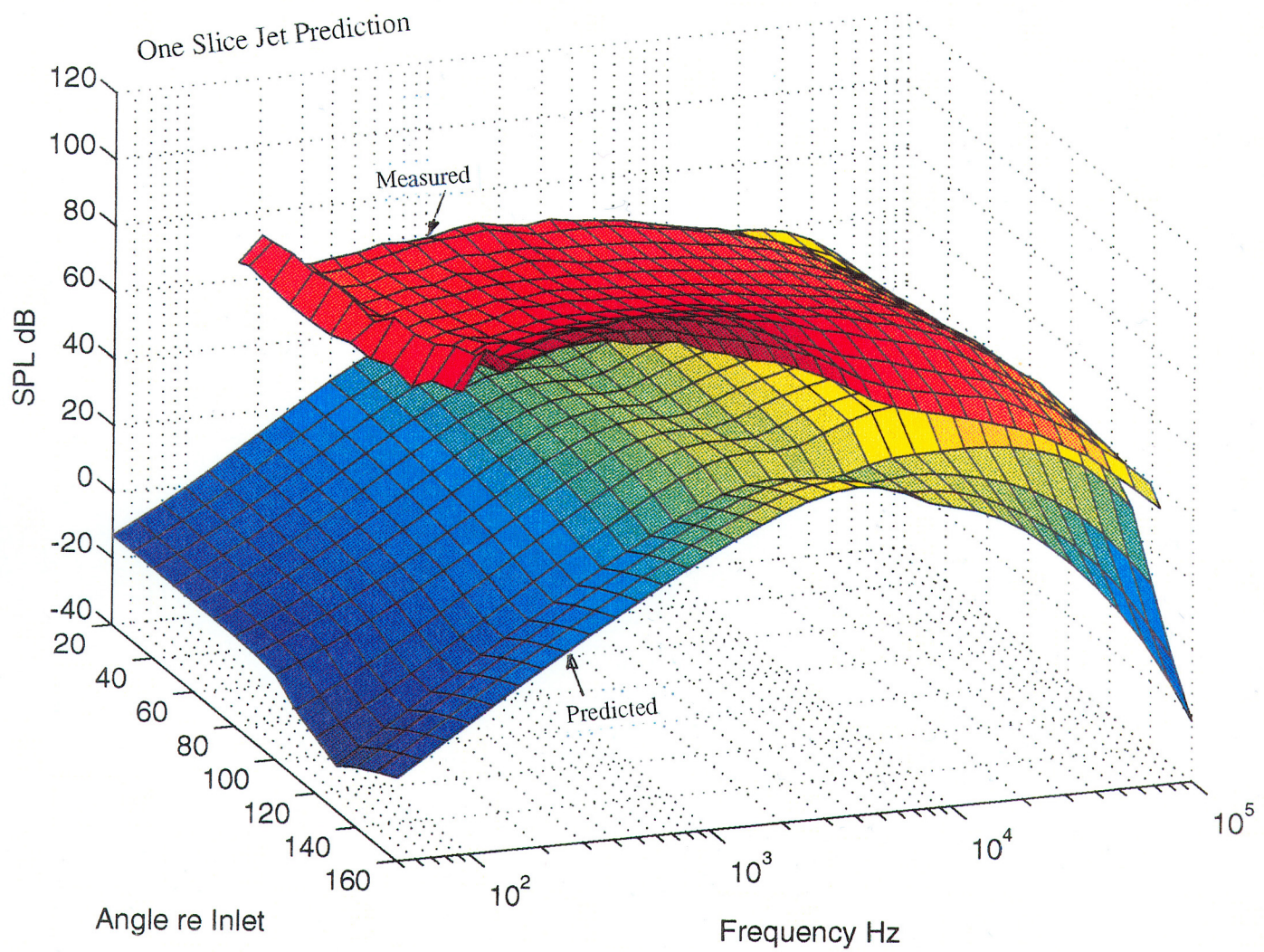


Figure C-11. Comparison between measured and predicted sound pressure level surface contour plots for a confluent mixer (V1) at static condition; nozzle pressure ratios and total temperatures are 1.6 &  $540^{\circ}\text{R}$  for fan stream and 1.631 &  $1454^{\circ}\text{R}$  for core stream (E<sup>3</sup>MFC - TP75).

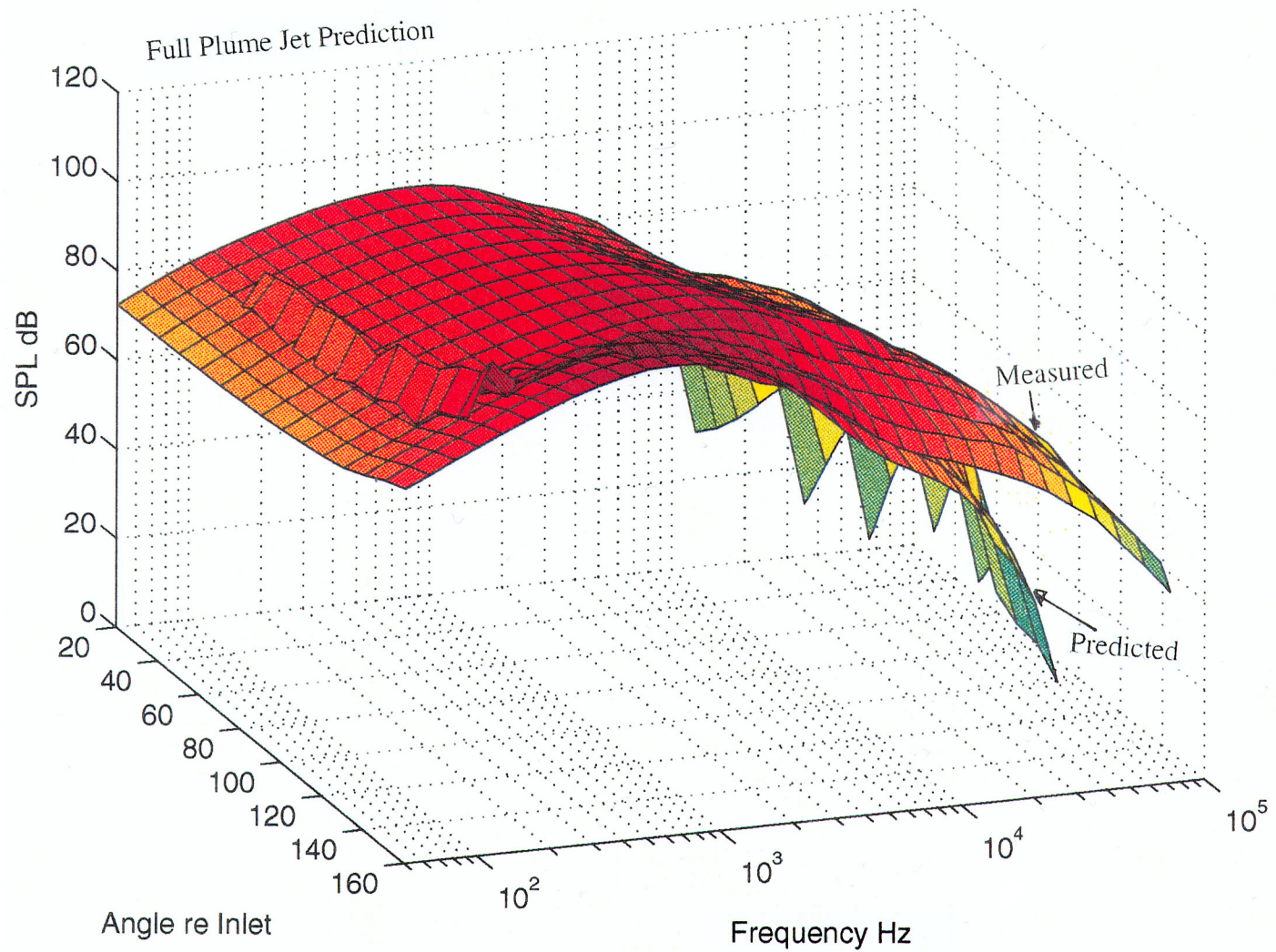


Figure C-12. Comparison between measured and predicted sound pressure level surface contour plots for an equivalent coannular nozzle at static condition; nozzle pressure ratios and total temperatures are 1.6 & 545°R for fan stream and 1.631 & 1444°R for core stream (E<sup>3</sup>MFC - TP75).

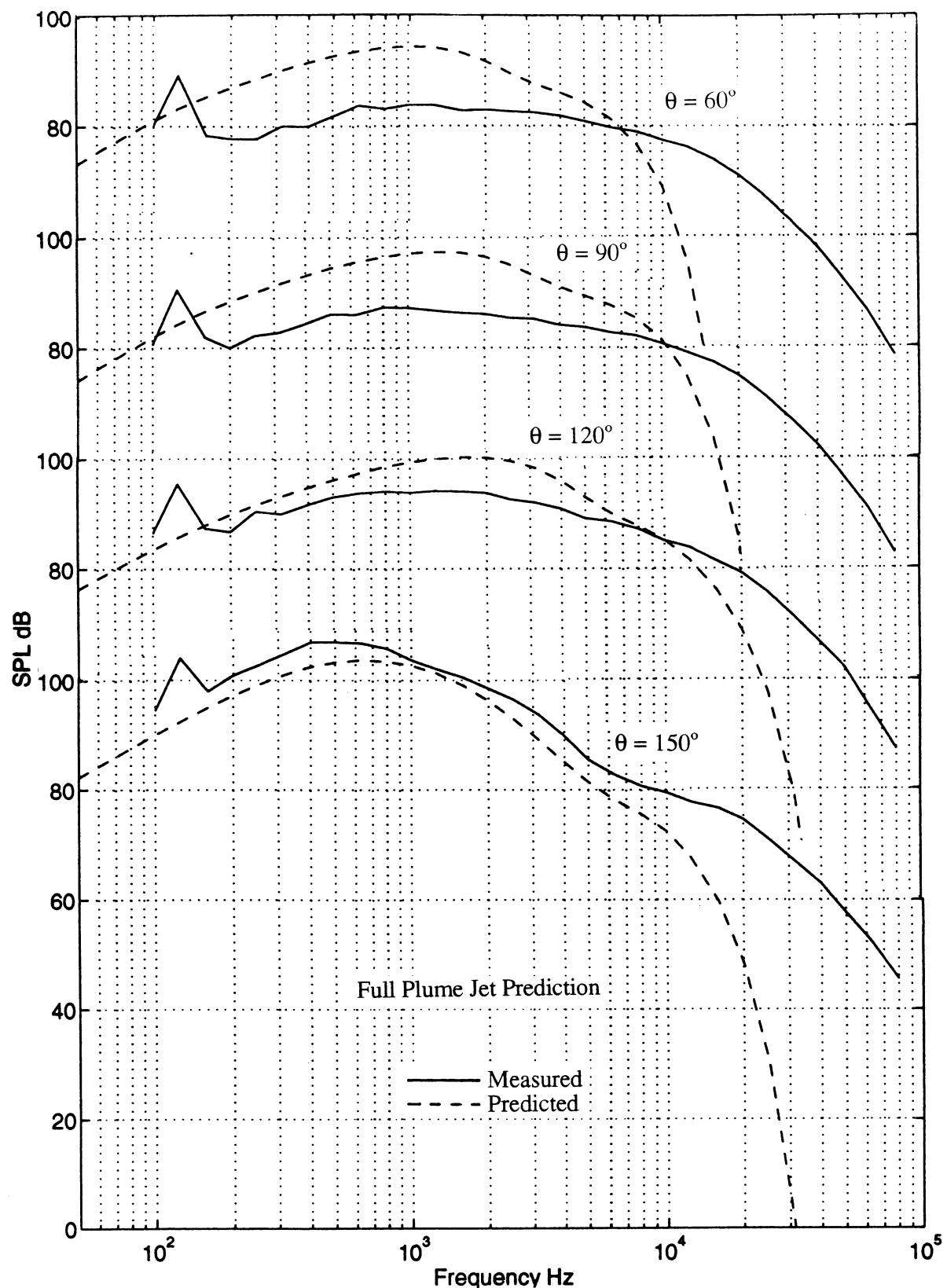


Figure C-13. Comparison between measured and predicted sound pressure level spectra at various polar angles,  $\theta$  for an equivalent coannular nozzle at static condition; nozzle pressure ratios and total temperatures are 1.6 & 545°R for fan stream and 1.631 & 1444°R for core stream (E<sup>3</sup>MFC - TP75).

<b>REPORT DOCUMENTATION PAGE</b>			<i>Form Approved OMB No. 0704-0188</i>
Public reporting burden for this collection of information is estimated to average 1 hour per response, including the time for reviewing instructions, searching existing data sources, gathering and maintaining the data needed, and completing and reviewing the collection of information. Send comments regarding this burden estimate or any other aspect of this collection of information, including suggestions for reducing this burden, to Washington Headquarters Services, Directorate for Information Operations and Reports, 1215 Jefferson Davis Highway, Suite 1204, Arlington, VA 22202-4302, and to the Office of Management and Budget, Paperwork Reduction Project (0704-0188), Washington, DC 20503.			
1. AGENCY USE ONLY (Leave blank)	2. REPORT DATE	3. REPORT TYPE AND DATES COVERED	
	September 2002	Final Contractor Report	
4. TITLE AND SUBTITLE		5. FUNDING NUMBERS	
Acoustic and Laser Doppler Anemometer Results for Confluent, 22-Lobed, and Unique-Lobed Mixer Exhaust Systems for Subsonic Jet Noise Reduction		WU-781-30-12-00 NAS3-26617	
6. AUTHOR(S)		7. PERFORMING ORGANIZATION NAME(S) AND ADDRESS(ES)	
M. Salikuddin, S. Martens, H. Shin, and R.K. Majjigi		General Electric Aircraft Engines Company Mail Drop A411 One Neumann Way Cincinnati, Ohio	
9. SPONSORING/MONITORING AGENCY NAME(S) AND ADDRESS(ES)		8. PERFORMING ORGANIZATION REPORT NUMBER	
National Aeronautics and Space Administration Washington, DC 20546-0001		E-13385	
11. SUPPLEMENTARY NOTES		10. SPONSORING/MONITORING AGENCY REPORT NUMBER	
Project Manager, James Bridges, Structures and Acoustics Division, NASA Glenn Research Center, organization code 5940, 216-433-2693.		NASA CR—2002-211598	
12a. DISTRIBUTION/AVAILABILITY STATEMENT		12b. DISTRIBUTION CODE	
Unclassified - Unlimited Subject Categories: 07 and 34		Distribution: Nonstandard	
Available electronically at <a href="http://gltrs.grc.nasa.gov">http://gltrs.grc.nasa.gov</a> This publication is available from the NASA Center for AeroSpace Information, 301-621-0390.			
13. ABSTRACT (Maximum 200 words)			
The objective of this task was to develop a design methodology and noise reduction concepts for high bypass exhaust systems which could be applied to both existing production and new advanced engine designs. Special emphasis was given to engine cycles with bypass ratios in the range of 4:1 to 7:1, where jet mixing noise was a primary noise source at full power takeoff conditions. The goal of this effort was to develop the design methodology for mixed-flow exhaust systems and other novel noise reduction concepts that would yield 3 EPNdB noise reduction relative to 1992 baseline technology. Two multi-lobed mixers, a 22-lobed axisymmetric and a 21-lobed with a unique lobe, were designed. These mixers along with a confluent mixer were tested with several fan nozzles of different lengths with and without acoustic treatment in GEAE's Cell 41 under the current subtask (Subtask C). In addition to the acoustic and LDA tests for the model mixer exhaust systems, a semi-empirical noise prediction method for mixer exhaust system is developed. Effort was also made to implement flowfield data for noise prediction by utilizing MGB code. In general, this study established an aero and acoustic diagnostic database to calibrate and refine current aero and acoustic prediction tools.			
14. SUBJECT TERMS		15. NUMBER OF PAGES	
Acoustic measurement; Laser doppler velocimeters; Noise prediction; Noise reduction; Scale models; Exhaust systems; Subsonic flow; Aeroacoustics; Jet aircraft noise		201	
		16. PRICE CODE	
17. SECURITY CLASSIFICATION OF REPORT	18. SECURITY CLASSIFICATION OF THIS PAGE	19. SECURITY CLASSIFICATION OF ABSTRACT	20. LIMITATION OF ABSTRACT
Unclassified	Unclassified	Unclassified	